Role of BMP4 and RHOA Signalling in Breast Cancer

A Thesis

Submitted in Partial Fulfilment of the Requirements for the Degree of

DOCTOR OF PHILOSOPHY

Submitted by

Renu Sharma

(156106045)

18th December 2023

Under the supervision of

Prof. Bithiah Grace Jaganathan

Department of Biosciences and Bioengineering

Indian Institute of Technology Guwahati

Guwahati-781039, Assam, India

Indian Institute of Technology Guwahati
Department of Biosciences and Bioengineering

DECLARATION

I do hereby declare that the content embodied in this thesis entitled "**Role of BMP4 and RHOA Signalling in Breast Cancer**" is the result of investigations carried out by me in the Department of Biosciences and Bioengineering, Indian Institute of Technology Guwahati for the award of the degree of Doctor of Philosophy, under the supervision of **Prof. Bithiah Grace Jaganathan**.

As per the general norms of reporting research findings, due acknowledgements have been made wherever the research findings of other researchers have been cited in this thesis.

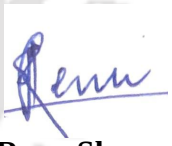

Date: 18.12.2023

Renu Sharma
(156106045)

Indian Institute of Technology Guwahati
Department of Biosciences and Bioengineering

CERTIFICATE

It is certified that the work described in this thesis entitled "**Role of BMP4 and RHOA Signalling in Breast Cancer**", by **Renu Sharma** (Roll No. 156106045) for the award of the degree of Doctor of Philosophy is an authentic record of the results obtained from the research work carried out under my supervision in the Department of Biosciences and Bioengineering, Indian Institute of Technology Guwahati, India. This work has not been submitted elsewhere for the award of any degree or diploma.

Date: 18.12.2023

Prof. Bithiah Grace Jaganathan
(Thesis Supervisor)

Table of contents

List of Figures

Abbreviations

ABCB1	Adenosine 5′-Triphosphate–Binding Cassette Subfamily B Member 1
ABCG2	ATP-Binding Cassette Subfamily G Member 2
AGTR1	Angiotensin II Receptor Type 1
AIF1L	Allograft Inflammatory Factor 1-Like
AMH	Anti-Müllerian Hormone
AMHR2	Anti-Müllerian Hormone Type II Receptor
ANXA1	Annexin-A1
AP-1	Activating Protein-1
APC	Adenomatous Polyposis Coli
BAMBI	Bmp and Activin Membrane-Bound Inhibitor
BAG6	Bcl-2-associated Athanogene 6
BMP	Bone Morphogenetic Protein
BMPR-2	BMP Receptor Type II
BMPR-IA	BMP Receptor Type IA
BMPR-IB	BMP Receptor Type IB
BNIP-2	BCL2 Interacting Protein 2
BORG	BMP/OP-Responsive Gene
BRCA1	Breast Cancer Gene 1
BRCA2	Breast Cancer Gene 2
CCM3	Cerebral Cavernous Malformations 3
CD44	Transmembrane Glycoprotein Cluster of Differentiation 44
CDDP	Cis-Diamminedichloroplatinum(II)
CDK	Cyclin Dependent Kinase
CERS6	Ceramide Synthase 6
CHRDL1	Chordin Like-1
circRNAs	Circular RNAs

ccRCC	Clear Cell Renal Cell Carcinoma
CK	Cytokeratin
CK1	Casein Kinase 1
CML	Chronic Myeloid Leukaemia
CRIM1	Cysteine-Rich Transmembrane BMP Regulator 1
CSCs	Cancer Stem Cells
CTGF	Connective Tissue Growth Factor
Cyr 61	cysteine-rich angiogenic inducer 61
DAAM1	Dishevelled-Associated Activator of Morphogenesis 1
DCIS	Ductal Carcinoma in Situ
DKK-1	Dickkopf 1
DLC1	Deleted in Liver Cancer 1
DMH1	Dorsomorphin homolog 1
Dsh	Dishevelled
EDV	Endothelium-Dependent Vascularization
EGFR	Epidermal Growth Factor Receptors
EMT	Epithelial-Mesenchymal Transition
ER	Estrogen Receptor
ERK	Extracellular Signal-Related Kinases
ET1	Endothelin 1
FAK	Focal Adhesion Kinase
FGF	Fibroblast Growth Factor
FOXF2	Forkhead Box Protein F2
FPPS	Farnesyl Pyrophosphate Synthase
FSTL1	Follistatin-Like Protein 1
GATA4	GATA Binding Protein 4
GEF	Guanine Nucleotide Exchange Factors
GLI1	Glioma-Associated Oncogene 1

GNA13	Guanine Nucleotide Binding Protein Alpha 13
GREM1	Gremlin-1
GSK3	Glycogen Synthase Kinase 3
HER2	Human Epidermal Growth Factor Receptor 2
HGF-Met	Hepatocyte Growth Factor Met Tyrosine Kinase
HMLH1	Human Mutl Homolog 1
HPTTG1	Human Pituitary Tumour-Transforming Gene 1
HSP90	Heat Shock Protein 90
HTR1A	5-Hydroxytryptamine Receptor 1A
IGF	Insulin Growth Factor
IP3	Inositol Trisphosphate
I-Smad	Inhibitory Smad
LATS1/2	Large Tumour Suppressor Kinases ½
LEF	Lymphoid Enhancer Factor
LIMK	LIM Kinase
LncRNA	Long Non-Coding RNA
LRP5/6	low-density lipoprotein receptor-related protein 5/6
MAPK	Mitogen-Activated Protein Kinase
M-CSF	Macrophage Colony-Stimulating Factor
MEK	Mitogen-Activated Extracellular Signal-Regulated Kinase
MLC2	Myosin Light Chain 2
MMPs	Matrix Metalloproteinase
MMTV-PyMT	Mouse Mammary Tumor Virus-Polyoma Middle Tumor-antigen
MORC2	Microrchidia Family CW-Type Zinc Finger 2
MRI	Magnetic Resonance Imaging
NEAT1	Nuclear Enriched Abundant Transcript 1
Net1	Neuroepithelial Transforming Gene 1
NF-κB	Nuclear Factor-Kappa B

NOV	nephroblastoma overexpressed
NRF2	Nuclear Factor Erythroid 2 Related Factor
OC-MSC	Ovarian Cancer Patient-Derived Mesenchymal Stem Cell
OVOL1	Ovo-Like Transcriptional Repressor 1
Pax-2	Paired Box 2
PBF	Pituitary Tumour-Transforming Gene (PTTG)-Binding Factor
PDGF	Platelet-Derived Growth Factor
PET	Positron Emission Tomography
PEEK	Polyetheretherketone
PGE2	Prostaglandin E2
PI3K	Phosphatidylinositol-3 Kinase
PLA	Polylactic Acid
PP2A	Protein phosphatase 2
PR	Progesterone Receptor
PROCR	Protein C Receptor
PTCH1	Patched Homolog-1
PTHrP	Parathyroid Hormone-Related Peptide
RAF	Rapidly Accelerated Fibrosarcoma
RANKL	Receptor Activator of Nuclear Factor Kappa Beta
RAS	Rat Sarcoma Virus
RHPN1	ROPN1 Interacting Protein Rhopillin-1
RHOA	Ras homolog family member A
RNF2	Ring Finger Protein 2
ROCK	Rho-Associated Coiled-Coil Kinase
ROPN1	Rhophilin-Associated Tail Protein 1
ROR2	receptor tyrosine kinase-like orphan receptor 2
RTK	receptor tyrosine kinase
R-Smad	Regulatory Smad

S/T Kinase	Serine/Threonine Kinase
S1PR1	Sphingosine-1-Phosphate Receptor 1
SDF-1	Stromal Cell-Derived Factor-1
SFRP1	Soluble Frizzled-Related Protein 1
SHH	Sonic Hedgehog
siRNA	Small Interfering RNA
SMO	Smoothened
SMURF1	SMAD-specific E3 ubiquitin protein ligase 1
SOSTDC1	Sclerostin Domain-Containing Protein-1
SPATS1	Spermatogenesis Associated Serine-Rich 1
TAK-1	Transforming growth factor-β-activated kinase 1
TAMs	Tumour-Associated Macrophages
TAZ	Transcriptional Co-Activator with PDZ-Binding Motif ccRCC
TCF	T Cell Factor
TERT	Telomerase Reverse Transcriptase
TGF-β	Transforming Growth Factor-Beta
Tiam1	T-Lymphoma Invasion and Metastasis-1
TKIs	Tyrosine Kinase Inhibitors
TNBC	Triple Negative Breast Cancer
TNF	Tumour Necrosis Factor
TNM	Tumour Node Metastasis
TRIM 21	Tripartite Motif Containing-21
UCA1	Urothelial Carcinoma Associated 1
USP8	Ubiquitin Specific Peptidase 8
VEGF	Vascular Endothelial Growth Factor
VM	Vasculogenic Mimicking
WAP-Cre	Whey Acidic Protein
WASP	Wiskott–Aldrich Syndrome Protein

Wnt	Wingless-Int-1
XIAP	X-Linked Inhibitor of Apoptosis Protein
YAP	Yes-Associated Protein
ZEB1	Zinc finger E-box-binding homeobox 1

Synopsis

Breast cancer is the second leading cause of cancer-related death in women worldwide and most of these deaths are due to metastatic breast cancer. Metastatic breast cancer is not easily treatable since it is invasive, and spreads to several organs. Targeted therapy is available for some breast cancer subtypes, based on their receptor expression and tumour stage. However, triple-negative breast cancer (TNBC), which lacks estrogen, Her2, and progesterone receptors, is aggressive and does not respond to hormone therapy. Surgery and chemotherapy are still the standard treatments for TNBC, however, they are effective only in the early stages. Therefore, one of the ways to effectively combat cancer is to understand the underlying signalling pathways that drive them so that they can be targeted for therapy. Although there is a myriad of interconnected signalling pathways that get activated in the spread of cancer, we have focused mainly on the BMP, WNT, and RHOA signalling pathways.

Four model breast cancer cell lines ZR75.1 (ER^+ PR^+ $HER2^+$), MCF7 (ER^+ PR^+ $HER2^-$), SKBR3 (ER^- PR^- $Her2^+$), and MDA-MB -231 (ER^- PR^- $HER2^-$) were used in this study. As per the cell surface marker expression, ZR75.1, MCF7 and SKBR3 are $CD24^+$ and $EpCAM^+$, while MDA-MB-231 is $CD44^+$. The three-dimensional spheroid growth represents that ZR75.1, MCF7, and MDA-MB-231 form dense, compact spheroids, whereas SKBR3 failed to form spheroids. Also, the migration analysis revealed that ZR75.1 and SKBR3 are majorly non-migratory, which may be responsible for tumour growth confined to a specific area, whereas MCF7 migrated at a rate of 2-3 µm/h and MDA-MB -231 had a migration speed of 6-8 µm/h, which correlates with their metastatic potential. The differential expression of BMP4, RHOA and β-catenin in these cell lines were analysed and accordingly, SKBR3, MCF7 and MDA-MB-231 were used for studying the BMP signalling and RHOA and Wnt signalling were analysed in detail in MCF7 and MDA-MB-231 cells.

Bone morphogenetic proteins, often known as BMPs, are proteins that control the fate of developing cells and also play a role in the progression of cancer. In this study, we explored the role of BMP4 in the proliferation of breast cancer cells, as well as its function in anoikis resistance, metastatic migration, and therapy resistance. In order to gain an understanding of the functional effect that BMP4 has on breast cancer, we used breast cancer cell lines as well as clinical samples that represent different subtypes. The involvement of the BMP pathway in breast cancer cells was further studied by utilizing the small molecule inhibitor LDN193189 hydrochloride (LDN), a BMP receptor inhibitor. Activation of BMP signalling through exogenous addition of BMP4 led to an increase in the expression of stem cell genes *CD44* and

ALDH1A3, as well as the anti-apoptotic gene *BCL2*, and boosted anoikis resistance in MDA-MB-231 cells. Additionally, LDN treatment downregulated anoikis resistance and the proliferation of anoikis-resistant breast cancer cells in an osteogenic milieu. BMP4 upregulated Notch signalling, which resulted in increased chemoresistance and accelerated self-renewal of MDA-MB-231. Conversely, BMP4 decreased anoikis resistance in MCF7 and SKBR3 cells, and downregulated proliferation, and colony-forming abilities, while LDN treatment enhanced the formation of tumour spheroids and growth. These findings suggest that BMP4 plays a context-dependent role in breast cancer cells. Furthermore, our findings with MDA-MB-231 cells, which represent triple-negative breast cancer, implying that BMP pathway inhibition may hinder the tumour's ability to colonise new sites and expand metastatically.

To better understand the signalling pathway that regulates the metastatic migration of breast cancer cells, the well-known RHO-ROCK signalling pathway associated with actin organisation was investigated. Breast cancer cells were treated with Y27632, a putative inhibitor of Rho-associated protein kinase (ROCK). Inhibition of ROCK significantly reduced 3D spheroid formation in MCF7 and SKBR3 cells but not in MDA-MB -231 cells. In MDA-MB -231, however, there was a decrease in the $CD44^{+}/24^{-}$ population, suggesting that ROCK is primarily responsible for cell proliferation. Both MDA-MB -231 and MCF7 breast cancer cells showed enhanced 2D (wound healing assay) and 3D migration (spheroid migration assay) when ROCK was inhibited. Additionally, the inhibition of ROCK resulted in a significant increase in the clonogenic potential of MCF7, while it had no impact on the proliferation of MDA-MB-231 cells. Thus, this part of the study suggests that an active RHOA pathway is required for proliferation, while downregulation of ROCK is required to promote metastasis and survival during breast cancer development.

Furthermore, both RHOA and β-catenin were silenced in order to obtain a comprehensive view of the effects of Wnt signalling on the progression of breast cancer. Multiple functional assays and gene expression analyses confirmed that silencing RHOA and β-catenin in MCF7 significantly reduced proliferation, self-renewal, migration, anoikis resistance, and shear stress tolerance. In contrast, self-renewal was inhibited in MDA-MB-231 by suppressing RHOA and β-catenin, but 3D growth and migration remained unaffected. Nevertheless, the most intriguing observation is that a higher expression of ERK under stress conditions provides a new perspective on where further research should be conducted by considering the ERK signalling in context. Doxorubicin treatment increased the ability of MDA-MB-231-shRHOA cells to form spheroids. The RHOA-silenced MDA-MB-231 cells

displayed greater tolerance to shear stress, as evidenced by a greater number of colonies, whereas β-catenin silencing significantly reduced the shear stress tolerance of MDA-MB -231.

The immunoblotting analysis further revealed that suppressing RHOA in MDA-MB-231 can upregulate β-catenin expression, indicating an increase in canonical WNT signalling. β-Catenin silencing in MDA-MB-231 decreased pERK1/2, but RHO silencing did not affect pERK1/2 levels. This finding suggests the existence of a cross-talk between the canonical and non-canonical pathways of WNT signalling in TNBCs, in which inhibition of one pathway leads to an increase in the activity of the other. The increased expression of pERK1/2 during shear stress and spheroid formation suggests that ERK signalling becomes hyper-activated when cells are subjected to stress. Gene expression analysis was performed to determine the interaction between BMP, RHOA, and WNT signalling. Concerning cross-talk, there appears to be a compensatory relationship between RHOA and β-catenin in a stage-specific manner in both cell lines. It has been observed that the Wnt/β-catenin signalling pathway modulates the BMP4 pathway, and BMP4 regulates RHOA signalling via some unknown transcription factors. Thus, there is a possibility that inhibiting Wnt signalling could serve as a potential treatment option for breast cancer. More research is needed to establish a comprehensive link between these three pathways and locate a central point at which the entire signalling cascade can be inhibited to control the progression of cancer.

Scientific Background

1.1 Cancer

Cancer is a disease characterised by the uncontrollable multiplication and dissemination of body cells (Boyce et al., 1999). Mutations in the genetic material significantly contribute to the transformation of normal cells into malignant cells (Figure 1.1) (Patel et al., 2017). If chemical substances such as heterocyclic amines (Wogan et al., 2004) and metal substances such as arsenic or cadmium (Z. Wang & Yang, 2019) cause cancer, then the substance is called a carcinogen and the process is called carcinogenesis. When cancer cells multiply and overgrow, a collection of abnormal tissue called a tumour is formed. Tumours that do not spread beyond their site of origin are called benign, while malignant tumours infiltrate surrounding organs (R. L. Siegel & Miller, 2021).

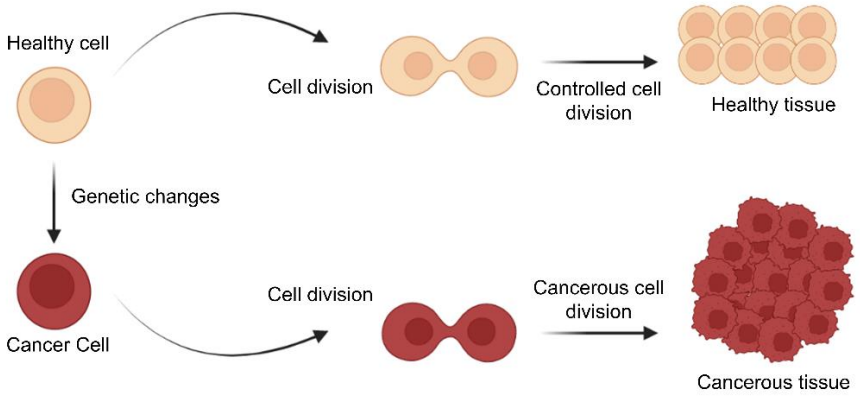

Figure 1.1: *Represents the development of normal and cancerous cells (Eldridge, 2022).*

1.1.1 Cancer types and their prevalence

The number of known cancer subtypes has risen to a hundred. The first method of classification is based on the cell type most adversely affected. The first group based on cell type affected by cancer is carcinoma, in which epithelial cells are altered to cause cancer predominately. Carcinoma is further divided into three subcategories, including Adenocarcinoma, which affects epithelial cells that produce secretions or fluids Squamous carcinoma, which affects epithelial cells that line the outside and inside of organs like the skin, stomach, lung, kidney, and bladder, and transitional carcinoma, which affects

epithelial cells that are a group of large and small cells that line the bladder, uterus, and kidney (renal pelvis) (Chhikara & Parang, 2023). Sarcoma is an additional kind of cancer that primarily affects bone, fibrous tissue (ligaments and tendons), and soft tissue (blood vessels, muscle) (Whooley et al., 2000). The third type of cancer is leukaemia, which affects blood cells. This type of cancer is characterised by a high number of abnormal blood cells that interfere with the function of healthy blood cells (*Leukemia*, 1958). Lymphoma, a type of cancer, develops when lymphocytes like B-cells and T-cells become cancerous, while multiple myeloma develops when plasma cells are affected (Cheson, 2004). Melanoma, on the other hand, affects cells that secrete melanin and pigment, and so can manifest as cancer of the skin or the eyes (Wang et al., 2023). For example, breast, lung, prostate, colon/rectal, melanoma (skin), bladder, non-Hodgkin's lymphoma, kidney (renal cell/renal pelvis), endometrial, ovarian, pancreatic, thyroid, biliary duct, and hepatic malignancies are classified based on their primary organ of manifestation.

According to the latest data, there are around 19,58,310 new cases of cancer and 6,09,820 deaths from cancer in the United States. In comparison, India has a reported incidence rate of 14,61,427 or an annual rate of 100.4 per 100,000 people. Research shows that prostate, lung, and breast cancer are the most common cancers among all other cancers (Mohamed et al., 2022). It was estimated that 1 in 13 men will be diagnosed with lung cancer at some point in their lives, while rates of colorectal cancer were 5.1 per 100,000 women and 7.2 per 100,000 men. Pancreatic cancer is the deadliest and most awful form of the disease, and it is often detected in older age groups (65-69) and at a later stage of the disease (Chhikara & Parang, 2023). According to most recent cancer statistics, prostate cancer in men and breast cancer in women lead the list of all cancers (Rebecca et al.,2023). A woman is diagnosed with breast cancer every four minutes, and a woman dies from the disease every thirteen minutes. It has surpassed lung cancer as the leading cause of global cancer incidence, accounting for 11.7% of all cancer cases with an estimated 2.3 million additional cases in 2020 (Mehrotra & Yadav, 2022). Two million individuals worldwide will be affected by breast cancer by 2030, according to epidemiological studies. 13.5% (178361) of all cancer cases and 10.6% (90408) of all fatalities in India can be attributed to breast cancer, which has a comorbidity rate of 2.81 (H. Sung et al., 2021)**.** The new cases of cancer in the all-female population are depicted in Figure 1.2.

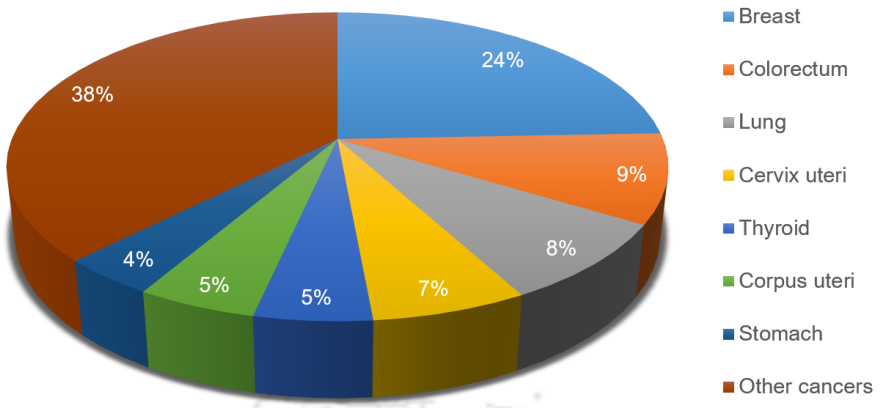

Figure 1.2: *Diagram depicting the estimated global number of new cases of female cancer across all age groups (Rebecca L Siegel et al., 2023)*

1.1.2 Development and progression of cancer

There are three main stages in the development of cancer: initiation, promotion, and progression (Vincent & Gatenby, 2008). Cancer begins with initiators that cause irreversible alterations in the genetic composition of normal cells. This process is known as "initiation." Initiators include not only genetic predisposition or a family history of genetic abnormalities, but also lifestyle choices, pesticide and virus exposures, radiation exposure, and excessive chemotherapy doses, among others (Trichopoulos et al., 1996). Once the initiators have completed their mandate, specialised or general promoters promote the proliferation; this action is known as "Promotion." Promoters cannot cause cancer unless they are exposed to a cancer-causing agent or carcinogen. Numerous promoters, including Catalytic Subunit Telomerase Reverse Transcriptase (TERT), Adenomatous Polyposis Coli (APC), Cyclin-dependent kinase inhibitor 2A (p16INK4), Human Mutl Homolog 1 (hMLH1), GATA Binding Protein 4 (GATA4), histone modification, DNA hypo- and hyper-methylation, and epigenetic modification, can function as promoters. (Derks et al., 2006; Heidenreich et al., 2014; Luczak et al., 2006). Promoters typically attach to receptors, which can be selective or non-specific, and increase cell proliferation instead of forming covalent bonds with molecules or DNA to affect internal processes. The next stage is Progression, in which cancer cells continue to develop after being exposed to promoter's multiple times. Several stages of development contribute to the progression; the first stage, hyperplasia, occurs when cells divide repeatedly but manifest normally; the second stage, dysplasia, occurs when both the cells and tissue created by these cells appear

aberrant. The third position is Carcinoma in situ refers to the growth of malignant cells at the site of origin. The fourth phase is in which cells depart their initial location, enter blood arteries or lymph vessels through intravasation, and travel to distant sites via circulation. This fourth stage of cancer allows abnormal cells to exit the artery and colonise a new location (X. Liu et al., 2017; Thiberville et al., 1995; J. Zhou et al., 2003). The chronology of metastatic cancer is displayed in Figure 1.3.

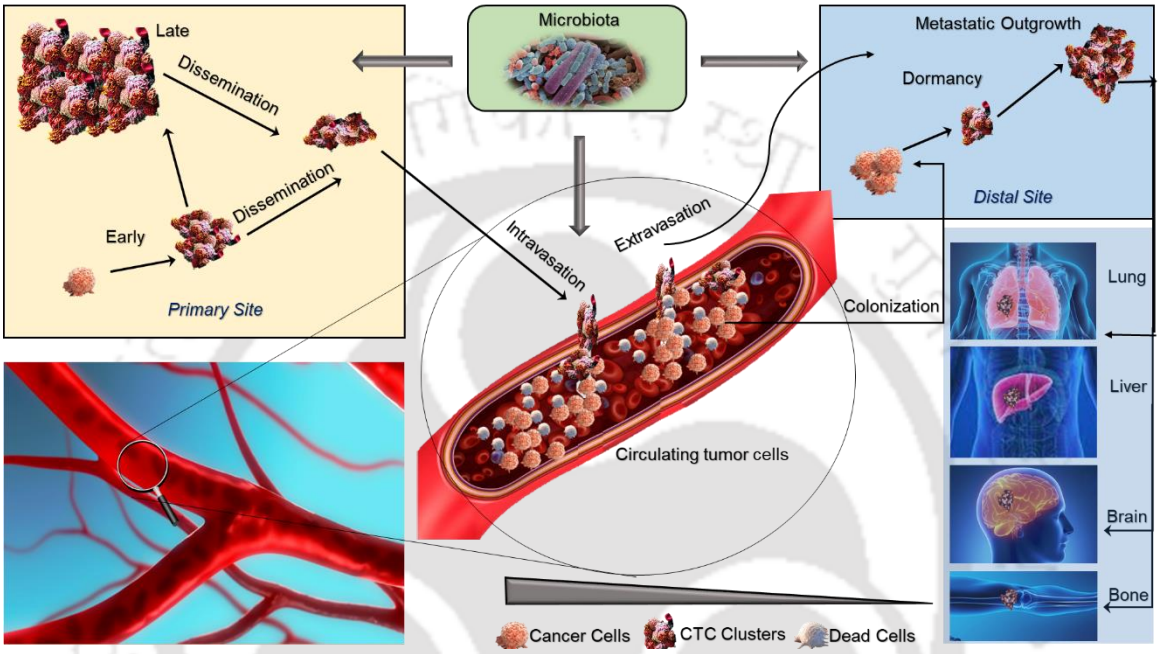

Figure 1.3: Development and progression of cancer. *The diagram illustrates the development of malignant cells at the primary site and their subsequent acquisition of mesenchymal characteristics after detachment. When malignant cells detach from their primary site and infiltrate a blood vessel, intravasation occurs. After overcoming fluid pressure and immune response, cancer stem cells extravasate from the blood vessel to colonise a new site. The new site could be the lung, the bone, the brain, or the liver (Fu et al., 2022).*

1.1.3 Significance of signalling pathways in cancer

The involvement of signalling pathways in cancer initiation and progression is crucial. Mutations in the master regulators of cell division and proliferation are responsible for the unchecked development and division of cancer cells. The signalling pathways that promote cell growth, survival, and migration are commonly activated by these alterations. The following examples highlight the significance of the signalling pathway in the emergence of cancer. The RAS-RAF-MEK-ERK signalling pathway is well-known for its role in cancer progression (Devetzi et al., 2016). Many different forms of cancer are associated with activating mutations in the RAS genes. The PI3K-AKT-mTOR pathway is another crucial signalling mechanism in the development and spread of cancer (Coutte et al., 2012).

This route promotes cell survival and development by suppressing programmed cell death (apoptosis) and fostering cell cycle advancement, and it is frequently active in cancer. It has long been understood that the Hedgehog and Wnt signalling pathways control the patterning and growth of embryos, but recently many studies have linked these pathways to the development of cancer (Anastas & Moon, 2013; Taipale & Beachy, 2001). Induced hepatocyte growth factor Met tyrosine kinase (HGF-Met) can also play a role in the progression of malignancy, which is typically governed by paracrine agonists supply (Cecchi et al., 2010). It is also known that the signalling system linked to vitamin D deficiency also causes cancer by promoting proliferation and suppressing apoptosis (Deeb et al., 2007). Numerous other cancers, including those of the colon, brain, lung, ovary, and prostate, are also caused by Notch signalling dysfunction (Venkatesh et al., 2018). The mevalonate route, which is often used to synthesise steroids, may interact with the aforementioned pathway and contribute to the development of cancer (Mullen et al., 2016). Not only do individual pathways contribute to carcinogenesis, but also their interactions. Crosstalk between Wnt/β-catenin and E-cadherin promotes cancer progression by enhancing epithelial-mesenchymal transition (EMT) (Ghahhari & Babashah, 2015). In conjunction with an inflammatory response, NF-kB signalling can also induce prostate cancer (Nguyen et al., 2014). VEGF signalling in conjunction with Akt/mTOR can also exacerbate ovarian cancer (Trinh et al., 2009). Disrupted Hippo signalling promotes cancer development, both independently and in concert with Wnt (Li et al., 2019) and long non-coding RNA (LncRNA) (Tu et al., 2020). In colorectal cancer, an epithelial-mesenchymal transition is induced by cross-talk between Notch and BMP signalling, and this synergistic interaction contributes to the disease's poor prognosis (Irshad et al., 2017). Several other cross-talks, including those between TGF-β and Integrin, which aids in wound healing (Margadant & Sonnenberg, 2010), PI3K/AKT/mTOR and miRNA, which contribute to cancer (Akbarzadeh et al., 2021), Integrin and E-cadherin, which increase metastasis and invasion (Canel et al., 2013), Ras-Rho, which promotes migration and self-renewal (Sahai et al., 2001), and PI3K/AKT with Circular RNAs (circRNAs), which contribute to cancer progression (Xue et al., 2021). The preceding examples illustrate the significance of understanding cancer signalling pathways and identifying therapeutic targets to treat the disease.

Given the substantial prevalence rate and the current constraints on therapeutic approaches to curing breast cancer, we must investigate signalling mechanisms as early as feasible in

the disease's progression**.** My research is primarily concerned with the development and spread of breast cancer. Cancer progression and normal development are strikingly comparable at the molecular level. Normal human growth is carefully regulated by intricate signalling pathways that allow cells to communicate with each other and their environment. It should not be shocking that Cancer Stem Cells (CSCs) and cancer cells have altered or hijacked several of these interconnected signalling pathways (Barbieri & Kouzarides, 2020). Cancer is essentially caused by genetic and epigenetic changes that allow cells to evade the mechanisms that normally control their migration, survival, and proliferation. Many of these changes are related to signalling systems that regulate cell motility, differentiation, proliferation, and death. Due to mutations that activate proto-oncogenes, certain signalling pathways may become overly active. However, when tumour suppressors are inactivated, the same signalling pathways become significantly less active (Feng et al., 2018). Breast cancer is known to be influenced by several well-known signalling pathways, including Notch, Hedgehog, ER, Her2, TGF-β, PI3K/mTOR, BMP, Rho-ROCK, Wnt and so on (Ghosh et al., 2019). The propensity of breast cancer cells to spread into the bone environment is facilitated by a gene associated with bone. Since BMP is the primary signal that regulates the bone microenvironment, studying BMP signalling in breast cancer could shed light on cancer's function in the bone microenvironment both before and after cancer cells have entered the bone. Subsequently, Wnt is believed to play a role in virtually every developmental stage and also plays a significant role in the bone microenvironment, investigating this pathway may provide a fantastic opportunity to combat cancer. For a comprehensive comprehension of cancer, the Rho-ROCK signalling pathway was further explored, as it is the most important signalling pathway for understanding the complete migration process. Therefore, we focused on understanding how BMP, Rho-ROCK, and Wnt signals contribute to the development of breast cancer.

1.2 Breast cancer

Breast cancer is defined as cancer that has grown in the breast tissue (Yerushalmi et al., 2009). The breast is a glandular organ consisting of fat, connective tissue and breast tissue that can make glands for milk synthesis (Jesinger, 2014). When breast tissue cells mutate, they can become malignant and spread to other organs, much like any other type of cancer. Although breast cancer is more common in women, men have also been diagnosed with the disease (Sharma et al., 2010). While most cases of breast cancer are diagnosed in women over the age of 50, the disease can affect people of any age. Breast cancer can

begin in either the milk ducts or the lobules, and when it becomes aggressive, it is classified as either ductal invasive or lobular invasive (Figure 1.4) (Burstein et al., 2004; Foote Jr & Stewart, 1941). Angiosarcoma is cancer that begins in a blood artery or lymph vessel of the breast (Vorburger et al., 2005); phyllodes tumour is cancer that begins in the connective tissue of the breast and may or may not spread to other parts of the body (Tse et al., 2010).

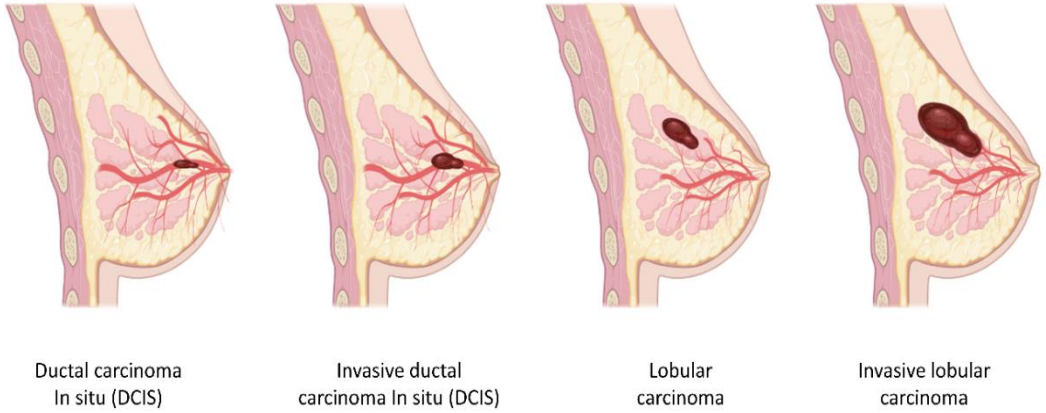

Figure 1.4: *The illustration depicts a ductal and lobular carcinoma.(Burstein et al., 2004; Foote Jr & Stewart, 1941)*

1.2.1 Breast cancer classification

Breast cancer can be categorized in several ways. Based on histopathology; lobular carcinoma, (begins in the milk-producing lobe) and ductal carcinoma (begins in the milk duct) (Malhotra et al., 2010). Invasive and ductal carcinoma may also be inflammatory and invasive (Costa et al., 2018). The other way of classification is based on the molecular signatures; luminales (luminal A and B), Her2 (luminal and enriched) and triple-negative (basal-like and non-basal-like) (Figure 1.5). Luminal A and B of the luminales group are ER^+, PR^+, and $Her2^-$, whereas the luminal and enriched group of Her2 categories are ER^+, PR^+, $Her2^+$, and ER^-, PR^-, $Her2^+$, respectively. Triple-negative tumours are ER^-, PR^-, and $Her2^-$ negative; however, their cytokeratin (CK) expression is different (Trop et al., 2014). $Her2^+$ cells are cytokeratin negative, whereas luminal A and B are positive. Basal-like cells are CK5/6/8/14/18 positive. Ki67 expression distinguishes between luminal A and B; the former has less than 14% and the latter has more than 14%. $Her2^+$ and basal-like cells exhibit Ki67-like luminal B cells (Sinn & Kreipe, 2013). While luminales fall under I and II-grade malignancy, $Her2^+$ and triple-negative breast cancers are often III-grade cancers.

Some other types of breast cancer are inflammatory (inflammation in the breast tissue) (Jaiyesimi et al., 1992), Paget's disease (eczema in the nipple and areola area) (Ashikari et al.,1970), mucinous (secretion of mucin in the breast tissue) (Marrazzo et al., 2020), and medullary (cancer in the inner lining of the breast) (Malyuchik & Kiyamova, 2008) and account for 2-3% of all breast cancers.

Characteristics	**Subtypes**				
	Luminal A	Luminal B HER2-	Luminal HER2+	HER2+ enriched	Triple negative
Hormonal receptor	ER+, PR+, HER2-	ER+, PR+, HER2-	ER+, PR+, HER2+	ER-, PR-, HER2+	ER-, PR-, HER2-
Ki67 Index	Low	High	High	High	High
Prognosis	Good	Intermediate	Intermediate	Intermediate	Poor
Therapy	Endocrine	Endocrine and chemo	Endocrine And targeted	Endocrine And targeted	Chemo
Prevalence	60-70%	10-20%	13-15%		10-15%

Figure 1.5: Breast cancer classification*: Illustrations of subtypes of breast cancer based on molecular characteristics, prognosis, and treatment options for each subtype of the disease. (Boix-Montesinos et al., 2021)*

1.2.2 Factors contributing to breast cancer

The leading cause of breast cancer is genetic and epigenetic alterations (D. B. Thomas, 1984). The most well-known examples are Breast Cancer Gene 1 (*BRCA1)* and Breast Cancer Gene 2 (*BRCA2)*. A female harbouring this is 85 % more likely to develop breast cancer. In addition to ataxia telangiectasia heterozygotes, oestrogen-receptor polymorphisms and *p53* are also cancer-causing genetic factors (Hulka & Stark, 1995). Some hormones generated by the adrenal cortex, such as androstenedione, are metabolised in the adipose cells of obese women to produce oestrogen is also responsible for cancer (Colditz, 1998). Omega-6 polyunsaturated fatty acids and heterocyclic amines in food increase the risk of developing cancer (Makarem et al., 2013). Lifestyle factors such as lack of exercise, excessive alcohol consumption, and tobacco use are also risk factors (Hashemi et al., 2014). Cancer is also caused by exposure to chlorinated pesticides, electromagnetic radiation, and ionising radiation. Preservatives, deodorants, and antiperspirants used on the

underarms contain some compounds that have been related to an elevated risk of breast cancer (Darbre, 2001).

1.2.3 Early signs and diagnoses of breast cancer

At first, patients with breast cancer may only encounter a few of the disease's common symptoms and indications. The presence of these symptoms is not usually indicative of breast cancer. The major indicators and symptoms of breast cancer can vary from individual to individual. Breast or armpit enlargement or lump in the breast, physiological changes and redness, breast flesh with dimples or puckers, inversion (turning in) or a discharge from the nipples (Parthasarathy & Rathnam, 2012), experiencing discomfort, and skin abnormalities, such as scaling or peeling, are some of the symptoms of breast cancer (Sambanje & Mafuvadze, 2012) (Figure 1.6). Self-examination of the breast is crucial for preventing life-threatening malignancy (S. A. Rahman et al., 2019). To find any anomalies or changes in the breast tissue, a biopsy is frequently used in conjunction with imaging studies to diagnose breast cancer.

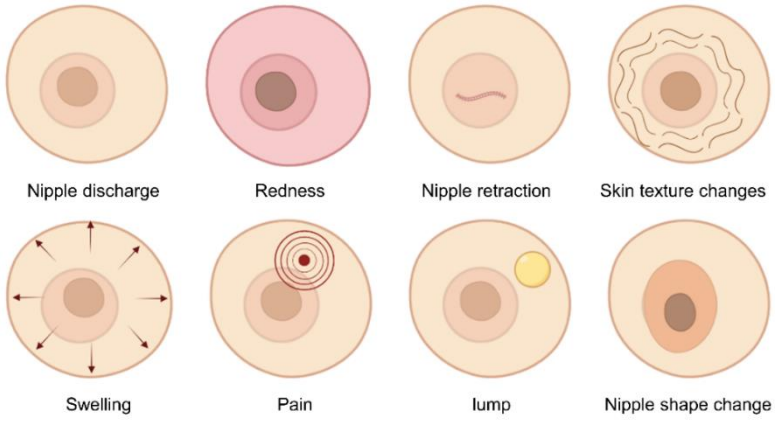

Figure 1.6: *The image highlights several early breast cancer symptoms (Sumbaly et al., 2014).*

A biopsy is carried out to remove a sample of tissue for additional investigation if a questionable area is discovered. A surgical biopsy removes the entire alarming area along with some nearby tissue, whereas a needle biopsy only takes a sample of the problematic tissue. The abnormal growth of malignant cells in the breast was imaged via mammography, which involved the use of X-ray technology (Sickles, 1984).

The lump in the breast was located using a technique known as ultrasonography or ultrasound, which involved the use of sound waves (Lulu Wang, 2017). Positron emission tomography (PET) is a method of diagnosis in which patients were given an injection of a particular kind of dye, and then images were acquired using a scanner. Positron emission tomography is an acronym for "some special kind of dye" (Flanagan et al., 1998; Mintun et al., 1988) MRI, or magnetic resonance imaging, serves as another technique that can be performed (Roganovic et al., 2015). With this procedure, magnetic fields and radio waves are combined to obtain an enhanced and clear picture of each region of the breast (Hylton, 2005).

1.2.4 Breast cancer staging and grades

The term "stage" refers to how far cancer has spread and how advanced it is. The abnormalities of cancer cells can be assessed by viewing them under a microscope. Staging breast cancer can be done in several ways. As a method of object classification, the TNM system has become very important in recent years (Benson, 2003). The TNM staging system is an abbreviation for tumour, node, and metastasis, where T stands for the size of the tumour, N for the malignancy in the lymph nodes, and M for the spread of cancer beyond the lymph nodes (Cserni et al., 2018) (J. Koh & Kim, 2019). Depending on the size and location of the tumour, breast cancer can be classified into one of five stages. The proliferation of cancer cells begins in stage 0 within a certain area. In stage 1, the tumour is up to 2 cm in size and stage 2 the size increase from 2-5 cm in size but has not yet affected surrounding tissue; in stage 3, it is up to 5 cm in size and has begun to damage nearby lymph nodes; and in stage 4, it has already spread to other parts of the body. Depending on which organs the cancer has metastasised to, patients may experience a variety of symptoms (Lobbezoo et al., 2015). While any organ may be affected, the brain, liver, bone, and lung are most vulnerable to metastasis from breast cancer. In contrast, microscopic analysis of the grades revealed subtle differences between healthy and malignant cells. There are four standard scaling categories. In oncology, Grade 1 is used to classify cancer cells and tissue that closely resemble healthy cells and tissue. Well-differentiated tumours within this grade are called low grade. In Grade 2, cancer cells and tissue show noticeable abnormalities and are classified as moderately differentiated, making them intermediate-grade tumours. In Grade 3, cancer cells lose their structural organization and pattern, becoming poorly differentiated and highly abnormal. This tumour is occasionally called a high-grade tumour. Grade 4 represents the highest level of tumour malignancy, marked by

fast growth and spread to other parts of the body. The cells observed are cancer cells that are undifferentiated and have different physical features compared to healthy cells. In contrast, microscopic analysis of the grades revealed subtle differences between healthy and malignant cells. There are four standard scaling categories. In oncology, Grade 1 is used to classify cancer cells and tissue that closely resemble healthy cells and tissue. Well-differentiated tumours within this grade are called low grade. In Grade 2, cancer cells and tissue show noticeable abnormalities and are classified as moderately differentiated, making them intermediate-grade tumours. In Grade 3, cancer cells lose their structural organisation and pattern, becoming poorly differentiated and highly abnormal. This tumour is occasionally called a high-grade tumour. Grade 4 represents the highest level of tumour malignancy, marked by fast growth and spread to other parts of the body. The cells observed are undifferentiated cancer cells and have different physical features compared to healthy cells. (Telloni, 2017).

1.2.5 Breast cancer metastasis to bone

The organ-specific translocation property of cancer cells from the site of origin to the distant site lies in the cancer cell itself and can be referred to as a preselected seed (Lu & Kang, 2007). The niche or environment present around the site of origin or within the cancer cells is also responsible for metastasis to a distant site and may be referred to as the pre-metastatic niche (Chu & Allan, 2012). The first step in the spread of metastases is an EMT of localized cancer cells. EMT gives cancer cells a shape that allows them to enter the lumen of blood vessels (Buyuk et al., 2022).

Cells moving through blood vessels must cope with stresses such as shear forces, the immune system, and matrix detachment before reaching their destination. To get around this, cancer cells attach to platelets and form emboli. Only a few cancer cells can invade the blood vessels of an organ and develop (Caswell-Jin et al., 2018). When a tumour grows large enough, it exerts pressure on blood vessels, causing them to rupture and that is how cancer spreads (Gunasinghe et al., 2012). By reversing the EMT, the cancer cells combine with the stromal cells and begin to colonize. Soon after, the malignant cells secrete parathyroid hormone, which activates osteoclasts. Breast cancer cells contain bone-related genes (BRGs) such as Forkhead Box Protein F2 (*FOXF2)* that help them mimic osteocytes when they metastasize and colonize in bone (Wang et al.,2019). Osteoclastic cells demineralize bone through an osteolytic activity that releases various substances, including

calcium, Fibroblast Growth Factors (FGFs), Insulin Growth Factors (IGFs), Bone Morphogenetic Proteins (BMPs), and Transforming Growth Factor-β (TGF-β). These secreted substances promote the proliferation of breast cancer cells, which leads to the release of more parathyroid hormone, a kind of positive feedback for osteolytic activity (Lu & Kang, 2007) shown in Figure 1.7. Some signalling pathways, such as Wnt, BMP, and IGF, were found to be present in both the bone microenvironment and mammary cells and to facilitate bone metastasis. CapG, a macrophage-covering protein discovered using genomics and proteomics, is a biomarker that can predict the extent of bone metastasis based on its presence in breast cancer cells (Boyce et al., 1999).

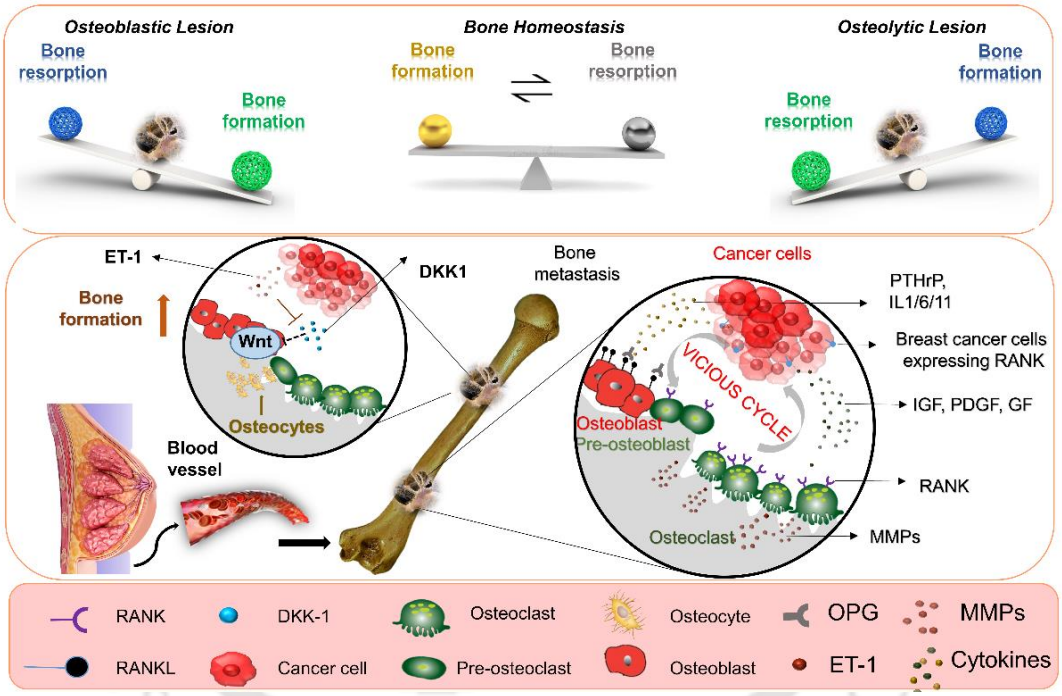

***Figure 1.7: Breast cancer metastasis to bone**. After acquiring the EMT property, cancer cells in the primary site enter blood vessels via intravasation and translocate to the bone site via extravasation. Once these cancer cells reach the bone, a vicious cycle begins that can disrupt the homeostasis of the bone. Depending on the secretion factors, breast cancer cells in the bone microenvironment can activate either osteolytic or osteoblastic activity. pTHrP (parathyroid hormone-related peptide), interleukin1/6/11, PGE2 (prostaglandin E2), TNF (tumour necrosis factor), M-CSF (macrophage colony-stimulating factor), RANKL (secreted by breast cancer cells) and RNAKL (secreted by osteoblast) bind to the RANK receptor and activate osteoclastogenic activity by increasing osteoclast differentiation. The osteoclastogenic activity increases HCl (hydrochloric acid), IGF-1 (insulin-growth factor 1), FGF (fibroblast growth factor), PDGF (platelet-derived growth factor) and MMPs (Matrix metalloproteinase) promotes the degradation of the collagen matrix as well as the proliferation of cancer cells. During the osteoblastic activity, breast cancer cells increase ET1 (endothelin 1) secretion, which inhibits DKK-1 expression. Reduced Dickkopf 1 (DKK-1) levels enhance Wnt signalling, leading to more bone production* (Venetis et al., 2021).

1.3 Signalling pathways involved in breast cancer progression

1.3.1 ER signalling and ER-Positive breast cancer

ER, signalling, in which each ER receptor consists of two parts - a membrane receptor and a nuclear receptor. In general, the membrane receptors consist of G-coupled proteins, whereas the nuclear receptors (ERα and ERβ) are transcription factors that become active when they bind to the correct ligand (Saha Roy & Vadlamudi, 2012). The binding of an estrogen ligand promotes the dimerization of ERα and ERβ, and this active dimer form causes conformational changes in the DNA-binding domain (Song & Santen, 2006). These changes affect downstream genes such as *CCND1, HIF1α*, and *IL6* (De et al., 2016) and also the formation of toxic metabolites that damage DNA leading to the progression of cancer. Inhibition of Nuclear Factor Erythroid 2 Related Factor (NRF2), a protein activated in response to oxidative stress (Xie et al., 2023), and Ubiquitin Specific Peptidase 8 (USP8) increase endocrine resistance (Zheng et al., 2023) may reduce the ER regulated breast cancer.

1.3.2 Her2 signalling and Her2 Positive breast cancer

A family of tyrosine kinase receptors known as human epidermal growth factor receptors (EGFRs or HERs) is expressed in healthy tissues as well as in various cancers. Human epidermal growth factor receptor-2, also known as Her2/NEU or c-ERBB2, is an EGFR. Similar to the other receptor tyrosine kinases, Her2 has an intracellular domain, a transmembrane domain, and an extracellular ligand-binding domain (Dean et al.,2008). The constitutively active version makes Her2 the preferred component for forming dimers with molecules other than Her1/3/4 and offers Her2 the potential to influence numerous cellular activities through multiple pathways. Several downstream signalling pathways, including mitogen-activated protein kinase (MAPK) and phosphatidylinositol 4,5-bisphosphate 3-kinase (PI3K), are activated by ligand binding (Weigelt et al.,2010). Breast tumour development is closely related to these signalling pathways, as they directly affect cell cycle progression and cancer cell survival (Yarden, 2001) (Iqbal & Iqbal, 2014).

1.3.3 Notch signalling

The Notch signalling pathway is thought to play a role in the development of breast cancer, making it a potential new treatment target. The Notch signalling pathway consists of five Notch ligands, which are single transmembrane proteins called Delta-like (DLL) 1, 3, 4

and Jagged (JAG) 1, 2. The binding of a Notch ligand from one cell to the extracellular domain of a Notch receptor from another cell is a prerequisite for the activation of one of the four Notch receptors, all of which function through the same basic signalling pathway. A series of important proteolytic cleavages of the Notch ligand-receptor complex gives rise to the extracellular Notch domain and the intracellular Notch domain (NICD). In one study, primary human breast cancer was found to have high expression of *Jag1* and/or *Notch1* genes in tumours, which is associated with poor prognosis (Reedijk et al., 2005). Mammosphere self-renewal was prevented by blocking Notch 4 or inhibiting the enzyme γ-secretase, and disruption of Notch signalling significantly reduced the efficiency of mammosphere development of Ductal Carcinoma In Situ (DCIS) (Politi et al.,2004). Notch 3 and Jag1 are critical regulators of cancer stem cell renewal and survival under hypoxia in primary breast cancer and tumour spheres derived from breast cancer cell lines (Feng et al., 2018). Notch3 can also inhibit breast cancer migration by upregulating Glycogen Synthase Kinase 3 β (GSK3β) (W. Chen et al., 2022). The Her2 signalling system, active in approximately 20% of breast tumours and associated with more aggressive diseases, interacts with the Notch signalling system. It has been discovered that dysregulation of the Notch signalling pathway in conjunction with the Wnt signalling pathway causes breast cancer metastasis (Sethi et al., 2011). Ezrin, a protein that links actin and plasma membrane, regulates breast cancer via Notch signalling in a Hes1-dependent manner (M. Chen et al., 2022). Patients resistant to tamoxifen showed upregulation of Hes1, Notch4, and nicastrin, another role of Notch signalling (Boustan et al., 2023).

1.3.4 Sonic Hedgehog (SHH) signalling

SHH signal transduction is required for the proper organization of cell proliferation and differentiation during embryonic tissue patterning, which is critical for the formation of the mouse mammary gland. When the Shh ligand is bound, the inhibitory action of Patched Homolog-1 or PTCH1 on Smoothened (SMO) is reduced, and SMO activation enhances Glioma-Associated Oncogene 1 (GLI1) translocation (Lee et al.,2017). Another research has shown that inhibiting GLI using GANT61 and knocking out SHH can significantly inhibit cancer progression and migration (Riaz et al., 2019). Disruption of PTCH1 and GLI-2, resulted in severe defects in ductal development (Edward et al., 2021). Cordycepin, a derivative of adenosine, demonstrated inhibitory effects on the growth and metastasis of triple-negative breast cancer (MDA-MB-231) in nude mice through the down-regulation of SHH, PTCH-1, GLI-1, and SMO expression (Wu et al., 2022)

1.3.5 PI3K/AKT/mTOR signalling

Oncogenic PI3K mutations (PIK3CA) are common in human breast cancer and can lead to dedifferentiation of luminal or basal mammary progenitor cells, giving them multilineage potential. Resistance to endocrine therapies may be caused by hyperactivation of AKT and consequently mTOR. Consequently, the level of phosphorylated S6 kinase (S6K), a downstream regulator of mTOR activation, may predict overall survival in patients with hormone receptor-positive breast cancer after adjuvant endocrine treatment (Paplomata & O'Regan, 2014). The ureido group of 5-ureidobenzofuranone can mimic the hydroxyl group in PI3K and mTOR, thus a reduction in PI3K and mTOR signalling was observed when added to cells, as confirmed by the reduction in S6, PaktS473, and pAKTT308 expression levels (Hussain et al., 2022).

1.3.6 Hippo signalling

The Hippo signalling pathway is one of the signalling mechanisms that can cause breast cancer to spread to other parts of the body. Large Tumour Suppressor Kinases ½ (LATS1/2), Mammalian Sterile-Twenty-like (MST1/2), MAP kinase kinase kinase kinases (MAP4Ks) and Yes-Associated Protein/transcriptional coactivator with PDZ-binding motif (YAP/TAZ) are the essential components of the Hippo signalling pathway (M. Fu et al., 2022). In malignant cells, activation of YAP /TAZ by methylation of MST1 at lysine position 59 is responsible for the upregulation of bone metastasis. Oxygen deficiency in the bone microenvironment is one of the factors contributing to tumour development. By regulating EMT, hypoxic inducible factor-1 acts as a promoter of breast cancer metastasis. This is achieved by binding to TAZ. In addition to binding to TAZ, the transcription factor STAT5 is also responsible for regulating metastasis (Wei et al.,2018). Deletion of ring finger protein 3 (RFN3) improved the proliferation and migration of MDA-MB-231 and also increase the relapse issue in patients (H. Yang et al., 2022). Similarly, Transducins repeat-containing protein (β-TrCP) has been shown to bind to YAP/TAZ and promote its degradation at low concentrations of ubiquitin E3 ligase (HERC3), whereas at high concentrations of HERC3, β-TrCP fails and promotes translocation of YAP/TAZ to the nucleus, promoting tumour progression (Yuan et al., 2023). This indicates that activating the hippo pathway can be a potential target to treat breast cancer as studied by (Xiang et al., 2022) where Paris saponin VII (steroid) was used to induce autophagy.

1.3.7 TGF-β signalling

TGF-β signalling is another mechanism by which TGF-β ligands bind to a heterodimeric complex and activate the Smad-dependent and Smad-independent pathways. The Smad-independent pathway activates p38 MAPK and c-jun NH2 kinase, which control bone growth and development. However, in a malignant state, TGF-β control is easily bypassed, and by upregulating EMT, it promotes metastasis. By activating Smad2/3/4, Smad-dependent pathways transmit their signal and thus control metastasis. It was discovered that inhibition of Smad 4 reduces bone metastasis (Drabsch & Ten Dijke, 2011). Recent studies have shown how TGF-β signalling is essential for breast cancer progression. TGF-β signalling is high in the presence of RNF2 because RNF2 degrades Inhibitory Smad (SMAD7), leading to breast cancer progression in both basal and luminal cancer. Further studies have shown that ring finger protein 2 is tightly regulated by phosphorylated Smad2 and Akt (Y. Huang et al., 2022). A mutation in O-GlcNAc transferase, the enzyme responsible for Microrchidia Family CW-Type Zinc Finger 2 (MORC2) activity, can lead to TGF-β mediated breast cancer progression. It was later found that glutamine-fructose-6-phosphate aminotransferase, which is regulated by TGF-β signalling, can also activate MORC2 function (Y. Liu et al., 2022). HTR1A (5-hydroxytryptamine receptor 1A) reacts with Tripartite Motif Containing-21 (TRIM 21) and PSMD7 to inhibit TGF-β signalling and thus the progression of triple-negative breast cancer, (Q. Liu et al., 2022) whereas TMEM I56 promotes breast cancer metastasis by upregulating TGF-β related EMT (Tong, et al., 2022). Some other protein like Ovo-Like Transcriptional Repressor 1 (OVOL1) shows an inverse relationship with EMT (Fan et al., 2022), reduced TGF-β signalling by degrading SMAD7 a positive modulator of TGF type I receptor. In the TGF-β family of cytokines, BMP has received the most attention because it jointly regulates cell fate determination and disruption of TGF-β/BMP can lead to various diseases such as autoimmune, skeletal and cardiac problems (Rahman et al.,2015).

In addition to the overhead mentioned pathways, the BMP, RHO-ROCK, and Wnt signalling pathways are discussed in detail from a research perspective to comprehend the significance of these three pathways in the progression, migration, metastasis, and chemoresistance of breast cancer.

1.4 BMP signalling

Marshall Urist discovered Bone Morphogenetic Protein, which promotes bone growth in muscle. Recombinant BMPs are effective in the treatment of bone and kidney diseases, while genetically engineered BMPs show promise for regenerative medicine and tissue engineering (Leung et al., 2023; Obradovic Wagner et al., 2010). Bone morphogenetic proteins are dimeric complexes synthesized in the cytoplasm of cells by the action of convertase on proprotein complexes already present in the cytoplasm, with the C-terminal mature peptide, N-terminal signal peptide, and prodomain having a regulatory function. In mammals, there are at least 15 different BMP molecules, each with multiple, sometimes redundant, functions (autocrine, paracrine, and endocrine). Bone shortening, also known as brachydactyly type A2, has been associated with bone morphogenetic protein receptor 1B (BMPR1B) deficiency. Myhre syndrome is characterized by short stature and facial dysmorphism due to a dysfunction of the Smad4 gene. Mutations in the BMPR1 receptor cause progressive fibro-dysplasia ossificans progressiva (FOP), a disease of the skeleton (S. Thomas & Jaganathan, 2022).

BMP utilizes both canonical and non-canonical signal transduction pathways (Nickel & Mueller, 2019). BMP molecules bind to a heterotetrameric complex consisting of dimeric S/T kinase receptors of types I and II (Brazil et al.,2015). There are seven different types of type I receptors and five different types of type II receptors (Nickel & Mueller, 2019; Yadin et al., 2016). Three receptors of each of these types bind to BMP-associated signals, including BMPR-IA, BMPR-IB, ActR- IA, BMPR-2, ActR-2A, and ActR-2B (Katagiri, et al., 2021). According to the study, BMP2 and BMP4 recruit type II while binding to type I, but BMP6 and BMP7 recruit type I while binding to type II (de Vinuesa et al., 2016; Gipson et al., 2020). The active heterotetrameric complex phosphorylates R-Smads (receptor-regulated Smads), which then interact with Co-Smad (co-mediator Smad). In the framework of BMP signalling, Smads 1–5 are R-Smads, Smad 4 is the Co-Smad, and Smads 6 and 7 are inhibitory Smads or I-Smads that prevent signal transduction from occurring (Christian, 2021). It has been shown that the extracellular environment and the influence of other signalling pathways can occasionally cause some BMP molecules to

activate non-canonical signalling pathways, such as PI3K/Akt, RHO-GTPase, and TGF-Beta-Activated Kinase-1 (TAK-1) (R. N. Wang et al., 2014) (Figure 1.8)

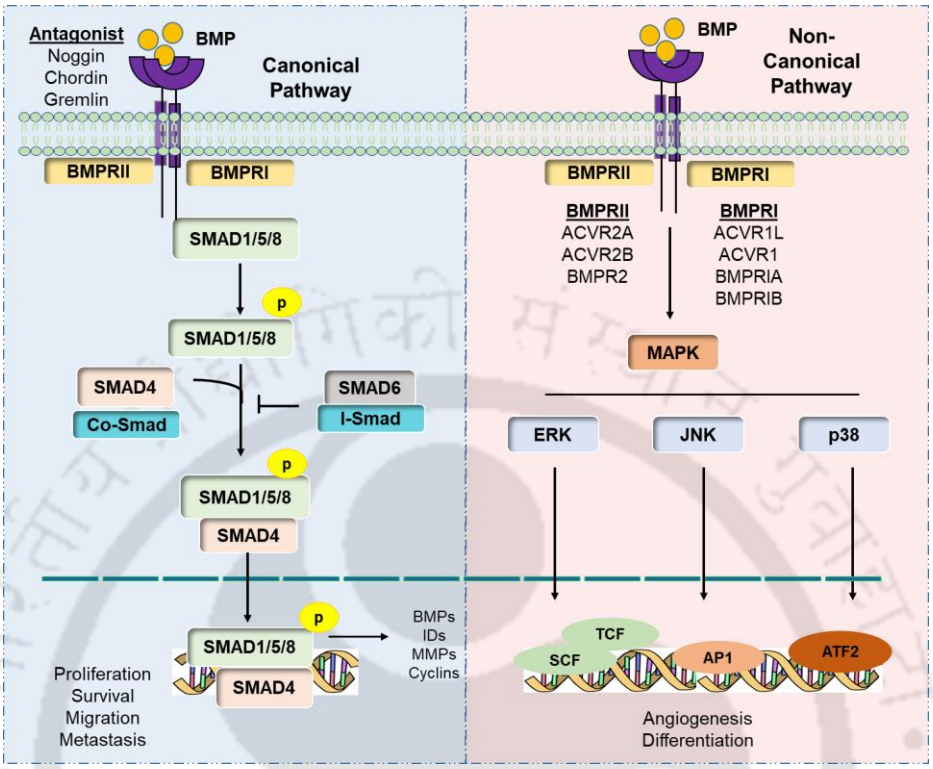

***Figure 1.8: BMP signalling pathway**. The image depicts the canonical and non-canonical BMP signalling pathways. When ligands of the BMP family bind, they phosphorylate the BMP receptors, activating both canonical and non-canonical signalling pathways. Smad1/5/8 and Smad4 collaborate to regulate canonical signalling, while the PI3K-JNK-ERK protein controls non-canonical signalling (Gomez-Puerto et al.,2019; Guyot & Maguer-Satta, 2019).*

Bone morphogenetic proteins (BMPs) serve crucial roles in the regulating of cell proliferation. The TGF-β (transforming growth factor beta) superfamily of proteins is involved in numerous biological processes, including cell proliferation, differentiation, and death. BMPs can induce cell cycle arrest, which allows cells to repair DNA damage or undergo differentiation. By increasing the expression of cyclin-dependent kinase inhibitors, BMP-2 has been demonstrated to induce cell cycle arrest in prostate cancer cells (Brubaker et al.,2004). Additionally, BMPs can increase cell proliferation, which is essential for tissue repair and regeneration. For instance, BMP-2 has been proven to stimulate the proliferation of osteoblasts (Chatakun et al., 2014), which are the cells responsible for the formation of bone structure. BMPs can affect the activity of other growth factors, such as the insulin-like growth factor (IGF) pathway, which regulates cell proliferation. It has been demonstrated that BMP-7 inhibits IGF signalling in breast cancer cells (Otsuka, 2010),

resulting in decreased cell proliferation. In certain circumstances, BMPs can have tumour-promoting actions, which can result in enhanced cell proliferation. For example, BMP-2 promotes the growth of pancreatic cancer cells by increasing cell proliferation and angiogenesis. Overall, BMPs play significant roles in the regulation of cell proliferation, with context-dependent effects.

1.4.1 BMPs in neuronal and muscular development

The signalling pathway known as BMP is of utmost importance in maintaining a delicate equilibrium between the proliferation and differentiation of muscle satellite cell progeny. In the initial stages, BMP signals elicit an upregulation in the quantity of primary satellite cells through the regulation of their proliferation. Following the process of cellular differentiation, there is an upregulation in the production of Chordin, which acts as an inhibitor for Bone Morphogenetic Protein (BMP). The presence of this negative feedback loop halts the process of cellular differentiation and facilitates the formation of myotubes. (Friedrichs et al., 2011). In conjunction with Notch signalling, BMP signalling exerts tight control on neuronal induction, specification, and differentiation (Shih et al., 2023). Research shows that a chemical inhibitor of BMP signalling, Dorsomorphin homolog 1 (DMH1), upregulates Her2 expression, a downstream target of Notch signalling, resulting in a decrease in the number of neuronal precursors; however, it is noteworthy that treatment of Her2 knock-out cells with DMH1 restores the decreased neuronal precursor, indicating the tight control of BMP-Notch signalling in neuronal proliferation, specification, and differentiation. In a separate investigation, supplying hypoxia-induced vascular smooth muscle cells with rhBMP2 boosted their proliferation by upregulating CD44, MMP2, and actin aggregation. Immune hybridization research revealed that CD44 has a direct relationship with vinculin aggregation, just like CD44 and MMP2, increasing migration(M. Yang et al., 2018).

1.4.2 BMPs in medical implants

In recent years, there has been a boom in interest in biomaterials that transport BMP-2 to damaged bone locations to enhance bone regeneration (Huang et al., 2020). Biodegradable polylactic acid (PLA) finds application in tissue engineering and medical devices. Cultivating MSCs on PLA material coated with bioactive compounds derived from mussels and BMP-2 promotes the development of MSCs, their specialisation, and mineral deposition. It has been discovered that bioactive compounds extracted from mussels

facilitate the attachment of MSCs to surfaces that are coated with BMP-2 and PLA. As a result, osteogenesis, the formation of new bone tissue, is stimulated (Chen et al., 2018). In order to facilitate the biofunctionalization of medical implants, scientists employ minerals and growth variables such as Titanium Dioxide (TiO2) combined with FGF2, BMP2/6, and fibronectin. (Ettelt et al., 2018). Immobilized FGF2 with heparin stimulates fibroblast proliferation, immobilized BMP2 with heparin stimulates osteoblast growth, and fibronectin improves osteoblast cell adherence to the TiO_2 surface. Biocompatibility, mechanical characteristics, and radiolucency make polyetheretherketone (PEEK) a popular thermoplastic polymer for medical implants. *In vitro,* studies have shown that micro-porous PEEK implants coated with phosphorylated gelatine and BMP-2 can increase bone marrow-derived mesenchymal stem cell (BMSC) adhesion, proliferation, and osteogenic differentiation, as shown by increased osteogenic marker expression (J. Wu et al., 2018).

1.4.3 BMP signalling in cancer proliferation

BMPs in breast cancer

Research is currently being conducted on the potential involvement of BMPs in the processes of self-renewal and differentiation of breast cancer stem cells. These cellular activities have been linked to the development and advancement of tumours. A study conducted demonstrated that the administration of BMP4 and BMP7 resulted in modifications to the gene expression profiles of seven distinct breast cancer cell lines at six different time intervals. The cell lines utilised in this study comprised of MDA-MB-231, MDA-MB-361, ZR-75-30, SK-BR-3, T47D, HCC1954, and HCC1419. (Rodriguez-Martinez et al., 2011). Through the utilisation of hierarchical clustering, researchers ascertained that distinct cell lines exhibit varying responses to bone morphogenetic proteins (BMPs), while specific genes demonstrate responsiveness to both ligands. The expression of BMP4 and BMP7 genes exhibited the highest abundance among synexpression clusters, thereby emphasising the significance of BMP targets in breast cancer research. BMP4 exhibited a notably substantial influence on gene expression in comparison to the other ligands. (Alarmo et al., 2007). In the zebrafish model, it was observed that the protein Smad6 exhibited regulatory control over the invasiveness of the human breast cell lines MCF10A and MDA-MB-231. On the contrary, the inhibition of Smad6 can elicit an inverse response, thereby reducing the aggressiveness of these cells. (De Boeck et al., 2016a). Recent scientific research suggests BMP6 and BMP7 may exhibit a potential preventive

effect against the development of breast cancer. Elevated levels of BMP6 and BMP7 were found to be correlated with heightened infiltration of immune cells in breast cancer cases characterised by the presence of oestrogen receptors. (Katsuta et al., 2019). Furthermore, the aforementioned study revealed a positive correlation between elevated levels of BMP6 and BMP7 expression and enhanced survival rates in oestrogen receptor-positive (ER^+) breast cancer cases. On the contrary, alternative investigations have examined the impact of BMP-6 on the reduction of metastasis *in vitro*, specifically focusing on highly invasive and metastatic MDA-MB-231 breast cancer cells. The activity of Activating Protein-1 (AP-1), which is known to influence the expression of Matrix Metalloproteinase-1 (MMP-1), was observed to be decreased by BMP-6 (Hu et al., 2016). Concurrently, further research has presented findings that indicate BMP6 inhibits the ability of MDA-MB-231 cells to metastasize *in vivo* also by reducing the expression of MMP-1, a crucial protein involved in the metastasis process (Ning et al., 2019). The literature survey revealed that BMP2 on its own is implicated in 17% of prostate and breast cancers, as well as 15% of lung cancers (Skovrlj et al., 2015).

BMPs in ovarian cancer

Recently, MSCs have been implicated in tumour microenvironment and carcinogenesis, especially in ovarian cancer (Whiteside, 2008). A study in Oncotarget investigated the impact of ovarian cancer patient-derived mesenchymal stem cells (OC-MSCs) on cancer stem cells (CSCs) and carcinogenesis. In vitro and in vivo, OC-MSCs enhanced the development and self-renewal of CSCs. Subsequent studies found that OC-MSCs exhibited changes in the production of bone morphogenetic protein (BMP), with a decrease in BMP2 and an increase in BMP4. Exogenous BMP2 or BMP4 inhibition reversed the effects of OC-MSCs on CSCs and tumorigenesis. (McLean et al., 2011). The observed effects of OC-MSCs on CSCs and carcinogenesis were attributed to the alteration in BMP production. (Thawani et al., 2010). The growth of serous ovarian cancer cells was significantly reduced both *in vitro* and *in vivo* when the BMP signalling system was inhibited using a small molecule inhibitor or siRNA targeting BMP ligands or receptors. In contrast, it has been discovered that in SK-OV-3 ovarian cancer cell lines, the introduction of rBMP2, a different BMP protein, resulted in an increase in cellular proliferation. This effect was attributed to the translocation of pSMAD5 from the cytoplasm to the nucleus. The administration of dorsomorphin to ovarian cancer cell lines resulted in the reversal of the

functional impact of BMP2. Based on the findings of the aforementioned study, it has been shown that there exists a negative correlation between the levels of pSMAD5 and the prognosis of ovarian cancer. (Peng et al., 2016). According to a scientific study, it has been observed that the expression of BMP2 is regulated by the long non-coding RNA Urothelial Carcinoma Associated 1 (UCA1). Consequently, the inhibition of lncRNA UCA1 leads to the enhancement of BMP signalling through the activation of pSMAD1/5/8, ultimately leading to a rise in the proliferation of osteoblast cells. (R. Zhang et al., 2019).

BMPs in kidney cancer

Renal cancer cell lines such as Caki-2 and ACHN exhibit notable proliferative and clonogenic capabilities as a result of heightened expression of ALDHbr, OCT4A, Nanog, and Pax-2. The administration of BMP2 has the potential to decrease the proliferative capacity of renal cancer cells. (Wang et al., 2015). In contrast to another molecule of the BMP family, BMP-6 encourages the growth of RCC cells both *in vitro* and *in vivo*. Further investigation showed that interleukin-10 synthesis by BMP-6 in the tumour microenvironment enhances the M2 polarization of tumour-associated macrophages (TAMs). RCC is one kind of cancer where M2-polarized TAMs are known to encourage tumour development and immune evasion (Lee et al., 2013). According to the findings, BMP1 is overexpressed in ccRCC tissues (Sun et al., 2021) as opposed to nearby healthy tissues. In ccRCC patients, increased BMP1 expression is strongly associated with advanced tumour stage, high histologic grade, and reduced overall survival. The study suggests that increased levels of BMP1 may promote the restructuring of the extracellular matrix (ECM) and the invasion of tumours, potentially leading to the aggressive characteristics of ccRCC. (Xiao et al., 2020).

BMPs in lung cancer

Patients diagnosed with non-small cell lung cancer exhibited alterations in the Epidermal Growth Factor Receptor (EGFR) gene (Passaro et al., 2021). EGFR tyrosine kinase inhibitors (TKIs) show promise in treating EGFR-mutant NSCLC, but resistance often emerges (Morgillo et al., 2016). Recent scientific research suggests that the activation of the bone morphogenetic protein (BMP)-BMP receptor (BMPR) pathway might play a role in the development of resistance to EGFR-TKI treatment in specific patients with non-small cell lung cancer (NSCLC). Scientifically, it has been established through research that the activation of the BMP-BMPR pathway can stimulate the synthesis of the transcription

factor Slug. This, in turn, leads to the suppression of EGFR expression and the initiation of signalling pathways downstream that augment cell viability and confer resistance to EGFR-TKIs (Z. Wang et al., 2015). According to one study, both organoids and *in-vivo* surveillance following pneumonectomy revealed a reduction in BMP signalling in type 2 alveolar and type 2 related stromal cells. Reduced BMP signalling promotes the proliferation of type 2 alveolar cells, while elevated BMP signalling promotes their differentiation into type 1 alveolar cells (Chung et al., 2018). By decreasing caspase activity, XIAP (X-linked inhibitor of apoptosis protein) is an anti-apoptotic protein that promotes cancer cell survival. TAK1 (TGF-activated kinase 1) is a protein kinase that activates multiple signalling pathways, including those involved in cell survival and inflammation. Inhibition of BMP and TGF-β receptors has been demonstrated to lower the expression of XIAP and TAK1 in lung cancer cells, resulting in increased apoptosis and decreased cell survival (Augeri et al., 2016).

In addition to its association with other cancers, a study also demonstrated the importance of BMP in the process of hair follicle regeneration. The BMP4/SMAD8 signalling pathway plays a vital role in regulating granulosa cell proliferation and follicle growth in various species, such as geese. The detection of BMP4 in both pre-hierarchical and hierarchical follicles indicates that the increased expression of BMP4 in white goose granular cells enhanced the rate of proliferation of these cells. Additional Chip-seq analysis confirmed the upregulation of Smad 8, a downstream effector of BMP4 signalling, and the downregulation of Bmp and Activin Membrane-Bound Inhibitor (BAMBI), an inhibitor of activin membrane binding, as contributing factors promoting cellular proliferation (Wei et al., 2023).

1.4.4 BMP signalling in metastasis

BMPs have been associated with the process of metastasis, which is the spread of cancer cells from the primary tumour to surrounding organs. Figure 1.9 depicts the changes epithelial cells undergo to acquire mesenchymal properties. BMPs have been demonstrated to influence the EMT process in several cancer types, including breast and lung cancer. BMP-7 can suppress EMT in breast cancer cells (Ying et al., 2015), for instance, by activating the Smad signalling pathway, which results in the overexpression of E-cadherin, a protein that is essential for maintaining cell-cell contact. BMP7 can also enhance the migration and invasion of pancreatic cancer cells, by stimulating the PI3K/Akt signalling

pathway (Gordon et al., 2009). BMPs can also affect the tumour microenvironment, which plays an essential part in the process of metastasis. For instance, BMP-2 can induce the differentiation of mesenchymal stem cells (MSCs) into osteoblasts (Garg et al., 2017), which can foster the formation and dissemination of bone metastases. Overall, BMPs can influence the metastatic process through a variety of methods, and their effects can vary depending on the context in question.

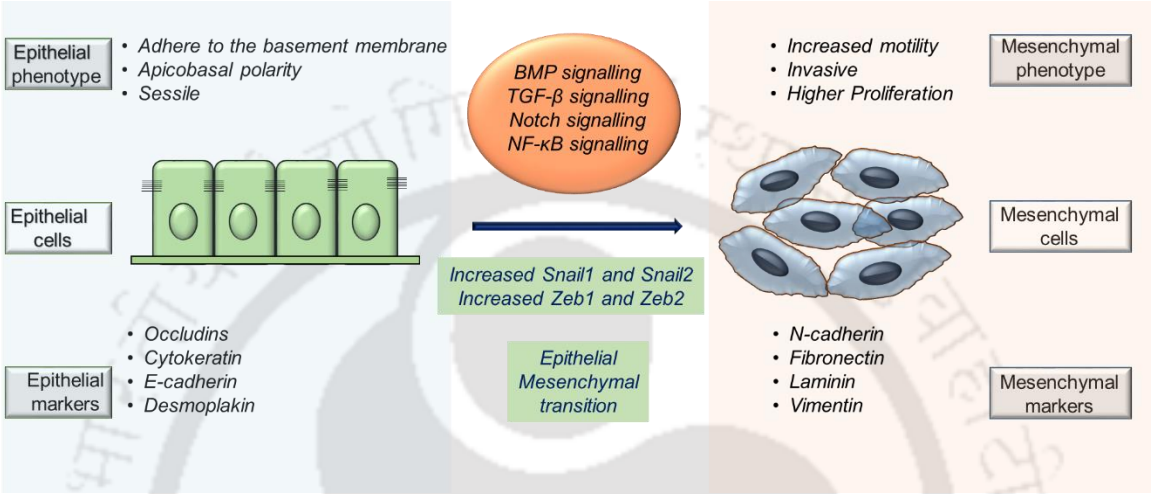

***Figure 1.9: Epithelial-mesenchymal transition**. This picture depicts the reprogramming of an epithelial cell into a mesenchymal one in response to signals from BMP, TGF-β, Notch, and NF-κB. signalling. Epithelial cells lose their high expression of E-cadherin, occludins, cytokeratin, and desmoplakin and acquire mesenchymal characteristics by expressing more N-cadherin, fibronectin, laminin, and vimentin. Epithelial cells lose adhesion to the basement membrane and become invasive and highly proliferative (Panda et al., 2022; Srivastava et al.,2013).*

Bone morphogenetic protein receptors, ligands, and antagonists play a role in regulating tumour growth and metastasis. In animal models lacking BMP signalling components, cancer spread was reduced, suggesting that blocking this pathway may be therapeutic (Bach et al., 2018). The migration, polarity, and dendritogenesis of mouse cortical neurons have all been demonstrated to be sensitive to alterations in canonical and non-canonical BMP signalling pathways. The loss of the BMP receptor BMPR1A in mouse cortical neurons, for instance, reduces dendritic complexity and spine density and causes abnormalities in dendritic arborisation and orientation by blocking canonical BMP signalling. Similarly, abnormalities in axonal development and migration of cortical neurons are observed when non-canonical BMP signalling is disrupted by blocking the MAPK/ERK pathway (Saxena et al., 2020).

The CCN protein, consisting of Cyr6, CTGF, and NOV, also known as cysteine-rich angiogenic inducer 61, connective tissue growth factor, and nephroblastoma overexpressed, is a matricellular protein that regulates signalling pathways and interactions between epithelial and stromal cells. The expression of CCN6, a matricellular protein, is found to be highly prevalent in breast epithelial cells. However, its levels decrease significantly in cases of aggressive and inflammatory breast cancer. (Kleer, 2016; Leask, 2016). The silencing of CCN6 leads to the activation of TAK1 (Transforming growth factor-β-activated kinase 1) and p38 MAPK, which in turn induces BMP signalling through a Smad-independent pathway (Giusti & Scotlandi, 2021). CCN6 controls integrin 6 (a key component of acinar polarity) and E-cadherin to maintain epithelial cells. Thus, a decrease in CCN6 can boost tumourigenic activity, which can be quickly restored by treating cells with rhCCN6, but overexpression of CCN6 can promote acinar development and limit invasion (Pal et al., 2012). Likewise, Chordin-Like 1 (CHL1) has been associated with inhibiting the migration and invasion of breast cancer cells. It has been demonstrated that CHL1 specifically inhibits BMP4, a protein that promotes the migration and invasion of breast cancer cells. The inclusion of CHL1 in a culture medium inhibits both cell migration and invasion, regardless of the presence of BMP4 (Cyr-Depauw et al., 2016).

According to a scientific study, it has been proposed that Smad6 exerts inhibitory effects on the metastasis of breast cancer cells. The sustained upregulation of Smad6 hampers the capacity of BMP6 to regulate the expression of mesenchymal markers in MCF10A M2 cells. The application of BMP6 resulted in enhanced intercellular communication in MDA-MB-231 cells, as observed through electron microscopy. In the zebrafish xenograft model, the inhibition of Smad6 did not have any impact on the MDA-MB-231 cells (De Boeck et al., 2016b). The activation of BMP-2 induces the Rb pathway, leading to an upregulation of epithelial-mesenchymal transition (EMT) and breast cancer stem cells (BCSCs). Breast cancer stem cells (BCSCs) exhibit the presence of CD44, a cell surface glycoprotein that plays a crucial role in facilitating cell adhesion, migration, and invasion processes. The BMP-2 protein enhances the expression of CD44 in cells of breast cancer, leading to an increase in breast cancer stem cells (BCSCs) and the development of tumours (P. Huang et al., 2017).

The receptor of the BMP signalling cascade may also influence tumour metastasis. Tumour initiation was found to be delayed when WAP-Cre (Whey acidic protein) was used to quench BMPRIA in Mouse Mammary Tumor Virus-Polyoma Middle Tumor-antigen

(MMTV.PyMT) mice. However, increased expression of keratin 5 and vimentin was observed in knock-out mice (Pickup et al., 2015). Zinc Finger E-box-binding homeobox 1 (ZEB1) is a transcription factor that controls EMT and cancer metastasis. ZEB1 binds to and stimulates the promoters of the noggin and gremlin genes. It is believed that noggin and gremlin, which are BMP inhibitors, facilitate bone metastases. ZEB1 can also stimulate genes associated with bone metastasis, such as S100A4, a calcium-binding protein that facilitates the metastasis of cancer cells (Mock et al., 2015). The Zinc Finger E-box-binding homeobox 1 (ZEB1) transcription factor is responsible for the regulation of epithelial-mesenchymal transition (EMT) and the process of cancer metastasis. The transcription factor ZEB1 exhibits direct binding and subsequent activation of the promoters of the noggin and gremlin genes. Noggin and gremlin, which are inhibitors of bone morphogenetic proteins (BMPs), are hypothesised to facilitate the development of bone metastases. ZEB1 has the ability to activate genes associated with bone metastasis, such as S100A4, a protein that binds to calcium and enhances the spread of cancer cells (Wang, et al., 2019).

Halofuginone is a tiny drug that exclusively targets the Smad3 transcription factor to block TGF-β/BMP signalling. Recent research indicates that the combination of halofuginone and zoledronic acid reduces breast cancer bone metastases synergistically. In preclinical models of breast cancer bone metastases, the combined therapy lowers considerably tumour burden, osteolysis, and tumour-induced bone remodelling. Halofuginone and zoledronic acid exert their synergistic effects by inhibiting TGF-β/BMP signalling pathways (Juárez et al., 2017). RNA-seq analysis of 4T1 mouse mammary cell lines 67NR (non-metastatic) and 66cl4 (metastatic) showed upregulation in 28 genes. KM Plotter showed that GREM1 expression is highly associated with lower recurrence-free survival in ER breast cancer patients. Low Crossveinless-2, CHRDL1, CRIM1 and Sclerostin Domain-Containing Protein-1 (SOSTDC1) expression in ER^+ patients and high CRIM1, GREM1 and SMAD6 expression in ER^- patients worsened recurrence-free survival. GREM1 amplification regulates ECM via collagen production, ECM patterning, and EMT promotion, according to TCGA data from 421 breast cancer patients. Deletion of GREM1 from the 66cl4 cell line reduces tumour growth and lung metastasis in mice compared with controls (Neckmann et al., 2019). In another study, researchers have found that Gremlin-1 (Sung et al., 2020) and BMP2 (Kim et al., 2015) increase breast cancer and colon cancer metastasis respectively, by activating the STAT3 signalling pathway. This, in turn, leads to increased synthesis of

matrix metalloproteinase 13 (MMP13), an enzyme linked to extracellular matrix degradation and cancer cell invasion. The treatment of MMTV-PyVmT animals with DMH1, an antagonist of BMP signalling, decreased lung metastasis by modifying the macrophages, blood vessels, and fibroblasts in the microenvironment that typically favour metastasis (Owens et al., 2015). JAG1, a downstream target of Notch1 signalling, was reduced by knocking down transcriptional enhanced associate domain and suppressing YAP1. Similar to the knockdown of Notch, the expression of YAP1 was reduced and degradation of YAP1 was accelerated by the knockdown of NICD, suggesting that Notch1 contributes to the stability of YAP1 by blocking its ubiquitination by TrCP (Zhao et al., 2022). The research suggests that YAP1 and Jag1/Notch1 have a positive association. It is interesting to note that overexpression of YAP1 decreases Smad1/5 expression and, YAP1 in conjunction with Notch1, promotes metastasis to the lung. Follistatin-like protein 1 (FSTL1) is a secreted glycoprotein that stimulates the nuclear factor kappa B (NFκB) signalling pathway to promote the proliferation, migration, invasion, and chemoresistance of oesophageal squamous cell carcinoma (ESCC). FSTL1 regulates the proliferation, differentiation, and metastasis of cells by activating nuclear factor NFκB and BMP signalling pathway (Lau et al., 2017).

1.4.5 BMP signalling in chemoresistance and relapse

BMP has the ability to elicit chemoresistance through multiple mechanisms. The upregulation of anti-apoptotic genes by BMPs is a contributing factor to the development of chemoresistance (Zhuo Chen & Xu, 2016). The nuclear factor kappa B pathway, which is activated by BMP signalling, is a key player in tumour promotion and chemoresistance (Ghasemi et al., 2019). Upregulation of multiple anti-apoptotic genes, including survivin and Bcl-xL, by BMP2 in esophageal squamous-cell carcinomas cells (Moniuszko et al., 2016) has been linked to increased chemoresistance. To add remarks to a medical condition, BMP signalling can also control the expression of drug transporters such as ATP-Binding Cassette Subfamily G Member 2 (ABCG2) and Adenosine 5′-Triphosphate–Binding Cassette Subfamily B Member 1 (ABCB1) (Binello & Germano, 2011) which play a role in drug efflux and contribute to chemoresistance. Downregulation of BMP6 in breast cancer stimulates ERK signalling and downstream targets of ERK signalling, such as cyclin-D1 and B-cell lymphoma 2 result in higher proliferation, whereas total knockdown of BMP6 induces chemoresistance (Lian et al., 2013). ERK is a protein kinase that is triggered by a

variety of stimuli, such as growth hormones and stress signals, and promotes cell proliferation and survival.

Lack of Smad4 and *p53* has been associated in certain studies with the development of colorectal cancer. Loss of Smad4 and *p53* stimulates β-catenin, leading to an increase in Wnt signalling, while loss of Smad4 and *p53* causes cells to activate DKK1, decreasing Wnt signalling. This two-way communication aids in the development of resistance in colorectal cancer cells (Voorneveld et al., 2015). Research has shown that anti-Müllerian hormone (AMH) and its type II receptor, AMHR2, play a role in TGF-β/BMP signalling and EMT in lung cancer, a field in which they were previously solely thought to play a role in gonadal tissue. Chemoresistance is triggered by depleting AMH or AMHR2, but cells become more sensitive to the Heat Shock Protein 90 (HSP90) inhibitor ganetespib thereafter. To better understand TGF-β/BMP resistance-associated signalling and to develop novel EMT therapeutics, AMH/AMHR2 can be a potential target (Beck et al., 2016). The tumorigenesis and resistance to chemotherapy of colorectal tumours can be traced back to the PSMD14-ALK2 axis, which initiates the BMP6 signalling pathway (Seo et al., 2019). *Nanos3* is a well-known germline cancer gene responsible for proliferation and chemoresistance. In one study, the deletion of *Nanos3* increased the sensitivity of glioblastoma cells to doxorubicin and temozolomide, confirming its function in chemoresistance (Zhang et al., 2020). The protein SMAD-specific E3 ubiquitin protein ligase 1 (SMURF1) was discovered to be increased in Head and neck squamous cell carcinomas and to be related to poor clinical outcomes. SMURF1 is involved in the control of BMP signalling. Increased expression of CD44 and SMURF1 in spheroids compared to monolayer cells indicates reduced BMP signalling, as shown by quantitative polymerase chain reaction (qPCR) and western blotting analyses. As a result of decreased BMP signalling, an environment is created where BMP inhibitors thrive, heightening chemoresistance to the medication cisplatin (Khammanivong et al., 2013).

Imatinib is a regularly used targeted medication for the treatment of Chronic Myeloid Leukaemia (CML). According to the study, the adherence of CML cells to stromal cells in the microenvironment of the bone marrow may lead to Imatinib resistance. When CML cells come into contact with stromal cells, they activate signalling pathways such as the ERK pathway, which promotes the upregulation of anti-apoptotic proteins, and the bone BMP pathway, which increases the expression of stem cell-related genes that promote cell survival and resistance to Imatinib (Kumar et al., 2017). The research done by authors

implies that MSCs from acute myeloid leukaemia patients cause K562-ADM cells to change into fusiform shapes and exhibit chemoresistance, which is demonstrated by enhanced expression of CTGF as determined by qPCR and FISH (fluorescence in-situ hybridization) (H. Li et al., 2019). Carboplatin is a chemo-drug that is used to treat many different types of cancer. An increase in *BORG*, which is a BMP/OP responsive gene, is caused when carboplatin is used to treat colorectal cancer. This causes *p53* to be downregulated, which in turn leads to increased proliferation and chemoresistance in the cancer cells (J. Li et al., 2020). Carboplatin treatment for ovarian cancer led to increased expression of BMP2, suggesting that BMP2 should be targeted to better comprehend chemoresistance (Fukuda et al., 2020). Palbociclib and 4-hydroxytamoxifen inhibit cell proliferation and prevent tumour growth in MCF7 and T47D (Shee et al., 2019).

To create new therapeutic approaches for treating cancer, researchers need a better understanding of the mechanisms underlying the role of BMPs in cancer proliferation. There is some evidence that BMPs play a role in both the development of tumours and the spread of cancer to the bones in breast cancer. Chemotherapy failure and disease recurrence are significant worries because of chemotherapy resistance. The tumour's microenvironment can amplify pre-existing drug resistance and foster the formation of chemoresistance by providing a haven for cancer cells. Therefore, the discovery of effective drugs that can target both the primary tumour and bone metastases in breast cancer require achieving a BMP signalling equilibrium in this disease. Treatment efficacy and disease recurrence risk could be enhanced by using biomarkers to forecast chemoresistance and customise treatment plans for individual patients.

1.5 RHO-ROCK Signalling

RHO GTPase

Numerous cellular processes, such as cell migration, proliferation, and cellular adhesion, are regulated by very small signalling proteins known as Ras homolog family member guanosine triphosphatases (Rho GTPases). It has been suggested that cancer development is linked to the dysregulation of Rho GTPases (Shang et al., 2013; Zeng et al., 2019). Numerous biomolecules act as signal transducers for these cells and influence tumour progression and proliferation. In this context, the GTPase family is one of the most studied enzymes as it alters cell signalling leading to uncontrolled cell growth. The Rat sarcoma

virus (Ras) GTPase superfamily is a group of molecular switches regulating various cellular functions including mitogenesis, cytoskeletal organization, vesicle trafficking, and nuclear transport (Pulgar et al., 2005). RHO GTPase is a member of the Ras GTPase family (20 members), mainly as homolog family member A (RHOA), Ras-related C3 botulinum toxin substrate 1 (Rac1) and Cell division control protein 42 homolog (CDC42), which together with their activating proteins, guanine nucleotide exchange factors (GEFs), are cancer oncogenes (Aspenström, 2022). RHO GTPase is overexpressed in cancer cells such as breast, testicular and liver cancer (Kalpana et al., 2019). Hence, the major challenges are to understand the role of RHOGTPase expression in the formation of cancer. The 20 RHO GTPases in humans can be categorised into different subfamilies based on their structural similarities and the way they are controlled. Most studies have focused on the RHO (RHOA, RHOB, and RHOC), RAC (RAC1, RAC2, RAC3, and RACG), and CDC42 (CDC42, RHOQ, and RHOJ) families (Hodge & Ridley, 2016). The C-terminal sections of RHOA, RHOB, and RHOC are where most of their differences lie; otherwise, the three proteins share an extremely similar primary protein sequence (about 85% identity) (Eckenstaler et al., 2022). The switch 1 and 2 domains, as well as most of the amino acids involved in GTP binding and hydrolysis, are located in the N-terminal regions of RHOA GTPase (responsible for the conformational transition between the GTP-bound and GDP-bound states). RHOA, RHOB, and RHOC undergo a variety of posttranslational changes, such as prenylation of a conserved C-terminal cysteine, methylation, and proteolytic removal of the terminal three amino acids (Bagnell et al., 2022). RHOA and RHOB protein levels and function are reduced in the presence of inhibitors of enzymes that generate prenyl groups, indicating that prenylation of Rho proteins is essential for their stability (Shang et al., 2013).

The term "RHO-ROCK signalling" describes a biochemical pathway involving the serine/threonine kinase family ROCK (Rho-associated coiled-coil protein kinase) and the Rho family of small GTPases (Y. Tang et al., 2018). The cytoskeletal system, cell migration, proliferation, and differentiation are just a few of the operations in which this pathway is crucial (Hanifa et al., 2023). RHOA functions passively when bound to GDP but actively when bound to GTP as depicted in figure 1.10. GEFs, GAPs, and GNIs control the activity and localization of RHOA (GDIs). GEFs enhance GTP binding of RHOA by stimulating the release of GDP. GAPs hydrolyze the GTP substrate of RHOA to stop its action. GDIs sequester GDP in the membrane to maintain the position of RHOA. Nearly

145 GEFs and GAPs are found in the diverse tissues to control RHO functioning (Jiang et al., 2023; Müller et al., 2020; Y. Zhang et al., 2022). RHOA interacts with downstream effectors to alter cellular activity. RHOA regulates migration, adhesion, survival, cell proliferation, gene expression, and vesicle transport (Filić & Weber, 2023; Schmidt et al., 2022; Zhou et al.,2013). G protein-coupled receptor ligands, extracellular matrix proteins, and other growth proteins stimulate GTPase activity by binding to their respective receptors, which in turn activates RHO, RAC1, and CDC42. The signal from activated RHO is transduced to Citron (Bishop & Ann, 2000), which controls cell cycle and cytokinesis, and protein kinase N (PKN), which supports membrane trafficking (Filić & Weber, 2023). The downstream targets of activated RHO, ROCK and mouse version of the diaphanous homolog 1 (mDIA), control actin dynamics and actomyosin contractility (Kimura et al., 1996). Rac1 stimulates Serine/threonine-protein kinase (PAK), which controls actin dynamics via LIM-Kinase, and nicotinamide adenine dinucleotide phosphate hydrogen oxidase, which supports cell proliferation (Sauzeau, et al., 2022). The last component, cdc42, promotes myotonic dystrophy kinase related-Cdc42 related kinases (MRCK), which in turn activates Myosin Light Chain 2 (Amano et al., 1996) and assists actomyosin in contraction, and (Wiskott–Aldrich syndrome protein) WASP, which controls cell motility (Figure 1.10).

Rho pathway mutations can cause many diseases. Breast, lung, and gastric cancers have RHOA gene mutations. Mutations can over-activate RHOA signalling, increasing cell proliferation, migration, and invasion. Mutations in the *Rac1* and *Cdc42* (Lionarons et al., 2019) genes have been linked to developmental disorders like Duane syndrome and developmental delay and intellectual disability, respectively. Hypertension and coronary artery disease are linked to *ROCK2* gene mutations. Some RHO mutations that were produced in the lab, such as G14V and Q63L (Khosravi-Far et al.,1995), show a gain of function characteristics and are easily compatible with active mutants that already exist. It was also found that these mutations tend to cluster in the interaction areas of regulators and that they have an influence on downstream effectors. R5, G17, and Y42 (Network, 2014) were shown to be the three most common mutation hotspots in RHOA. It was observed that 90% of peripheral T-cell lymphoma cases and roughly 15-20% of stomach cancer cases both displayed mutations in RHOA (Kakiuchi et al., 2014; K. Wang et al., 2014). According to the TCGA database, E40Q, G17A, and R5W mutations were also observed in breast cancer (Svensmark & Brakebusch, 2019). Differential signalling occurs in RHOA

mutant cells since mutations in RHOA can affect both downstream effectors and upstream regulators, favouring or downregulating the function.

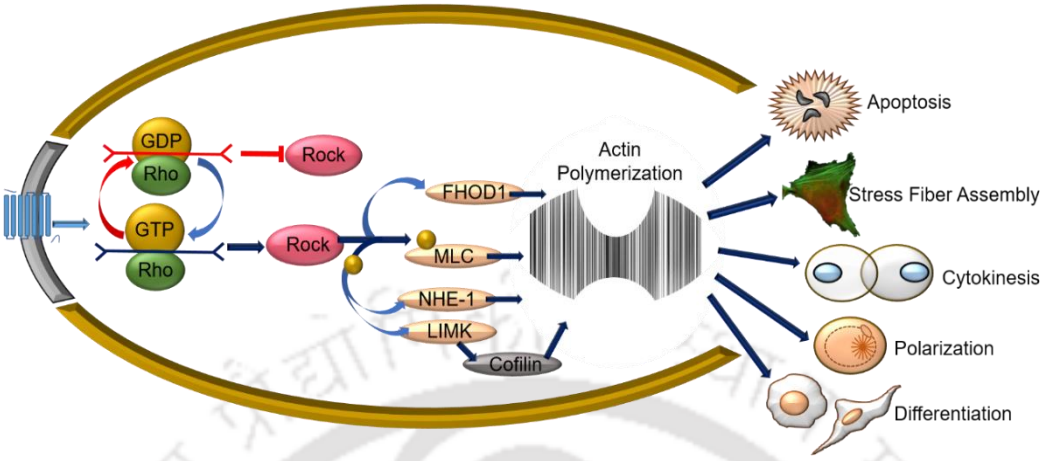

Figure 1.10: Switching between RHO-GDP/GTP and downstream signalling. *As depicted, Rho-GDP inhibits ROCK activity whereas Rho-GTP stimulates ROCK activity. By phosphorylating FHOD1 and multiple cofilins activating factors, ROCK activation promotes actin polymerization. The actin organisation (polymerization and depolymerisation) regulates apoptosis, stress fibre assembly, cytokinesis, polarisation, and differentiation (Saadeldin et al., 2021).*

1.5.1 RHOA in cancer progression

Tumour initiation, metastasis, and treatment resistance have all been linked to the Rho family of small GTPases, which includes RHOA, Rac1, and Cdc42. RHOA is overexpressed in many malignant tumours and has been linked to tumour expansion, invasion, and blood vessel formation (Rathinam et al., 2011; Ridley et al., 2008). Oncogenes and tumour suppressor genes are responsible for the transition of normal cells into malignant cells early in the course of cancer (Pulciani et al.,1985). Among the characteristics of malignant cells include unregulated cell division, apoptosis resistance, and the ability to grow without supporting structures. By modifying the cytoskeleton architecture of the cells, these malignant cells can also regulate the stress fibres (Anne J et al.,1992).

Local tumour invasion of healthy tissue initiates the metastatic process. As cancer cells lack the resources to multiply and survive in their surrounding environment, local invasion is adaptive (García-Jiménez & Goding, 2019). In normal organisms, cells can migrate as a group, such as epidermal keratinocytes during skin wound healing, or singly, such as leukocytes to an inflammatory region. (Friedl et al., 2012). To move the plasma membrane and the cell body, cells use four different actin-based projections (García-Jiménez &

Goding, 2019). Lamellipodia are thick actin protrusions near the cell periphery, while filopodia are thin actin structures that serve as exploratory protrusions to probe the cell's environment. Invadopodia degrade the matrix, while blebs are massive spherical protrusions (Charras et al., 2006) that form when an area of the plasma membrane detaches and inflates due to increased hydrostatic pressure caused by strong actomyosin contraction (Anne J Ridley, 2015). When cells lose their adherence to the matrix and develop polarity, migration can start. High Rac1 and low cdc42 activation in the anterior half of migrating cells regulate their elongated shape, and contraction of actomyosin at the posterior end encourages the protrusion known as lamellipodia. RHOA simultaneously encourages retraction along with mDIA at the anterior end and ROCK at the posterior end. The capacity to retract and create a protrusion must be properly balanced during the migration process (Bolado-Carrancio et al., 2020). Actin-myosin contraction in the lateral area via Rho-ROCK and cdc42-MRCK controls collective cell movement (Gaggioli et al., 2007). Figure 1.11 illustrates the variations in actin and stress fibre formation during cell migration. Intravasation was studied in the zebrafish model. It was found that cdc42- WASP promotes intravasation and overexpression of RHOC in migrating cells facilitates intravasation by giving the cells a round and amoeboid shape as they circulate in the blood arteries (Stoletov et al., 2007).

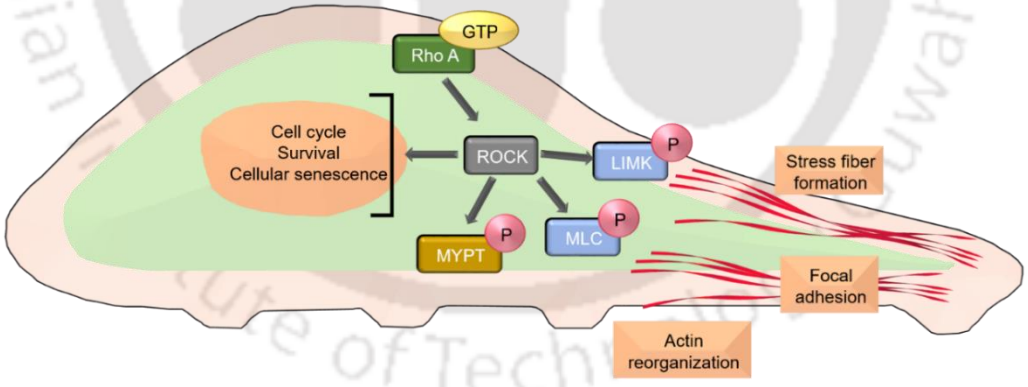

Figure 1.11: RHOA-ROCK in cancer progression. *Activated Rho-associated kinase (ROCK) phosphorylates LIMK (Lim kinase), MLC (myosin light chain), and MYTP (myosin phosphatase target), as depicted, to promote stress fibre formation, increase focal adhesion, and regulate actin organisation. The active ROCK is directly responsible for regulating the cell cycle as well as cellular survival and senescence (Kim et al.,2021).*

Not only in migration and intravasation but RHO-ROCK signalling also regulates extravasation and colonization at distant sites. It was studied that ROCK with NF-kB promotes lung colonization (Georgouli et al., 2019) by disrupting the cell-cell attachment,

similarly, RHOC with caveolin-1 protein helps prostate cancer to metastasise in in-vitro conditions (Gligorijevic et al., 2012). The majority of cancer deaths are caused by distant metastases. The interaction between SDF-1α and CXCR4 causes distant metastases in many solid tumours. This substance promotes migration and distant colonisation. Many chemokine factors that promote homing and recruitment to distant locations appear to attract RHOA mutant cells at concentrations of 100ng/ml of SDF-1α and CXCR4, increasing the likelihood of bone marrow host cells binding them (Pasquier et al., 2015).

During the process of microtubule disintegration, GEF-H1 can drive RHOA activation, but only if BCL2 Interacting Protein 2 (BNIP-2) is present. BNIP-2 is a BCH domain-containing protein that binds RHOA and GEF-H1 and migrates with kinesin-1. In breast cancer cells of the MDA-MB-231 subtype, loss of BNIP-2 leads to a reduction in RHOA activity and an increase in cell motility. Nocodazole-induced microtubule disintegration enhances BNIP-2-GEF-H1 interaction, while BNIP-2 knockdown uncouples RHOA activation and cell rounding. BNIP-2 acts as a scaffold for GEF-H1 and RHOA, which allows for more precise control of RHOA activity and cell motility. (Pan et al., 2020). Tiam1 (T-lymphoma invasion and metastasis-1) is a different GNEF that controls Rac *in vivo* and Rac-cdc42 *in vitro* by catalysing nucleotide exchange (Minard et al., 2004). Tiam1 controls RHOA's GDP-GTP state in conjunction with the cytoplasmic protein Ankyrin. Tiam1 was expressed more strongly when breast cancer was of a higher grade (Bourguignon et al., 2000). In addition to GEF, RhoGAP also controls the level of activated Rho signalling, which in turn affects cancer. When p190RhoGAP is overexpressed in cells, it inhibits RHOA activity, which decreases nestin expression, reduces cell proliferation, and lengthens cellular processes (Wolf et al., 2003). RhoGAP protein ARHGAP10 is an additional member of the RhoGAP family that suppresses cell migration, invasion, and adhesion by deactivating cdc42 via GTP hydrolysis (Luo et al., 2016). Breast cancer patients (Li et al., 2019) and 77.3% of ovarian cancer patients (Teng et al., 2017) and had lower levels of ARHGAP10, which shows that it governs the way cancer expands. In addition to ovarian cancer, overexpression of ARHGAP10 reduced the production of MMP2 and MMP9 and stimulated the expression of β-catenin and c-Myc, which prevented lung cancer from migrating, invading, and metastasizing (Teng et al., 2017). In contrast to non-cancerous tissue, prostate cancer patients were shown to have increased levels of ARHGAP10, and this protein has a negative relationship with wnt signalling (Gong et al., 2019; Teng et al., 2017).

RHOA or RhoC overexpression in breast cancer is associated with a poor prognosis; RHOA or RhoC suppression using anti-siRNA curtailed cell proliferation and invasion more effectively than conventional Rho cell signalling inhibitors (Pillé et al., 2005). Matrigel invasion experiment, flow cytometry, and qPCR all revealed that silencing the *syndecan-1* gene induced an increase in migration of MDA-MB-231 and MCF7 cells by upregulating vinculin, cadherin-11, MMP2 and RHOA/C and downregulation of Cyclin-dependent Kinase 6 (CDK6) and MMP9 (Ibrahim et al., 2012). Additionally, given that Cdc42, a member of the Rho signalling family, governs malignancy, the fact that TT17C knockdown increased the expression of Rap1 and Cdc42 in breast cancer samples shows TT17C has a negative correlation with malignancy (J. Zhang et al., 2023). Silencing *DLC1* (deleted in liver cancer 1) in PCa cells increased proliferation, as demonstrated by the CCK-8 assay and cell cycle analysis, whereas Y27632 restored *DLC1* function, indicating an inverse relationship with ROCK and a potential target to control tumourigenesis (Gong et al., 2023). In prostate cancer cells that had been treated with enzalutamide, an enhanced expression of RHOA, p38, androgen receptor, and ROCK2 was observed in enzalutamide-resistant cells; however, the resistance could be overcome by inhibiting RHOA through the RHOA/ROCK2/p38 pathway (X. Chen et al., 2023). The proliferation and migration-promoting properties of C-X-C-motif ligand-1 (CXCL1) in tongue cancer cells, secreted by LNMTCa8113 lymphatic endothelial cells were validated by the CCk-8 assay and the transwell assay, respectively. CXCL1 is also capable of activating RhoGTPase, which in turn promotes cytoskeleton reorganisation, a crucial step in migration (S. Zhang et al., 2023). According to the findings of one study, Bcl-2-associated Athanogene 6 (BAG6), a chaperone protein that maintains protein quality and proteostasis inhibits the ubiquitination of RHOA and promotes the formation of stress fibres. In cells lacking BAG6, RHOA levels and the formation of stress fibres are both reduced. BAG6 may assist RHOA in maintaining its stability and producing stress fibres (Miyauchi et al., 2023). miR-31 is a microRNA with anti-fibrotic actions in multiple organs, including the kidney. It was discovered that Nuclear Enriched Abundant Transcript 1(NEAT1) acts as a shield for miR-31, preventing it from binding and blocking its downstream targets. This results in an increase in the activation of the RHOA/ROCK signalling pathway, which has been implicated in the aetiology of renal fibrosis. The connection between miR-31 and NEAT1 or RHOA was confirmed using RNA immunoprecipitation (RIP), fluorescence in situ hybridization (FISH), and luciferase reporter assays (Y. Chen et al., 2023).

1.5.2 RHOA in metastasis

Several investigations have been conducted to learn how RHO-ROCK signalling contributes to the development and spread of breast cancer. High RHOA and low RHOB messenger RNA expression strongly regulate the actin cytoskeleton and cell motility in eight breast cancer cell lines. RHOB inhibition boosted invasion, but RHOA inhibition decreased stress fibre formation. Restoration of *BRCA1* expression in a basal-like cell line impedes migration. Reduction of RHOA and increase of RHOB cause this behavioural change. These results suggest that *BRCA1* regulates the expression of RHOA and RHOB in basal-like malignancies (Privat et al., 2020). Voltage-gated Na+ channels (VGSCs) also support cancer cell migration and invasion. Researchers looked at how RHOA changes Nav1 protein in MDA-MB 231 and MCF-7 breast cancer cell lines. Silencing RHOA decreased both the production of Nav1.5 channels and the flow of sodium, which led to less cell growth and invasion. Knocking out Nav1.5 also lowered RHOA protein levels, which shows that RHOA and Nav1.5 work together to make tumours more aggressive (Dulong et al., 2014). Cell proliferation, metastasis, and invasion can be inhibited in MCF7 and MDA-MB-231 by activating NRF2 alpha receptors, which control the oxidative stress response. Mechanistic studies conducted recently demonstrate that NRF2 binds to the promoter of ERR1 (oestrogen receptor) and reduces protein function. The expression of RHOA can be reduced by inhibiting NRF2, which improves the prognosis of breast cancer (C. Zhang et al., 2016). In the same context, Neuroepithelial Transforming Gene 1 (Net1), a RHOA subfamily GEF, is increased in several human cancers. PyMT-expressing Net1-deficient animals show decreased tumours and metastasis. Net1 loss reduces tumour angiogenesis and enhances tumour cell death. Net1 is required for RHOA activation and tumour cell motility. PyMT cannot activate ERK1/2 and PI3K/Akt1 without Net1. Primary tumour cells transplanted without Net1 diminish tumour angiogenesis and lung metastasis. Net1 signalling increases proliferation and PI3K pathway activation in 10% of human breast cancers. Net1-expressing patients have lower distant metastasis-free survival (Y. Zuo et al., 2018).

Recent whole genome sequencing studies suggest that RHOA limits tumour development. Researchers used a syngeneic triple-negative breast cancer mouse model to examine how reduced RHOA expression affects tumour development, metastasis, and invasion. Suppression of RHOA *in vivo* did not affect breast cancer cell proliferation or clonogenesis, despite encouraging results *in vitro*. Cancer-associated fibroblasts and macrophages

enhance the tumour-friendly CCL5-CCR5 and CXCL12-CXCR4 chemokine axes of the primary tumour. RHOA-deficient breast cancer tumours spread aggressively to the lungs and lymph nodes due to chemokine receptor suppression (Kalpana et al., 2019). Basal-like carcinoma, an aggressive breast cancer, has no targeted treatment. Septins, 13-headed GTP-binding proteins, are the fourth cytoskeleton component. SEPT9 on Chr 17q25 affects cell motility, proliferation, shape, and cytokinesis. SEPT9 i1 increases breast tumour growth and cell migration. SEPT9 Overexpressed MCF-7 cells injected into mice's mammary fat pads and tail veins caused palpable tumours in the fat pad but no metastases in the lung or liver. Knocking down SEPT9 decreased p-FAK (Y397, Y576/577, and Y925), p-Src (Y416), p-Paxillin (Y118), and p-ROCK1 (T455 + S456). After treatment with the FAK inhibitor PF-573228, Y-27632 decreased FAK/Src/paxillin signalling but did not affect RHOA-ROCK1 signalling activity, confirming the involvement of RHOA-ROCK1 (Zeng et al., 2019). FAK/RHOA was shown to be triggered by AngII/AGTR1 (angiotensin II receptor type 1). AGTR1 increases FAK/RHOA and its downstream effectors ROCK1, ROCK2, and MLC. AGTR1 activates G12/13 and interacts with Rho-GEF G to influence RHOA. In vascular smooth muscle cells, losartan inhibits FAK phosphorylation caused by Ang II production (Y. Ma et al., 2019). AIF1L (allograft inflammatory factor 1-like) appears to regulate cell motility through FAK/RHOA signalling. By adopting a more circular shape and producing fewer protrusions, AIF1L-transfected MDA-MB -231 cells were able to reduce their propensity to spread. Moreover, GSEA suppressed AIF1L expression, resulting in increased COL4, COL6, COL5, and COL1 expression. Consequently, it was hypothesized that AIF1L affects FAK/RHOA expression by sabotaging cell-ECM communication (Liu et al., 2018). Moesin is a protein that can both initiate and arrest tumours. Activated intracellular moesin directly upregulates the expression of Scr, LRP5, MMP9, Snail2, and viability and thus migration, whereas activated extracellular moesin downregulates FAK and RHOA along with these genes (Ahandoust et al., 2023).

TNBC cells with a high migration rate express RhoGAP ARHGAP18. ARHGAP18 levels are lower in breast cancer survivors who have not had a recurrence or metastasis. ARHGAP18 deletion increased RHOA while decreasing TNBC growth, migration, and metastasis. Overexpression of MiR-200b stimulates RHOA, improves focal adhesions and actin stress fibres, and inhibits migration and metastasis. Stable miR-200b reduced RHOA activity while increasing cell mobility. ROCK inhibition reduced RHOA signalling and

reversed the effects of miR-200b inhibition on cell movement. TNBC cell motility and metastasis are inhibited by ARHGAP18 and miR-200b (Humphries et al., 2017). Together with Rac1, the other ARHGAP8 (pro-metastatic Rho GAP) is transported to the lamellipodia region to generate cell polarity. Under the effect of EGF, BPGAP1 maintains a balance between the activation of RHOA and Rac1. BPGAP1 recruits RacGEFVav1 to activate Rac1 in the lamellipodia area and RhoGAP to inhibit RHOA activity. Reduced RHOA and elevated Rac1 are necessary conditions for cell migration (Wong et al., 2023).

TNBC cell lines have more RHOA pathway activity than normal cancer cell lines because rhophilin-associated tail protein 1 regulates it (ROPN1). Silencing ROPN1 inhibits cell migration and invasion while overexpression stimulates them. Silencing RHPN1 (ROPN1 interacting protein rhopillin-1) separates RHOA and ROPN1, showing it is needed for all functions. Drug or suppressing RHOA decreases migration in cell tracking, wound healing, and transwell penetration experiments. Dephosphorylation of cofilin reduces stress fibre formation in RHOA-deficient cells (Q. Liu et al., 2020). ANXA1, also known as Annexin-A1, activates p38, JNK, ERK, and MAP-kinases to impact proliferation, actin cytoskeleton, membrane trafficking, and apoptosis in certain malignancies. Paxillin staining showed more focal adhesion spots in ANXA1-silenced MCF7. This suggests that ANXA1 overexpression may increase migration and metastasis by inversely expressing focal adhesion sites. U0126, a MEK1/2 inhibitor, increased wound closure time in MCF7 cells transfected with or without ANXA1. ANXA1-MCF7 showed a greater rise. ANXA1 overexpression increased CXCL12-induced RHOA signalling in cells. In normal MDA-MB-231 cells, RHOA, Rac1, and cdc42 overexpression boosted NF-kB activity by 2–20-fold. In response to CXCL12, MCF7 cells overexpressing RHOA, cdc42, and Rac1 activated NF-kB but not Rac1. CXCL12-induced NF-kB activation requires RHOA. Thus, ANXA1 enhances wound healing via ERK-RHOA-NF-kB signalling pathways (Bist et al., 2015).

TNBC cells exhibit more of the Protein C Receptor (PROCR) gene family, which is linked to purpura fulminans and thrombophilic disorders, than ER^+/PR^+ and $Her2^+$ cells. PROCR overexpression causes c-Myc, cyclin D1, ERK, PI3K-Akt-mTOR, and RHOA-ROCK signalling cascades. Increased PROCR expression made BT549 cells more elongated than controls, demonstrating that this gene regulates cell shape and morphology. PROCR's cytoprotective action in several cell types may be mediated by the G protein-coupled F2R

receptor. Knocking down F2R only inhibited RHOA-ROCK and p38 signalling, which had been boosted by PROCR overexpression, but did not affect ERK or PI3K-Akt-mTOR signalling (Daisong Wang et al., 2018). EDV (endothelium-dependent vascularization) and vasculogenic mimicking (VM) angiogenesis boost tumour growth. S1PR1 (sphingosine-1-phosphate receptor 1) is involved in all EDV-dependent human cancers. RHOA phosphorylates VE-cadherin. RHOA activity was higher in S1PR1-expressing MDA-MB-231 and MCF-7 cells. The RHOA inhibitor boosted VE-cadherin expression and decreased phospho-VE-cadherin (Y731) and β-catenin expression, but S1PR1 expression was unaffected. In response to the inhibitor, RHOA signalling induces tumour endothelium-dependent vasculature and decreased VM development through elevating S1PR1 (S. Liu et al., 2019).

G proteins, combined with receptors, send cell signals via subunits like G-α/β/γ. Aggressive breast cancer cells upregulate GNA13 component G-α13. Kallikrein genes, including KLK3, produce prostate-specific antigen (PSA), a prostate cancer marker. Gene expression and immunoblot profiles demonstrate that GNA13-expressing cells decrease KLKs, specifically KLK-5, KLK-6, KLK-7, KLK-8, and KLK-10. GNA13 knockdown enhances KLK6/7 in aggressive breast cancer cells like MDAMB-157. Many breast cancer patient samples show that GNA13 inhibits KLK-5/6/7/8/10. Rhotekin pull-down experiment showed that GNA13-overexpressed cells downregulated RHOA. RHOA controls KLK, as C3 toxin (RHOA inhibitor) lowered active and total RHOA levels and KLK gene profile in MCF-10A. GNA13 decreases RHOA and KLK gene expression and suppresses KLK gene expression via the RHOA-ROCK pathway (Teo et al., 2016). Researchers found that not only G-protein, but type IV collagen stimulates Dishevelled-Associated Activator of Morphogenesis 1 (DAAM1) and RHOA and promotes haptotaxis of MDA-MB -231 and MDA-MB-453 breast cancer cells on Boyden chamber membranes, a process blocked by cycloheximide (RGDfK). ShRNA-mediated DAAM1/N-DAAM1 reduction decreased collagen-induced RHOA activity, stress fibre assembly, invadopodia enlargement, and cell haptotaxis. An inhibitor (CCG-1423) or a dominant-negative mutant (RHOA-N19) reduced collagen-induced invadopodia expansion and haptotaxis in MDA-MB -231 and MDA-MB-453 cells. Integrin γ3/DAAM1/RHOA type IV signals collagen-induced invadopodia growth and haptotaxis in breast cancer cells (T. Yan et al., 2018). Human pituitary tumour-transforming gene 1 (hPTTG1) encodes human securin, which regulates the cell cycle during mitosis by segregating sister chromatids; DNA damage repair by interacting with

Ku70; the cell cycle by interacting with PBF, PP2A, p53, and Ku70; and expression of c-Myc and fibroblast growth factor 2. MDA-MB -231 and MDA-MB-453 that formed metastases expressed more hPTTG1 than MCF7, T47D-D, and BT-483 cells. Overexpression of hPTTG1 or GEF-H1 increased migration and invasion of MDA-MB -231 and MCF7, but not proliferation. In SCID mice, MDA-MB-231-KD-hPTTG1 and MDA-MB-KD-shGFP were injected into mammary fat pads for *in vitro* studies. As expected, injection of hPTTG1 knockdown decreased tumour size and tumour volume compared with MDA-MB-231-sh-GFP. Thus, hPTTG1 could treat breast cancer (Liao et al., 2012). MCF-7-14-3-3T-FLAG cells outperformed MCF-7-empty vector cells in migration and invasion. EGF increases actin ring filament production, making 14-3-3T MCF7 cells motile and less adherent. Mammary fat pad xenografts are more common in nude mice implanted with stable MCF7-14-3-3T-FLAG than MCF7 empty cells. 14-3-3T directly activates the Rho/ROCK signalling pathway, which enhances tumour development, pelvic cavity invasion, and lymph node metastases, resulting in poor survival. Thus, 14-3-3T may inhibit cancer spread (Xiao et al., 2014).

Enzalutamide, an androgen receptor antagonist, regulated cell cycle genes like cyclins D, E, A, and B in ER^+ breast cancer cells and inhibited proliferation in the S phase. The other inhibitor of Arv7, a version of AR, did not directly affect cell growth but downregulated c-Myc in treated cells. Enzalutamide inhibited growth and migration, as seen by greater E-cadherin expression and lower MMP9/2 and ROCK1 and 2 activities. Enzalutamide inhibits angiogenesis by decreasing VEGF expression (Ali et al., 2023). 30% of ErbB-2-expressing breast cancers are metastatic and have a bad prognosis. ErbB-2 overexpression in human breast cancer cell lines phosphorylates and activates plexin-B1, which is needed to activate the pro-metastatic small GTPases RHOA and RhoC and promote invasiveness. Plexin-B1 ablation in ErbB-2-overexpressing animals reduced metastasis. ErbB-2-overexpressing breast cancer patients with low plexin-B1 had excellent prognoses (Worzfeld et al., 2012).

1.5.3 RHOA in cancer chemoresistance and relapse

Patients are resistant to chemotherapy, immunotherapy, and radiotherapy as a result of the heterogeneity of their tumour populations. In addition, cancer cells of a heterogeneous population have a high proliferation capability due to stem cell markers $CD24^-$, $CD44^+$ and $ALDH^+$ (Zhang et al., 2022) and the ability to commence tumour growth via differentiation.

Changes in tumour signalling cascades and bone microenvironment may account for acquired medication resistance (Zahra et al., 2022). There were several drugs used to inhibit Rho signallings, such as Rhosin which inhibits RHOA (Shang et al., 2012), NSC23766 which inhibits Rac1(Gao et al., 2004), casin which inhibits cdc42 (Sakamori et al., 2014), ZCL278 which inhibits cdc42 by binding to GEF (Aguilar et al., 2019), and Y16 which inhibits LARG by binding to RHOA (Evelyn et al., 2009). ROCK is inhibited by Y-27632 (Nagumo et al., 2000), Fasudil (Nagumo et al., 2000), Wf-536, RKI-1447 (R. A. Patel et al., 2012), and AT13148 (Yap et al., 2012) by competing with ATP. PAK is inhibited by K252 (Kaneko et al., 1997), OSU-03012 (Porchia et al., 2007), PF-3758309 (Murray et al., 2010), and FRAX597 (Licciulli et al., 2013) by competing with ATP, whereas IPA-3 (Deacon et al., 2008) inhibits PAK by generating autoinhibited conformation. To determine the most effective treatment, we must therefore comprehend the process underlying medication resistance. Consequently, numerous investigations have been done to determine the cause.

Even though PAK family inhibitors like PF-3758399 have been employed to treat solid tumours, their significance has been diminished due to poor bioavailability and anaemic responses. There is evidence that ROCK inhibitors can be used as a target, as Fasudil and Ripasudil have been effective in treating glaucoma and cerebral vasospasm, and AT13148 has been effective in treating solid tumours of colorectal carcinoma in Asia (Crosas-Molist et al., 2022). Mechanical stress requires a fast cell and tissue response to maintain homeostasis. Mechanotransduction mechanisms tighten the actomyosin cytoskeleton under mechanical stress. Due to extracellular matrix stress, mechanotransduction is over-activated in diseases like cancer, despite its relevance in epidermal regeneration. Acute compressive stress increases RHOA-GTP levels and ROCK-mediated phosphorylation of myosin, actomyosin contractility, and tension in cells and tissues in 3D. This shows that short-term, high-intensity compression stresses may produce RHO/ROCK-dependent cellular homeostasis alterations that may be therapeutic for cancer (Boyle et al., 2020). Similarly, (Y. Li et al., 2020) soft matrices like polyacrylamide hydrogel coated with fibronectin have been reported to foster the stemness property of cancer cells. According to (Patwardhan et al., 2021), the different behaviour of cancer cells on different matrices can be attributed to the secretion of exosomes. In this study, researchers showed that the addition of GW4869, an inhibitor of exosome sequestration, can reverse the stiffness-mediated changes in cell shape, adhesion and lamellipodia production of cancer cells which

improves motility. The results of the TCGA study indicate that thrombospondin 1 is a potential regulator of exosome secretion, and knocking down thrombospondin 1 confirms that it uses FAK and MMP proteins to promote migration. CCM3 (Cerebral cavernous malformations 3) discovered by (S. Wang et al., 2021) can also govern stiffness-oriented alterations via YAP/TAZ signalling, in addition to thrombospondin. Mechanotransduction is primarily driven by focal adhesion kinase binding to paxillin to fine-tune the FAK/Src/paxillin pathway, which activates YAP/TAZ. The study found that CCM3 can bind to paxillin competitively in place of FAK, which is why knocking down CCM3 in a mouse model resulted in failed tissue remodelling and matrix alterations that reversed the YAP/TAZ signalling and led to metastasis. RICH1, a RhoGTPase-activating protein 17, also activates kinases that inhibit YAP /TAZ translocation by dislodging the Amot-p80 member of the Merlin complex. The poor prognosis of cancer and high migration and proliferation of triple-negative breast cancer is inversely related to RICH1 expression (Tian et al., 2022).

Furthermore, more investigation has shown that topographic change can influence the receptivity of cancer cells to chemotherapy agents. When cancer cells SKOV3 and OVCAR-5 were seeded on a convex bio imprint coated in polystyrene as opposed to a flat surface, they were less responsive to the chemotherapy drug carboplatin. Similar to carboplatin alone, rho inhibition eliminated the chemo-response disparity across substrates but intriguingly made it proliferate rather than reduce metabolic activity (Sarwar et al., 2020). It is also known that WASP family member WAVE3 promotes migration by controlling actomyosin contraction. In general, drugs like doxorubicin, paclitaxel, and cisplatin influence the phosphorylation status of WAVE3 (W. Wang et al., 2022). When administered to MDA-MB-231 and 4T1, *in vitro* and *in vivo* growth, invasion, and metastasis are inhibited in 2D as well as 3D, respectively. However, the function of WAVE3 can be restored if the phosphorylated version of WAVE3 is re-expressed, indicating that the presence of WAVE3 without phosphorylation is insufficient. The cisplatin-resistant MDA-MB-231 demonstrated increased expression of pWAVE3 and β-catenin, as well as an increase in survival to 80%, indicating that WAVE3 modulates wnt-β-catenin signalling. Sphingolipid biosynthesis, which maintains cell activity, produces ceramide synthase 6. CERS6 (Chen et al., 2022) is linked to ovarian, stomach, and lung cancer. It may be involved in breast cancer, particularly lymph node-metastatic breast cancer. CERS6 overexpression in MDA-MB-468 and BT-549 causes doxorubicin,

cisplatin, paclitaxel, and 5-fluorouracil chemoresistance without affecting cell migration or proliferation. CERS6 inhibits active RHOA, pMYTP1, MLC, and EGFR/mTOR pathway components, suppressing TNBC. Possible effects of dexamethasone on cell migration and cytoskeleton were attributed to the AKT/mTOR/RHOA pathway. The growth of T47D cells was successfully suppressed by dexamethasone, whereas the drug did not eradicate the cells. In the treatment of advanced breast cancer, dexamethasone and glucocorticoids have shown encouraging results (Meng & Yue, 2015). Additionally, miR124a and miR373 are chemo-sensitive. One study discovered that following neoadjuvant chemotherapy, HR^+ breast cancer patients had higher expression of miR124a and lower expression of miR373 (Ryspayeva et al., 2022).

Much research in recent years has looked into RHOA-ROCK and its possible connection to the onset and spread of breast cancer. Although these studies have provided useful information, they do have significant restrictions that should be taken into account. Due to a lack of diversity, many studies have only looked at one subset of breast cancer, such as triple-negative breast cancer, which may not be representative of the disease. However, the complexity of actual malignancies may not have been adequately represented in these studies because researchers have mostly used the cell line model. Studies have revealed possible therapeutic targets related to RHOA-ROCK signalling in breast cancer; however, there is a lack of clinical data to support their efficacy in human patients. Correlational studies have shown a link between RHOA-ROCK signalling and breast cancer progression, but establishing a fundamental relationship is difficult due to the complex and multifactorial nature of cancer development and progression.

1.6 Wnt Signalling

Wingless-Int-1 is abbreviated as "Wnt" both "Int1" and "Wingless" stand for the same thing. All metazoans, embryonic and adult, produce and secrete Wnts, which are Cys-rich glycol-lipoproteins. 19 human genes code for Wnts, and they all communicate with each other to trigger intracellular signalling cascades (De Boer et al., 2004). Wnt signalling pathways utilize both paracrine and autocrine mechanisms. The transition from fruit flies to humans has been fairly smooth (Klaus & Birchmeier, 2008) Wnt1, Wnt3, and Wnt7a are among the strongest WNTs in terms of transformation. Wnt2, Wnt4, Wnt5a, Wnt5b, Wnt6, and Wnt11, on the other hand, are not. Frizzled proteins, also known as PDZ receptors, are involved in both the canonical and non-canonical modes of signal transduction. The Wnt

signalling system affects cell motility, cell polarization, and cell fate determination, in addition to its role in organogenesis and brain development (Schinner, 2009). Cancer is associated with the disruption of the 42 Wnt signalling pathway. Figure 1.12 depicts the hallmark of cancer associated with Wnt signalling dysregulation.

1.6.1 Wnt signalling targets

The Wnt signalling pathway also has two types of effects: canonical and non-canonical (planar cell polarity and calcium pathway) (Huelsken & Behrens, 2002). When the signalling pathway is activated, the Wnt ligand binds to the Frizzled receptor (a G-coupled receptor) along with other proteins such as low-density lipoprotein receptor-related protein 5/6 (LRP5/6), receptor tyrosine kinase RTK and receptor tyrosine kinase-like orphan receptor 2 ROR2 (Zhou et al., 2014). From there, the signal is relayed to Dsh, which can then lead to one of three pathways. Stable β-catenin is translocated to the nucleus by the canonical pathway, where it activates T-cell factor/lymphoid enhancer factor TCF/LEF, which would otherwise be destroyed by the destruction box (Axin, APC, Protein phosphatase 2 (PP2A), GSK3, and CK1)(Ghosh et al., 2019). The activated Dsh forms a complex with DAAM1 in the non-canonical (Akoumianakis et al., 2022) planar cell polarity, which activates the RHO pathway (reconstruction of the cytoskeleton) (Figure 1.13). The Fz receptor is directly associated with the G protein and Dsh in the non-canonical calcium pathway. The activated complex then phosphorylates PLC, IP3 and PKG, to control cell adhesion and migration (Duchartre et al., 2016). Two molecules, referred to respectively as Small Frizzled-Related Protein (sFRP) and Dickkopf (Dkk) kinase, can regulate Wnt signalling. When sFRP molecules bind to Wnt ligands, canonical signalling is activated; however, when Dkk molecules bind to the subunits of the Wnt receptor, this activation is prevented. Compared to the huge sFRP family (which includes sFRP, WIF1, and Cerberus), the dynein light chain family lacking kinesin (Dkk) is quite small (Dkk1 to Dkk4). By analyzing the expression pattern of endogenous Wnt antagonists, the authors can infer the presence of a Wnt feedback loop during the process of osteoblast formation in mice (S. Thomas & Jaganathan, 2022). In addition to cancer, the dysregulation of Wnt signalling can induce some other disorders, such as loss of trabecular bone caused by LRP6 mutations in adult osteoblasts, whereas low bone mineral density is associated with LRP5 mutations (heterozygous mice with LRP5 and LRP6 receptor mutations exhibit limb deformities (Riddle et al., 2013) However, a mutation in the coding sequence of LRP5

causes gain of function and resistance to inhibition by Dickkopf 1 (Dkk1), resulting in increased bone density (Ai et al., 2005). Reduction of Wnt expression after conditional deletion of Wls (wntless) was found to negatively affect osteoblast growth and mineralization (Regard et al., 2012).

1.6.2 Wnt in breast cancer

Defective Wnt signalling is associated with a variety of cancers, including breast cancer. Blocking Wnt causes breast cancer cells to become less aggressive and develop more slowly. Malignant mammary gland neoplasms arise in mice with mutations in the Wnt signalling system (Howe & Brown, 2004). Slug, a key regulator of the epithelial-mesenchymal transition (EMT) system was discovered to be regulated by the canonical Wnt/GSK3/β-Trcp1 axis. Early-onset basal-like breast cancer is characterized by high levels of Slug and low expression of the tumour suppressor gene breast cancer 1, and recent research suggests that Wnt signalling may play a role in its development (BRCA1). Slug directly suppresses *BRCA1* expression by activating the chromatin demethylase LSD1 by interacting with an E-box motif in the BRCA1 promoter. These results suggest that Slug, EMT, and BRCA1 expression are regulated by canonical Wnt signalling (Wu et al., 2012). The small drug CWP232228 decreased the viability and proliferation of BCSCs generated from both primary and metastatic breast cancer cell lines. BCSCs exhibited decreased expression of Wnt/β-catenin target genes, decreased nuclear localization of β-catenin, and increased apoptosis in response to the inhibitory effects of CWP232228. Notably, CWP232228 inhibited the growth of BCSCs more effectively than non-BCSCs, showing its preference for targeting BCSCs (Jang et al., 2015).

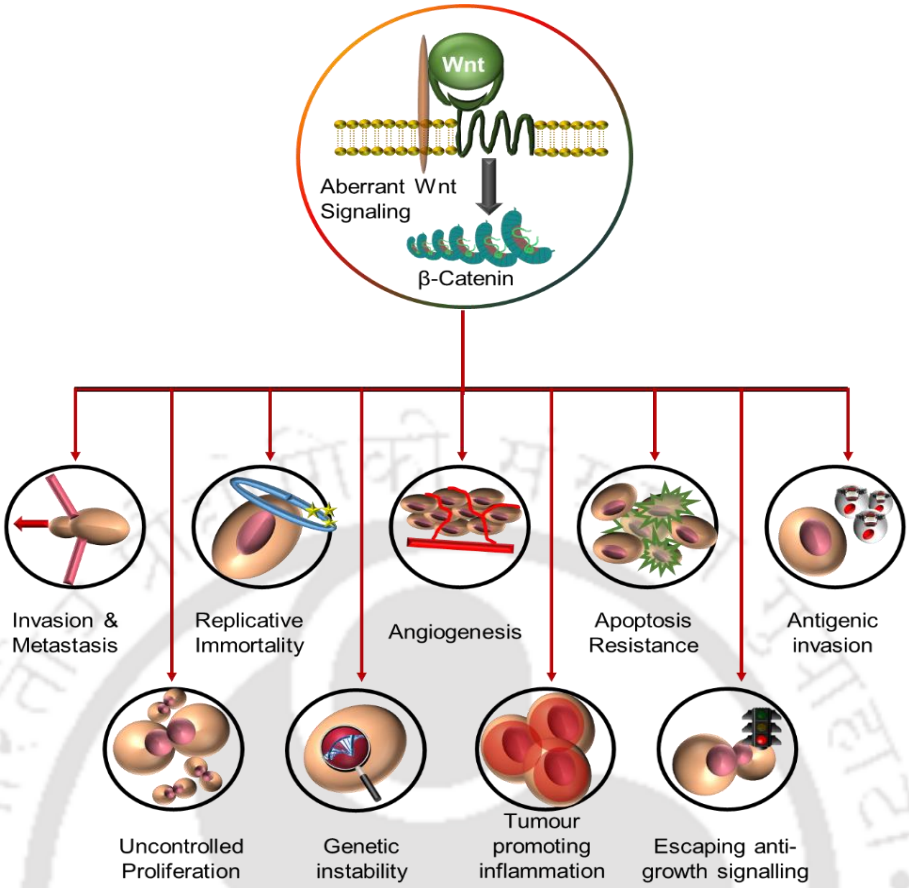

Figure 1.12: Wnt signalling in cancer*. The image depicted an essential characteristic of cancer governed by Wnt signalling. The binding of Wnt to its receptor prevents the degradation of β-catenin, stabilises its translocation to the nucleus, and regulates multiple functions that promote malignancy. Apoptosis-resistant cells evade programmed cell death, an essential step for maintaining a healthy ratio of healthy to unhealthy cells. Invasion and metastasis, which encourage cancer cells to invade adjacent tissue and colonise new sites, are a second characteristic. The combination of replicative immortality and unbridled proliferation encourages unrestricted cell division. For cancerous cells to develop unrestrictedly, new blood vessels are required to supply them with nutrients continuously. Escaping antigrowth signals and immune invasion contribute to the progression of cancer's growth. Nonetheless, genetic instability is the greatest threat to cancer development, as irreversible genetic alterations and unstable DNA content continuously produce mutated or malignant cells (Zhong et al.,2020).*

One of the research suggests that c-Myb may enhance the invasion and metastasis of breast cancer via the Wnt/β-catenin signalling pathway. c-Myb boosted Wnt/β-catenin signalling mechanistically by elevating the expression of β-catenin and its downstream target genes, including Axin2. In consequence, Axin2 downregulation contributed to the activation of the Wnt/β-catenin pathway and improved the invasion and metastasis of breast cancer cells (Yihao Li et al., 2016).

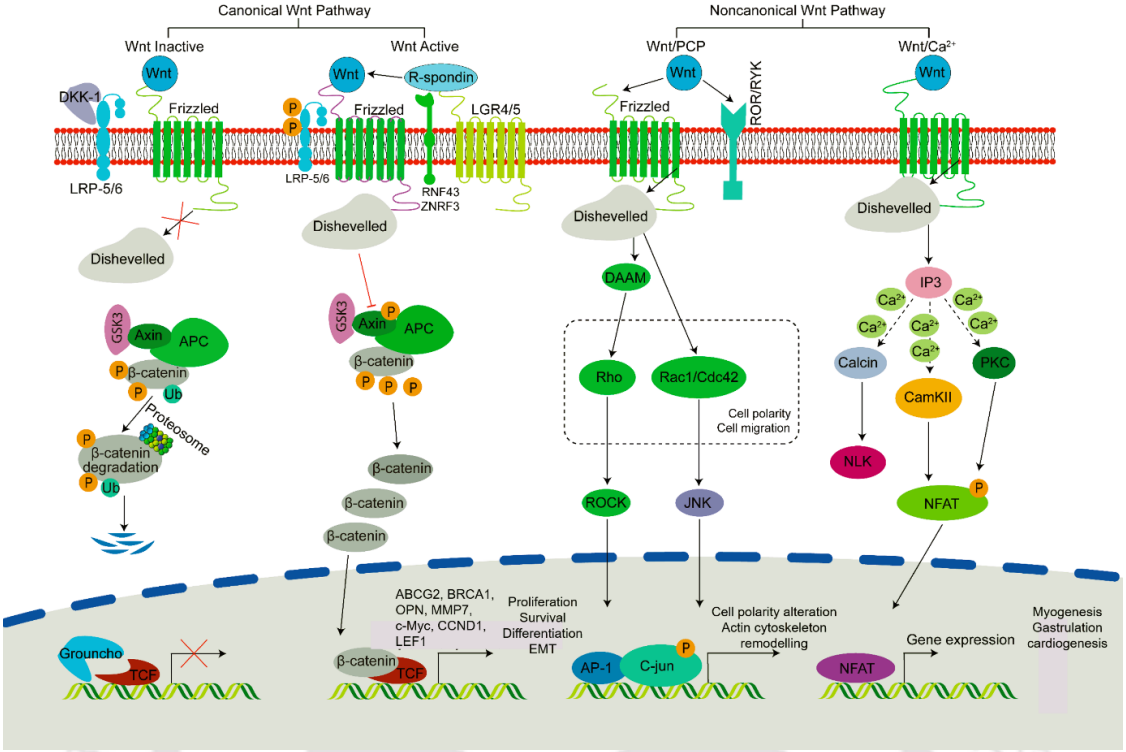

Figure 1.13: Wnt signalling pathway*. The binding of a Wnt ligand to a receptor complex on the cell surface starts a sequence of intracellular signalling events that make up the Wnt signalling pathway. The canonical pathway and the non-canonical pathway are the two primary branches of the Wnt pathway. The canonical Wnt pathway also called the β-catenin pathway, activates β-catenin and subsequently controls the expression of several genes, including ABCG2, MMP7, cMyc, CCND1, BRCA1, LEF1, and many more, promoting survival, differentiation, proliferation, and EMT. Again, two mechanisms control the non-canonical Wnt pathway: Rho/Rac1/cdc42, which activate ROCK and JNK, and control cell polarity and actin-cytoskeleton remodelling. The other approach is calcium-dependent planar cell polarity, in which signals are transferred by IP3 and then processed by calcin, CamKII, and PKC. The signals from calcin are transmitted via NLK and CamKII, and PKC transmits via NFAT. The activated NFAT regulates downstream transcription factors which regulate myogenesis, cardiogenesis and gastrulation (Haseeb et al., 2019).*

Several studies have shown that SPATS1(Spermatogenesis associated serine-rich 1) regulates gene transcription by blocking the traditional Wnt signalling pathway (Zhan et al., 2017). Some believe that the role of FSTL1 in regulating cellular signalling networks is one way it contributes to disease. This finding supports the idea that FSTL1 is required for CDDP (cis-diamminedichloroplatinum(II)) and doxorubicin chemoresistance in breast cancer cell lines. FSTL1 enhances Wnt/β-catenin signalling via integrin 3 in top/flip-out during colony formation and tumour sphere assays. Using luciferase studies to screen for additional microRNAs, it was discovered that miR-137 inhibits both mRNA and protein expression of FSTL1. The miR-137/FSTL1/integrin/3/5/Wnt/β-catenin axis regulates stem cell formation and chemoresistance in breast cancer (Cheng et al., 2019). Recent research

reveals that breast cancer spread can be facilitated by a kind of inflammation triggered by the loss of the tumour suppressor gene *p53*. According to the results, chronic neutrophilic inflammation is triggered when *p53* is depleted because cancer cells release more of IL-1β. The inflammatory response facilitates the metastasis of cancer cells to other organs (Wellenstein et al., 2019). Due to its occurrence in human cancers, the Wnt/β-catenin signalling system has been the focus of many potential cancer treatment discoveries (Jung & Park, 2020).

In breast cancer, crosstalk has been documented between the Wnt pathway and other signalling pathways, such as the estrogen receptor (ER) and Her2 pathways. For instance, estrogen can activate the Wnt pathway by inducing the production of Wnt ligands and receptors. By decreasing GSK-3, a negative regulator of the Wnt pathway, Her2 signalling can also activate the Wnt pathway. Targeting the Wnt pathway is a potential therapeutic method for the treatment of breast cancer. Multiple Wnt inhibitors have been produced and are now being assessed in preclinical and clinical trials. These include small chemicals that target the Wnt pathway, antibodies that inhibit Wnt ligands or receptors, and naturally occurring substances that regulate the Wnt system. To completely comprehend the complicated role of Wnt signalling in breast cancer and to create successfully targeted therapeutics, additional study is required.

1.7 Cross-talk between BMP4, RHOA and WNT signalling

Bone morphogenetic proteins (BMPs), RHO family GTPases, Rho-associated protein kinases (ROCKs), and Wnt signalling pathways are all essential regulators of several cellular processes, such as cell proliferation, differentiation, migration, and apoptosis. The dysregulation of these pathways has been linked to the genesis and progression of numerous cancer types. Both embryonic and adult cell development are affected by BMP and Wnt signalling pathways. The discovery of common signalling pathways has allowed researchers to map the interconnected gene networks in humans, frogs, zebrafish, and fruit flies. Recent research has shown that BMP signalling pathways are associated with both apoptosis and proliferation. The link between mitogen-activated protein (BMP) and the Wnt signalling pathway was discovered by (Huang et al., 2004) through mutations in mammalian cells.

To comprehend the overall process of cancer advancement, several studies were conducted to determine the intricate relationship between distinct signalling pathways. In

gastrointestinal (GI) epithelial cells, epithelial Hedgehog promotes WNT2B and BMP4, whereas mesenchymal BMP creates IHH. An increase in SHH and WNT2B expression is associated with NF-κB and inflammatory bowel disease (IBD). Overexpression of WNT2B has deleterious effects on embryonic development, normal tissue function, and tumourigenesis (Masuko Katoh & Katoh, 2009). In the same context, another research was done which said that WNT and FGF cross-talk increases β-catenin and nuclear factor of activated T cells (NFAT). The transcription factors SFRP1, JAG2, and FOXL1 become activated in response to hedgehog signals. The WNT-FGF-Notch and BMP-Hedgehog signalling pathways must be properly controlled to preserve stem and progenitor cell homeostasis (Masaru Katoh, 2007).

A similar study concluded that osteolytic cancer cells produce Gli2-dependent PTHrP from TGF-β signalling. Oncogenic tumour cells that damage bone express Gli2 via Wnt signalling. Overexpression of β-catenin/TCF4 or LiCl increased Gli2 and PTHRP in osteolytic cancer cells. Therefore, treatments that target TGF-β are being developed to disrupt Wnt signalling and thereby reduce cancer cell vulnerability to the bone microenvironment (Turner et al., 2014). The expression of SMAD4, p53, and β-catenin was examined in CRC invasive fronts. To a high extent, β-catenin is present in CRCs lacking SMAD4 and/or in which p53 is aberrant (84%). BMP suppresses Wnt signalling in Colorectal cancer when p53 and SMAD4 are functional. Activation of Wnt signalling by BMP is possible when SMAD4 is absent. The effect of BMP on Wnt requires the presence of p53 (Voorneveld et al., 2015).

FPPS is an enzyme that makes isoprenoids, which are lipid molecules that are needed for signalling and the formation of cell membranes. The study discovered that TGF-1 caused NSCLC cells to make more FPPS and that if FPPS was turned off, TGF-1's ability to cause invasion and EMT was stopped. The study also demonstrated that TGF-1 turned on the RHOA/Rock1 signalling pathway, which was needed for invasion and EMT caused by TGF-1. When FPPS was taken away, TGF-1's effect on the RHOA/Rock1 pathway was stopped. This suggests that FPPS controls invasion and EMT caused by TGF-1 through the RHOA/Rock1 pathway (Parrotta et al., 2021). The study discovered that the WNT pathway dynamics were transient in the absence of TGF-β signalling, implying that the route was only engaged briefly during the early phases of differentiation. However, there was a synergy between the TGF-β and WNT pathways when TGF-β signalling was present, which resulted in long-lasting WNT pathway activation. The maintenance of the

pluripotent state and the inhibition of differentiation were the outcomes of this long-term stimulation of the WNT pathway (Massey et al., 2019).

Ganoderal A, a naturally occurring substance derived from the medicinal mushroom Ganoderma lucidum, promoted the differentiation of human amniotic mesenchymal cells into osteoblasts by increasing bone-specific markers such as alkaline phosphatase, osteocalcin, osteopontin, and runt-related transcription factor 2. More research indicates that ganoderal A can stimulate both Wnt and BMP signalling, hence speeding osteogenesis, demonstrating cross-talk between the Wnt and BMP pathways (Wang et al., 2020).

However, colorectal cancer is not triggered by RHOA activation. Over-activation of Wnt/β-catenin by RHOA inactivation promotes colorectal cancer progression and metastasis. Similar to what is seen in mouse intestinal carcinogenesis, inactivating RHOA in human colon cancer cells enhances Wnt/β-catenin signalling and leads to increased proliferation, invasion, and de-differentiation. By enhancing Wnt/β-catenin signalling, RHOA suppresses the progression of colorectal cancer (Rodrigues et al., 2014a). Studies have shown that the activation and nuclearization of RHOA can represent the loss of the chondrocyte phenotype through its interaction with the Wnt signalling pathway. Blocking RHOA signalling causes the expression of 2D surface chondrogenic markers and reduces Wnt signalling. Wnt signalling activation results in the production of 2D chondrogenic markers, demonstrating the context dependence of RHOA's activity (Öztürk et al., 2017). The study found that the dysregulation of the Wnt signalling pathway in iPSC-derived Arrhythmogenic right ventricular cardiomyopathy was associated with the activation of the Rho signalling pathway. Specifically, the study showed that the overexpression of the Wnt signalling pathway led to the activation of RHOA, which in turn caused a decrease in the levels of Connexin-43 (Cx43), a protein responsible for maintaining the electrical coupling between cardiomyocytes (Parrotta et al., 2021).

According to new research, statin use may reduce the occurrence of colon cancer by 50% and increase patient lifetime through unidentified processes. In APC^{min} mice, lovastatin treatment improved colon cancer, spleen enlargement, and peripheral anaemia. Researchers discovered that lovastatin suppressed Wnt/β-catenin and YAP/TAZ signalling in colonic mass tissues using RT-PCR. Transcriptomic analysis revealed that lovastatin influenced cell growth pathways in RKO. When lovastatin is injected into RKO cells, it prevents β-catenin, TAZ, and p-LATS1 from acting. Lovastatin inhibited RHOA activity, which

reduced Wnt/β-catenin and Wnt-YAP/TAZ signalling in colon cancer cells. Colorectal cancer treatment options may include the use of statins, which have been shown to inhibit tumour growth. These findings support the idea that statins have applications beyond cardiovascular disease and suggest new approaches to the cancer problem (Yi Xiao et al., 2022).

Wnt plays a function in cancer initiation and progression, although its relevance in stem cell biology is uncertain. In recent years, however, research has led to a greater understanding of the receptors involved in tumour growth, allowing the development of drugs that target this system directly. The Wnt pathway is important in cancer biology and drug resistance (Shaw et al., 2019).

Recent research indicates that the BMP, RHO-ROCK, and Wnt signalling pathways interact extensively in cancer. This crosstalk is regulated by multiple molecular processes, such as protein-protein interactions, transcriptional control, and post-translational changes. BMP signalling inhibits Wnt signalling by promoting the production of the Wnt antagonists secreted frizzled-related proteins (sFRPs) and Dickkopf-1 (DKK-1). Additionally, BMP signalling can stimulate RHOA, which in turn promotes RHO-ROCK signalling, resulting in enhanced cell motility and invasion. By stimulating the production of BMP ligands and antagonists, Wnt signalling can control BMP signalling. Wnt signalling can also stimulate RHO-ROCK signalling by elevating the expression of RHO GTPases and ROCKs, resulting in enhanced cell motility and invasion. In addition to activating Wnt signalling, RHO-ROCK signalling increases the expression of Wnt ligands and receptors. Overall, the cross-talk between the BMP, RHO-ROCK, and Wnt signalling pathways plays a significant role in the formation and progression of cancer. Targeting these pathways singly or in combination may provide a potential therapeutic strategy for the treatment of numerous cancer types.

1.8 Cancer treatments and limitations

Breast cancer treatment options range from surgery and radiation to chemotherapy and targeted therapies; choosing the right one for each patient depends on factors including their general health and the disease's stage of progression. While these treatments have greatly improved the prognosis for patients whose cancer has not spread to other parts of the body, metastatic cancer remains a major health risk. To fully comprehend and control the spread of metastatic cancer, extensive research into various aspects of the disease is still

necessary. Although research has improved medical science's efforts to treat cancer, there are still several restrictions that lower cancer therapy success rates. Here are a few examples of this limitation: Chemoresistance has been the most problematic issue in cancer treatment. The majority of individuals acquire resistance to the available chemotherapy drugs. The side effects of chemotherapy medications, such as decreased immunity, nausea, hair loss, and exhaustion, are also cause for concern. People are unable to afford combined chemo, surgery, and radiation therapy sessions. Cancer patients are not the only ones who experience worry, stress, and sadness; their loved ones are also affected. Furthermore, the majority of women were unaware they had breast cancer until it had progressed to other regions of their bodies, which could be owing to a lack of general knowledge or a limited screening system or facility in their area. Due to these constraints, we were obligated to examine the underlying core biology of breast cancer to discover an effective therapeutic target to combat cancer and improve patient outcomes.

Aim and Objectives

2.1 Aim

Several signalling pathways contribute to cancer development and metastasis. Although several studies have been done to identify the signalling pathways important for cancer metastasis, effective treatment strategies are still not available. Recent shreds of evidence have found a role for BMP signalling in regulating several stages of cancer progression, such as proliferation, survival, metastasis and chemoresistance. Studies have shown that BMP signalling plays a context-dependent role in breast cancer progression and metastasis. BMP signalling has been implicated in the progression of other cancer types; for example, BMP2 inhibits pancreatic cancer but promotes breast cancer. On the contrary, BMP7 inhibits breast cancer but promotes pancreatic cancer, and BMP6 promotes renal cancer and inhibits breast cancer. The context-dependent behaviour of BMP molecules has made it difficult to utilize or target BMP signalling for therapeutic purposes.

The purpose of our study is to understand the various mechanisms through which BMP signalling controls the progression of different breast cancer sub-types. The study also aims to understand whether there is a stage-specific role for BMP signalling in controlling breast cancer proliferation, metastasis and chemoresistance. In addition, the study also focused on understanding the role of the RHO-ROCK signalling pathway in regulating breast cancer progression. RHO-ROCK signalling modulates motility and invasion by modifying the actin cytoskeleton. Abundant proteins, such as BNIP-2, Net1, NRF2, RhoGAPs (ARHGAP10, ARHGAP18), BAG6, Tiam1, and many others, have been studied for their ability to inhibit cell growth and migration. These proteins primarily affect the function of PAK, ROCK, and MRCK, which modifies the downstream signalling. In this study, in addition to inhibiting ROCK, the GTPase RHOA was silenced and its effect on breast cancer cells was analysed. RHO-ROCK signalling pathway is activated by a variety of growth factors, but it is also regulated by a non-canonical Wnt signalling pathway.

Recent research has made Wnt an immensely popular subject signalling pathway in the quest of curing osteolysis.

Blocking Wnt signalling through the BMP, Rho-ROCK, Notch, and FGF-regulated pathways appeared to be successful in the case of breast cancer. It is unclear, though, whether the process only involves forward signalling or if there is also some reverse or feedback signalling that inhibits cancer. Therefore, in the current study, the role of BMP, Rho-ROCK, and Wnt signalling was studied as a means of combinatorial therapy for combating metastatic breast cancer.

2.2 Objectives

Given the high incidence and mortality rate associated with breast cancer, the current study aimed to investigate the role of BMP, RHOA, and Wnt signalling in cancer metastasis at each stage of the disease.

1. Screening of BMP4, RHOA and Wnt signalling components in breast cancer cells
2. To study the role of BMP4 signalling in breast cancer proliferation, migration and chemoresistance.
3. To investigate the role of RHOA and Wnt signalling in breast cancer proliferation and migration
4. To understand the crosstalk between BMP4, RHOA and Wnt signalling pathways for developing a combinatorial therapeutic strategy.

Materials and Methods

3.1 Cell culture

3.1.1 Materials

3.1.1.1 Chemicals and reagents

1X Trypsin (0.25%)

Diluted in ice-cold sterile 1X PBS at a ratio of 1:10 for working stock Aliquots were stored at -20℃ for long-term storage.

Trypan blue (0.4%)

0.4 g of trypan blue powder (dye composition 40%) was added to 100 ml of 1X PBS. Sterilized by filtration with a sterile filtration unit (0.22 µM) and stored at 4℃ for long-term storage.

Crystal violet (0.5%)

Crystal violet is prepared by dissolving in water with 25% methanol (v/v).

Paraformaldehyde solution (4%)

4 g of paraformaldehyde was added to 80 ml of 1X PBS and heated at 55 until it dissolved well. The pH was adjusted to 7.2-7.4 by dropwise addition of 5N-HCl with constant stirring. The volume was adjusted to 100 ml with 1X PBS, filtered with a 0.22µM filter and stored at -20°C for long-term storage.

Formaldehyde solution (4%)

37%-41% formaldehyde solution diluted in 1X PBS at a ratio of 1:10 as a working stock

Noble agar (1%)

1 g of noble agar was dissolved in 100 ml of 1X PBS, autoclaved for 15 minutes at 15 lbs pressure (121℃) and stored at 4°C.

Ponceau Stain

A pinch of Ponceau powder was added to 10ml of ddH_2O with 300µl of glacial acetic acid and the final volume was made up to 40ml.

Propidium iodide solution

1mg/ml of PI was dissolved in 1X PBS and stored at -20℃ in the dark.

Triton-x-100 solution 0.1% (v/v) prepared in 1X PBS

Tween® 20 for synthesis 0.1%(v/v) prepared in 1X TBS

Sure Cast Acrylamide: bis-acrylamide (29:1) solution

SureCast TEMED (N, N, N', N-tetramethylethylenediamine)

SureCast APS (Ammonium persulfate)

PEI (polycation polyethylenimine)

Polybrene

Puromycin (2 µg/ml)

PowerUp™ SYBR™ Green Master Mix

Bio-Rad ECL (Enhanced chemiluminescence) with peroxide reagent and luminol/enhancer reagent.

MitoSOX™ Red mitochondrial superoxide indicator

4',6-diamidino-2-phenylindole (DAPI) solution (1mg/ml)

Recombinant human BMP4

LDN193189- dihydrochloride

Y27632- dihydrochloride

Doxorubicin hydrochloride

collagen solution from calfskin

Pure Link™ RNA mini kit

High-Capacity cDNA Reverse Transcription Kit

3.1.1.2 Buffers

Phosphate-buffered saline (PBS)

80 g NaCl, 2 g KCl, 14.4 g Na2HPO4, and 2.4 g KH2PO4 were dissolved in 800 ml autoclaved, deionized, distilled water to prepare 10X, 1 L PBS. The pH was adjusted to 7.2-7.4 by dropwise addition of 5N-NaOH with constant stirring. The volume was made up to 1000 ml and filtered with a 0.22µM filter and stored at room temperature. For the working concentration, the stock was diluted 1:10 with distilled water.

RBC lysis buffer

2.005 g NH_4Cl, 9.25 mg ethylenedinitrilotetraacetic acid disodium salt titriplex- III reagent and 0.21 g $NaHCO_3$ dissolved in 200 ml autoclaved deionized distilled water. The pH was adjusted to 7.2-7.4 by dropwise addition of 5N-HCl with constant stirring. The volume was adjusted to 250 ml and filtered with a 0.22µM filter and stored at 4°C.

RIPA buffer

Add 25mM Tris-Cl (pH-7.4), 150mM NaCl, 1% Na-deoxycholate, 1%, NP -40, 0.1% sodium dodecyl sulfate, 1mM-EDTA and a 1mM protease inhibitor in distilled water.

5X SDS Loading Sample buffer

Add Tris-Base 0.25M (pH 6.8), 20% SDS, 50% glycerol and a pinch of bromophenol blue to distilled water. Vortex, aliquot and store at 4°C.

Note: Add β-mercaptoethanol (10% v/v) just before use.

SureCast Resolving buffer (1.5M Tris base, pH 8.8)

SureCast Stacking buffer (0.5M Tris-HCl, pH 6.8)

Tris-Glycine SDS-Running buffer

30 g Tris-Base and 144 g glycine were dissolved in 800 ml autoclaved, deionized, distilled water to make 10X, 1 L. The pH was adjusted to 8.3 and the volume was made up to 1000 ml. To the final solution, 1% SDS was added.

Tris-Glycine-Transfer buffer

30.2 g Tris base and 144 g glycine were dissolved in 800 ml autoclaved, deionized, distilled water and made up to 1 L to prepare 10X.

Note: pH adjustment is not required. 20% methanol was added before the use

Tris Buffered Saline buffer

24 g of Tris base and NaCl-88 g were dissolved in 800 ml of autoclaved, deionized, distilled water to make up 10X, 1 L. The pH was adjusted to 7.6 and the volume was made up to 1000 ml.

Note: 0.1% Tween-20 was added before the use.

Tris-acetate EDTA buffer

60.5 g of Tris base, 16.275 ml of glacial acetic acid and 25 ml of 0.5M EDTA were dissolved in 200 ml of deionized, distilled water and the volume was made up to 250 ml to prepare 50X.

Note: pH adjustment is not required

Staining buffer

0.5% (w/v) bovine serum albumin in 1X PBS

2% (v/v) FBS in 1X PBS

Blocking buffer

5% (w/v) Bovine Serum Albumin in 1X PBS

Skim Milk Powder in 1X-TBST

3.1.1.3 Antibodies

Fluorescently conjugated antibodies (anti-human antibodies)	Western blot Primary antibodies (anti-human antibodies)
• CD44 (Cat #555478) • CD24(Cat #17-0247-42) • EpCAM (Cat #MA5-38715) • CD49b (Cat #555498) • CD49c (Cat #556025) • CD49e (Cat #555617) • CD49f (Cat #555736) • N-cadherin (Cat #561554) • pSMAD1/5/8 (Cat #BS-3418R) • pSMAD2/3 (Cat #PA5-36125) • pERK1/2 (Cat #612592)	• E-cadherin (Cat #13-5700) • N-cadherin (Cat #MA5-15633) • β-catenin (Cat #500-8864) • pERK1/2 (Cat #MA5-15134) • pSMAD1/5/8 (Cat #BS-3418R) • BCL2 (Cat #13-8800) • BMP4 (Cat #MA5-15572) • BMPRIA (Cat #MA5-17036) • BMPRII (Cat #PA5-47949) • RHOA (Cat. # ARH04) • GAPDH (Cat #MA1-16757)

Immunostaining antibodies

Phalloidin-TRITC (Cat # R415), E-cadherin (Cat #13-5700), RHOA (Cat #ARH04), and β-catenin (Cat #500-8864).

HRP-conjugated secondary antibodies

Donkey-anti-rabbit (Cat # A-31573), Goat anti-mouse (Cat # 31430), Donkey-anti-goat (Cat # A-21082).

Note: Anti-RHOA antibody was obtained from Cytoskeleton (USA), while primary antibodies against anti-GAPDH, anti-E-cadherin, anti-N-cadherin, anti-phospho ERK1/2, anti-phospho SMAD1/5, anti-beta catenin, anti-BCL2, anti-BMP4, anti-BMPRIA, and anti-BMPRII were acquired from Invitrogen (ThermoFisher Scientific, India). Donkey

anti-goat, goat anti-rabbit, and goat anti-mouse HRP conjugated secondary antibodies were acquired from Invitrogen (ThermoFisher Scientific, India). BD Biosciences (India) supplied fluorescently conjugated antibodies targeting phospho-SMAD1/8, phospho-SMAD2/3, CD44, CD49F, and KI67. Invitrogen supplied fluorescently conjugated anti-CD24 and anti-EPCAM.

3.1.1.4 Media

DMEM- HG (Dulbecco's Modified Eagle Medium-High Glucose)

Supplemented with 3.7g/L sodium bicarbonate, 100X penicillin/streptomycin and 10% fetal bovine serum. Filtered with a 0.22µM filter and stored at 4°C.

DMEM- LG (Dulbecco's Modified Eagle Medium-low Glucose)

Supplemented with 3.7g/L sodium bicarbonate, 100X penicillin/streptomycin and 10% fetal bovine serum. Filtered with a 0.22µM filter and stored at 4°C.

RPMI 1640 (Roswell Park Memorial Institute)

Supplemented with 2g/L sodium bicarbonate, 100X penicillin/streptomycin, 10% fetal bovine serum and 2mM L-glutamine. Filtered with a 0.22µM filter and stored at 4°C

McCoy's 5A Medium

Supplemented with 2.2g/L sodium bicarbonate, 100X penicillin/streptomycin and 10% fetal bovine serum. Filtered with a 0.22µM filter and stored at 4°C.

HEK media

DMEM- HG media supplemented with 100mM sodium pyruvate, 100X non-essential amino acids and 2mM L-glutamine. Filtered with a 0.22µM filter and stored at 4°C.

3.1.1.5 Cell lines

ZR75.1 (ER^+ PR^- $Her2^-$)

MCF7 (ER^+ PR^+ $Her2^-$)

SKBR3 (ER^- PR^- $Her2^+$)

MDA-MB-231 (ER^- PR^- $Her2^-$)

Stromal Cells

3.1.2 Methods

3.1.2.1 Maintenance of breast cancer cell lines

Breast cancer cell lines ZR75.1, MCF7, SKBR3, and MDA-MB -231 were obtained from the National Center for Cell Science (NCCS) in Pune, India. MCF7 and MDA-MB -231 were cultured in HG-DMEM, SKBR3 in McCoy's-5A, and ZR75.1 in RPMI media supplemented with 10% fetal bovine serum and 1X penicillin/streptomycin solution.

The well-grown cells were aseptically transferred to the BSL2 chamber, and the medium from the cell culture dish was transferred to a Falcon tube. The plate was then rinsed with sterile 1X PBS, followed by the addition of 0.25% 1X trypsin-EDTA. After 3 to 4 minutes (incubation time varies depending on cell type), the dish was examined under a microscope to determine if any cells had detached. Harvested cells were collected and reseeded at the correct density. MDA-MB -231, MCF7, and ZR75.1 cells were sub-cultured every 3 to 4 days at a ratio of 1:3, whereas SKBR3 cells were sub-cultured every 5 to 6 days at a ratio of 1:2.

3.1.2.2 Cryopreservation and thawing of cancer cell lines

Harvested cells were pelleted by centrifugation at 300g for 7 min at 4°C before resuspension in FBS. The beforehand prepared 20% DMSO in FBS was added to the resuspended cells at a ratio of 1:1. The vials were placed directly in the cryocooler, where they were refrigerated for approximately 16 hours before being stored at -80°C for long-term storage (6-8 months).

The frozen vial was thawed by placing it in a 37°C water bath for 10 to 15 seconds, or until half of the contents began to thaw. The vial was then aseptically transferred to BSL2 and the cells were shifted to a Falcon tube containing pre-warmed growth media. The cells were centrifuged at 300g for 5-7 minutes at 4°C and the pellet was resuspended in fresh growth media. The cells were seeded into a cell culture dish and incubated for 18 to 24 hours until adherence. The next day, all medium was renewed and cells continued to grow until they reached 70-80% confluence.

3.1.2.3 Adherent culture

Cancer cell lines ZR75.1, SKBR3, MCF7 and MDA-MB-231 were seeded on tissue culture-treated plates. To ensure proper adhesion of the cells, the plates were incubated at

37°C in a humidified incubator containing 5% CO_2. The cells were treated with recombinant human BMP4 protein (10ng/ml), LDN193189 (1µM/ml), Y27632 (10µM/ml) and doxorubicin (5µM/ml) the next day and incubated for 48 hours. These treated cells were used for various experiments such as cell count analysis, live/dead population estimation, cell cycle/Ki67, phenotyping, MitoSOX staining, immunostaining, colony formation assay, wound healing assay (2D), gene expression analysis by RT-PCR, Western and flow cytometry.

3.1.2.4 Non-adherent culture

i. Under non-adherent conditions, cells were seeded together with the compounds on agar-coated wells for 48 hours. These cells were collected and the wells were rinsed with 1X PBS to ensure their thorough eradication. The collected cells were centrifuged at 300g for 7 minutes at 4°C and then resuspended in the experimentally required buffer. Cell count analysis, live/dead population estimation, phenotyping, colony formation assay, and Western blot analysis of gene expression were performed.

ii. In different situations with non-adherent conditions, cells were seeded on agar-coated wells for an extended period to measure spheroid development, spheroid migration, and protein expression using the Western blot technique.

3.1.2.5 Suspension culture

For the suspension culture, cells were seeded in a Falcon tube and placed in an incubator at 37°C and 100 RPM for 24 hrs. The cells were collected and processed for phenotyping, colony formation assay, and Western blot analysis.

3.1.2.6 Coculture of breast cancer cells with Stromal cells

The patient's bone marrow sample was used to isolate stromal cells. The stromal cells were sub-cultured and seeded at a seed density of 5000 cells/cm^2 in a flat bottom 96-well plate. Meanwhile, MDA-MB -231 and MCF7 were seeded at a seeding density of 500 cells/250 µl on agar-coated wells along with BMP4, LDN193189, and Y27632 in 48 well plates. The breast cancer cells were incubated in non-adherent conditions for 48 hours and entire cells were removed from each well in a separate Eppendorf. The Eppendorf was centrifuged at 300g for 5 minutes at 4°C and the cell pellet was re-suspended in 0.4ml of the new medium. From this cell mixture, 100µl of cells were added to 4 different wells of previously seeded

stromal cells and incubated for 10 days to form colonies. The number of colonies was counted under the microscope. After the 10th day of co-culture, ALP staining was performed and pictures were taken.

3.1.2.7 Cell count analysis

Cell number determination was performed using the trypan blue exclusion method. Adherent cells were trypsinized whereas cells seeded in a non-adherent environment and suspension were taken directly. The cells were washed with 1X PBS by centrifuging at 300g for 7 minutes at 4℃ and diluted with 0.4% trypan blue staining solution at a 1:1 ratio. The trypan blue-stained cells were placed between the hemocytometer (Neubauer chamber) and the glass coverslip. Since only the dead cells are stained with trypan blue, the dead cells appear blue and the live cells appear white. For the final cell count, the cell counts in four chambers (A, B, C, and D) were substituted into the following formula.

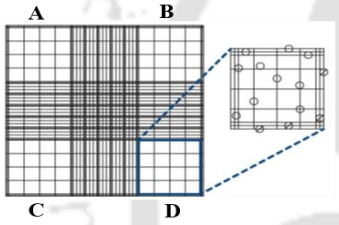

$$\frac{\text{Total Number of cells counted in 4 quadrant}}{\text{Number of quadrant (4)}} \times \text{Dilution factor} \times 10^4$$

The breast cancer cells were seeded at a specific seeding density. A cell count was performed for three consecutive passages to determine the length of time it takes for the cells to undergo two rounds of division. The final cell count that was acquired was entered into the formula that is provided below to calculate the amount of time that it takes for cancer cell lines to replicate.

$$\frac{\text{Time interval between two successive passage (hours)} \times \log 2}{\log(\text{final number of cells obtained}) - \log(\text{initial number of cells seeded})}$$

3.1.2.8 Live/dead analysis

Propidium iodide staining was used to determine the proportion of live and dead cells within a given population. Propidium iodide stains only dead cells. In adherent culture, cells were seeded and treated after 24 hours of cell adhesion, whereas in non-adherent conditions, cells were seeded onto agar-coated (1% noble-agar) wells along with the compounds. Similarly, for shear stress assay, cells were seeded at a density of 2*10^5/ml

in a Falcon tube and placed in an incubator at 37℃ and 100 RPM for 24 hours. Adherent culture cells were trypsinized and collected in RIA vials, whereas cells seeded on agar-coated wells and in suspension for shear stress were taken directly and collected in a tube. Cells were pelleted and washed with 1X PBS by centrifugation at 300g for 7 minutes at 4℃. Cells were resuspended in 2% FBS-PBS solution, and then 2µg/ml propidium iodide was added. The tubes were vortexed for 15-20 seconds to mix thoroughly and incubated in the dark for 15 minutes. Cells were examined using a BD FACSCalibur and changes in fluorescence shifts were measured. The percentage was first estimated by gating the population in the forward and side scatter channels. Then, the gated population was displayed in the forward side scatter channels and PI to calculate the percentage of live and dead cells.

3.1.2.9 Cell cycle/Ki67 analysis

Trypsinized cells were washed with 1X PBS by centrifugation at 300g for 7 min at 4℃. The cell pellet was fixed by dropwise addition of 1 ml of 70% ice-cold ethanol under constant vortexing at 1500 rpm. After overnight incubation at -20℃, the cells were washed with 1X PBS at a ratio of 1:9 (1 ml of cell mixture and 9 ml of 1X PBS) and centrifuged at 300g for 10 minutes at 4℃ to remove the ethanol. After washing with PBS, the cell pellet was resuspended in 100µl of 2%- FBS-PBS and the anti-Ki67 antibody was added. The tubes were vortexed for 30 seconds to ensure thorough mixing before incubation in the dark at room temperature for one hour. To reduce nonspecific binding, cells were washed with 1X PBS and incubated in RNase solution (100µg RNase-H in 1ml 1X PBS) for 30 minutes at 37℃ in a water bath. Cells were washed with 1X PBS and propidium iodide solution (50µg/ml) was added. After incubation for 15 minutes in the dark, cells were analysed by flow cytometry. The gated population of forward and side scatter were plotted in the PEA against PEW channels to obtain a singlet population, and a histogram was generated for the PEA channel to obtain the percentage of the population in the G1/S/G2 phase. To determine Ki67 negative populations, the gated population of forward and side scatter was plotted in the FITC against the PI channel.

3.1.2.10 Colony formation assay

To measure the ability of a single cell to form a colony of at least 50 cells by unrestricted cell division, in adherent culture, MDA-MB -231 and MCF -7 were seeded at 100 cells/well, whereas SKBR3 and ZR75.1 were seeded at 500 cells/well in a tissue culture-

treated 6-well plate. In non-adherent cultures, MDA-MB -231 and MCF -7 were seeded at 500 cells/well, while SKBR3 and ZR75.1 were seeded at 2000 cells/well for 48 hours on agar-coated wells along with compounds. Similarly, for suspension colony assay 10,000 cells/ml were seeded in a Falcon tube at 37°C for 24 hours with 100 RPM along with compounds. After incubation, non-adherent cells and suspension cells were collected and transferred to tissue-culture plates to form colonies.

To study the effects of pre-treatment, the medium was replaced with a fresh medium after 48 hours of incubation with the compounds. To study the effects of continuous treatment, cells were maintained in the media containing compounds until colonies were formed. MDA-MB -cell lines 231 and MCF -7 were incubated for 14 days, while SKBR3 and ZR75.1 were incubated for 21 days to form colonies. Colony plates were placed on ice and the medium was discarded. The plates were carefully rinsed with ice-cold 1X PBS and fixed on ice with 100% ice-cold methanol for 10 min. Crystal violet solution (0.5% crystal violet in 25% methanol) was added to the colony plates and incubated at room temperature for 2-3 hours or overnight at 4°C to allow the crystal violet dye to bind to the colonies. Colonies were counted and imaged using a microscope. Fiji software was used to calculate the colony area.

3.1.2.11 Spheroid formation assay

To mimic the 3D model of an *in vivo* culture, a test for spheroid formation was performed. For this purpose, the 96-well plate with U-bottom was coated with sterile 1% noble agar prepared in 1X PBS. The well-grown cell culture dish was trypsinized and the required number of cells was taken separately and placed in growth media. In advance, a medium containing rhBMP4, LDN193189, Y27632, and doxorubicin was prepared by reserving 2-fold of the desired concentration. Cells were seeded at a density of 2500 cells per 150 µl of medium and then another 150 µl of medium containing the compounds was added. The plates were centrifuged at 200g for 20 min at room temperature and kept in a CO_2 incubator at 37°C. Images were taken at four-day intervals to determine the effect of the compounds on spheroid formation and growth. Fiji software was used to calculate the area of the spheroid.

3.1.2.12 Phenotyping

Flow cytometry was used to study cell surface markers. The cells were processed as mentioned in the 3.14.5 section. The cell pellet was re-suspended in 2% FBS-PBS and

fluorescently labelled antibodies (CD44, CD24, EpCAM, CD49b, CD49c, CD49e, and CD49f) were added. Tubes were vortexed for 15 to 20 seconds before incubation on ice in the dark for 30 minutes. To avoid nonspecific signals, cells were washed with 1X PBS and propidium iodide (2 µg/ml) was added to distinguish between live and dead populations. Based on the excitation of the fluorescently conjugated antibodies, flow cytometric analysis was performed by gating populations from PI against forward-side scatter channels into the designated fluorophore channels.

3.1.2.13 Immunostaining

To observe the alignment and localization of the intracellular protein, cells were seeded on glass coverslips and treated with the compounds for 48 hours. The coverslip containing the cells was rinsed twice with 1X PBS and fixed with 4% paraformaldehyde (prepared in 1X PBS) by incubation at room temperature for 20 minutes. After washing, 0.05% Triton-X-100 (prepared in 1X PBS) solution was added to the coverslips to make the cell membrane permeable. Cells were washed and blocked with 5% bovine serum albumin or 2% FBS-PBS for one hour at room temperature or overnight at 4°C to avoid non-specific binding. Then, the primary antibody prepared in 2% FBS-PBS was added and incubated overnight at 4°C. To eliminate unbound primary antibodies, five 5-minute washes with 2% FBS-PBS were performed. The secondary antibody was then added and incubated overnight at 4°C. To detect the location of the nucleus, DAPI (1:2000) was added from a stock of 1 mg/ml after washing the cells with 2% FBS-PBS. The coverslips were placed on a glass slide along with a fluorescent mounting medium from Dakocytomation and dried for 24 hours. Images were then taken using a fluorescence microscope.

3.1.2.14 Migration assays

i. **2D migration assay**

To understand the effect of the compounds on the migration potential of breast cancer cells, MDA-MB -231 was seeded at a seeding density of 20,000 cells/cm^2, MCF -7 at 30,000 cells/cm^2, and SKBR3 at 40,000 cells/cm^2 and allowed to adhere for 24 hours. Once the cells reached 85-90% confluence, a 24-hour serum starvation was performed to inhibit the proliferation potential of the cells. A scratch was then created using a 200µl tip. The dead cells and debris were removed by washing the cells with 1X PBS. To test the effect of BMP4 protein, LDN193189 and Y27632 on migration, medium enriched with 2%-FBS was added along with the compounds

after creating a wound or scratch. Microscopic images of the scratched area were taken at regular intervals, maintaining the same reference point to estimate cell migration. T-Scratch software was used to calculate the area closed by the migrating cells and the formula below was used to calculate the migration rate of the cells in µm/hours.

$$\frac{(\text{Initial Open Area- Final Open area}) \times \text{Image Length (1280)} \times \text{Image Width (960)} \times \text{Magnification}}{(\text{Time interval} \times \text{Front} \times \text{Image Width (960)})}$$

The T-scratch software was used to measure the initial and final areas, and the image length and width are shown in pixels. The magnification value (5X) was 1.25, and since the cells migrate in both directions, the value for the front was set to 2. The time intervals were usually specified as 4 hours.

ii. 3D migration assay

First, spheroids were synthesized by seeding cells at a density of 2500 cells/well in U-bottom plates coated with noble agar. To generate proper spheroids, the plates were centrifuged at 200 g for 20 min at room temperature and incubated in a CO_2 incubator at 37°C for 5 days. Meanwhile, 96-well flat bottom tissue culture plates were coated with collagen (50µg/ml) prepared in 0.02N acetic acid and incubated for 2 hours at room temperature in a biosafety level 2. After the removal of the collagen solution, the wells were rinsed once with 1X PBS. Blocking was performed for one hour with 1% BSA prepared in 1X PBS at room temperature. After washing the plates with 1X PBS, 100 µl of 1X PBS was added to prevent drying before use. Once spheroids were formed, they were transferred to coated 96 flat bottom plates using a micropipette. The medium containing BMP4 (10ng/ml), LDN (1µM) and Y27632 (10µM/ml) was added slowly from the side of the wells to prevent displacement. The plates were left in the incubator for 30 minutes to allow spheroids to adhere. Images were then taken at 6-hour intervals to track the invasion of migrating cells derived from the spheroids through the collagen matrix. Fiji software was used to quantify the area covered by the cells.

3.1.2.15 Gene expression analysis

i. RNA isolation from breast cancer cells

To determine the changes in gene expression profile, treated cells were washed with ice-cold 1X PBS and cells were collected in lysis buffer and RNA isolation was done as described in the Pure Link™ RNA mini kit.

ii. RNA isolation from the tissue sample of breast cancer patients

Tissue samples were collected in collaboration with Dr Gayatri Gogoi from patients diagnosed with breast cancer and referred to the pathology department of Assam Medical College, Dibrugarh. Ethical approval for the study was obtained from the hospital and IIT Guwahati. Tumour samples were preserved in RNA-later aqueous solution immediately after surgery and stored at -80℃. To isolate RNA from the tumour samples, the tissue was removed from the RNA-later solution and placed in a mortar and pestle treated with DEPC. The tumour sample was crushed in the presence of liquid nitrogen and Trizol was added to the finely crushed tissue sample. The entire extract was collected in Eppendorf and centrifuged at 13000 rpm for 10 minutes to remove tissue debris. RNA was then isolated by the Trizol method. The RNA pellet was resuspended in RNase-treated water.

iii. Reverse transcription

The isolated 2µg RNA was reverse transcribed using the High-Capacity cDNA Reverse Transcription Kit followed by a thermal cycling condition of 25℃ for 10min, 37℃ for 120min and 85℃ for 5min.

iv. Real-time PCR

Real-time PCR was performed to quantify gene expressions. The reaction was performed in a CFX96 real-time PCR instrument. The conditions for RT-PCR were as follows: initial denaturation at 95℃ for 2 minutes, followed by 95℃ for 10 minutes. The cycling phase began with denaturation at 95℃ for 15 seconds, primer annealing and extension at 60℃ for 45 seconds for 35 cycles. The final extension was performed at 72℃ for 10 minutes. To obtain a melting curve, the temperature gradient is set as follows: 95℃ for 15 seconds, 60℃ for 1 minute, 95℃ for 30 seconds, and 60℃ for 30 seconds. PowerUp™ SYBR™ Green Master Mix was used to perform RT-PCR. The fold change in expression level was calculated using the ΔΔCt method.

v. Protein expression analysis using western blot techniques

To establish the protein profile, cells were seeded and incubated according to the experimental design. For adherent culture, cells were seeded and treated after 24 hours of cell adhesion. BMP4, LDN, and Y27632 were added and incubated for 48 hours. For the non-adherent conditions, cells were seeded into agar-coated wells along with the compounds and incubated for 48 hours. For shear stress conditions, cells were seeded at a density of 2*10^5/ml in a Falcon tube and incubated in an incubator at 37℃ and 100 RPM for 24 hours. MDA-MB -231 and MCF7 were also seeded on agar-coated wells to form spheroids for 11 days. The adherently seeded cells were then washed with ice-cold 1X PBS and RIPA buffer was added directly to the cells. Cells were scraped off with a scraper and the lysate was collected in an Eppendorf tube. For cells seeded onto agar-coated, suspension conditions and spheroid formation were collected directly in an ice-cold Falcon tube and washed with 1X PBS by centrifugation at 500g for 10 minutes at 4℃. Then the cell pellet was resuspended in RIPA buffer. The lysate was incubated on ice for 30 minutes and sonicated for 30 seconds, at an amplitude of 25 and ON-OFF cycles for 1 second and 4 seconds, respectively. To remove debris, cells were centrifuged at 13000 rpm for 10 minutes at 4℃. The supernatant was then collected and stored at -80℃ for long-term storage. To perform a Western blot, 5X- SDS loading dye (final 1X) and β- ME (10%) were added to the protein sample and incubated at 95℃ for 5 minutes, followed by 5 minutes on ice. The prepared samples were loaded onto a 10% acrylamide gel and transferred to a 0.22µM nitrocellulose membrane using a semi-dry transfer technique. The membrane was blocked with 5% skim milk to prevent non-specific antibody binding. A primary antibody (prepared in 1X TBST) was then added and incubated at 4℃ for 24 to 36 hours on a shaker. The membrane was washed five times with 1X TBST and then incubated with the appropriate HRP-conjugated secondary antibodies for approximately one hour. ECL substrate was used for detection after the membrane was washed with 1X TBST.

vi. Phospho-protein analysis using flow cytometry

Flow cytometric analysis was performed to determine the changes in phospho-protein levels. The MDA-MB -231 and MCF7 were seeded at a seed density of 5000 cells/cm^2 and incubated for 48 hours. After successful incubation, the dishes were removed and immediately placed in a water bath already set at 37℃ to maintain the cells in a phosphorylated state. The medium was discarded and the

dishes were washed with pre-warmed (37℃) 1X PBS. Trypsin was added and the dishes were incubated in a water bath for a few minutes to dislodge the cells. FBS (fetal bovine serum) was added to deactivate the effect of trypsin and the cells were immediately fixed with 4% paraformaldehyde. Cells were collected in RIA vials and incubated for 20 minutes at room temperature. Cells were pelleted and washed with a staining solution (0.5% BSA in PBS) by centrifuging the cells at 500g for 10 minutes at 4℃. For subsequent fixation, ice-cold 100% methanol was added dropwise to the pellet under continuous vortexing at 1500 rpm and incubated at 4℃ for 16 hours. The next day, cells were harvested and washed with a staining solution by centrifuging the cells at 500g and 4℃ for 10 minutes. Fluorescently labelled antibodies were added and incubated at room temperature for 1 hour in the dark. Washing was then performed to remove the nonspecific binding. Flow cytometric analysis was performed by plotting the gated population of FSC against SSC in specific fluorescence-conjugated antibody channels.

3.1.2.16 Lentiviral transduction of mammalian cells

i. Transfection

HEK293T cells were seeded at a seeding density of 70,000 cells/cm^2 in a 35-mm tissue culture dish and incubated at 37℃ with 5% CO_2 for 24 hours. The medium was replaced with a new medium just before the 2-hour transfection, and the transfection mixture (mentioned below) was carefully added dropwise to the plates.

Preparation of the transfection mixture

The transfection mixture was prepared in 100 µl of incomplete medium containing the plasmid of interest (2.38 µg) and the packaging plasmid (pMD -0.75 µg, p8.74-1.87 µg) with a total DNA amount of 5 µg. The PEI solution was added to the mixture so that the final concentration was 12 µg. The mixture was pulse vortex for 15 seconds and then incubated at room temperature for 10 minutes. After incubation, 600 µl of complete medium (37℃) was added to the transfection mixture.

After 2 hours of incubation of the cells with the transfection mixture, another 2 ml of media was added to the dish and kept back in the incubator. At the end of 18 hours of transfection, the old media was replaced with the virus-collecting medium (HG-DMEM with 2% FBS) and incubated at 5% CO_2. The virus-containing medium is collected after 24 and 48 hours

and centrifuged at 500g for 15 minutes at 4℃. The virus supernatant was collected and stored at 4℃ for immediate use and at -80℃ for long-term use.

ii. Transduction

MDA-MB -231 and MCF7 cells were seeded 24 hours before transduction at the appropriate density (10,000 cells/cm2). Virus-containing media collected after 24 and 48 hours (1st and 2nd harvest) of transfection are added together with 4µg/ml of polybrene and serum so that the final serum concentration should be 10%, and incubated at 37℃ and 5% CO_2 for 24-48 hours. Finally, the complete medium is added to the transduced cells and selection was performed with Puromycin (2µg/ml).

3.1.2.17 Data analysis

To compare between treated and untreated groups, a paired t-test was used. Primary patient sample data was analyzed by the Mann-Whitney non-parametric variables test. The association between the expression levels of different genes in the primary patient samples was determined by bivariate Pearson correlation analysis using SPSS software. p values < 0.05 were considered statistically significant. Colony area, 3D spheroid migration, and the spheroid area were analyzed using Fiji software, and 2D cell migration was analyzed with TScratch software. FlowJo software (Flow-Jo, LLC) was utilized to analyze flow cytometry data.

3.2 Bacterial culture

3.2.1 Materials

3.2.1.1 Chemicals and reagents

SMARTPURE Plasmid Isolation Kit

Ampicillin (100 µg/ml)

$CaCl_2$ solution (50mM)

3.2.1.2 Buffers

Tris-acetate-EDTA (TAE) buffer

3.2.1.3 Plasmids used for silencing

Scramble

shRHOA

shβ-catenin

3.2.1.4 Media

LB-Growth Top Agar

32 grams dissolved in 1000 ml double distilled water, autoclaved at 15 lbs pressure (121℃) for 15 minutes and stored at 4°C.

Luria Bertani HiVeg TM Broth, Miller

25 grams, dissolved in 1000 ml double distilled water, autoclaved at 15 lbs pressure (121℃) for 15 minutes and stored at 4°C.

SOC (Super Optimal broth with Catabolite repression) medium

34.1 grams, dissolved in 1000 ml double distilled water, autoclaved for 15 minutes at 15 lbs pressure (121℃) and stored at 4°C.

3.2.2 Methods

3.2.2.1 Transformation

The Top 10 (E. coli) competent cells were used to perform the transformation. 50 µl of the Top 10 competent cells were thawed on ice and 5 µg of the plasmid was added. Mixed gently with a micropipette and incubated on ice for 30 minutes. A heat shock of 45 seconds at 42℃ was administered and incubated again on ice for 5 minutes to recover. The medium SOC (Super Optimal broth with Catabolite repression) was added to the mixture and incubated at 37℃ for 1 hour at 180 rpm. The culture was spread on LB agar plates containing ampicillin antibiotics and incubated at 37℃ for 18 hours. The next day, ampicillin-resistant colonies were collected and inoculated into LB broth containing ampicillin antibiotics. The inoculated broth was incubated at 37℃ for 16-18 hours at 180 rpm. The culture was collected in a Falcon tube and the plasmid was isolated using the SMARTPURE plasmid isolation kit.

3.2.2.2 Plasmid isolation

The inoculated broth was incubated at 37℃ for 16-18 hours at 180 rpm. The culture was collected in a Falcon tube and the plasmid was isolated using the SMARTPURE plasmid isolation kit.

BMP, RHOA and Wnt Signalling Components in Breast Cancer

4.1 Introduction

The current study focuses on BMP, RHOA, and Wnt signalling to understand their role in breast cancer progression and to check whether these signalling pathways can be modulated for therapeutic purposes. For this, the expression levels of the signalling components in the presentative breast cancer cell lines were determined. Breast tumours formed in breast cancer patients are generally hormone-dependent and around 75% of them express estrogen receptors (Ding et al., 2021). The breast tumours are classified as luminal (ER^+, PR^+), Her2-enriched ($Her2^+$), and basal-like (ER^-, PR^- and $Her2^-$) (Eliyatkın et al., 2015) types. To understand the expression of the various signalling components, four breast cancer cell lines that represent different breast cancer subtypes were utilized: ZR75.1 (ER^+, PR^+, $Her2^+$), MCF7 (ER^+, PR^+, $Her2^-$), SKBR3 (ER^-, PR^- and $Her2^+$), and MDA-MB-231 (ER^-, PR^- and $Her2^-$). ZR75.1 lacks Tp53 function, unlike SKBR3, which expresses the Tp53 gene (Chin et al., 2006). According to ATCC, ZR75.1 was isolated from the mammary gland of a patient with ductal carcinoma, SKBR3 from a pleural effusion with adenocarcinoma, and MCF7 and MDA-MB-231 from the mammary gland with adenocarcinoma. The ideal model chromosome number is 72 for ZR75.1 and 84 for SKBR3 with the hyper triploid chromosome and the aneuploid cell line MDA-MB -231 has 64 and 82 for MCF7 in which the chromosome number ranged from hyper triploidy to hypo tetraploidy. The Her2/neu gene is abundantly expressed in the aggressive breast cancer SK-BR-3 cell line. This fact makes it a useful tool for researching the efficacy of Her2-targeted medicines in the treatment of breast cancer. ZR75.1 breast cancer cell lines are also used to study drug susceptibility, vascular development and apoptosis. MCF7 cells are regularly used in breast cancer research, hormone signalling, novel medicine discovery, and other forms of cancer research. They are also used to investigate the impact of tamoxifen and other anti-estrogen drugs used in the treatment of ER^+ breast cancer (Comşa et al., 2015). MDA-MB-231 is an ideal model for investigating the biology of triple-negative breast cancer due to the absence of ER, PR, and Her2 receptors. These cells are also used extensively to investigate the mechanisms of breast cancer metastasis due to their invasive nature (Welsh, 2013). Several experiments were conducted to comprehend the functional

properties of cells, and gene expression analysis was performed to quantify BMP4, RHOA, and β-catenin expression.

4.2 Results

4.2.1 Morphology of breast cancer cells

Breast cancer cell lines were obtained from the National Centre of Cell Sciences (NCCS, Pune, India) and cultured as recommended. Morphology was first studied by culturing the cells in an ideal environment and observing them under a microscope. ZR75.1 contained small clusters of round-shaped cells, whereas MCF7 exhibited a sheet-like structure of polygonal cells. Similarly, the SKBR3 cell line had both round and polygonal cells, while the MDA-MB-231 cells were spindle-shaped as presented in Figure 4.1.

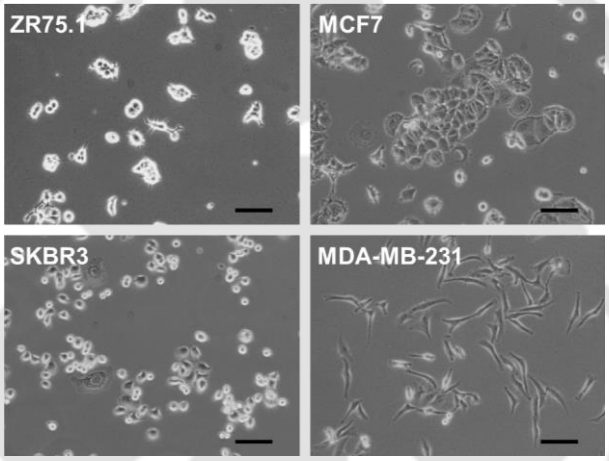

Figure 4.1: Morphology of breast cancer cells*: The cancer cell lines were allowed to grow in a proper cell culture environment and images were taken using a microscope. The figure displayed the morphology of ZR75.1, MCF7, SKBR3 and MDA-MB-231. The black line in the images represents the scale bar (100µm).*

4.2.2 Doubling time and cell cycle

In addition, the doubling time was calculated, which indicates the time it takes for a single population to double in size. For this purpose, the cancer cells were seeded at a precise seeding density and the number of cells was counted at different time intervals. The doubling time was calculated using the formula (Korzyńska & Zychowicz, 2008) mentioned in the materials and methods. MCF7 and ZR75.1 had a doubling time between 36 and 45 hours, whereas SKBR3 required approximately 120 hours. MDA-MB-231 triple-negative breast cancer cells had the lowest doubling time of 20 hours (Figure 4.2 A). The difference in doubling time inspired me to investigate the dynamics of the cell cycle. The

cell cycle is a complicated sequence of processes that meticulously control DNA replication and cell division. The proportion of cells, at each stage of the cell cycle, was estimated using propidium iodide labelling and the cells were analysed by flow cytometry. The G1 phase accounts for 50% of the cell population in ZR75.1, MCF7, and MDA-MB -231 cells, whereas SKBR3 has a G1 phase that is close to 70% of the total cell population. SKBR3 has about 20% of its population in the S phase, while ZR75.1, MCF7 and MDA-MB-231 have approximately 30-40% in the S phase. The G2 phase in ZR75.1 and SKBR3 accounts for about 6% of the total population, while MCF7 and MDA-MB -231 contain about 15% of the cells (Figure 4.2 B and C). Thus, doubling time and cell cycle analysis revealed that MDA-MB-231 as the most proliferative and SKBR3 as the least, while MCF7 and ZR75.1 are intermediate in their proliferation.

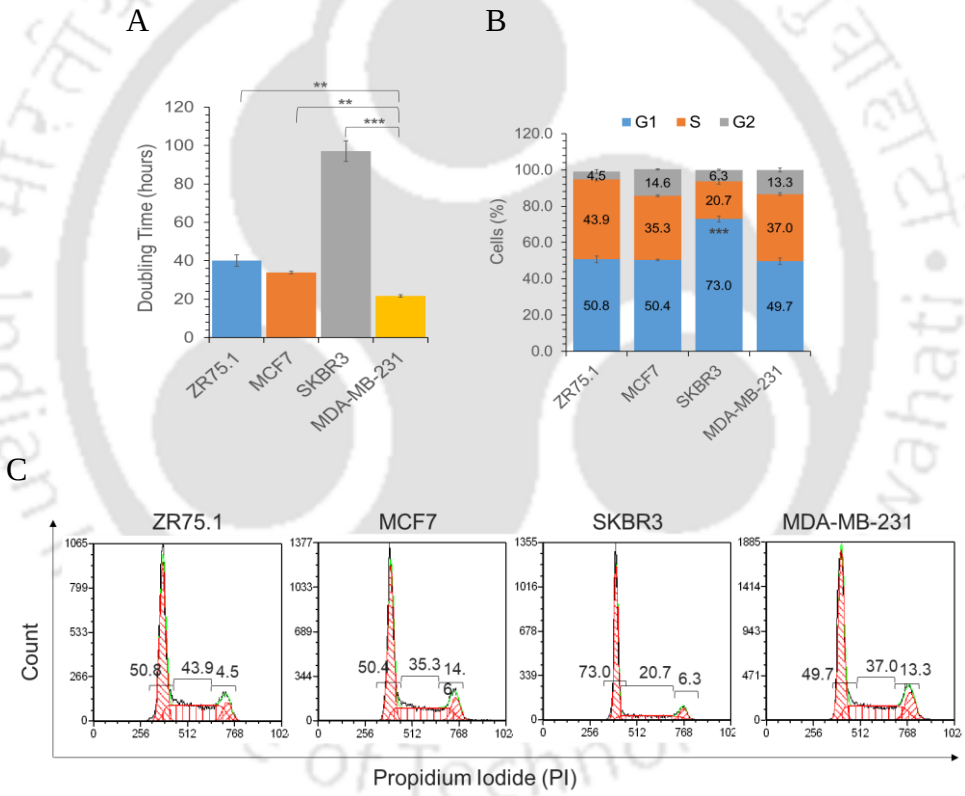

Figure 4.2: Doubling time and cell cycle analysis. *Trypan blue method was used to calculate the doubling time and propidium iodide staining was used to identify the cells based on the amount of DNA.* ***A.*** *represents the doubling time and* ***B.*** *represents the percentage of the population in different phases and* ***C.*** *represents the histogram of the cell cycle in ZR75.1, MCF7, SKBR3 and MDA-MB-231 respectively. Statistical significance was calculated with respect to MDA-MB-231. Values are mean ± SE, n=3-4 independent samples, *p<0.05, **p<0.005, ***p<0.0005.*

4.2.3 Cell surface marker profile

Cell surface receptors are integral membrane proteins that are anchored in the plasma membrane and play an important role in maintaining communication between internal cellular mechanisms and various extracellular signals.

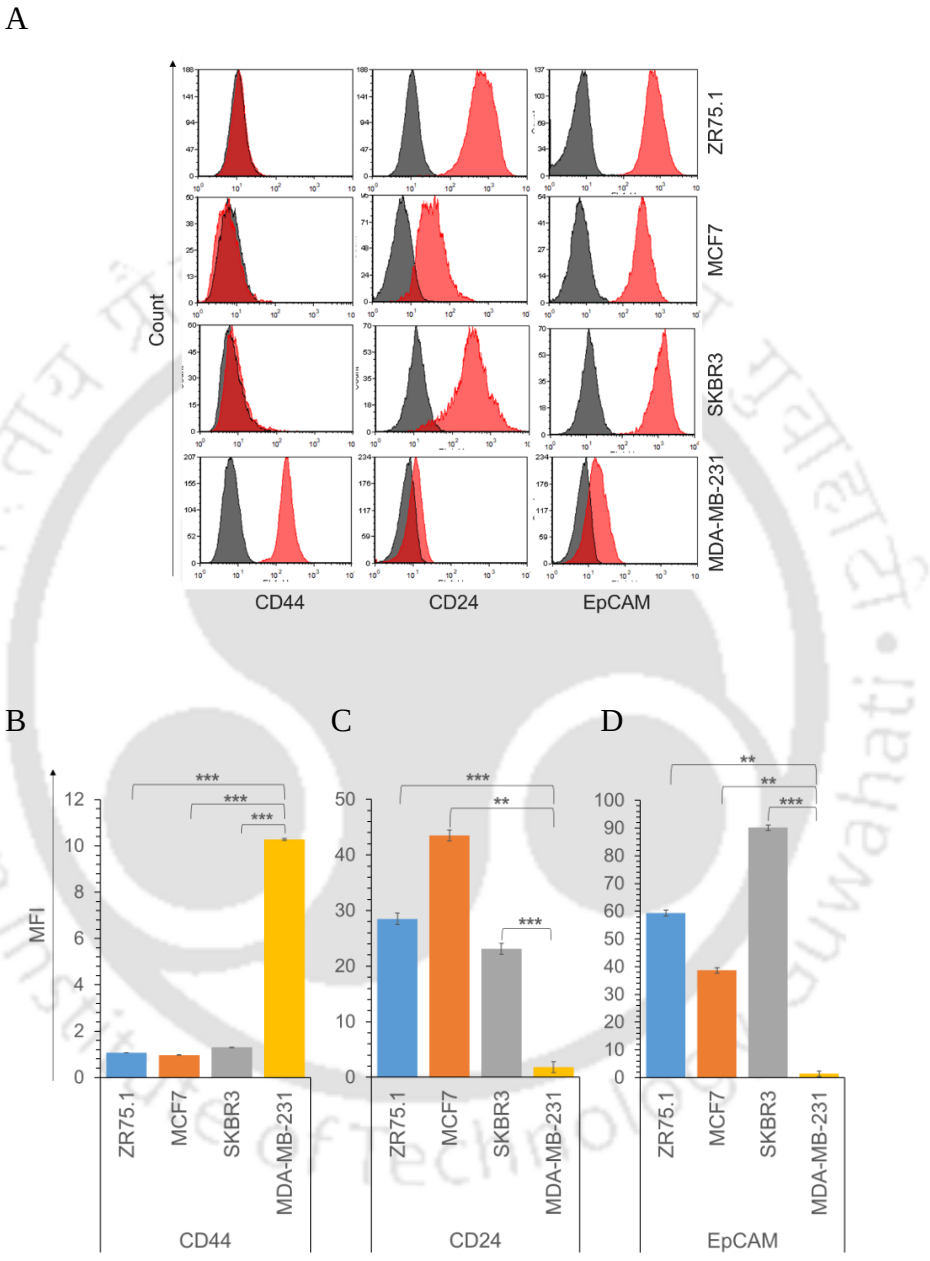

Figure 4.3: Phenotyping of breast cancer cells*. The cells were incubated with fluorescently labelled antibodies for 30 minutes on ice. Propidium iodide was added to distinguish between live and dead cell populations. The mean fluorescent intensity was calculated with respect to unstained.* ***A.*** *represents the histogram and* ***B.*** *represents the MFI of CD44* ***C.*** *for CD24 and* ***D.*** *for EpCAM expression in ZR75.1, MCF7, SKBR3 and MDA-MB-231. Statistical significance was calculated in reference to MDA-MB-231. Values are mean ± SE, n=3-4 independent samples, **p<0.005, ***p<0.0005.*

Numerous cell surface receptors are clinically important in determining the cancer stage of a tumour. Expression of CD44, CD24, and ALDH1 in combination or alone represent

cancer stem cell markers (Horimoto et al., 2016). The combination of CD44 and EpCAM is also considered a tumour-initiating marker, and cells with this combination have a high capacity for self-renewal (Hoe et al., 2017). For this purpose, cells were trypsinized and incubated with fluorescently labelled antibodies and analysed by flow cytometry.

ZR75.1, MCF7 and SKBR3 were positive for CD24 and EpCAM expression but negative for CD44 expression, whereas MDA-MB-231 was positive for CD44 but negative for CD24 and EpCAM (Figure 4.3).

4.2.4 Clonogenic ability

The self-renewal property represents the capacity of a cell to generate its progeny and is directly related to the stemness of the cell; therefore, we choose colony assay, the most effective method for identifying the self-renewal property of an individual cell (Figure 4.4 A). Breast cancer cells were seeded at a seeding density of 100 cells/well and allowed to form colonies for 10-15 days. The colony-forming ability was relatively higher in MCF7 and MDA-MB-231 compared to ZR75.1 and SKBR3 (Figure 4.4 B).

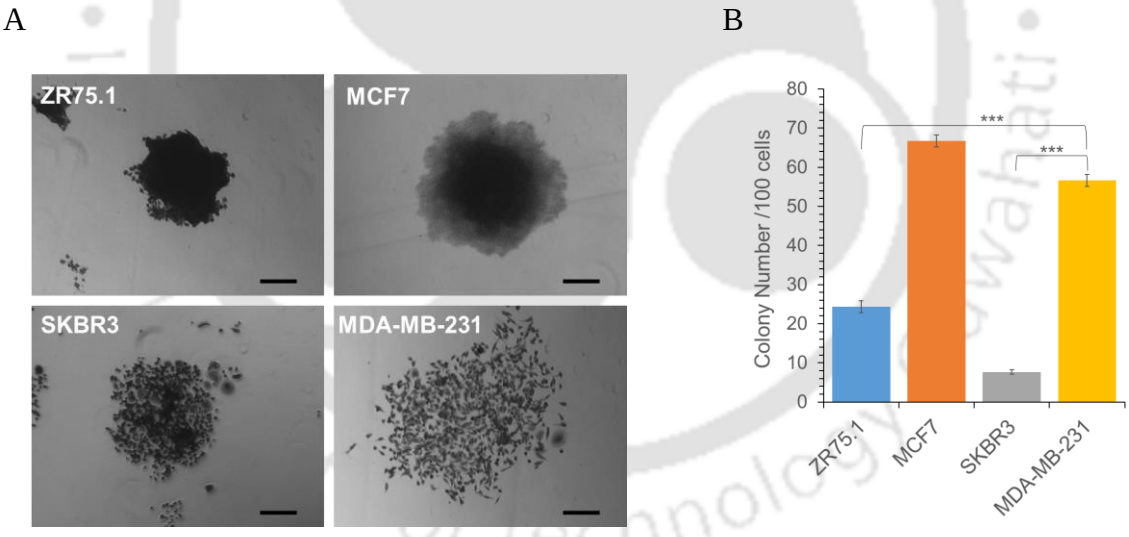

Figure 4.4: Colony formation ability. *The clonogenic capacity of cells is measured by seeding a specific number of cells and incubating them to form colonies for 14 days. The colonies were fixed with methanol and stained with a crystal violet solution. A colony is defined as having 50 or more cells. Colonies were counted and photos were obtained with a microscope. The area covered by each colony was measured using Fiji software.* ***A.*** *Represents the colony images (scale = 200 µm) and* ***B.*** *represents the graph indicating colony number in ZR75.1, MCF7, SKBR3 and MDA-MB-231. Statistical significance was calculated in reference to MDA-MB-231. Values are mean ± SE, n=5-6 independent samples, ***p<0.0005.*

4.2.5 3D spheroid formation ability

Three-dimensional growth is another way to describe proliferation and self-renewal, which illustrates how cell-cell interactions contribute to growth alongside their expanding potential. The efficiency of tumour sphere formation was determined using a spheroid formation assay, which determines the proportion of cancer cell cultures capable of forming 3D spheroids. For this purpose, a predetermined number of cells were seeded on non-adherent wells and allowed to form a spheroid. While ZR75.1, MCF7 and MDA-MB-231 cells formed dense and compact spheroids, SKBR3 grew as a clump of cells rather than forming spheroids (Figure 4.5 A). In addition, ZR75.1, MCF7, and SKBR3 showed good proliferation ability as a 3D spheroid compared to MDA-MB-231 (Figure 4.5 B).

A B

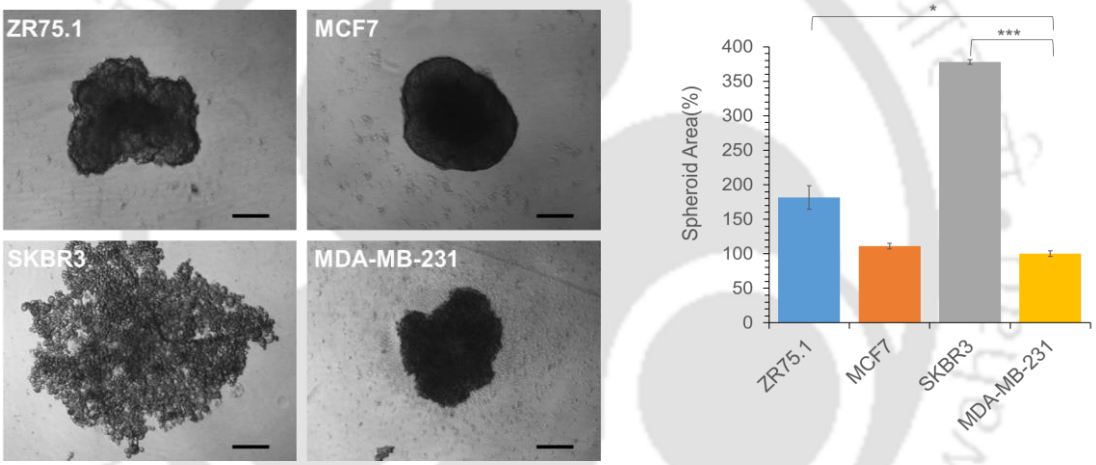

***Figure 4.5: Spheroid formation ability**. The breast cancer cells were seeded in anchorage-independent conditions to form a spheroid and the area covered by the spheroid was analysed using Fiji software. **A.** Represents spheroid images (scale = 200 µm) and **B.** represents the spheroid area of ZR75.1, MCF7, SKBR3 and MDA-MB-231 calculated as the percentage of the area with respect to 7th day. Values are mean ± SE, n=5 independent samples.*

4.2.6 F-actin arrangement

Because the cytoskeleton builds the foundation and acts as the engine for motile cells, remodelling of the intracellular cytoskeleton is considered to be the most significant event in cell migration (Wang et al., 2020). The migration fronts are determined by the amount, orientation, and location of actin within the cells. Similar to lamellipodia, where actin accumulates at the periphery of the cell membrane, and filopodia, where actin accumulates during the migration-related protrusion of cells. Healthy, growing cells were fixed, labelled for F-actin, and imaged under a fluorescence microscope. F-actin content was higher in

MCF7 and MDA-MB-231 cells, while it was low in SKBR3. ZR75.1, on the other hand, expressed lower F-actin than MCF7 and MDA-MB-231 but higher than SKBR3 as shown in Figure 4.6.

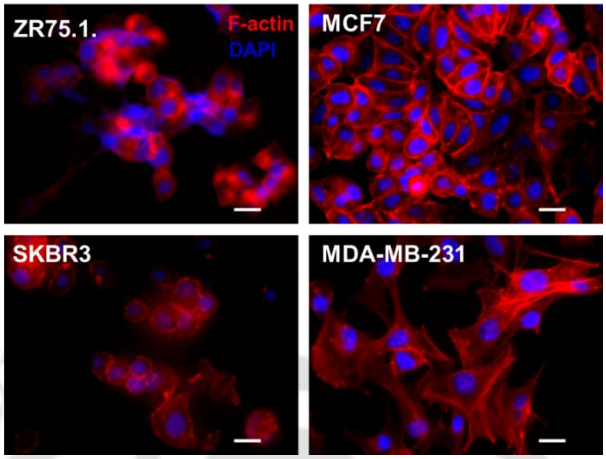

Figure 4.6: F-actin immunostaining*. The cells were processed, fixed and stained with fluorescent-conjugated Phalloidin-TRITC (Red colour) which stains F-actin and DAPI (blue colour) was added to identify nuclear locus in cells. The white line in the images represents the scale bar (50µm).*

After estimating F-actin expression, we conducted a wound-healing assay to ascertain whether the amount of actin present in cells correlated with migration.

4.2.7 Migration ability

Invasion of malignant cells into surrounding tissues and the vascular system is the first stage of cancer progression. To achieve this, cancer cells must migrate chemotactically, controlled by the anteroposterior activity of the cell membrane and its connection to the extracellular matrix (Yamaguchi et al., 2005). To correlate the F-actin level with the migration ability of the cells, wound healing assay was performed, and the migration rate was calculated in µm/hour. On average, MCF7 migrated at a rate of almost 2 µm/hour, MDA-MB-231 at a rate of 5-6 µm/hour, while SKBR3 did not show any migration ability (Figure 4.7 A and B). Based on the above results, F-actin content might correlate with their migration speed.

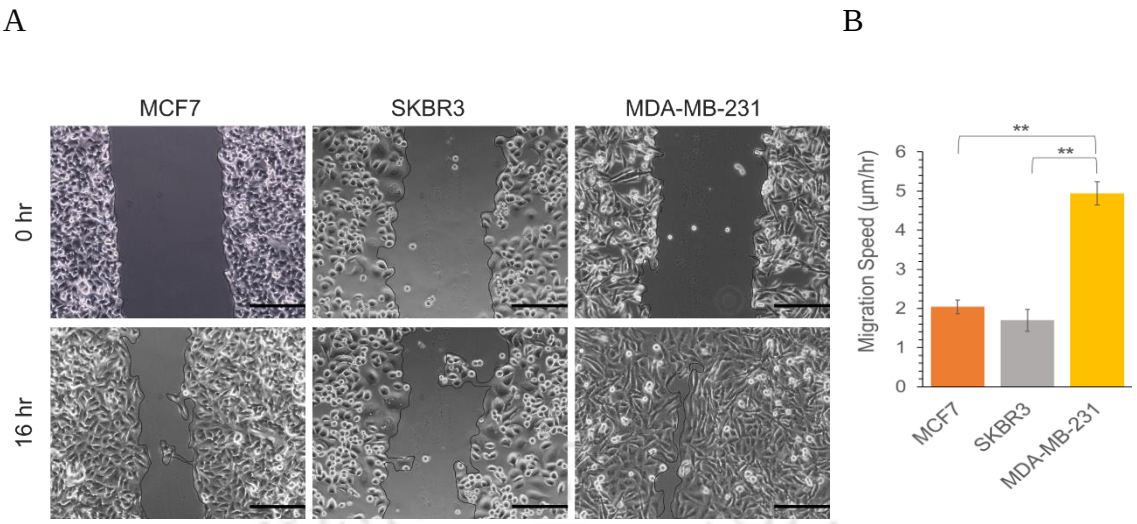

Figure 4.7: Wound healing assay. *To perform the wound healing assay, the cells were implanted and serum starved once they reached a confluence of 90-95% to cease growth. After that, a scratch was made and cells were permitted to move in the scratched area. The area covered in 28 hours by the migrating cells was determined using T-Scratch software and the migration rate was calculated in µm/hour.* ***A.*** *represents the microscopic images and* ***B.*** *represents the migration speed of MCF7, SKBR3 and MDA-MB-231 cells. The black line in the images represents the 100µm scaling bar. Statistical significance was calculated in reference to MDA-MB-231. Values are mean ± SE, n=5-6 independent samples, **p<0.0005.*

4.2.8 *In vitro* metastatic growth of breast cancer cells

Metastasis of breast cancer cells into bone microenvironment is very well known and this activates osteoclast activity which results in bone resorption (Mercatali et al., 2017). Breast cancer cells were seeded on a monolayer of bone marrow-derived stromal cells to examine their ability to form breast cancer colonies and proliferate. MCF7 cells were able to form well-formed colonies on the stromal layer, however, SKBR3 and MDA-MB-231 cells proliferated in a dispersed manner (Figure 4.8).

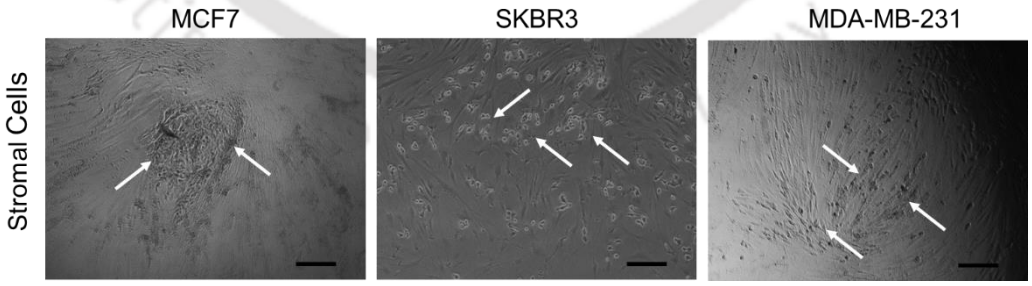

Figure 4.8: Co-culture of breast cancer cells on stromal cells*. To comprehend the metastatic development of breast cancer cells, the cancer cells were co-cultured with bone marrow-isolated stromal cells. The images were taken on the 7th day of co-culture to observe the interaction of different cancer cell lines with stromal cells. The black line in images represents the scale bar (200µm).*

4.2.9 Components of BMP signalling in breast cancer cells

After gaining an understanding of the functional properties of breast cancer cell lines, we sought to identify the signalling components of BMP, RHOA, and Wnt, to comprehend the role of these signalling pathways in cancer progression. The linked elements of these signals were estimated by immunoblotting and real-time PCR analysis. Intracellular expression levels of BMP4 were determined by immunocytochemistry staining and immunoblotting. Intracellular BMP4 expression was identified in both MCF7 and MDA-MB-231 cells and immunoblotting analysis showed that MDA-MB-231 cells had significantly higher expression of BMP4 compared to MCF7 and SKBR3 (Figure 4.9 A and B). The expression of BMP receptors was also determined by immunoblotting; interestingly, BMPR1A protein expression was identified in MCF7 and SKBR3, however, MDA-MB-231 showed *BMPR1A* expression at the mRNA level. A high level of BMPR2 expression was identified in MDA-MB-231 cells whereas it was relatively low in SKBR3 cells. To understand whether the BMP signalling pathway was active in the breast cancer cells, phospho SMAD1/5 (pSMAD1/5) levels were determined in these cell lines. SKBR3 cells showed low pSMAD1/5 expression levels whereas MCF7 and MDA-MB-231 had similar expression levels (Figure 4.9 C). Thus, the differential levels of the BMP signalling components indicate that BMP signalling might be modulated differentially in these breast cancer cell lines representing distinct breast cancer subtypes.

4.2.10 Expression of RHOA and Wnt signalling components in breast cancer cells

The expression levels of RHOA and β-catenin in the breast cancer cells were determined at the protein and mRNA levels. In the context of RHO-ROCK signalling, we estimated the expression profile of RHOA at both the mRNA and protein levels. RHOA expression could be detected by immunocytochemistry, immunoblotting and real-time PCR. MDA-MB-231 cells showed significantly high levels of RHOA (Figure 4.10 A and B) compared to MCF7 cells suggesting an active RHOA signalling pathway in MDA-MB-231 cells.

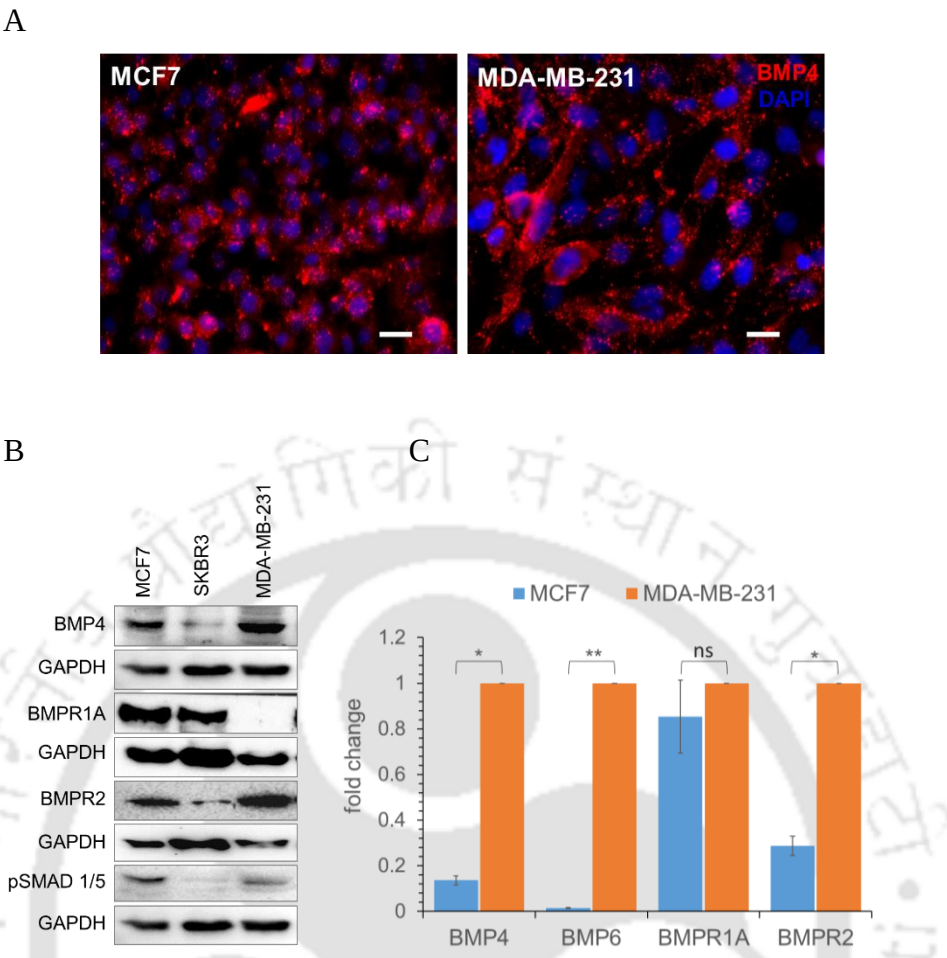

Figure 4.9: Components of BMP signalling in breast cancer cells. *Immunocytochemistry, immunoblotting and Real-time PCR techniques were used to determine the expression level of BMP signalling components.* ***A.*** *represents the fluorescence image of MCF7 and MDA-MB-231 cells stained with anti-BMP4 (Red) and DAPI (Blue) antibodies, respectively. The white line in the images represents the scale bar (20 µm).* ***B.*** *depicts a western blot of MCF7, SKBR3, and MDA-MB-231 cells for BMP4 (~34 KDa), BMPRIA (~55 KDa), BMPR2 (~115 KDa), and pSMAD1/5 (~55 KDa), and GAPDH (~37 KDa) expression. Using Real-time PCR, the mRNA transcript level of BMP4, BMP6, BMPRIA, and BMPR2 was analysed, and fold change was calculated relative to MDA-MB-231 represented in* ***C.*** *Statistical significance was calculated in reference to MDA-MB-231. Values are mean ± SE, n=4 independent samples, *p<0.05, not significant (ns), p>0.05.*

Similarly, the β-catenin expression could be detected in both MCF7 and MDA-MB-231 cells in the protein as well as mRNA level by immunocytochemical staining, immunoblotting and real-time PCR analysis. The β-catenin was found to be significantly higher in MCF7 cells compared to MDA-MB-231 cells suggesting that β-catenin might function differently in these cell types (Figure 4.10 B and C).

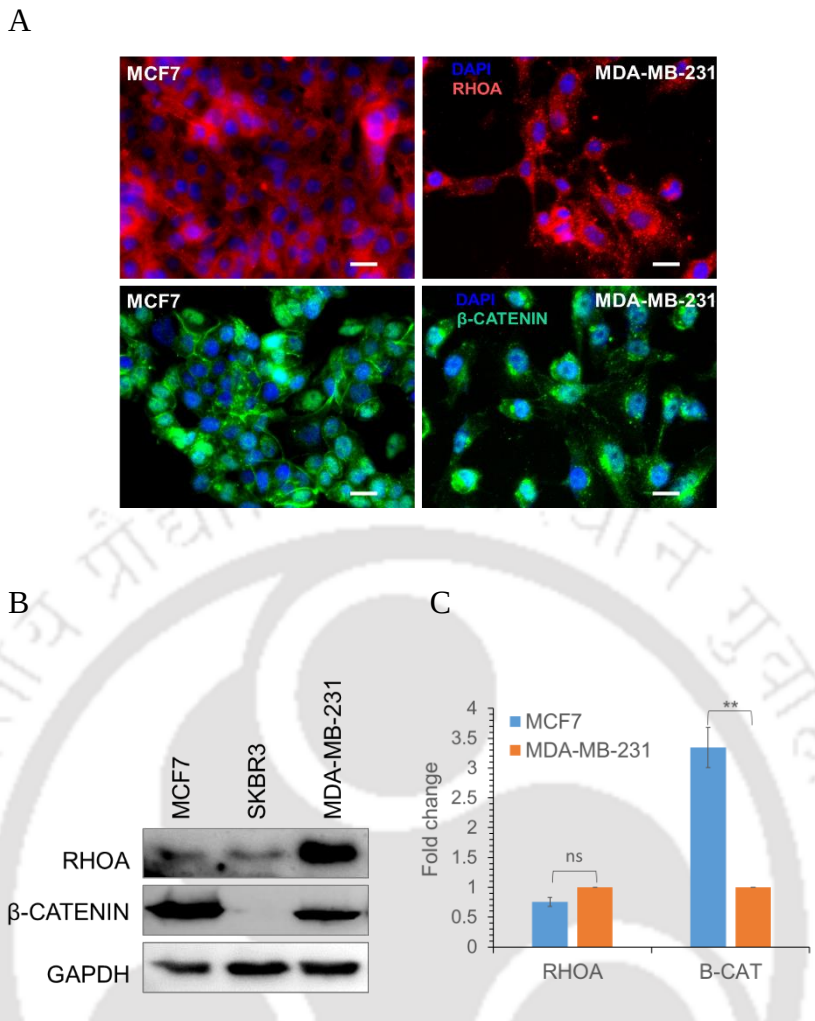

Figure 4.10: Signalling components of RHOA and Wnt in breast cancer cells. *The expression of RHOA and β-catenin was also evaluated using immunocytochemical staining, western blotting, and Real-time PCR.* ***A.*** *displays the fluorescence image stained with anti-RHOA (Red), anti- β-catenin (Green), and DAPI (Blue) for both MCF7 and MDA-MB-231. In the images, the white line represents the scale gauge (20 m).* ***B.*** *depicts western blot images of RHOA (~21 KDa), β-catenin (~92 KDa) and GAPDH (~37 KDa) in MCF7, SKBR3, and MDA-MB-231 cells. Real-time PCR was used to analyse the gene expression profile for RHOA and β-catenin, and the fold change was calculated with reference to MDA-MB-231 represented in* ***C.*** *Values are mean ± SE, n=4 independent samples, **p<0.005, not significant (ns), p>0.05.*

4.3 Discussion

Each subtype of breast cancer cells responds differently in terms of prognosis and treatment due to heterogeneity in terms of molecular characteristics, receptors present on them, cell culture environment, and many other factors; therefore, it was necessary to choose the appropriate cell lines for the study (Holliday & Speirs, 2011). Taking into account the wide variety of breast cancer subtypes, we selected four distinct cell line types to study. The cell lines were ZR75.1 (ER^+, PR^+, $Her2^+$), MCF7 (ER^+, PR^+, $Her2^-$), SKBR3 (ER^-, PR^-, $Her2^+$) and MDA-MB-231(ER^-, PR^-, $Her2^-$).

Each cell type had distinct morphological characteristics, where MDA-MB-231 cells have a spindle shape and SKBR3 cells have a mixed population of polygonal and round shapes, which are consistent with previously reports (Hollestelle et al., 2013). MCF7 has a sheet-like polygonal structure, and ZR75.1 has a sheet-like spherical globular structure, both of which are similar to those reported earlier (Gadalla et al., 2011). The doubling times of MDA-MB-231 and MCF7 were as reported earlier (Tesauro et al., 2019) and (R. Y. Koh et al., 2017). We found that MCF7 and ZR75.1 had nearly comparable doubling times of 36-45 hours, aligning with the earlier research (Stepp et al., 2019).

CD44 high and CD24 low is the primary marker for identifying breast cancer stem cells (Sheridan et al., 2006; Vikram et al., 2020). We also determined the baseline expression of CD44 in breast cancer cells and found that MDA-MB-231 had a positive expression for CD44, while MCF7, ZR75.1, and SKBR3 were negative for CD44 as reported by others (Fillmore & Kuperwasser, 2008; W. Li et al., 2017) (Meyer et al., 2010) (Moradian & Rahbarizadeh, 2019) (Meyer et al., 2009). As reported by Ghaedi et al, MDA-MB-231 and MCF7 possess a higher level of F-actin and migrate faster than SKBR3 cells (Ghaedi et al., 2019). Similarly, the clonogenic ability of MCF7 and MDA-MB-231 were similar to each other as reported by other studies (Ren et al., 2019). Some studies, however, reported that MDA-MB-231 cells have higher clonogenic potential than MCF7 (Mokhtari et al., 2021).

When breast cancer cells and stromal cells are co-cultured, it becomes clear that all breast cancer cell lines can colonise at a distant place. This finding suggests that the microenvironment of stromal cells also fosters the growth of breast cancer cells. Some proteins like SDF-1, CXCL1/2/5/6/10/12, interleukins, OPN and several others secreted by breast cancer cells are beneficial to their survival in the stromal cell milieu, and this has already been researched (Hill et al., 2020).

Further, MCF7 and SKBR3 express BMPRIA and MDA-MB -231 express BMPR2, which may suggest that MCF7 and SKBR3 activate BMP signalling via BMPRIA and MDA-MB -231 activate BMP signalling via BMPR2. Similarly, the higher β-catenin expression in MCF7 and lower expression in MDA-MB-231 were consistent with one of the studies published by et al (Bleckmann et al., 2016). RHOA expression was evaluated among the cell lines and found to be highest in MDA-MB-231, followed by MCF7, and then SKBR3. For the current study, MCF7, SKBR3, and MDA-MB-231 were selected to investigate the BMP signalling pathway and its significance.

4.4 Conclusion

Although all the cell lines ZR75.1, MCF7, SKBR3, and MDA-MB-231 utilized for the study were derived from breast cancer patients, there was a significant difference in their morphology, growth properties and expression of key signalling molecules. These cell lines represent different molecular subtypes and the differential expression of the signalling molecules related to BMP, RHOA and Wnt signalling suggest that a context-dependent regulation might occur in different breast cancer subtypes and could be utilized for therapeutic purposes.

BMP4 Signalling in Breast Cancer Progression

5.1 Introduction

BMP4, a member of the BMP family was found to be overexpressed in breast cancer and involved in both the growth and invasiveness of breast cancer cells including the development of chemotherapy resistance. Therefore, understanding the function of BMP4 might help in developing new treatment strategies for breast cancer. BMP functions in both canonical (SMAD-dependent) and non-canonical (SMAD-independent) signalling pathways (Goldman et al.,2022). Regulatory Smad (R-SMAD) and inhibitor Smad (I-SMAD) are involved in the canonical pathway (Lai et al., 2022), whereas ERK, p38 MAPK, and JNK are involved in the non-canonical (Chmielowiec et al., 2022) pathway. BMPs are known to play a dual role. For instance, BMP4 prevents the spread of breast cancer to other parts of the body by stopping NF-kB activity in human and mouse tumour lines. However, another study showed that BMP4 promotes tumour growth and metastasis by causing CD8+ T cell-mediated immunosuppression (Bach et al., 2018). BMP4 is known to stimulate endothelial cell migration by upregulating FoXO3 and ROS generation, in addition to tumour growth and metastasis, as demonstrated in (Q. Li et al., 2022). The development of "chemoresistance" by cancer stem cells is the primary source of failure in cancer therapy. Research has shown that blocking BMP4 and BMP2 can reduce tumour development and aggressiveness (S. Li et al., 2022). The context-dependent function of BMP signalling in different cancers prompted us to investigate the significance of BMP signalling at different stages of cancer progression. Multiple assays and microenvironments were used to investigate the role of BMP signalling in cancer proliferation, self-renewal, migration/EMT, anoikis resistance, metastasis, and chemoresistance. The effect of BMP signalling on breast cancer cells was determined by treating them with recombinant human BMP4 protein, the BMP receptor inhibitor LDN193189 (LDN), and a combination of these two compounds.

5.2 Results

5.2.1 Determining the efficiency of recombinant human BMP4 and LDN193189

Before initiating multivariate experiments, the optimal concentration of both BMP4 and LDN193189 (LDN) was determined.

5.2.1.1 LDN concentration curve

Reports have shown that high doses of LDN are toxic to cells, the optimal concentration was determined by a concentration curve. The breast cancer cell lines were seeded and treated with various concentrations of LDN ranging from 0µM to 10µM. The cell viability was unaffected with the LDN concentration between 0µM to 1µM, whereas a significant decrease in live cells was observed at 2µM, and LDN was highly cytotoxic at a concentration of 5µM and above (Figure 5.1). Thus, 1µM of LDN was utilized for further experiments.

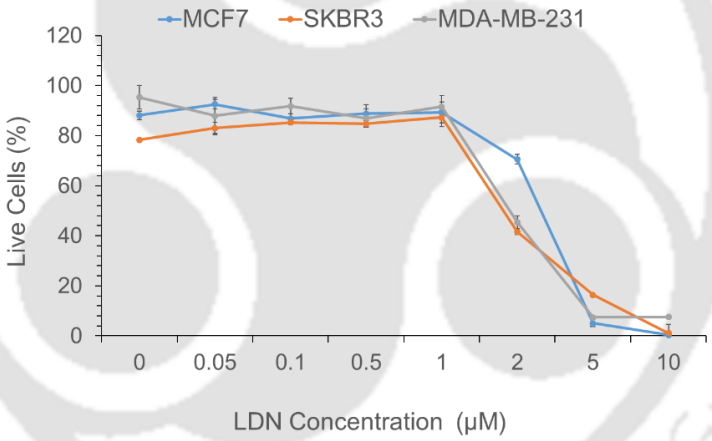

Figure 5.1: LDN concentration curve*. MCF7, SKBR3, and MDA-MB-231 cell lines were seeded and treated with LDN varying from 0.05µM to 10µM for 48 hours. The treated cells were processed and stained with propidium iodide to determine the percentage of living and dead cells. The corresponding line graph displays the percentage of viable cells across different LDN193189 concentrations. Values are mean ± SE, n=3 independent sample.*

5.2.1.2 Time course analysis of BMP4 and LDN

To determine the optimal treatment time for the breast cancer cells with BMP4 (10ng/mL) and LDN (1µM/mL), a time course analysis was performed. Cells were seeded, treated and then counted at different time intervals using the trypan blue method. Cell number did not change significantly in the first 24 hours after treatment with BMP4, LDN, or simultaneous treatment of BMP4 and LDN (BMP4+LDN). However, a significant increase in cell

number was observed after 48 hours of treatment with BMP4. In contrast, neither LDN nor concomitant treatment with BMP4 affected cell numbers. A decrease in cell number was observed after 72 hrs of LDN treatment and 48 hrs of treatment was sufficient to activate or inhibit the SMAD signalling with BMP4 and LDN treatment, respectively (Figure 5.2 A). To further corroborate the substantial effect of LDN on SMAD signalling, flow cytometric analysis was also conducted. The results showed that LDN (inhibitor) administration significantly reduced the expression profile of pSMAD1/8 (Figure 5.2 B).

A B

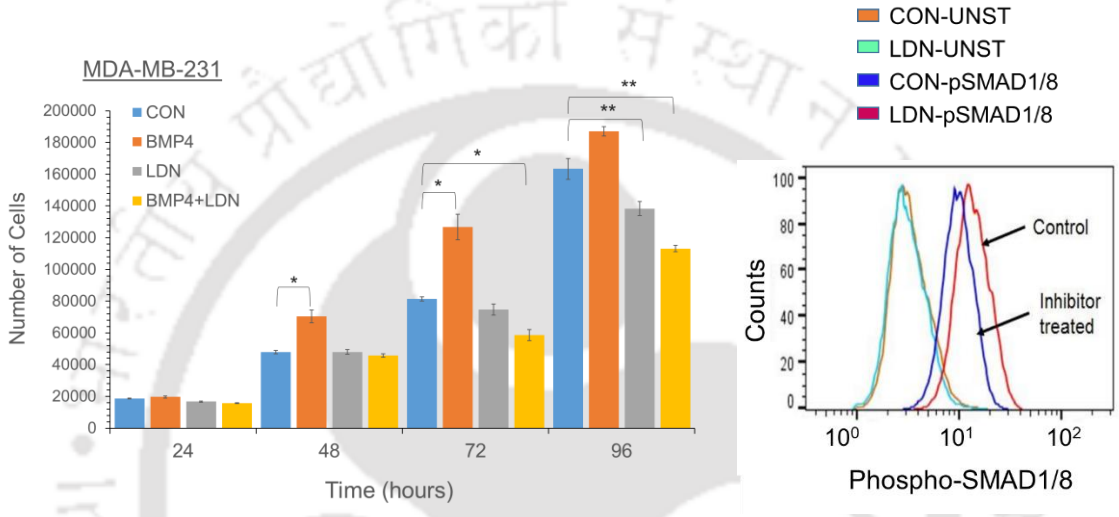

Figure 5.2: Time course analysis of BMP4 and LDN. *MDA-MB-231 with a seeding density of 5000 cells/cm^2 seeded in tissue culture-treated plates along with BMP4(10ng/ml) and LDN(1µM/ml). The cells were trypsinized and counted at regular time intervals of 24, 48, 72 and 96 hours using the trypan blue method. The above bar graph in* ***A.*** *represents the number of cells obtained at different time points in MDA-MB-231 where cells left untreated (CON), or treated with BMP4, LDN or BMP4+LDN are represented. Anti-Smad1 (pS463/pS465)/Smad8 (pS465/pS467) antibody (PhosphoSMAD1/8) was used to stain MDA-MB-231 cells. Cells were either left untreated (Control) or treated with the BMP inhibitor LDN193189 (Inhibitor). The orange line represents the unstained control for the control cells, whereas the light blue line represents the unstained control for the inhibitor-treated cells in* ***B****. Values are mean ± SE, n=4 independent samples, *p<0.05, **p<0.005.*

5.2.2 BMP4 facilitates canonical signalling in breast cancer cells

In order to understand the signalling pathway activated by BMP4 and LDN treatment, whether it follows canonical or non-canonical BMP pathway or both, the components of the BMP signalling was determined by immunoblotting and real-time PCR analysis. BMP4 treatment significantly increased the pSMAD1/5 (Figure 5.3 A and B), pSMAD2/3 (Figure 5.3 C and D) and pSMAD1/8 (Figure 5.3 E) protein levels in MDA-MB-231, whereas LDN treatment significantly downregulated these proteins.

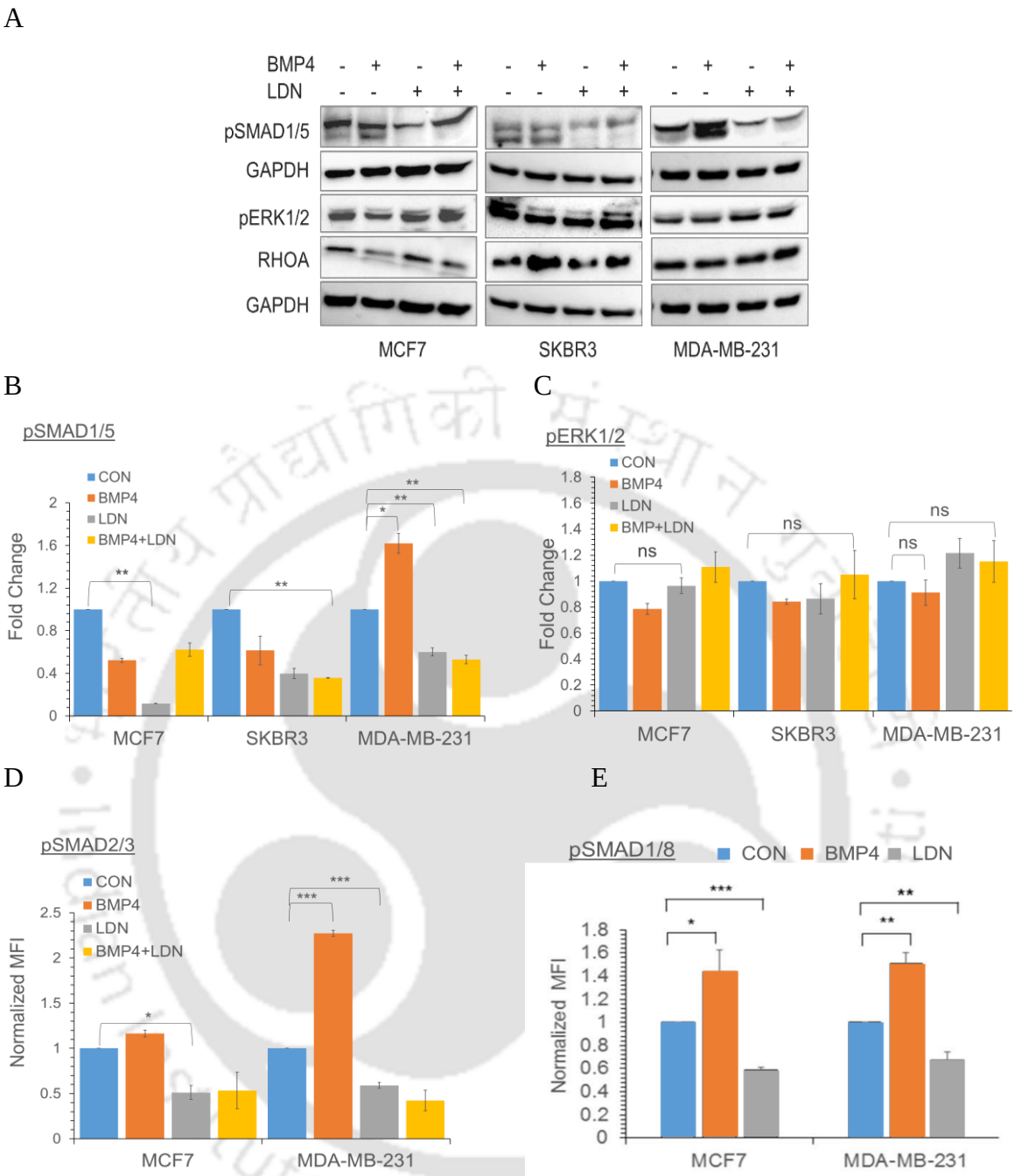

Figure 5.3: BMP4 and LDN treatment alters canonical signalling proteins*. The protein profiles of BMP canonical signalling in breast cancer cells treated with BMP4(10ng/ml) and LDN(1µM/ml) for 48 hours were examined using immunoblotting and flow cytometry. The protein lysate was extracted in RIPA buffer and separated on a polyacrylamide gel before being transferred to a nitrocellulose membrane for immunoblotting analysis. A primary antibody and an HRP-conjugated secondary antibody were used to incubate the membrane. To create a chemiluminescent picture of the blot, the ECL reagent was used.* ***A.*** *Blots represent the expression of pSMAD1/5(~55 KDa), pERK1/2(~42-44 KDa), RHOA (~21 KDa), and GAPDH (~37 KDa) proteins, while* ***B.*** *represents the fold change in pSMAD1/5 and* ***C.*** *represents the fold change in pERK1/2 expression in MCF7, SKBR3, and MDA-MB-231 cells respectively. The changes in phosphoprotein expression following treatment were examined using flow cytometry, in which cells were stained with fluorescently labelled antibodies and the change in intensity was evaluated. Normalised MFI was calculated by comparing fluorescence intensity to untreated conditions.* ***D.*** *and* ***E.*** *show the normalised MFI of pSMAD2/3 and pSMAD1/8 for MCF7 and MDA-MB-231, respectively. Values are mean ± SE, n=4 independent samples, *p<0.05, **p<0.005, ***p<0.0005, not significant (ns), p>0.05*

However, the levels of pERK1/2 and RHOA was unaffected upon treatment with either BMP4 or LDN in all the breast cancer cell lines tested proteins (Figure 5.3 A and F). Thus, the results indicate that BMP4 treatment primarily activates the canonical pathway in breast cancer cells.

Considering the above observation that BMP4 and LDN treatment has a striking effect on the canonical pathway, it was hypothesized that these treatments would also alter the expression of downstream targets of the Smad-dependent pathway. Among the important downstream mediators of the BMP pathway is the large family of proteins known as ID proteins. IDs play a significant and distinct role in controlling the expression of genes involved in cell differentiation and proliferation (J. Yang et al., 2013).

To investigate the effects of treatment with BMP4 and LDN on the expression of these IDs and other BMP proteins in breast cancer cells, gene expression analysis was performed. BMP4 treatment resulted in a dramatic increase in *ID1* and *ID2* levels in MCF7 cells, whereas LDN treatment resulted in a significant decrease in *ID1*, *ID2*, and *ID4* expression. The expression levels of *BMP4*, *BMP6*, *BMPRIA*, and *BMPR2* were also analysed, but neither BMP4 nor LDN had a noticeable effect on them as shown in Figure 5.4 A. In contrast, in MDA-MB-231 cells, BMP4 treatment increased the expression of *BMP6*, *ID1*, and *ID2*. In contrast to the expression of other ID genes, which were increased by BMP4 treatment and downregulated by LDN, *ID4* expression was downregulated by BMP4 treatment in MDA-MB-231 (Figure 5.4 B). In addition, there was a significant decrease in the expression of proliferation genes *KI67* (p=0.0203) and *PCNA* (proliferating cell nuclear antigen) (p=0.0112) in BMP4-treated MCF7 cells. Although BMP4 treatment induced *CCND1* expression (p=0.0111) in MCF7 cells, this effect appears to have been abrogated by the increase in *CDKN1A* (cyclin-dependent kinase inhibitor 1 A) expression (p=0.0019). Conversely, treatment with LDN increased the expression of *KI67* (p=0.0333) and *CCNE2* in MCF7 cells. In MDA-MB-231 cells, the expression of *CDKN1A* (p= 0.0543) increased after LDN treatment (Figure 5.4 C). Thus, BMP4 treatment activates the canonical BMP signalling and its downstream effectors whereas LDN treatment significantly inhibits the BMP expression and the downstream effector molecules.

A

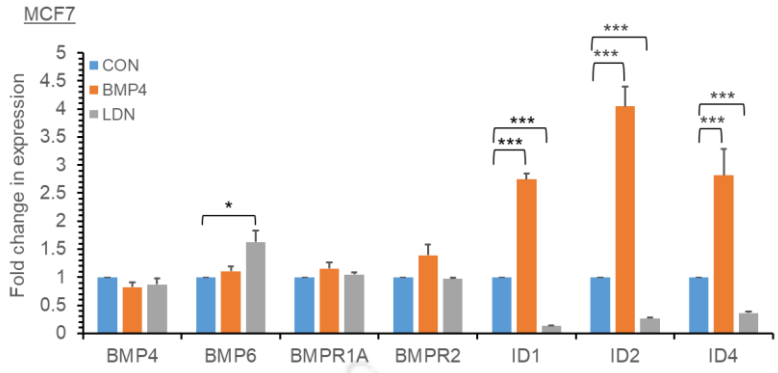

B

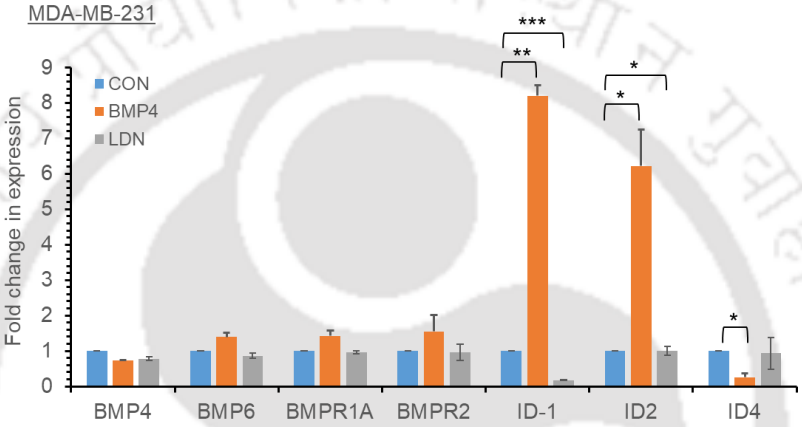

C

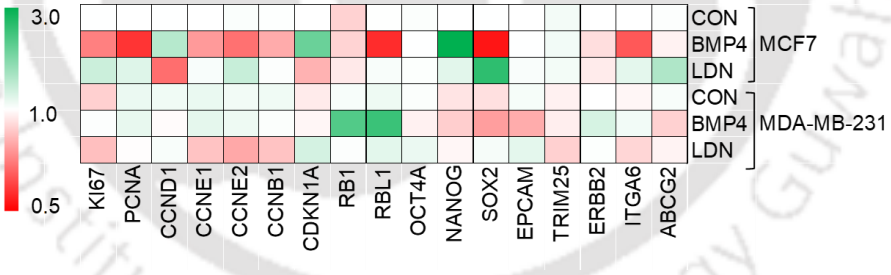

Figure 5.4: BMP4 and LDN regulate downstream targets of BMP signalling*. MCF7 and MDA-MB-231 cells were lysed and processed for RNA isolation after being treated with BMP4(10ng/ml) and LDN(1µM/ml) for 18 hours. The RNA was reverse-transcribed into cDNA, and real-time PCR was performed to analyse changes in the downstream targeted gene. After normalising with GAPDH expression, the fold change in expression level was estimated using the Ct method. The bar graph displays the fold change in gene expression profiles of BMP4, BMP6, BMPR1A, BMPR2, ID1, ID2, and ID4 of* ***A.*** *MCF7 and* ***B.*** *MDA-MB-231, whereas the heat map depicts fold change expression in Ki67, PCNA, CCND1, CCNE1, CCNE2, CCNB1, CDKN1A, RB1, RBL1, OCT4A, NANOG, SOX2, EPCAM, TRIM25, ERBB2, ITGA6 and ABCG2 of MCF7 and MDA-MB-231displyed in* ***C.*** *Values are mean ± SE, n=4 independent samples, *p<0.05, **p<0.005, ***p<0.0005.*

Although the BMP pathway was activated by BMP4 treatment in both MCF7 and MDA-MB-231 and LDN downregulated or inhibited the effector gene expression, it produced a contradictory effect on the proliferation genes. Interestingly, while BMP4 treatment

increased the KI67 expression in MDA-MB-231 cells, it significantly downregulated KI67 levels in MCF7 suggesting a context-dependent effect on the breast cancer cells.

5.2.3 BMP4 regulates proliferation and self-renewal of breast cancer cells

Given the fact that BMP4 or LDN treatment had a contradictory effect on the expression of proliferation-related genes, the role of BMP4 and LDN treatment in regulating the cell cycle profile was determined. Upon treatment with BMP4, the percentage of cells at the G1 stage of the cell cycle was significantly high in MCF7 and SKBR3 cells whereas an increase in G1 percentage was observed in MDA-MB-231 when treated with LDN (Figure 5.5 A). To determine whether the cells at the G1 phase are quiescent or cycling, the percentage of cells at the G0 stage of the cell cycle was determined by KI67 staining. KI67 staining helps in differentiating the cycling and non-cycling cells, where cells that are quiescent or exited the cell cycle have low or negative KI67 expression (Figure 5.5 B). As expected, BMP4 treatment significantly increased the G0 percentage in MCF7 and SKBR3 cells, whereas LDN treatment increased the percentage of cells at G0 in MDA-MB-231 cells (Figure 5.5 C). These results suggest that BMP4 and LDN have opposite effects on cell growth, with BMP4 inhibiting growth in MCF7 and SKBR3 and LDN in MDA-MB-231.

Furthermore, to understand the role of BMP4 in self-renewal and proliferation, BMP4 and LDN-treated breast cancer cells were analysed for their proliferation by cell counting. Treatment with BMP4 significantly inhibited cell proliferation reducing their cell number, whereas there was a significant increase in MDA-MB-231 cell number. Conversely, treatment with LDN, which inhibits BMP signalling, increased the MCF7 and SKBR3 cell numbers while that of MDA-MB-231 decreased. The cell numbers of MCF7 and SKBR3 were not affected by simultaneous treatment with BMP4 and LDN, whereas MDA-MB-231 showed a marked decrease, as shown in Figure 5.5 D. This suggests that LDN promotes proliferation in MCF7 and SKBR3, whereas BMP4 promotes proliferation in MDA-MB-231.

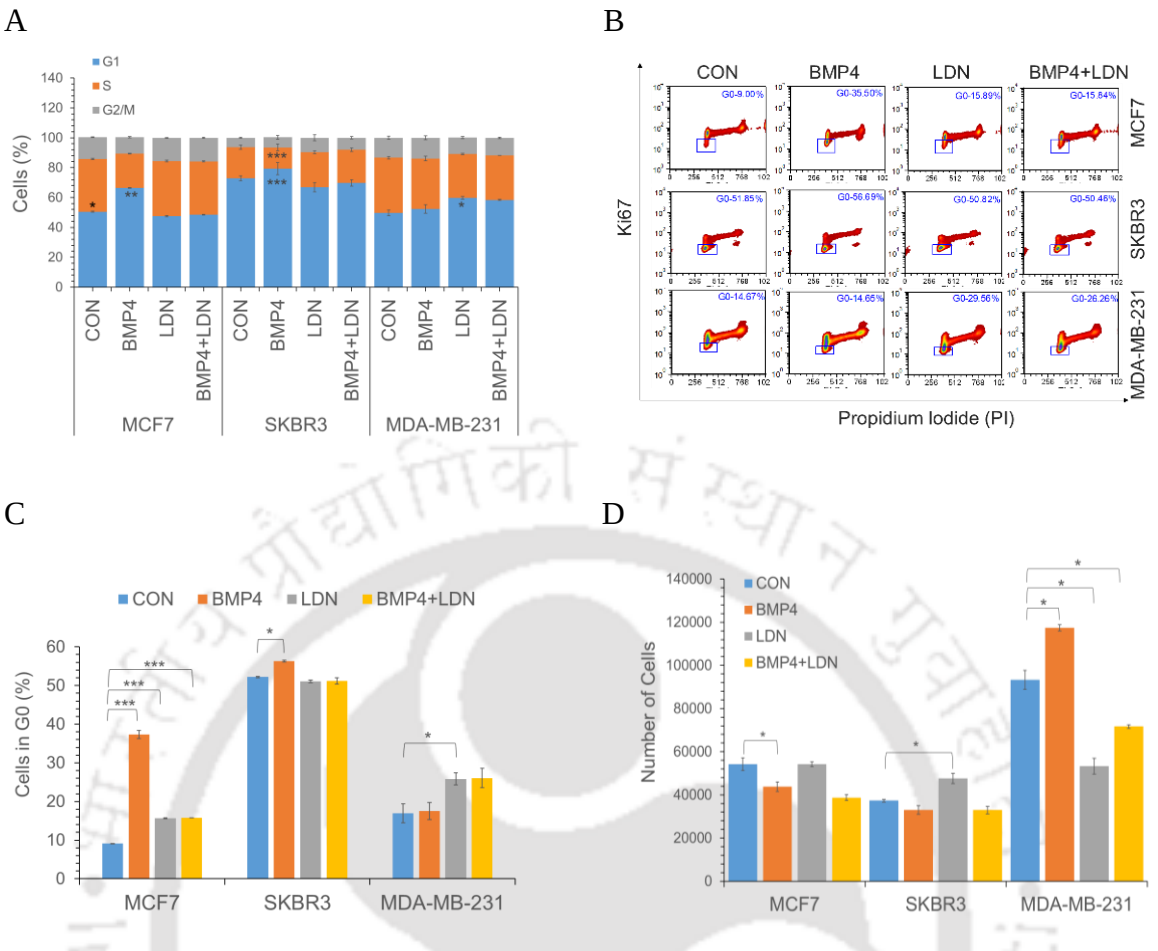

Figure 5.5: Impact of BMP4 and LDN on cell cycle and Ki67 staining. *Using propidium iodide and Ki67 staining, the variations in cell cycle phases were analysed. In addition to cell cycle analysis, alterations in cell number following treatment with BMP4(10ng/ml) and LDN(1µM/ml) for 48 hours were determined using the trypan blue method.* ***A.*** *Represents the percentage of cells in G1, S and G2 phases of cell cycle.* ***B.*** *Represents the density plot generated by flow cytometry analysis for G0 phase population by Ki67/PI staining and* ***C.*** *represents the percentage of G0 population in a graph and* ***D.*** *represents the changes in cell number of MCF7, SKBR3 and MDA-MB-231 when treated with BMP4 and LDN. In graph, CON represents untreated control. Values are mean ± SE, n=3-4 independent samples, *p<0.05, ***p<0.0005.*

To determine how BMP signalling regulates the 3D growth of breast cancer cells, a spheroid formation assay was performed in the presence of BMP4 and LDN. The breast cancer cells were allowed to form spheroids and their growth was monitored periodically. When treated with LDN alone or in combination with BMP4, MCF7 and SKBR3 cell lines showed increased spheroid growth, whereas treatment with BMP4 resulted in decreased spheroid size in MCF7, indicating reduced growth. Neither BMP4 nor LDN had any effect on the three-dimensional growth of MDA-MB-231, as shown in Figure 5.6. These findings suggest that BMP signalling is crucial for controlling cell development in three dimensions as well.

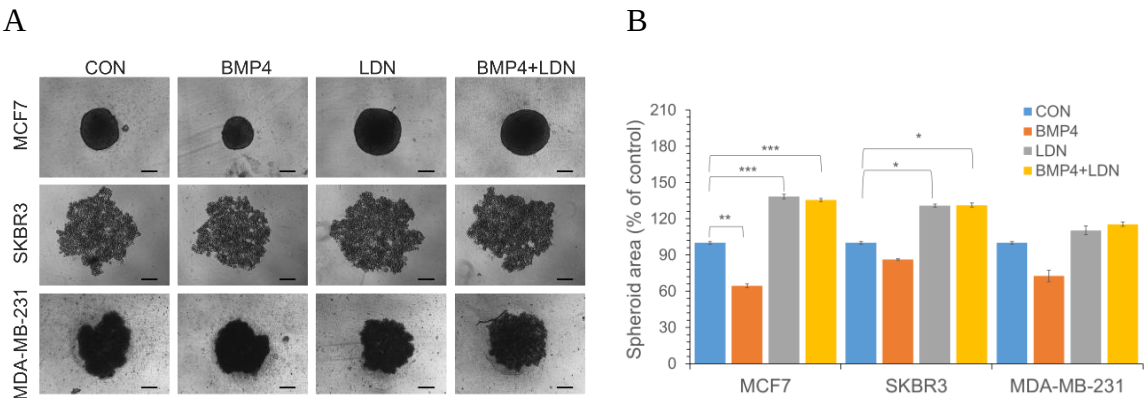

Figure 5.6: Effect of BMP4 and LDN on the growth of breast cancer spheroids. *To ascertain the effect of BMP4(10ng/ml) and LDN(1µM/ml) on three-dimensional growths, breast cancer cells were seeded on agar-coated wells, the spheroids were observed for 14 days, and the area covered by the spheroids was analysed with Fiji software.* ***A.*** *Displays spheroid images for left untreated (CON) or treated with BMP4, LDN or BMP4+LDN conditions (scale = 200 µm) and* ***B.*** *Displays the spheroid area of MCF7, SKBR3, and MDA-MB-231 in percentage concerning their controls. Values are mean ± SE, n=5 independent samples, *p<0.05, **p<0.005, ***p<0.0005.*

To understand the effect of BMP signalling on the self-renewal ability of breast cancer cells, a clonogenic assay was performed with BMP4 and LDN-treated cells. The cells were either pre-treated with BMP4 and LDN for 48 hrs or the treatment period was extended to 14 days for the entire duration of the colony formation assay (Figure 5.7 A). Treatment with both BMP4 and LDN diminished the colony formation ability of MCF7 cells; however, LDN treatment for 48 hr significantly increased the colony area. On the other hand, when the treatment with LDN was extended to 14 days, the colony area decreased significantly, and simultaneous treatment with BMP4 and LDN resulted in decreased colony number and area in MCF7 cells. In the case of SKBR3, treatment with BMP4 significantly decreased the self-renewal ability as seen with the reduced colony number and colony area during 48 hr and 14 days of treatment. Conversely, treatment with LDN for 14 days resulted in increased colony number, and simultaneous treatment with BMP4 and LDN for 14 days inhibited colony formation and colony area in SKBR3 cells.

In MDA-MB-231 cells, however, treatment with BMP4 significantly increased the self-renewal ability, and LDN treatment dramatically decreased the colony number and colony size. Co-treatment of BMP4 with LDN did not reverse the inhibitory effects of LDN on the colony-forming ability of MDA-MB-231 cells. Treatment of MDA-MB-231 with LDN for 48 hr was sufficient to inhibit their self-renewal ability even in the presence of BMP4, making it an interesting option for inhibiting the self-renewal and proliferation ability of breast cancer cells represented by MDA-MB-231 cells (Figures 5.7 B and C).

A

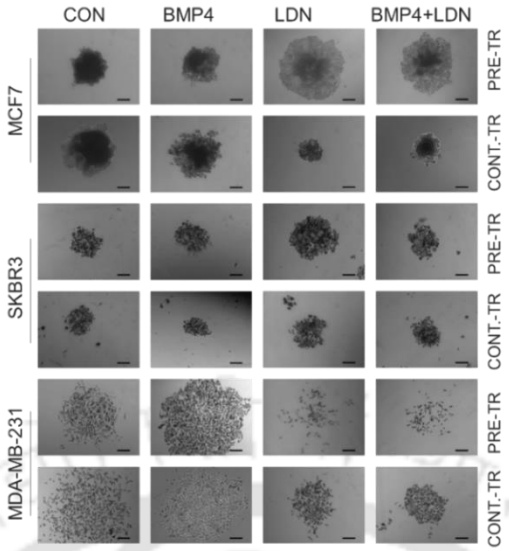

B

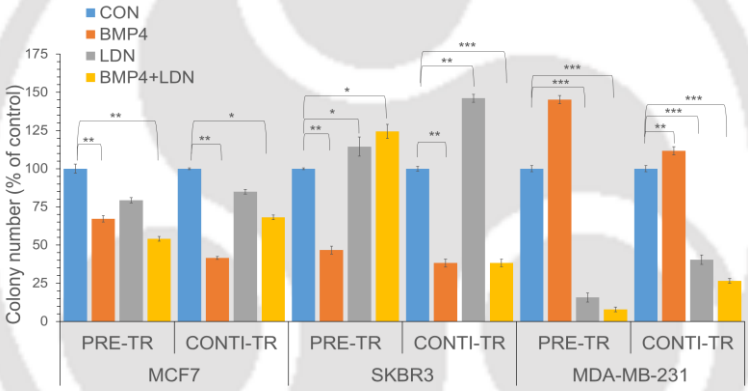

C

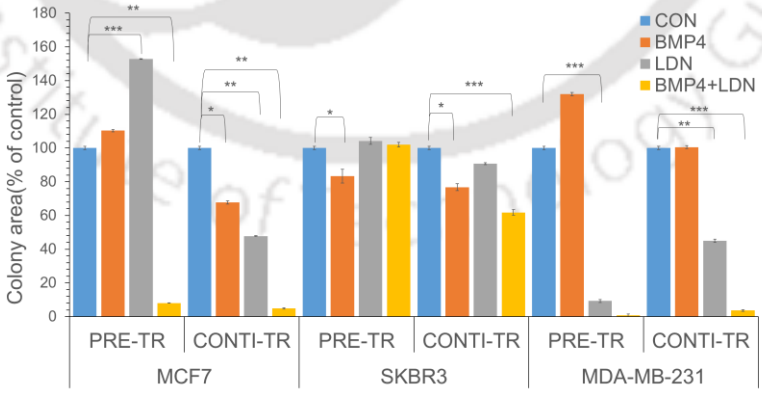

Figure 5.7*: *Effect of BMP4 and LDN on colony formation assay. *Breast cancer cells were treated with BMP4(10ng/ml) and LDN(1µM/ml) for 48 hours ("Pre") and 14 days ("Continuous") to evaluate their clonogenic capacity. Crystal violet solution was utilised for staining the colonies that had developed, and only those with 50 or more cells were considered to be actual colonies. Fiji software was used to measure colony size.* ***A.*** *Represents the colony images (left untreated (CON), or treated with BMP4, LDN or BMP4+LDN) (scale = 200 µm) and* ***B.*** *represents the graph indicating colony number, and* ***C.*** *represents the percentage of colony area calculated concerning their control condition for MCF7, SKBR3, and MDA-MB-231 respectively. Values are mean ± SE, n=5-6 independent samples, *p<0.05, **p<0.005, ***p<0.0005.*

Several reports suggest that the proliferation and self-renewal properties of cancer cells are related to their stemness. Stemness is defined as the ability of the cells to self-renewal and possesses a molecular signature for continuous proliferation. Breast cancer stem cells are defined as $CD44^{+}/CD24^{-}$ and $CD24^{+}$ indicates a $Her2^{+}$ enriched tumour. To understand the role of BMP signalling in the stem-cell-like population of breast cancer cells, the expression of cell surface markers in the presence of BMP4 and LDN was analysed.

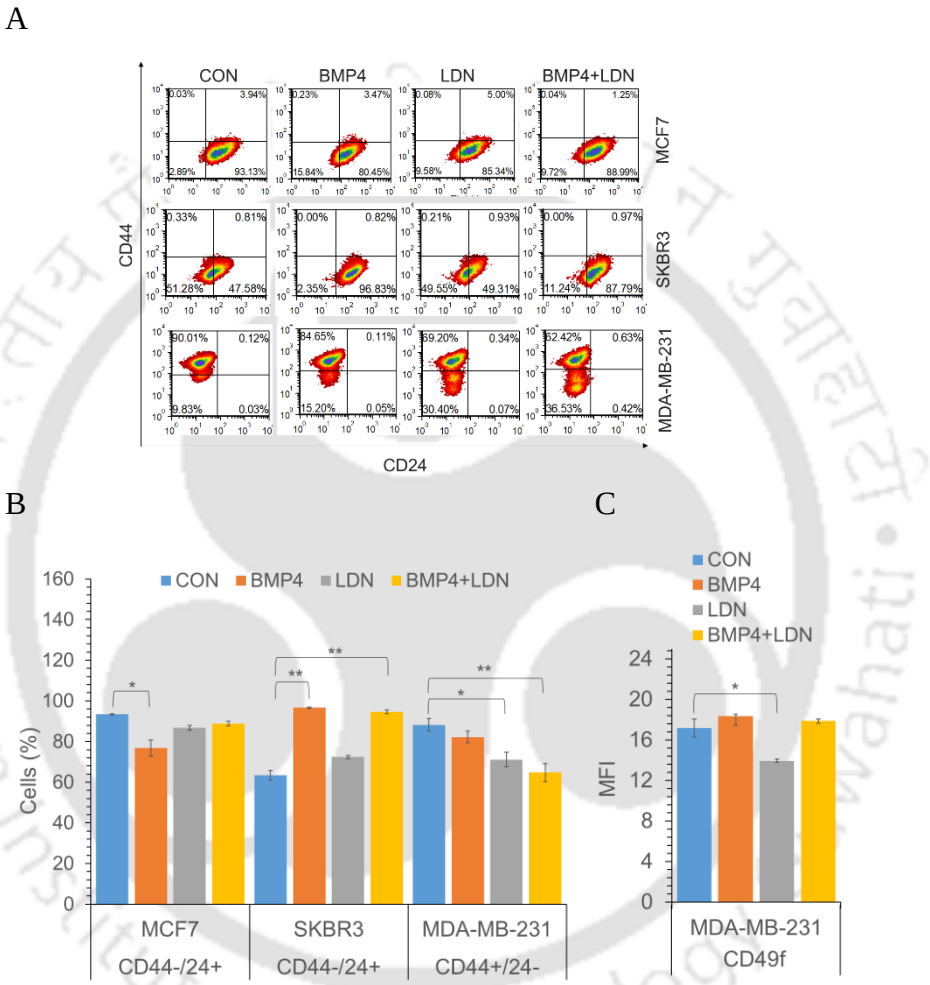

Figure 5.8: Effect of BMP4 and LDN on cell surface markers. *To assess alterations in cell surface markers, treated breast cancer cells with BMP4(10ng/ml) and LDN(1µM/ml) for 48 hours were incubated with fluorescently tagged antibodies CD44, CD24, EPCAM, and CD49f. Propidium iodide was also administered prior to flow cytometry analysis to discriminate between living and dead cells. The density figure in* ***A.*** *represents the fraction of the population that is CD44-/24+ in MCF7 and SKBR3, and $CD44^{+}/24^{-}$ in MDA-MB-231.* ***B.*** *Represents the percentage of the population that is CD44-/24+ in MCF7, SKBR3, and $CD44^{+}/24^{-}$ in MDA-MB-231, as well as the mean fluorescence intensity for the CD49f marker in MDA-MB-231 represented in* ***C.*** *Values are mean ± SE, n=3 independent samples, *p<0.05, **p<0.005.*

BMP4 treatment decreased the proportion of $CD44^{-}/CD24^{+}$ cells in MCF7, but neither LDN nor BMP4 co-treatment had any effect on the expression of the markers (Figure 5.8 A). In contrast, BMP4 and LDN co-treatment in SKBR3 showed an increase in the proportion of $CD44^{-}/CD24^{+}$ cells. The stem cell population in MDA-MB-231, as measured by

$CD44^+/CD24^-$ cells, was downregulated by treatment with LDN alone or in combination with BMP4 (Figure 5.8 B). In addition, the expression of CD49f was reduced when MDA-MB-231 was treated with LDN, however, expression was restored when BMP4 was added along with LDN (Figure 5.8 C). This indicates that BMP signalling plays a crucial role in regulating the expression of cell surface markers.

Furthermore, to understand the functional changes observed with BMP4 or LDN treatment, gene expression analysis was performed for the breast cancer cells treated with either BMP4 or LDN. BMP4 significantly upregulated the expression of stem cell-related genes *CD44* (p= 0.0455), aldehyde dehydrogenase 1A3 (*ALDH1 A3*) (p= 0.0171) and Notch signalling pathway genes *NOTCH2* (p= 0.0276), *NOTCH3* (p= 0.047), and *DNER* (Delta and Notch-like epidermal growth factor-related receptor) (p= 0.0003) in MDA-MB-231 cells. In addition, the expression of EMT-related genes such as *SNAI1* (p= 0.048), *SNAI2* (p= 0.0031) and *FOSL1* (Fos-related antigen 1) (p= 0.0158) also increased in BMP4-treated MDA-MB-231 cells. In MCF7 cells, LDN treatment downregulated E-cadherin (*CDH1*) and upregulated N-cadherin (*CDH2*, p= 0.0133) transcript levels (Figure 5.9). Thus, the BMP pathway controls the expression of EMT and stem cell genes in breast cancer cells.

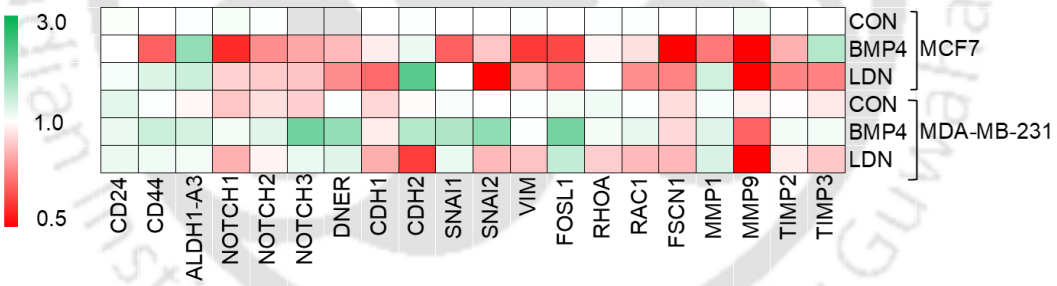

Figure 5.9: BMP4 regulates stemness and migration-related genes. *Using Real-time PCR, the effects of BMP4 and LDN on genes when cells were treated with BMP4(10ng/ml) and LDN(1µM/ml) for 18 hours analysed. In addition, the fold change of CD24, CD44, ALDH1A3, and FOSL1 genes associated with sameness, CDH1, CDH2, SNAI1, SNAI2, VIMENTIN, RHOA, RAC1, FSCN1, MMP1, MMP9, TIMP2 and TIMP3 genes associated with migration, and NOTCH1, NOTCH2, NOTCH3, and DNER genes associated with notch signalling were determined. After normalising the gene of interest with GAPDH, a heat map was generated and displayed as shown in the image above. Values are mean ± SE, n=3 independent samples.*

5.2.4 BMP4 modulates migration and EMT

Since BMP signalling modulated the expression of EMT genes, the role of BMP4 and LDN treatment in regulating the migration of breast cancer cells was determined. Firstly, changes in the actin cytoskeleton arrangement upon BMP4 and LDN treatment were determined. It is known that changes in actin organisation are one of the important aspects of cell

migration, as actin is directly involved in attachment and detachment via a variety of membrane protrusions. Neither BMP4 nor LDN significantly affected actin cytoskeleton organization in MCF7 cells. However, MDA-MB-231 cells treated with BMP4 formed a spindle-shaped morphology with increased polarization as represented in Figure 5.10. Polarisation caused by BMP4 treatment indicates its role in cell membrane protrusion or contraction.

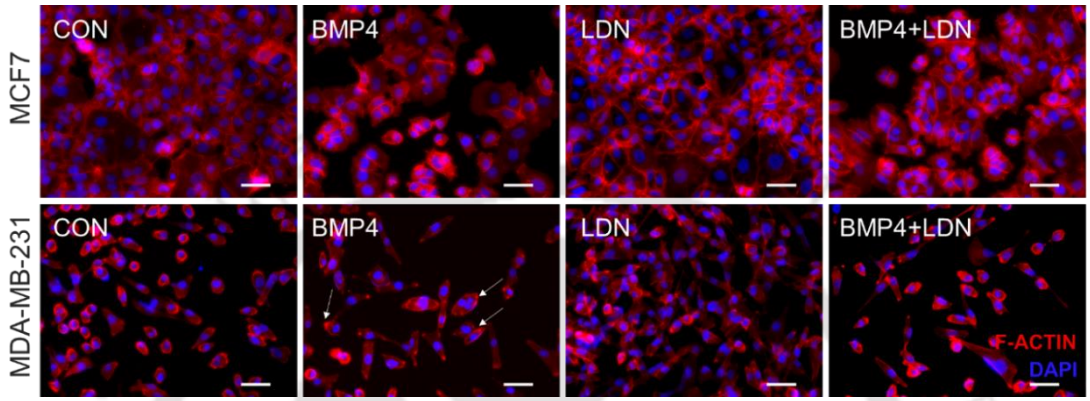

Figure 5.10: Effect of BMP4 and LDN on the actin cytoskeleton. *To observe the effect on actin arrangement and organisation, treated MCF7 and MDA-MB-231 cells with BMP4 (10ng/ml) and LDN (1μM/ml) for 48 hours were processed, fixed, and stained with fluorescent-conjugated Phalloidin-TRITC (Red) which stains F-actin and DAPI (Blue) to identify the nuclear localization in cells. The white arrows indicate the polarization of the cells and the white line in the images represents the scale bar (50μm).*

The migration of breast cancer cells was investigated by wound healing assay as well as through spheroid migration assay. MCF7 cells did not respond to treatment with BMP4 or LDN, but MDA-MB-231 showed a decrease in a migration after treatment with LDN and an increase in migration after treatment with BMP4 in the wound healing migration assay (Figure 5.11 A and B).

To understand how the BMP signalling modulates the invasion of cells in a collagen matrix, a spheroid migration assay was performed. When MCF7 cells were treated with LDN, migration was enhanced, as evidenced by a larger area occupied by the cells, whereas treatment with BMP4 slightly decreased the migration ability. Also, in cell line MDA-MB-231, the migration ability increased when BMP4 was added and decreased when LDN was added. However, the data obtained were not statistically significant. Moreover, the combination treatment of BMP4 and LDN showed no discernible effect in either of the cell lines as shown in Figure 5.12 A and B. This indicates that comparable to wound healing, the invasive potential of only MDA-MB-231 was altered in the presence of BMP4, whereas the effects of BMP4 on MCF7 remain unclear.

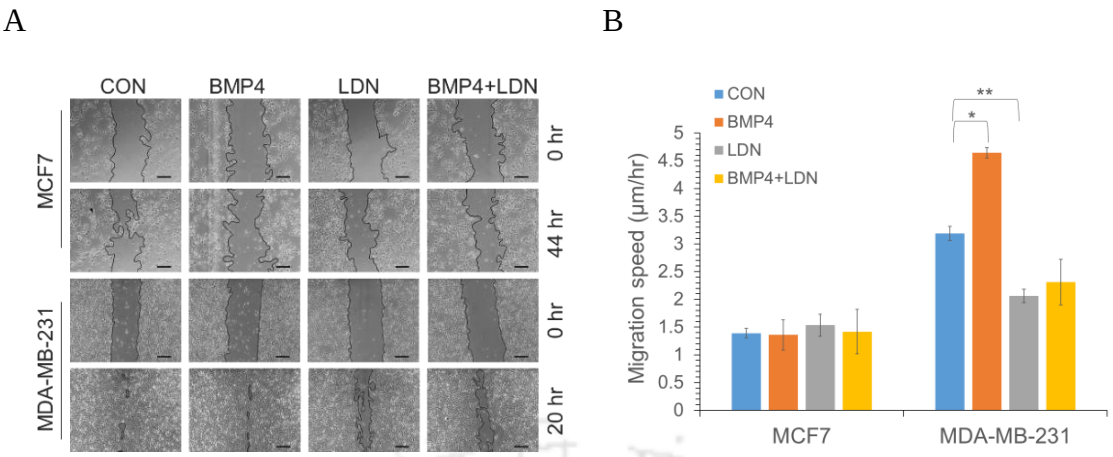

Figure 5.11: Effect of BMP4 and LDN on 2D migration. *An assay for wound healing in which a scratch was produced and cells were allowed to move into the scratched area. Cell mobility in the presence of BMP4(10ng/ml) and LDN(1µM/ml) suggests chemotactic cell migration The area covered by cells in 44 hours in MCF7 and 20 hours in MDA-MB-231 was calculated using T-scratch software and speed was calculated using a formula mentioned in the materials and methodology section.* ***A****. Represent the images of the wound healing assay (left untreated (CON), or treated with BMP4, LDN or BMP4+LDN) and* ***B.*** *is a graphical representation of the migration speed of MCF7 and MDA-MB-231 cells under different conditions. The black line in images represents the scale bar of 200µm. Values are mean ± SE, n=3 independent samples, *p<0.05, **p<0.005.*

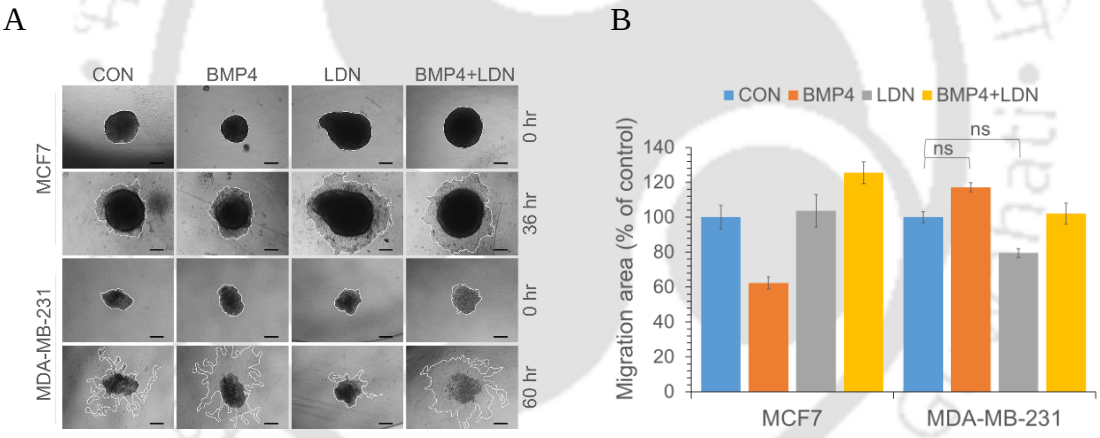

Figure 5.12: Effect of BMP4 and LDN on 3D migration. *The invasive potential of breast cancer in the presence of BMP4(10ng/ml) and LDN(1µM/ml) was also evaluated by transferring preformed spheroids to a flat-bottomed plate and permitting them to invade the collagen matrix. The area covered by the migratory cells in 36 hours of MCF7 and 60 hours in MDA-MB-231 from the spheroids was calculated using Fiji software.* ***A.*** *Represents the images of spheroid migration (left untreated (CON), or treated with BMP4, LDN or BMP4+LDN) and* ***B.*** *represents the graph of the area covered by migrating cells of each treatment condition calculated against their respective controls. The black line in images represents the scale bar (200µm). Values are mean ± SE, n=5 independent samples, not significant (ns), p>0.05*

Two important proteins that aid in controlling the epithelial-mesenchymal transition are E-cadherin and N-cadherin. Cells grown as 3D spheroid in the presence of either BMP4 or LDN were analysed for the expression of the cadherin. Both LDN and co-treatment of LDN and BMP4 decreased the expression of E-cadherin in MCF7. In MDA-MB-231 cells, the

expression of N-cadherin increased by BMP4 treatment and simultaneous treatment with LDN, as shown in Figure 5.13 A and B.

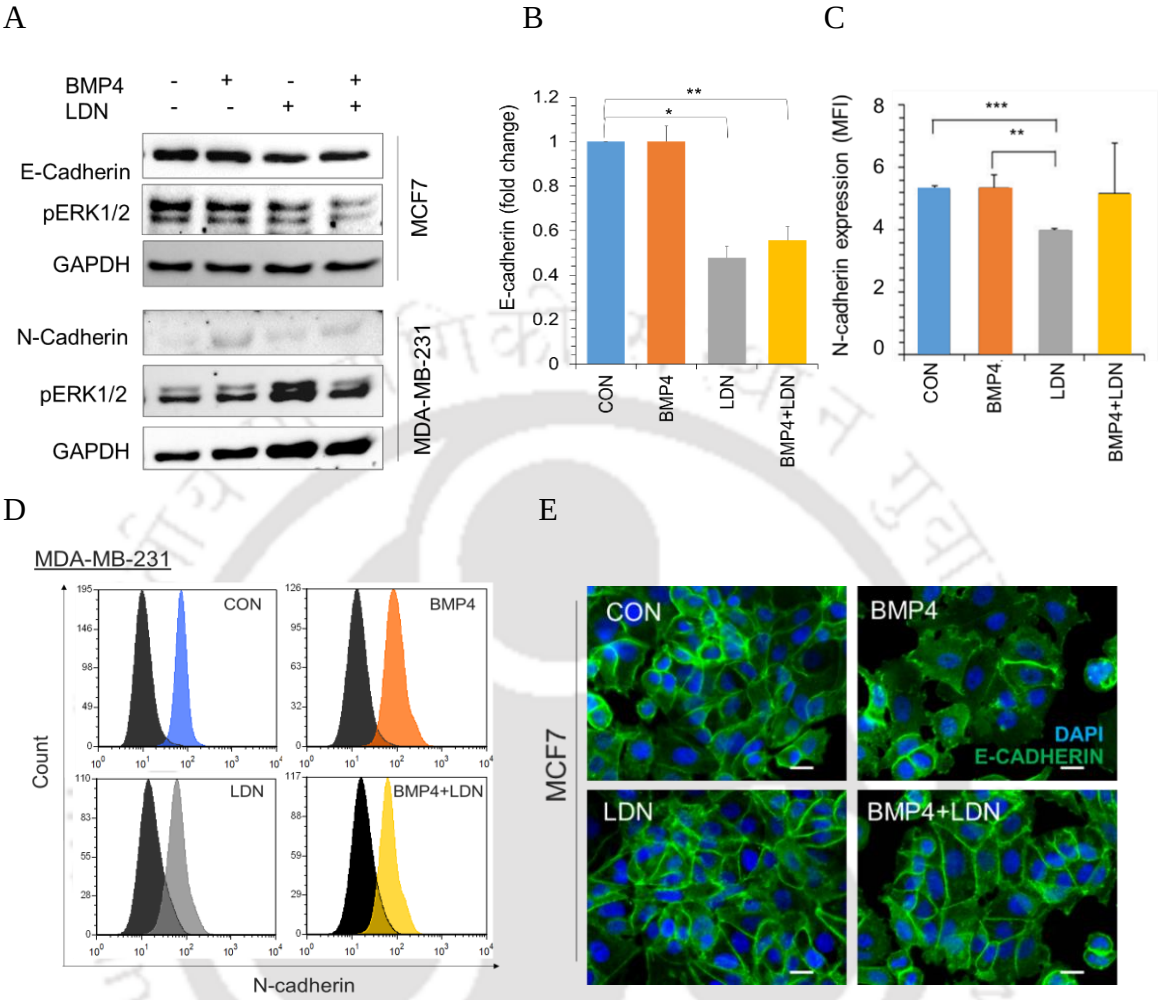

Figure 5.13: Effect of BMP4 and LDN on the expression of cadherin. *Using Western blot, flow cytometric, and immunocytochemical staining, the expression of cadherins was determined. E-cadherin and N-cadherin are the two most important proteins implicated in the EMT transition; consequently, the expression of these proteins was evaluated using a variety of techniques after treating breast cancer cells with BMP4(10ng/ml) and LDN(1µM/ml) for 48 hours.* ***A.*** *Represents the western blot image of E-Cadherin (~110 KDa), pERK1/2 (~42-44 KDa), and GAPDH (~37 KDa) expression in MCF7 and N-cadherin (~140 KDa), pERK1/2 (~42-44 KDa), and GAPDH (~37 KDa) in MDA-MB-231 and, followed by* ***B.*** *Indicates fold change in E-cadherin in MCF7* ***C.*** *represents normalized MFI of N-cadherin expression.* ***D.*** *Represents the histogram of N-cadherin expression where black peaks represent the unstained sample for respective treatment conditions and coloured peaks represent the stained samples of Control, BMP4, LDN and BMP4+LDN-treated conditions in MDA-MB-231* ***E.*** *Immunocytochemistry images of MCF7 where green colour indicates E-cadherin and blue colour represents the nucleus. The white line in the images represents the scale bar (20 µm). Values are mean ± SE, n=3 independent samples, *p<0.05, **p<0.005, ***p<0.0005.*

In addition, flow cytometric analysis showed that LDN and co-treatment with BMP4 decreased N-cadherin expression in MDA-MB-231 (Figure 5.13 C and D). When MCF7 were stained for E-cadherin, BMP4 treatment resulted in diffuse expression of E-cadherin throughout the cytoplasm, as shown in Figure 5.13 E.

5.2.5 BMP4 in anoikis resistance

During metastasis, the cells detach from their extracellular matrix, they undergo programmed cell death known as anoikis. When cancer cells avoid their programmed death signals, this phenomenon is referred to as anoikis resistance, and the cells themselves are called anoikis-resistant cells. Since anoikis resistance is an important aspect of cancer metastasis, its relationship with BMP signalling in breast cancer cells was investigated. Breast cancer cells were cultured in an anchorage-independent suspension culture, and then cell viability was determined. SKBR3 cells showed no response to BMP4 and LDN treatment, as no significant change in cell number was observed (Figure 5.14 A). However, BMP4 therapy resulted in a slight decrease in the percentage of viable cells (Figure 5.14 B). In contrast, MDA-MB-231, LDN treatment and co-treatment with BMP4 significantly reduced the number of cells and the percentage of viable cells. This data indicates that the anoikis resistance of SKBR3 and MDA-MB-231 cell lines is differentially regulated by BMP signalling.

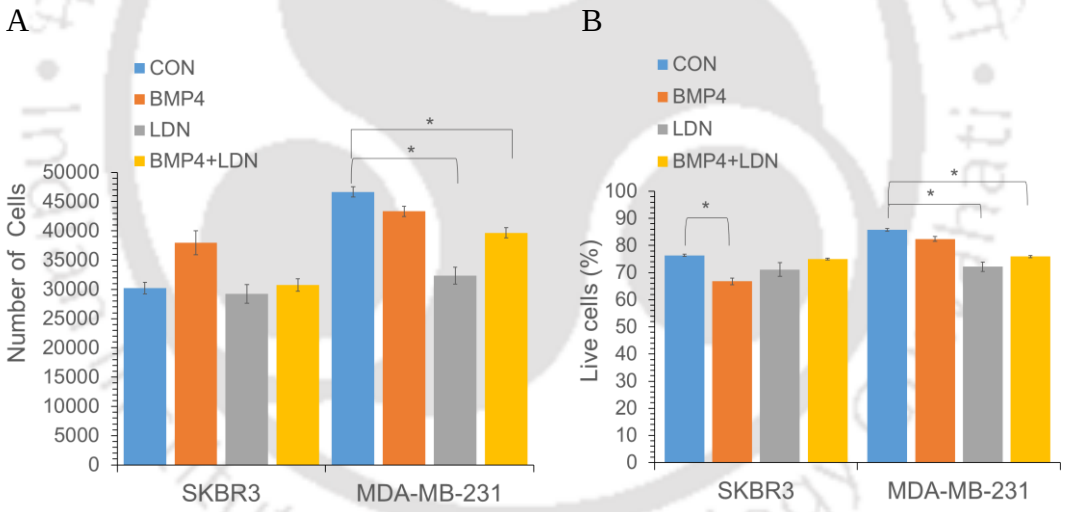

Figure 5.14: Effect of BMP4 and LDN on survival of anchorage-independent cultured cells. *Cell survival in non-adherent conditions was assessed using the trypan blue method to determine cell number and the propidium iodide staining method to determine the percentage of live and dead cells. The graph above depicts the number of cells in* ***A.*** *and the percentage of live cells in* ***B.*** *for both the SKBR3 and MDA-MB-231 cell lines when treated with BMP4(10ng/ml) and LDN(1µM/ml) for 48 hours. Values are mean ± SE, n=3 independent samples, *p<0.05.*

To understand further the effect of BMP4 and LDN on the anoikis resistance of breast cancer cells, cells grown in anchorage-independent conditions were analysed for their cell surface marker expression. A decrease in the percentage of $CD44^{+}/CD24^{-}$ and $CD44^{+}/EpCAM^{-}$ populations was observed in MDA-MB-231 cells treated with LDN (Figure 5.15 A), whereas CD49f expression increased after treatment with BMP4 (Figure

5.15 B). The fact that LDN treatment reduced stem cell marker expression while BMP4 treatment enhanced CD49f expression suggests that BMP signalling is important in maintaining the stemness of anoikis-resistant cells.

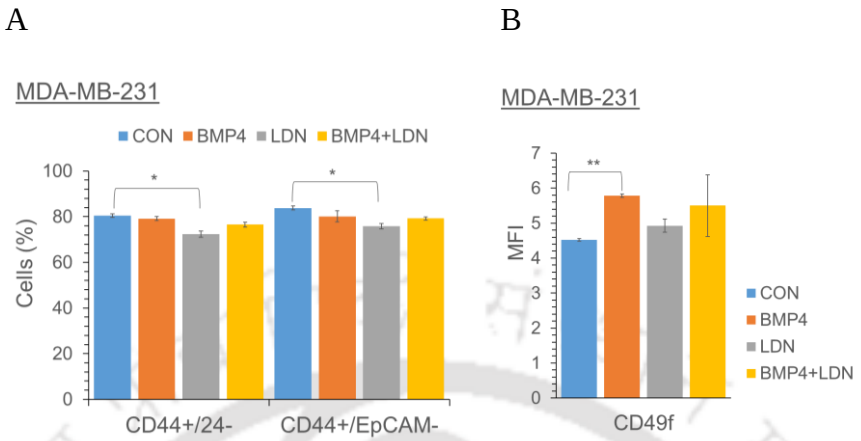

Figure 5.15: Effect of BMP4 and LDN on the phenotype of anchorage-independent cultured cells*. The expression of cell surface markers was examined further in non-adherent cell cultures. The cells were seeded along with BMP4(10ng/ml) and LDN(1µM/ml) for 48 hours and stained with antibodies against CD44, CD24, EPCAM, and CD49f that were fluorescently tagged. Using two distinct fluorescence at once, the percentage of the double-positive/negative population was determined, and normalised MFI was calculated by normalising the fluorescence intensity of treated samples versus the fluorescence intensity of unstained samples. Graph* ***A.*** *represents the percentage of $CD44^+/24^-$ and $CD44^+/EpCAM^-$ cells and* ***B.*** *represents the MFI of CD49f expression in MDA-MB-231. Values are mean ± SE, n=3 independent samples, *p<0.05, **p<0.005.*

To confirm the importance of BMP signalling in anoikis resistance, the clonogenic potential of breast cancer cells was also assessed. To address this, cells were grown under anchorage-independent conditions in the presence of BMP4 or LDN. The "pre-treated cells" (PRE-TR) refers to cells treated with BMP4 or LDN for 48 hours under anoikis conditions, and "continuously treated cells" (CONTI-TR) refers to cells that were additionally treated with BMP4 or LDN during colony formation (Figure 5.16 A). In MCF7, a decrease in both colony number and colony area was observed with both LDN and BMP4 treatment. However, when treated continuously with LDN and BMP4+LDN, a significant decrease in colony number and area was observed. SKBR3 responded very differently in this regard.

Treatment with LDN alone or with BMP4+LDN increased colony numbers under both "pre" and "continuous' conditions. At the same time, the colony area increased dramatically under both conditions, although it was slightly lower under continuous treatment. Furthermore, treatment with BMP4 did not affect the clonogenic capacity of SKBR3. Under anoikis conditions, treatment of MDA-MB-231 cells at both PRE-TR and CONTI-TR conditions with BMP4 resulted in increased colony numbers. Colony area also increased, although to a lesser extent at CONTI-TR compared with PRE-TR.

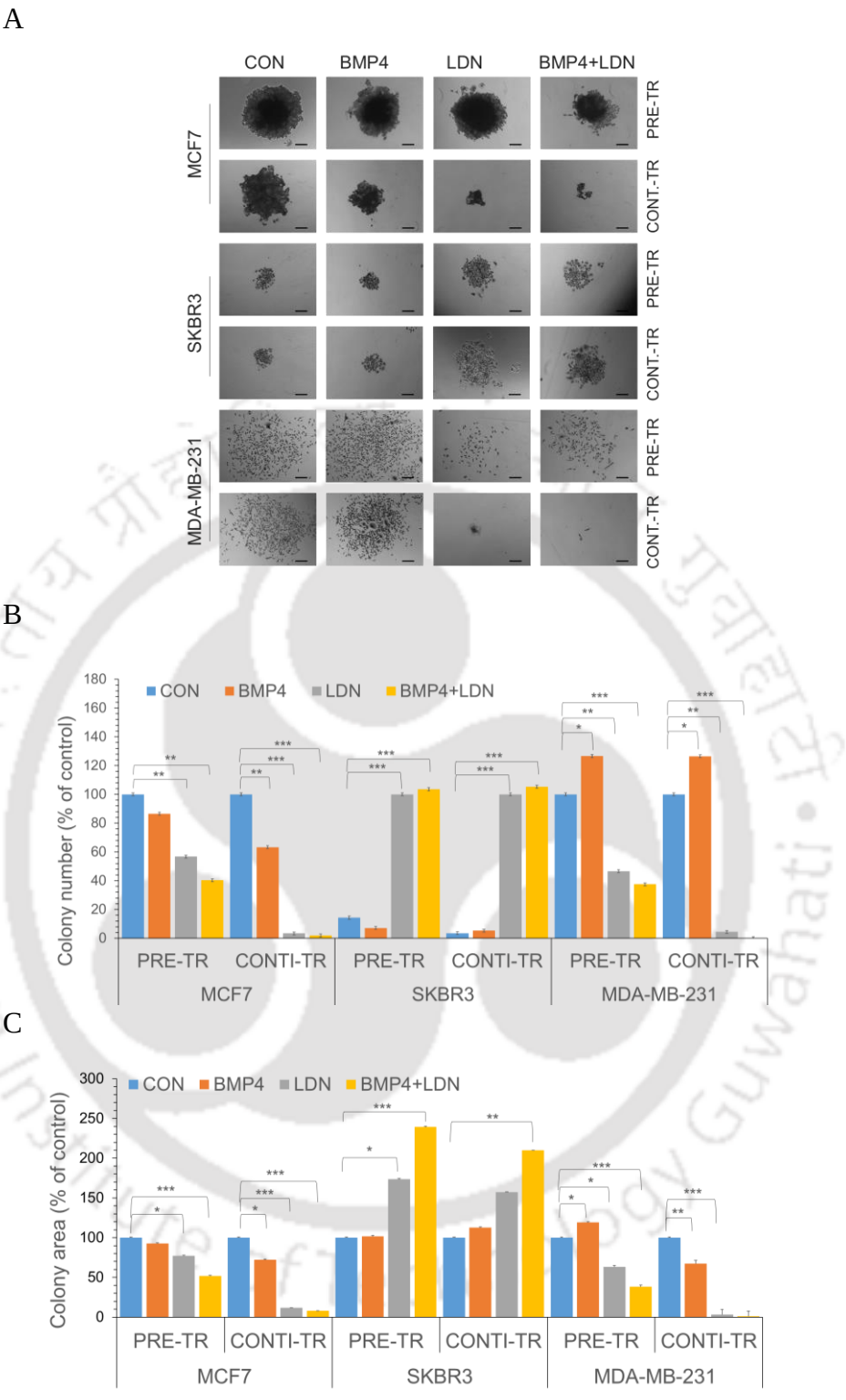

Figure 5.16: Effect of BMP4 and LDN on colony formation assay of anoikis-resistant cells. *Non-adherent cells cultured in the presence of BMP4(10ng/ml) and LDN(1µM/ml) were tested for anoikis resistance. BMP4 and LDN were given to pre-treated cells for 48 hours; continuous therapy (14 days) included treatment until the end of the experiment. Crystal violet solution was used to stain the colonies, and colonies with at least 50 cells were considered intact. Colonies were counted and the area was measured using Fiji software.* ***A.*** *Represents the colony images of left untreated (CON), or treated with BMP4, LDN or BMP4+LDN conditions (Scale bar = 200µm) and* ***B.*** *represents the graph of colony number and* ***C.*** *the colony area for MCF7, SKBR3 and MDA-MB-231 in percentage. Values are mean ± SE, n=5-6 independent samples, *p<0.05, **p<0.005, ***p<0.0005.*

Similarly, LDN or co-treatment with BMP4 resulted in a decrease in colony number and colony area, but the effect was more pronounced with continuous treatment (Figure 5.16 B and C). Thus, BMP regulated the anoikis resistance properties of breast cancer cells and treatment with either BMP4 or LDN can either increase or decrease the anoikis resistance ability based on the cell type. The cancer cells activate survival signals to overcome the anoikis conditions during metastasis, while the cells are circulating through the circulatory or lymphatic system. The BCL2 (B-cell lymphoma 2) protein family is critical for the regulation of apoptosis. BCL2 protein inhibits apoptosis by maintaining the integrity of the mitochondrial membrane as its hydrophobic carboxyl-terminal domain is attached to the outer membrane (Neinavaie, et al., 2021).

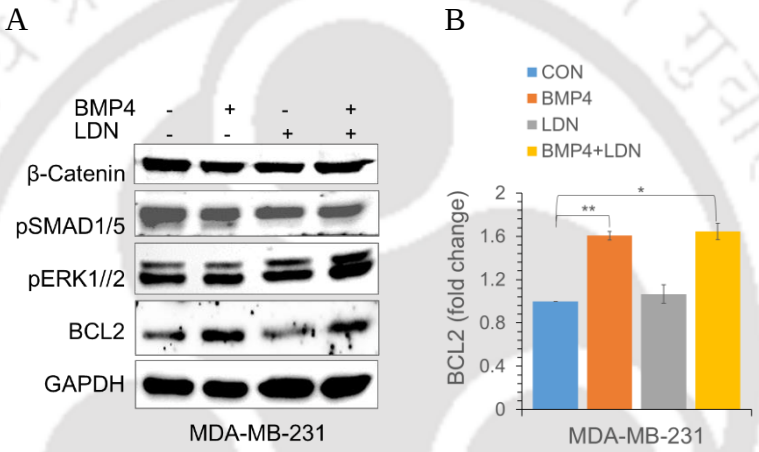

Figure 5.17*: *Effect of BMP4 and LDN on the protein expression of anchorage-independent cultured cells. *Protein lysates from anchorage-independent cells treated with BMP4(10ng/ml) and LDN(1µM/ml) for 48 hours were used in the western blot analysis. The lysate was put onto an acrylamide gel before being transferred to a nitrocellulose membrane. After blocking, the membrane was incubated with primary and secondary HRP-conjugated antibodies. A detection and representation of the chemiluminescence produced by the chemical reaction between the HRP and the ECL substrate are shown above.* ***A.*** *The blots represent the expression of β-catenin (~92 KDa), pSMAD1/5 (~55 KDa), pERK1/2 (~42-44 KDa), BCL2 (~26 KDa), and GAPDH (~37 KDa) in MDA-MB-231 and* ***B.*** *the graph represents the fold change in BCL2 expression. Values are mean ± SE, n=4 independent samples, *p<0.05, **p<0.005.*

Therefore, BCL2 expression in anchorage-independent conditions during treatment with BMP4 and LDN was determined by immunoblotting. BCL2 expression increased significantly under BMP4 and BMP4+LDN treatment conditions, whereas LDN treatment did not affect BCL2 expression in MDA-MB-231 cells (Figure 5.17 A and B). Interestingly, the expression of β-catenin and pERK1/2 were not affected by BMP4 or LDN treatment. These results confirm that BMP signalling improves cell survival by increasing BCL2 expression in MDA-MB-231 cells.

5.2.6 LDN193189 diminishes chemoresistance and proliferation on stromal cells

Chemoresistance is the next stage of cancer development, where cancer cells develop resistance to chemotherapy drugs that lead to excessive proliferation of the cancer cells even in the presence of chemotherapeutic drugs. Experiments were carried out in the presence of doxorubicin, a well-known chemotherapy drug that inhibits the topoisomerase enzyme that unwinds the DNA during replication. The role of BMP4 and LDN in the chemosensitization of breast cancer cells was investigated by treating them with doxorubicin in combination with BMP4 and LDN. Cell survival and viability were assessed, and the combination of LDN and doxorubicin reduced the viable cell number in MCF7. In SKBR3, treatment with BMP4 in combination with doxorubicin increased cell viability. When MDA-MB-231 cells were treated with LDN in combination with doxorubicin, a decrease in proliferation and cell number was observed (Figure 5.18 A and B).

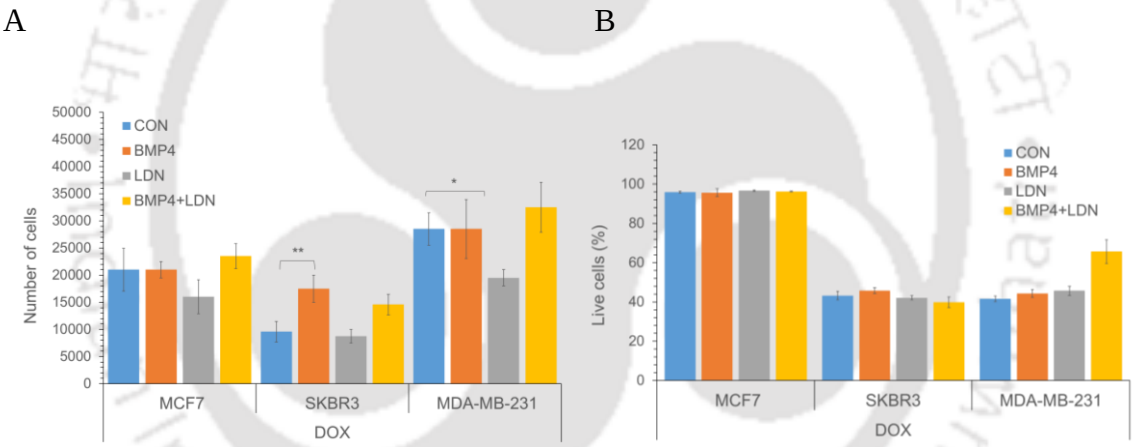

Figure 5.18: Effect of BMP4 and LDN on survival of doxorubicin-treated cells. *Cell survival of doxorubicin treated in combination with BMP4(10ng/ml) and LDN(1µM/ml) for 48 hours was assessed using the trypan blue method to determine cell number and the propidium iodide staining method to determine the percentage of live and dead cells. The above graph* ***A.*** *represents the change in cell number and* ***B.*** *depicts the percentage of live cells in MCF7, SKBR3 and MDA-MB-231 respectively. Values are mean ± SE, n=4 independent samples, *p<0.05, not significant (ns), p>0.05*

The chemosensitivity of breast cancer cells was further evaluated using a three-dimensional spheroid assay, as it is conceivable that a particular chemotherapeutic agent can affect 2D and 3D cultures differently. For this purpose, cancer cell lines were seeded with BMP4 and LDN in combination with doxorubicin to form spheroids. Three-dimensional growth was monitored at regular intervals by measuring spheroid size. Regardless of the cell line, treatment with doxorubicin resulted in a significant reduction in spheroid size. In MDA-MB-231 spheroids, co-treatment with doxorubicin and LDN or BMP4+LDN resulted in

smaller spheroids. In contrast, the spheroid size of MCF7 cells increased when treated with LDN and doxorubicin, whereas the spheroid size of SKBR3 decreased when treated with BMP4 and doxorubicin (Figure 5.19 A and B).

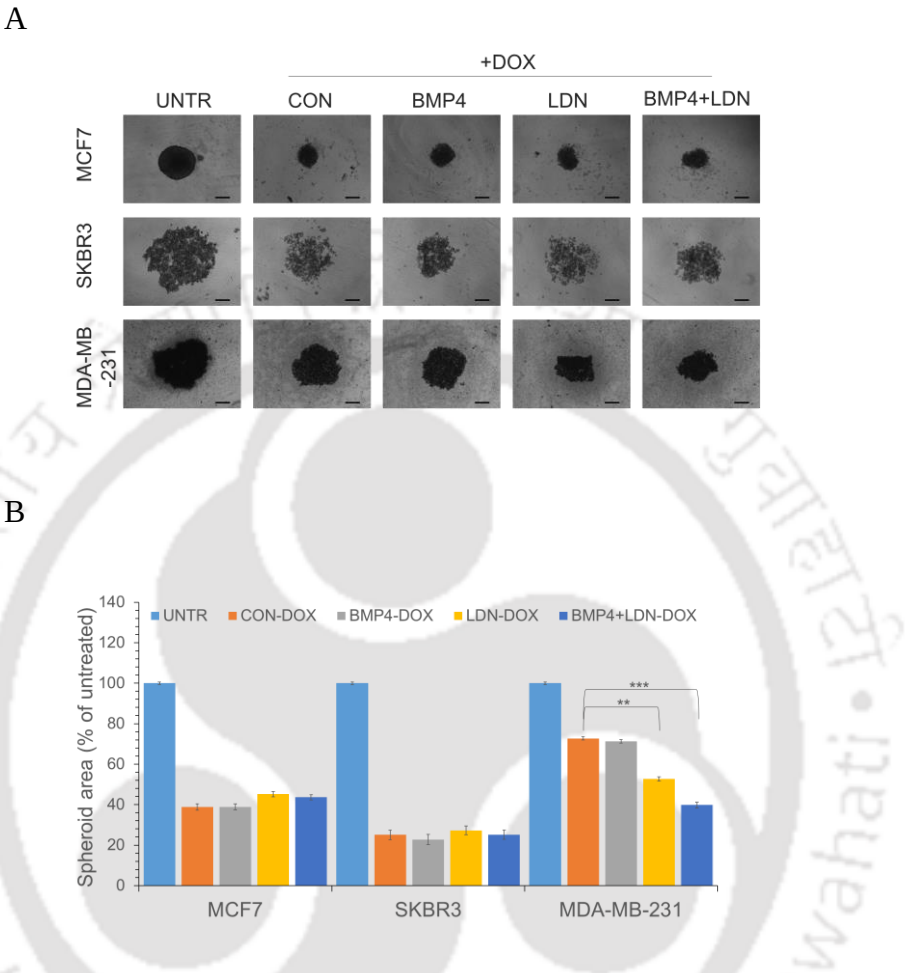

Figure 5.19: Effect of BMP4 and LDN on chemosensitivity of spheroids*. The chemosensitivity of breast cancer cells was also assessed in a three-dimensional environment, where cells were cultured in the presence of doxorubicin(5µM/ml), BMP4(10ng/ml) and LDN(1µM/ml) for 17 days to see if the supplied substances (BMP4 and LDN) may confer chemoresistance. The spheroids were monitored, and photos were collected every four days. The area covered by the growing spheroids was analysed using Fiji software.* ***A.*** *Represents the spheroid images of left untreated (CON), or treated with BMP4, LDN or BMP4+LDN and* ***B.*** *Represents the spheroid area of MCF7, SKBR3 and MDA-MB-231 under each treatment calculated as the percentage of the area of their respective controls. The black line in images represents the scale bar (200µm). Values are mean ± SE, n=5 independent samples, **p<0.005, ***p<0.0005.*

Thus, modifying the BMP signalling chemosensitizes the breast cancer cells to the chemotherapeutic drug, doxorubicin. To determine whether BMP signalling can modulate the chemosensitivity of anoikis-resistant cells, breast cancer cells were cultured under anchorage-dependent anoikis-inducing conditions. The cells were treated with BMP4, and LDN in the presence of doxorubicin for 48 hr and the resulting cells were tested for their colony-forming ability. This is to simulate the secondary growth of breast cancer cells during chemo-drug treatment during activation or inhibition of BMP signalling. The ability

of MDA-MB-231 cells to form colonies was completely abolished when treated with LDN and doxorubicin. However, BMP4 treatment enabled the cells to resist doxorubicin treatment, allowing them to form an increased number of colonies and larger colonies compared to the control cells.

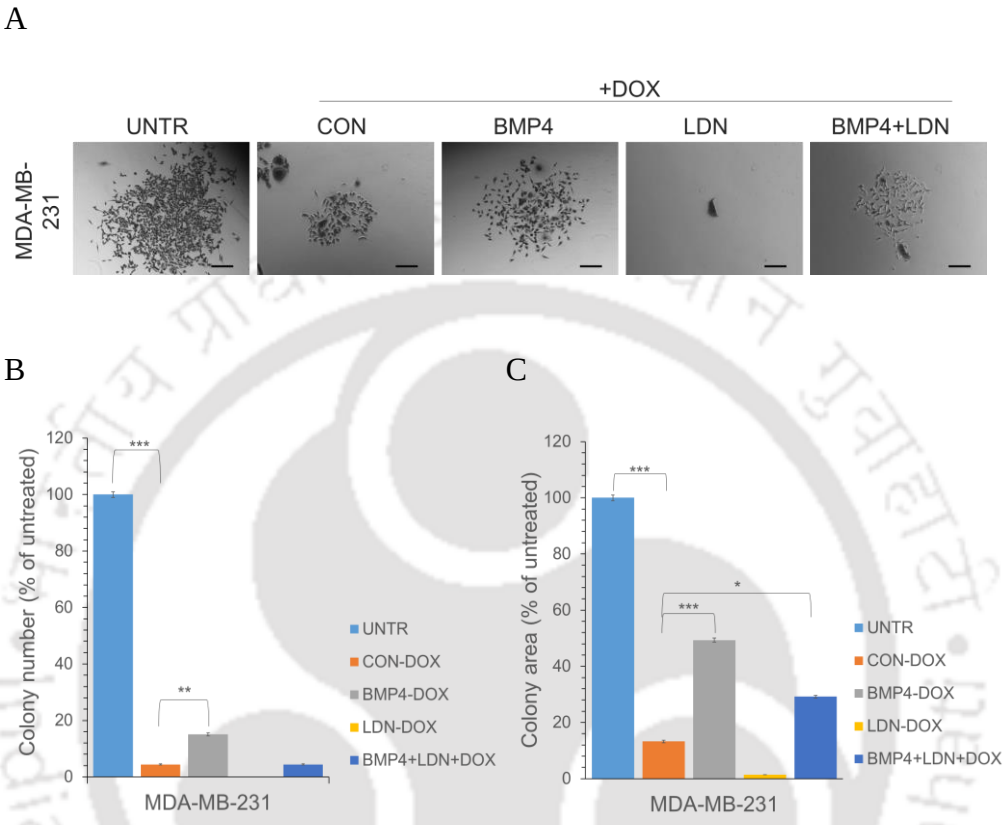

Figure 5.20: Effect of BMP4 and LDN on chemosensitivity of anoikis-resistant cells*. The chemosensitivity of anoikis-resistant cells was assessed after they were exposed to doxorubicin(5µM/ml), BMP4(10ng/ml) and LDN(1µM/ml) in non-adherent conditions and allowed to form colonies for 14 days. The combination of BMP4 and doxorubicin lowered the chemosensitivity of breast cancer cells, as evidenced by a high colony number. The colonies were stained with crystal violet solution, and their area was measured using Fiji software.* ***A.*** *Represents the colony images left untreated (UNTR), or treated alone with Dox (CON), or treated with BMP4, LDN or BMP4+LDN in conjunction with Dox and (Scale bar = 200µm) and* ***B.*** *represents the graph of colony number and* ***C.*** *the colony area for MDA-MB-231 cells. Values are mean ± SE, n=3 independent samples, *p<0.05, **p<0.005, ***p<0.0005.*

When doxorubicin was administered under BMP4+LDN conditions, the inhibitory effect of LDN was partially reversed, resulting in the formation of colonies, albeit in smaller numbers than with BMP4+doxorubicin treatment (Figure 5.20).

Bone marrow is one of the primary sites of metastasis for breast cancer cells. To analyse whether the presence of BMP4 or LDN can modulate the metastatic loci formation ability of breast cancer cells, breast cancer cells were first cultured under anoikis conditions. During anoikis culture, the cells were treated with either BMP4 or LDN and the resulting cells were allowed to proliferate on the bone marrow stromal layer. The ability of the cells to form colonies in the bone marrow microenvironment was analysed.

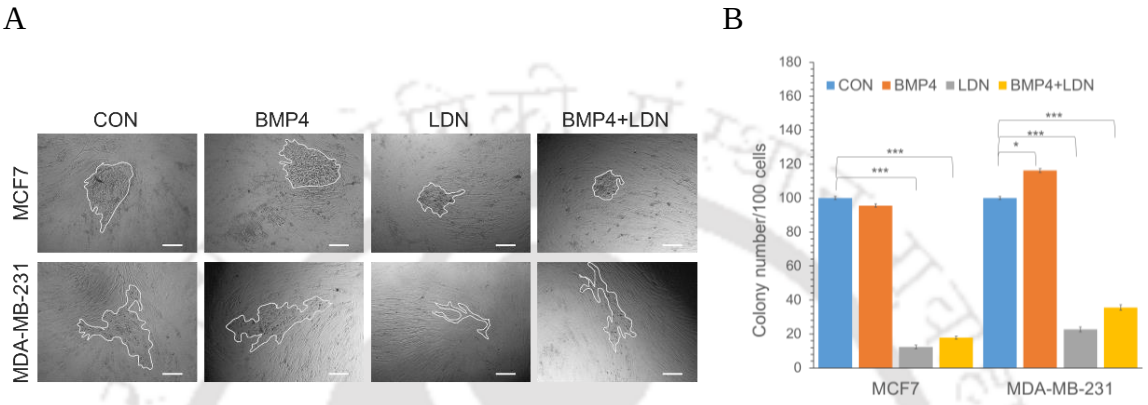

Figure 5.21: Effect of BMP4 and LDN on bone metastasis of anoikis-resistant cells. *The in vitro metastatic potential of breast cancer cells treated with BMP4(10ng/ml) and LDN(1µM/ml) for 48 hours in a non-adherent environment was assessed by co-culturing these cells with stromal cells derived from bone marrow samples. Using a microscope, the number of colonies generated by these breast cancer cells resistant to anoikis was determined.* ***A.*** *Represents the colony images of MCF7 and MDA-MB-231 of left untreated (CON), or treated with BMP4, LDN or BMP4+LDN formed on stromal cells (Scale bar = 200µm) and* ***B.*** *represents the graph of the colony number under each condition. Values are mean ± SE, n=12 independent samples, *p<0.05, ***p<0.0005.*

Both MCF7 and MDA-MB-231 formed more and larger colonies upon treatment with BMP4. However, LDN treatments significantly reduced the colony-forming ability, with the cells forming fewer and smaller colonies compared to the control untreated cells (Figure 5.21). Taken together, these data suggest that activation of BMP signalling induces anoikis resistance and supports metastatic growth of breast cancer cells which can be effectively controlled by inhibiting the BMP signalling.

5.2.7 BMP4 expression correlates with EMT genes in breast cancer patient samples

To determine the relevance of our results with the model breast cancer cell lines in the patients, the expression of BMP4 and genes related to proliferation, EMT, etc. were determined. For this, patient samples belonging to different subtypes based on their hormone receptor expression were analysed for the expression of different gene sets. *BMP4* expression was significantly high in ER-/PR- tumours regardless of Her2 expression (Figure 5.22 A). Furthermore, BMP4 mRNA expression showed a positive correlation with

EMT (epithelial-mesenchymal transition)-related genes such as *SNAI2* (p=0.0086), *CDH2* (p=0.049), *RHOA* (p = 0.006), *MMP9* (matrix metallopeptidase 9) and *ALDH1 A3* (p= 0.011) (Figure 5.22 B).

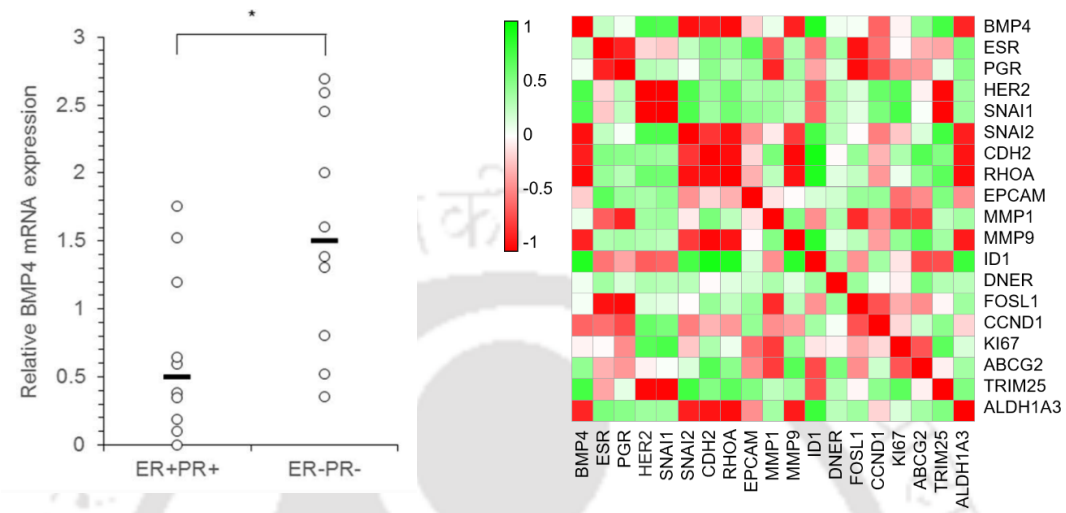

Figure 5.22: BMP4 expression correlates with EMT genes*. The expression of BMP4 in patient samples classified based on ER, PR, and Her2 expression was analysed by real-time PCR.* ***A.*** *represents the graph, where each open circle symbolizes an individual sample, and the line represents the median value.* ***B.*** *Heatmap of bivariate Pearson correlation coefficient values for the indicated genes in patient samples. n=6 independent samples ($ER^+ PR^+$ - 3 samples; $ER^- PR^-$ - 3 samples)****,*** **p<0.05, **p<0.005, ***p<0.0005.*

Thus, BMP signalling modulates the various aspects of cancer cells such as proliferation, EMT, anoikis resistance, chemoresistance and the ability to form colonies in the bone marrow microenvironment.

5.3 Discussion

This chapter describes the role of BMP4 signalling in breast cancer progression. BMP4 was found to control multiple aspects of cancer cells including their proliferation, EMT, anoikis resistance and chemoresistance. Breast cancer model cell lines MDA-MB-231, MCF7 and SKBR3 were utilized to understand how the BMP signalling regulates cancer progression and how it can be modulated for therapeutic purposes. Breast cancer patient samples were analysed to corroborate the results obtained with the breast cancer cell lines. The paracrine action of BMP4, which may be secreted by the tumour microenvironment (Cao et al., 2014) in breast cancer, was simulated by the exogenous addition of recombinant human BMP4. The BMP signalling pathway was inhibited by BMP receptor inhibitor LDN. Blood samples from patients with advanced breast cancer have been shown to have higher levels of BMP4 and BMPRII expression (Gul et al., 2015) compared to the control group, somewhat similar to what was seen with MDA-MB-231, a triple-negative breast cancer cell line, which showed high levels of BMPRII and BMP4 expression.

In the current study, BMP4 was found to have a cell-type-specific effect (Kallioniemi, 2012; Klumpe et al., 2022); it dramatically reduced the proliferation of MCF7 and SKBR3 accompanied by an increase in the percentage of cells at the G0 stage of cell cycle and increased CDKN1A expression. The proliferative effect observed in MCF7 was similar to that reported by Shee et al, that BMP4 inhibits the growth of ER^+ tumours in patients with breast cancer (Shee et al., 2019).

BMP4 generally modulates the proliferation and invasion of breast cancer by a canonical signalling route (Owens et al., 2013; Gang Yan et al., 2021). Chordin-like 1, a well-known BMP4 antagonist found to be increased in numerous breast cancer patients, blocks the migration and invasion generated by BMP4 (Cyr-Depauw et al., 2016). Another piece of research has shown that BMP4 plays an important part in the migration process (Ampuja et al., 2016a; Guo et al., 2012). Similarly, It has been demonstrated that BMPs encourage the migration of neural crest cells (Kanzler et al., 2000), which are crucial in the formation of the nervous system. On the other hand, BMPs can block the migration of smooth muscle cells (Dorai et al., 2000), which is crucial for the prevention of certain cardiovascular disorders. The breast cancer cell line MDA-MB-231 was able to migrate and invade more easily when exposed to BMP4 (Ampuja et al., 2016a), which was accompanied by an increase in the expression of EMT genes N-cadherin, *SNAI1*, *SNAI2*, and *FOSL1*, all of

which were blocked by LDN treatment. In contrast to this, one of the findings indicated that BMP4 reduces breast cancer propagated in animal models via Smad7 (Eckhardt et al., 2020a). Similarly, Cao et al, observed that the reduction of myeloid-derived suppressor cell activity at the tumour site reduced the metastasis of mouse mammary cancer cells overexpressing BMP4 (Cao et al., 2014).

The study conducted by Ampuja et al. presents evidence indicating that the injection of BMP4 leads to an earlier occurrence of bone metastases in comparison to the control group (Ampuja et al., 2016b). Likewise, the suppression of bone morphogenetic protein (BMP) signalling by utilising Noggin has been reported to hinder the spread of breast cancer cells to the bone, where the metastatic process is predominantly supported by the activity of FOFX2 (Wang et al., 2019). Another study corroborated the evidence that eliminating BMP4 from breast cancer cells, or administering a BMP signalling inhibitor, successfully inhibited the development of osteoclasts in bone metastases and decreased the activity of the Fam20C-regulated pathway (Zuo et al., 2021). In contrast, a distinct inquiry uncovered that when BMP4 acted as an autocrine mediator, it suppressed the dissemination of breast cancer cells to both the skeletal system and respiratory organs. This was accomplished by activating the BMP-SMAD7 signalling pathway (Eckhardt et al., 2020b). Additionally, a distinct inquiry has revealed that the inhibition of BMP4-Smad1/5, achieved by a positive feedback mechanism involving YAP1-Notch1, promotes the development of lung metastasis in breast cancer cells (Zhao et al., 2022). Therefore, data suggests that the autocrine BMP signalling inhibits metastasis, while the paracrine effect of BMP signalling promotes cancer cell mobility and metastasis.

Anoikis resistance is an indispensable requirement for cancer metastasis, which necessitates the hyperactivation of survival pathways and anti-apoptotic genes such as Mcl-1, Bcl-xL, and Bcl2. (Kim et al., 2012). This is precisely why for example, in the case of prostate cancer, researchers have begun to focus on anoikis resistance to halt the spread of the malignancy (Sakamoto & Kyprianou, 2010). Alternatively, BMPs can potentially have pro-anoikis effects. BMPs have also been demonstrated to increase cancer cell sensitivity to apoptosis by suppressing anti-apoptotic gene expression. BMP4 dramatically increased the survival of metastatic MDA-MB-231 cells under anoikis conditions via BCL2 overexpression, showing the importance of BMP signalling in the establishment of metastases. Furthermore, the functional effect of BMP4 extends beyond migration, invasion, and EMT, and the BMP pathway has also contributed to chemoresistance in many

types of malignancies. The function of BMP4 in chemoresistance was further reinforced by Ma et al (J. Ma et al., 2017), who showed that liver cancer cells have the potential to develop resistance to oxaliplatin by the EMT pathway. By suppressing the expression of drug-resistance genes, however, BMPs have been demonstrated to sensitise cancer cells to chemotherapy drugs. BMPs have also been discovered to promote apoptosis in chemotherapy-treated cancer cells, hence increasing the efficacy of chemotherapy. According to the findings of our research, BMP4 improved stem cell characteristics in MDA-MB-231 cells. This was demonstrated by an increase in the expression of *CD44*, *ALDH1A3*, and Notch signalling genes *NOTCH2*, *NOTCH3*, and *DNER* (Park et al., 2019). Notch signalling promotes the migration, metastasis, and therapy resistance of breast cancer cells (Giuli et al., 2019; Zhang et al., 2019). Notch inhibitors have anti-tumour effects, and breast cancer cells benefit from these inhibitors.

When BMP4 was present during doxorubicin treatment, it enhanced the colony-forming potential of MDA-MB-231 cells, whereas treatment with LDN completely eradicated colony formation ability in these cells. According to the findings of one of the studies, blocking BMP signalling with the drug LDN-214117 led to a reduction in cell viability seems to support our finding (Mihajlović et al., 2019). Therefore, the possibility of breast cancer cells surviving and, consequently, the risk of the disease recurring may be greatly increased by the presence of BMP4 in the microenvironment of the tumour.

Although previous research has demonstrated that BMP4 may operate as a metastasis suppressor (Eckhardt et al., 2020a), our findings imply that paracrine BMP4 may increase the metastatic potential of triple-negative breast cancer cells, particularly in the bone (Ampuja et al., 2016a). However, exogenous BMP4 may have therapeutic effects for decreasing proliferation in breast tumours with luminal-like characteristics (Shee et al., 2019). Our observations further suggest that the response of breast cancer cells to BMP4 may be mediated by the BMP receptor expression levels (Lowery & de Caestecker, 2010) and the presence of BMP antagonists in the tumour microenvironment.

5.4 Conclusion

BMPs can regulate the expression of genes involved in cancer cell survival, resistance to apoptosis, and chemoresistance through interactions with other signalling pathways. BMP4 influences breast cancer development and has a context-dependent role in breast cancer progression. Our findings suggest that LDN can inhibit cancer progression, and combined with the scarcity of treatments for triple-negative breast cancer, suggest that future therapeutics could investigate the possibility of disrupting BMP signalling to prevent breast cancer invasion and metastasis (Figure 5.23).

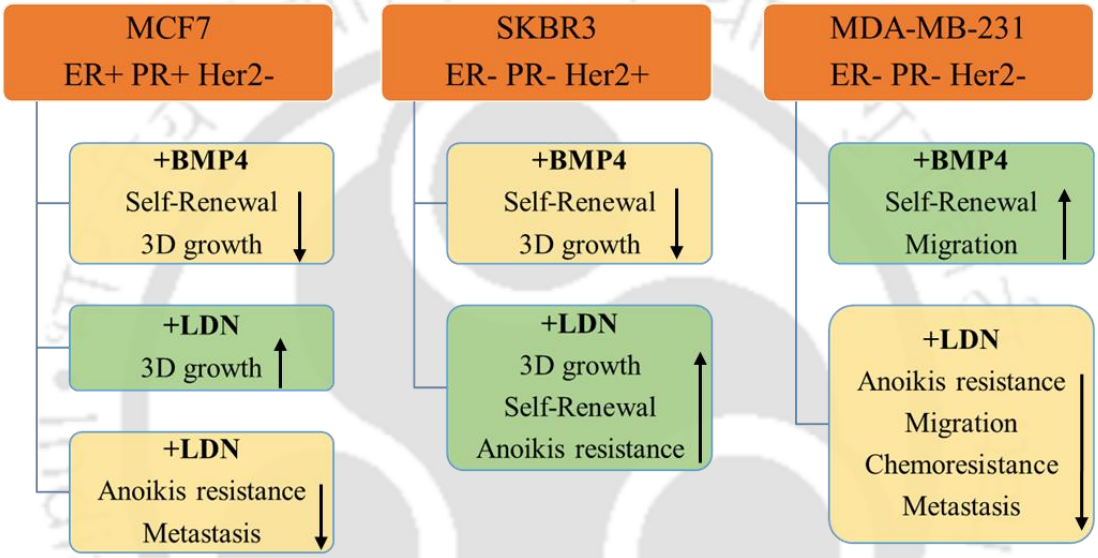

Figure 5.23: *Conclusive remark of BMP signalling in breast cancer cells.*

RHOA and Wnt Signalling in Breast Cancer Progression

6.1 Introduction

BMP signalling was found to regulate several aspects of cancer cells including proliferation, anoikis resistance and chemoresistance. However, to understand the signalling pathways that control migration and invasion, an important step in metastasis, RHOA signalling was studied. In addition, the role of the Wnt signalling pathway, which controls several aspects of cancer cells, was also explored.

RHO-ROCK signalling can be activated by several upstream targets in cells, but the non-canonical Wnt signalling pathway can also control RHO-ROCK signalling. Thus, RHOA and Wnt signalling pathways were studied simultaneously to understand the cancer progression and identify therapeutic targets for metastatic breast cancer. The expression profiles of RHOA and β-catenin showed that the level of RHOA expressed by MCF7 and SKBR3 is comparable, however, no β-catenin expression could be identified in SKBR3. In this study, two breast cancer cell lines MCF7 and MDA-MB-231 were utilized to understand RHOA and WNT/β-catenin signalling.

Several studies have documented the role of RHO-ROCK and Wnt signalling in the development of cancer. The primary function of RHO-ROCK signalling is the maintenance of the actin cytoskeleton in cells. The RHO family members also control cell migration; during migration, high Rac1 and low cdc42 maintain the formation of lamellipodia and filopodia (protrusion at the posterior end), whereas RHOA in association with mDIA and ROCK facilitate retraction at the anterior and posterior ends, respectively. In addition, RHO-ROCK and cdc42-MRCK aid in the collective mobility of cells. The function of RHO GTPases in controlling migration, proliferation, and metastasis, has been extensively investigated (Humphries et al., 2020). Inhibiting RHOA reduces the production of oestrogen receptors, resulting in the suppression of ER-positive malignancies (Rosenblatt et al., 2011). Similarly, studies on anoikis resistance in colon cancer show that RHO-ROCK and p38MAPK are the main targets of anoikis resistance, which motivates us to investigate the function of RHOA in anoikis resistance (Tanaka et al., 2013).

Wnt signalling is well-known for its essential role in embryogenesis; however, disruption in the signalling has been associated with numerous malignancies, including breast cancer. Both canonical and non-canonical Wnt signalling has been implicated in controlling various cellular processes. In canonical signalling, β-catenin translocate to the nucleus to control the transcription of genes related to proliferation, differentiation, apoptosis, and survival. The non-canonical Wnt signalling communicates via RHO-ROCK, which regulates migration, and calcium-dependent planar cell polarity, and supports myogenesis, cardiogenesis, and other processes

Since Wnt signalling can regulate RHO-ROCK signalling, we chose to examine both the canonical and non-canonical Wnt signalling pathways. Initially, the function of RHOA signalling was examined by treating MCF7 and MDA-MB-231 cells with Y27632 (inhibitor of ROCK), a downstream target of Rho-ROCK signalling, to determine its effect on cell proliferation, migration, and anoikis-resistance. To understand these signalling pathways further, RHOA and β-catenin was silenced by the lentiviral method and their effect on the breast cancer cells was determined.

6.2 Results

6.2.1 ROCK inhibitor influences the function of breast cancer cells

Y27632 inhibits ROCK-I and ROCK-II kinase activity by preventing them from binding to their catalytic site. Breast cancer cells were treated with Y27632 at a concentration of 10 μM/ml for 48 hours for the given study. The treated cells were then subjected to a series of experiments to determine the effect of Y27632 on cancer cells.

The microscopic images revealed that the Y27632 treatment caused morphology changes in MCF7 and MDA-MB-231 cells. As shown in Figure 6.1, the MCF7 cells acquired a morphology characterised by the increased protrusion, while the MDA-MB-231 cells developed a more spike-like structure. The depicted morphological images demonstrate that treatment with Y27632 reduces the cytoplasmic volume and matrix attachment of cells.

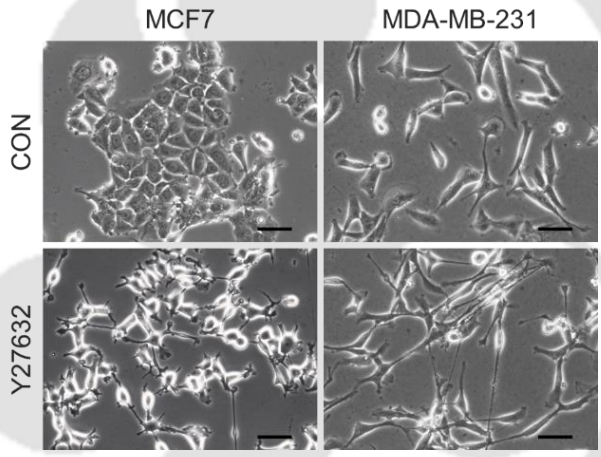

Figure 6.1: Effect of ROCK inhibitor on the morphology of cells. *To observe the effect of ROCK inhibitor on morphology, cells were treated with Y27632 (10μM/ml) for 48 hours and images were taken using a microscope. The morphology of MCF7 and MDA-MB-231 left untreated (control) or Y27632 treated conditions are shown in the illustrations. The black line in the images represents the scale bar (100μm).*

6.2.1.1 ROCK inhibition regulates clonogenic potential

Next, a colony formation assay was conducted to comprehend the significance of ROCK inhibitor on aspects of cell proliferation. An increase in colony number was observed in MCF7 in both pre and continuous treatment; however, the increase was substantially greater after continuous treatment. Similarly, treatment with Y27632 for 48 hours increased the colony number in MDA-MB-231; meanwhile, continuous treatment did not change the colony formation ability When treated with Y27632, MCF7 produced larger colonies, whereas the colony size was not altered during the treatment in MDA-MB-231. Count and

area measurements indicate that Y27632 treatment accelerated the proliferation of MCF7 cells, whereas the effect of Y27632 on MDA-MB-231 is time-dependent (Figure 6.2).

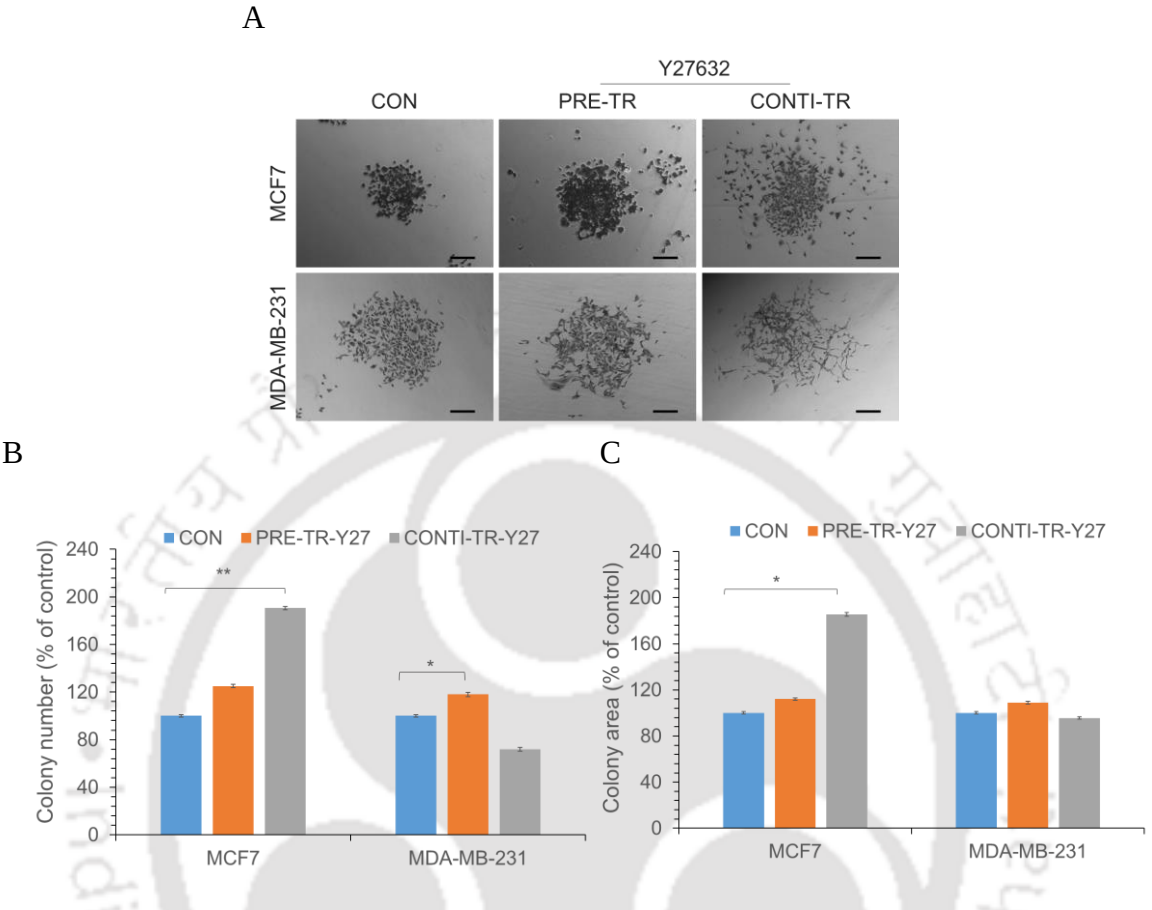

Figure 6.2: Effect of ROCK inhibitor on colony formation potential. *To understand proliferation, the colony assay was carried out in the presence of Y27632 (10µM/ml) for 48 hours (referred to as "Pre") and 14 days (referred to as "Continuous"). After successful incubation, the colonies were fixed and stained with a crystal violet solution. Colonies were counted using a microscope and the area was measured using Fiji software.* ***A.*** *Represents the colony images of left untreated (control) or Y27632 treated cells (scale = 200 µm) and* ***B.*** *represents the graph indicating colony number and* ***C.*** *area for MCF7, and MDA-MB-231. Values are mean ± SE, n=5-6 independent samples, *p<0.05, **p<0.005.*

6.2.1.2 ROCK inhibition reduces 3D growth

To understand the role of Y27632 further, its effect on spheroid formation was evaluated. Y27632 treatment resulted in reduced 3D growth, as seen by the reduced spheroid size in MCF7 cells, whereas no significant effect was observed in MDA-MB-231 cells (Figure 6.3 A and B).

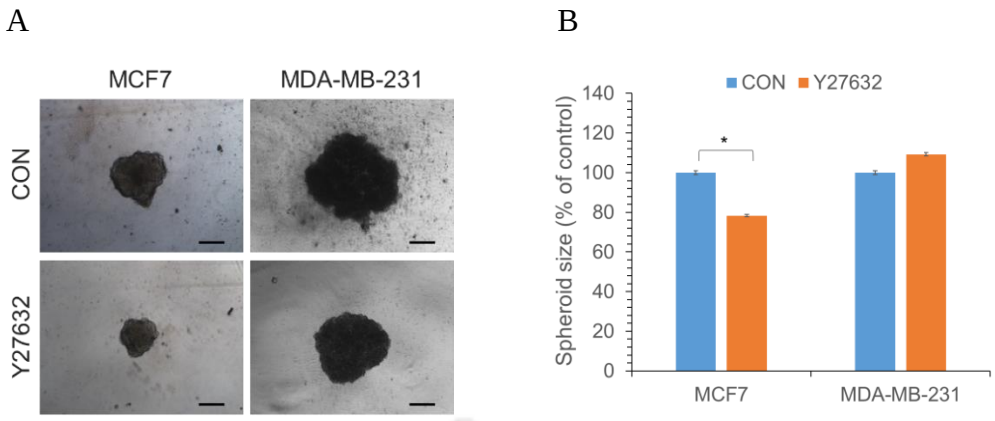

Figure 6.3: Effect of ROCK inhibitor on spheroid formation potential of cells. *Cancer cells were seeded with Y27632 (10µM/ml) for 17 days and incubated in order to ascertain the effect of ROCK inhibitor on spheroids formation. Images were taken on regular intervals of 3-4 days and the area was analysed using Fiji software.* ***A.*** *Represents spheroid images of left untreated (control) or Y27632 treated cells (scale = 200 µm) and* ***B.*** *Represents the spheroid area of MCF7 and MDA-MB-231 for each condition, calculated as a percentage of the area of their respective controls. Values are mean ± SE, n=5 independent samples, *p<0.05.*

6.2.1.3 ROCK inhibition enhances migration

Since RHO GTPases are one of the major regulators of cell migration, the effect of Y27632 treatment on the migration of breast cancer cells was carried out through a 2D as well as a 3D spheroid migration assay. Interestingly, the presence of Y27632 significantly increased the migration ability of both MCF7 and MDA-MB-231 (Figure 6.4 A and B). Immunoblotting analysis showed that MCF7 treated with Y27632 had significantly reduced E-cadherin expression further confirming the migration-promoting effect of Y27632 (Figure 6.4 C). As previously stated, the cancer cells migrate in a 3D environment from the tumour, spheroid migration assay was performed. Here, MCF7 or MDA-MB-231 spheroids were transferred onto a collagen matrix and allowed to invade and migrate in the presence of Y27632 (Figure 6.4 D). Figures 6.4 E and F demonstrate that similar to that observed in the wound healing assay, the addition of Y27632 to the cells significantly increased the migration. Thus, inhibiting ROCK activity in cells led to an increase in their propensity of cells to migrate, regardless of cell type.

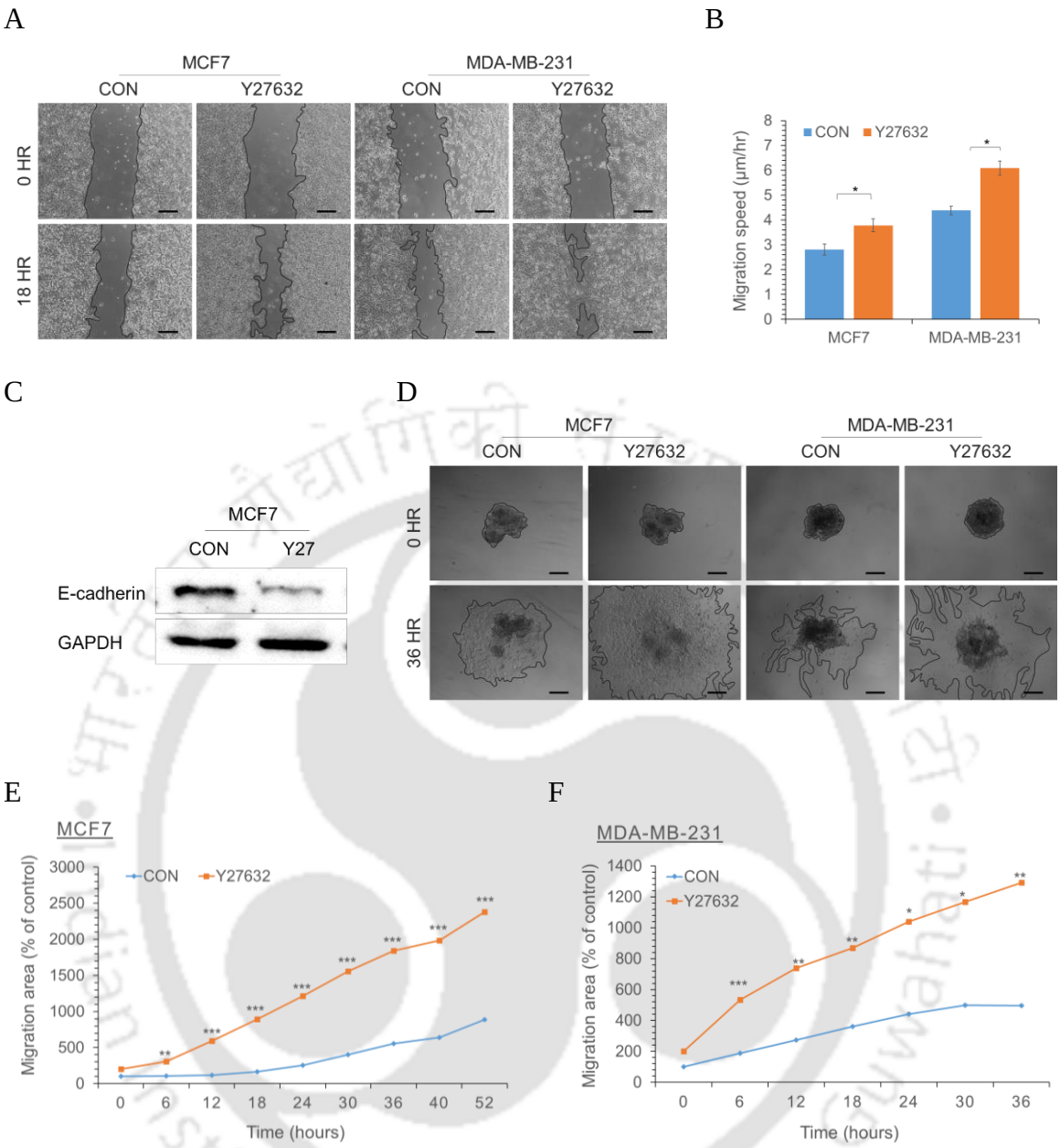

Figure 6.4: Effect of ROCK inhibitor on migration potential of cells*. The two-dimensional migration was evaluated using a wound healing assay in which breast cancer cells were permitted to migrate in a manually created wound or breach. The area covered by cells was computed using the T-scratch software, and migration velocity was computed in µm/hr.* ***A.*** *depicts the wound healing migration of MCF7 and MDA-MB-231 of left untreated (control) or Y27632 (10µM/ml) treated cells at 0 and 18 hours, whereas* ***B.*** *is a graphical representation of the migration velocity of MCF7 and MDA-MB-231 cells in the presence of Y27632 (10µM/ml).* ***C.*** *Depicts the results of a western blot image of E-cadherin (~110 KDa) and GAPDH (~37 KDa) expression in MCF7 cells. To assess invading potential, spheroids were transferred to a collagen-coated matrix and cells were allowed to permeate in the presence of Y27632 (10µM/ml)* ***D.*** *displays images of migrating cells of left untreated (control) or Y27632 (10µM/ml) treated cells from a spheroid at 0 and 36 hours. The percentage of area occupied by migratory cells during invasion assay cells is represented in line graph* ***E.*** *for MCF7 and* ***F.*** *for MDA-MB-231. The black line in images represents the scale bar (200µm). Values are mean ± SE, n=3 independent samples. *p<0.05, **p<0.005, ***p<0.0005.*

Since actin organisation and E-cadherin expression are essential modifications during migration, the distribution of E-cadherin and actin was assessed following the Y27632

treatment. Although the Y27632 treatment did not alter the total F-actin content in MCF7, it resulted in the formation of actin protrusions and filopodia formation. There was a discernible decrease in the E-cadherin levels at the cell surface and more cytoplasmic staining was observed (Figure 6.5 A), which requires further validation. In the case of MDA-MB-231, Y27632 treatment resulted in a slight decrease in the F-actin content, the cell size decreased and formed filopodia -like protrusions (Figure 6.5 B).

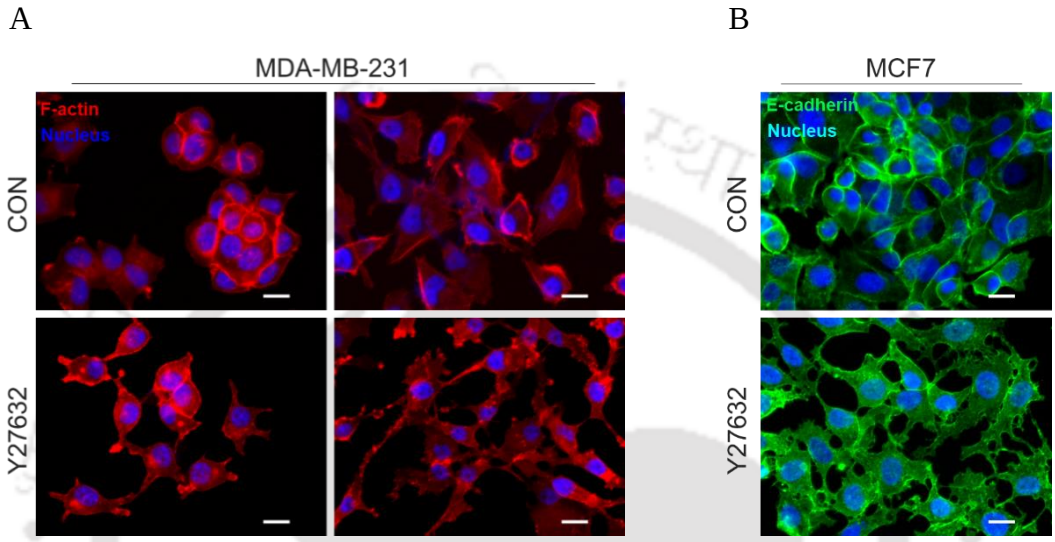

Figure 6.5: Effect of ROCK inhibitor on actin and E-cadherin staining*. Breast cancer cells were stained with fluorescent-conjugated Phalloidin TRITC antibody to stain f-actin, DAPI to stain nucleus, and anti-E-cadherin antibody to stain E-cadherin after 48 hours of treatment with Y27632 (10 M/ml).* ***A.*** *represents the expression of F-actin (in the red colour) in MCF7 and MDA-MB-231, while* ***B****. signifies the expression of E-cadherin (in the green colour) in MCF7. In both* ***A.*** *and* ***B.****, the nucleus location is denoted by the colour blue. Untreated cells are denoted as CON, while cells that have been treated with ROCK inhibitor are represented as Y27632. The white line in the images represents the scale bar (50μm).*

6.2.1.4 ROCK inhibitor in anoikis resistance

Numerous studies have highlighted the significance of RHO-ROCK signalling in anoikis resistance. So, the breast cancer cells were treated with ROCK inhibitor during non-adherent anoikis-inducing conditions. Anoikis-resistant cells were tested for colony formation ability with or without Y27632 treatment during non-adherent culture and colony formation. Continuous treatment of MCF7 with Y27632 during anoikis culture and colony formation significantly increased the number of colonies and colony size compared to the control cells. In contrast, the MDA-MB-231 showed a decrease in colony number under both pre-treatment as well as continuous-treatment conditions. However, the colony size was similar to that of the control cells in MDA-MB-231 under different treatment

conditions (Figure 6.6). These results suggest that ROCK inhibition might differentially regulate anoikis resistance in breast cancer cells belonging to different subtypes.

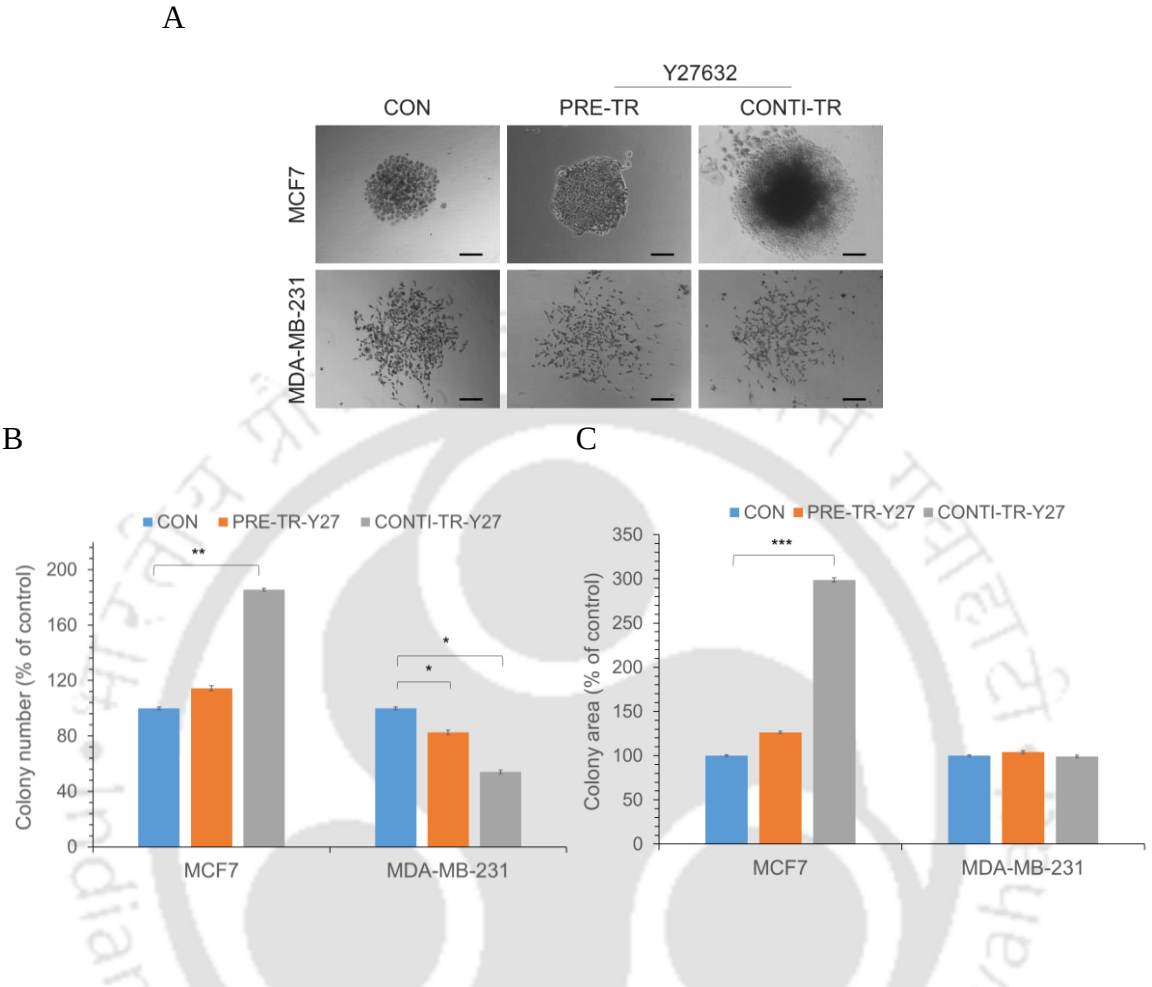

Figure 6.6: Effect of ROCK inhibitor on anoikis-resistance of cells*. To measure the resistance to anoikis, cells were seeded with Y27632 (10μM/ml) on an anchorage-independent surface. The administration was restricted to a 48-hour period known as "PRE-TR" and "CONTI-TR" during which treatment was administered until the conclusion of the experiment (14 days). The colonies were stained with a solution of crystal violet. Under a microscope, colonies were counted and the area was measured using Fiji software.* ***A.*** *Colony images (Scale bar = 200μm) of untreated (CON) and Y27632-treated (pre and continuous) cells.* ***B.*** *represents the graph of colony number, and* ***C.*** *represents the percentage of colony area for MCF7 and MDA-MB-231 for the control, Pre-treated, and Continuously treated conditions. Values are mean ± SE, n=5-6 independent samples, *p<0.05, **p<0.005, ***p<0.0005.*

6.2.2 RHOA and β-catenin downregulation

Treatment with the ROCK inhibitor has shown that interrupting the RHOA signalling potentially modifies the self-renewal, migration and anoikis resistance abilities of the breast cancer cells. In order to further understand the role of RHOA signalling in breast cancer progression, RHOA was lentivirally silenced in the breast cancer cells MCF7 and MDA-MB-231. It is known that RHOA also mediates non-canonical Wnt signalling, which plays

an important role in cancer progression. In parallel, canonical Wnt signalling was also studied by silencing β-catenin expression in breast cancer cells.

MCF7 and MDA-MB-231 cells were transduced with lentiviral particles containing shRHOA, shβ-catenin or scramble sequence. The transduced cells were selected using puromycin, expanded and utilized for further studies. To validate the level of gene silencing, gene expression analysis was performed by real-time PCR and immunoblotting. There was an ~ 10-fold reduction in β-catenin expression in shβ-catenin transduced MCF7 and MDA-MB-231. shRHOA transduced cells showed ~40%-60% reduction in RHOA levels in MCF7 and MDA-MB-231 cells (Figure 6.7).

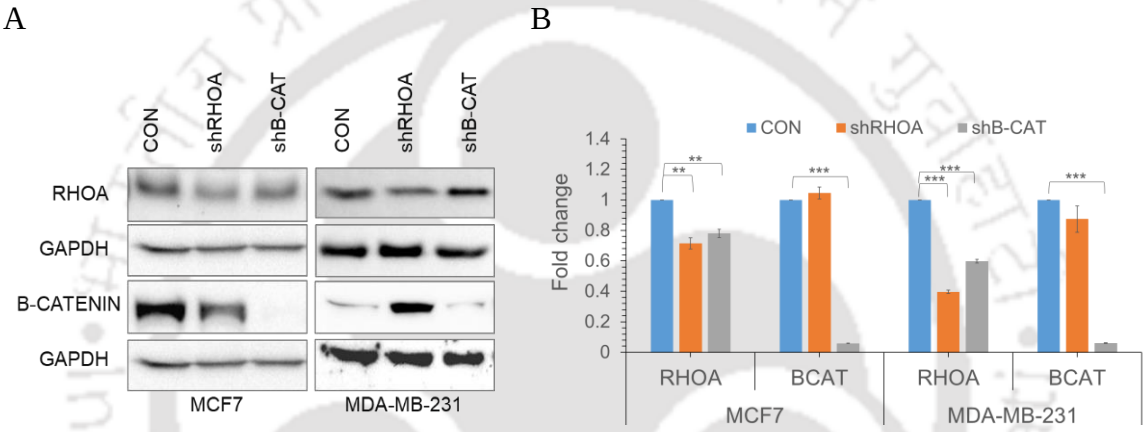

Figure 6.7: Silencing of RHOA and β-catenin. *Immunoblotting and Real-time PCR were conducted on control (transduced with scramble) and RHOA and β-catenin silenced breast cancer cells to determine the extent of gene silencing. The change in RHOA (~21 KDa) and β-catenin (~92 KDa) expression levels in silenced MCF7 and MDA-MB-231 cells is depicted as western blot images in* ***A.*** *and the fold change in gene expression measured by RT-PCR is shown in* ***B.*** *Using control cells as a benchmark, the fold change in gene expression was computed. Values are mean ± SE, n=5-6 independent samples, *p<0.05, **p<0.005, ***p<0.0005.*

6.2.2.1 RHOA silencing decreases F-actin polymerization in cells

Given that the downstream targets of RHOA signalling affect actin cytoskeleton and cell morphology, the morphology changes in shRHOA and shβ-catenin were determined. No discernible changes in the morphology were observed in shRHOA cells whereas β-catenin silencing was found to increase the cell-cell attachment in MCF7 cells (Figure 6.8 A). Furthermore, RHOA silencing reduced the F-actin content in both MCF7 and MDA-MB-231 cells whereas β-catenin silencing induced the formation of filopodia-like structures in MDA-MB-231 cells (Figure 6.8 B).

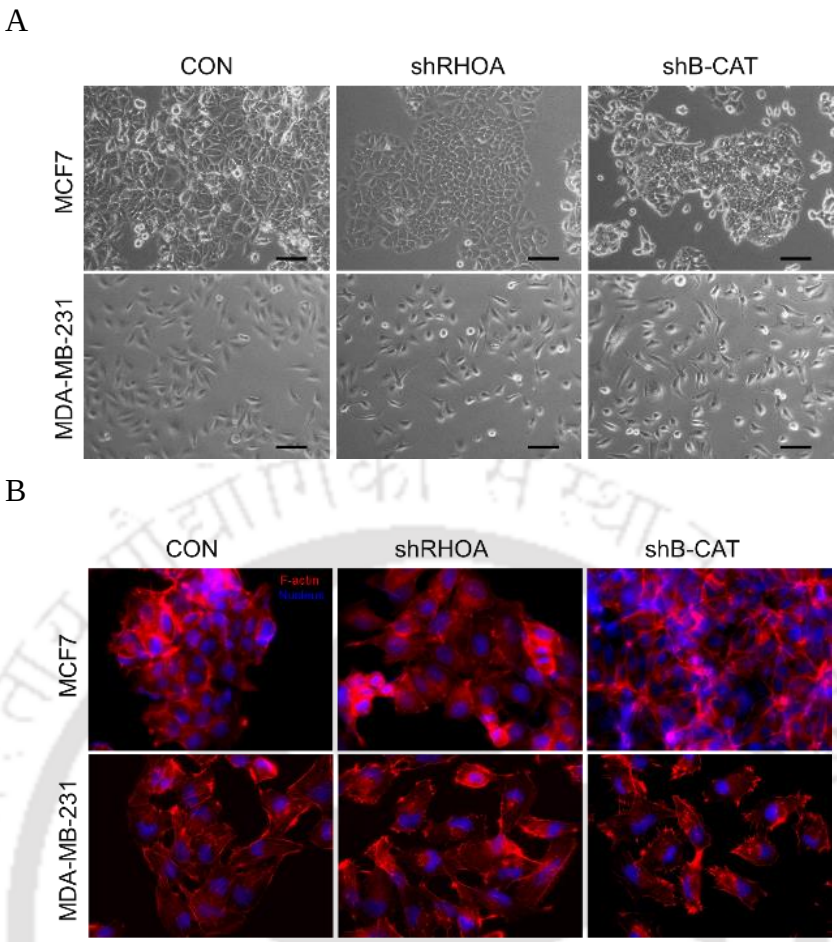

Figure 6.8: Effect of silencing on the morphology and actin organization of cells. *The silenced breast cancer cells (scramble, RHOA, and β-catenin) MCF7 and MDA-MB-231 were grown and microscopy images were acquired to examine their morphology, as shown in* ***A.*** *The black line in the images represents the scale bar (100μm). To examine the actin organisation, these selected cells were processed and stained with Phalloidin-TRITC (Red), which stains F-actin, and DAPI (Blue), which stains the nucleus of cells, as shown in* ***B.***

6.2.2.2 β-catenin silencing decreases Ki67 breast cancer population

To understand whether RHOA and β-catenin are required for proliferation and maintaining the cell cycle profile of the breast cancer cells, cell cycle analysis was performed and the percentage of cycling cells was determined by Ki67 staining. While there was a slight decrease in the percentage of G0 cells in shRHOA-MCF7 cells compared to the control cells, β-catenin silencing significantly decreased the percentage of Ki67 positive cells in both MCF7 and MDA-B-231 population (Figure 6.9). RHOA silencing also resulted in a significant increase in the G0 percentage of MDA-MB-231 cells.

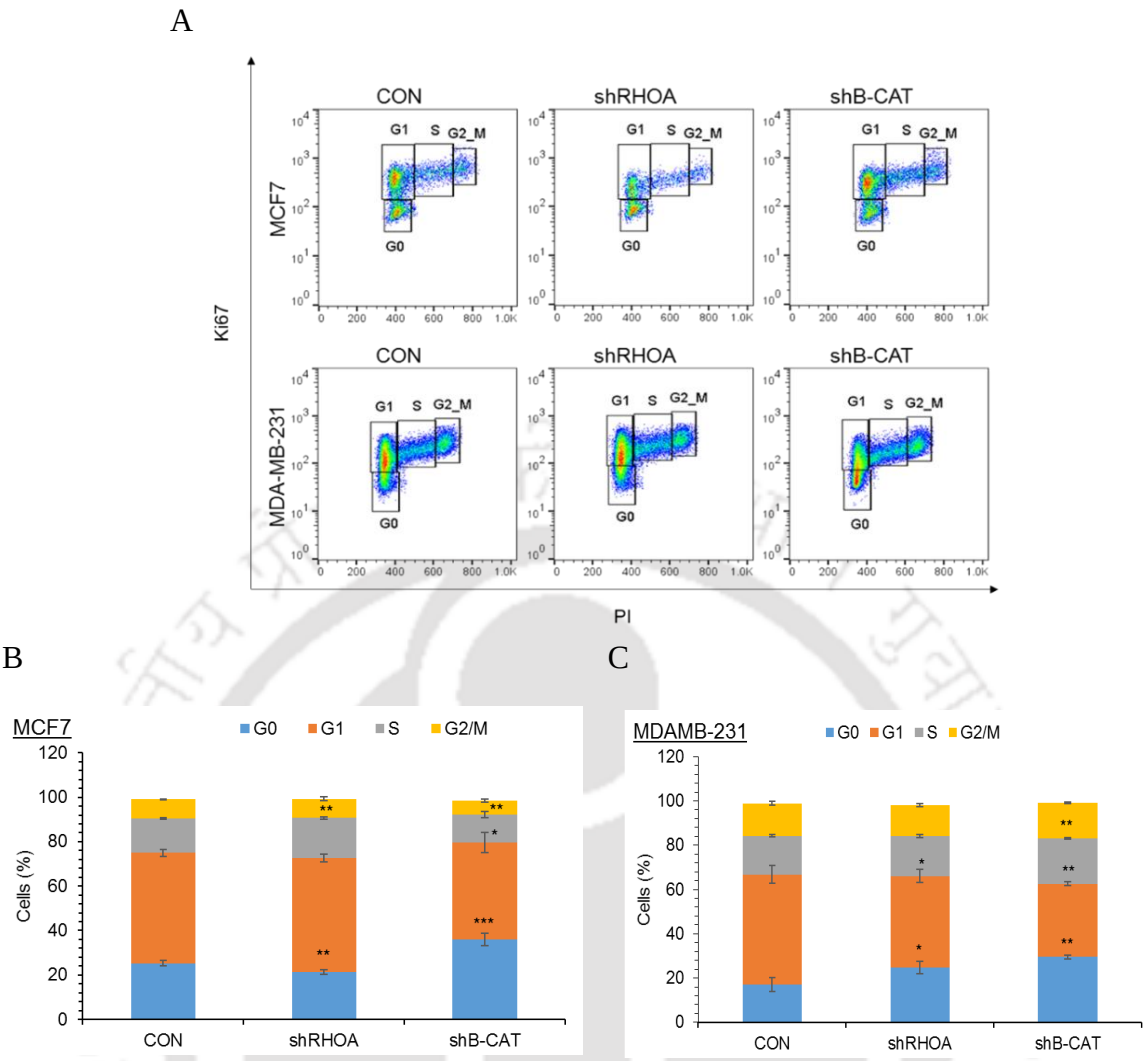

Figure 6.9: Effect of silencing on Ki67 breast cancer population. *Ki67 and Propidium iodide were utilised for the simultaneous analysis of the proliferation-specific marker (Ki-67) and cellular DNA content, which, respectively, distinguish resting/quiescent cell populations (G0 cell) and quantify cell cycle distribution (G1, S, or G2/M). Flow cytometry was utilised to analyse the stained cells by plotting the population in a dot plot between the Ki67 and Propidium iodide axes for control (transduced with scramble) and shRHOA and shβ-catenin cells, as depicted in* ***A.*** *whereas* ***B.*** *and* ***C.*** *represent the same quantified percentage of MCF7 and MDA-MB-231 cells silenced for control RHOA and β-catenin, respectively. Values are mean ± SE, n=3-4 independent samples, *p<0.05, **p<0.005, ***p<0.0005.*

To determine whether RHOA and β-catenin silencing has impacted the cell cycle-related genes, the expression of cyclin D1 (CCND1) and CDKN1A was analysed by real-time PCR. There was a significant decrease in the expression of CCND1 in both shRHOA and shβ-catenin MDA-MB-231 cells, however, a decrease in CDKN1A expression was also observed in shβ-catenin-MDA-MB-231 cells. No changes in the expression of the anti-apoptotic gene BCL2L1 at the transcript level were observed during RHOA or β-catenin silencing in MDA-MB-231 cells (Figure 6.10).

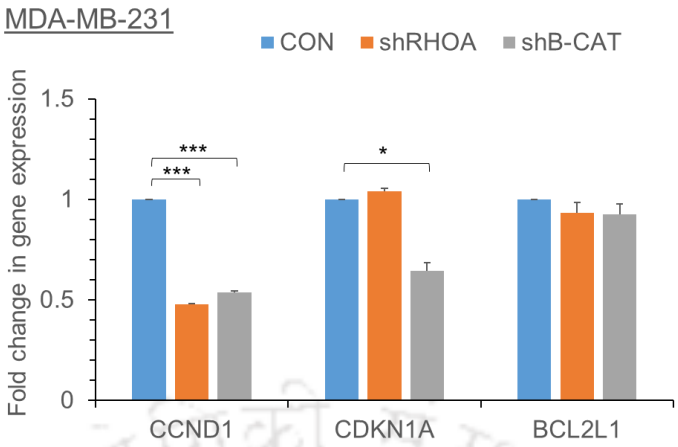

Figure 6.10: Effect of silencing on cell cycle-regulated gene. *The effect of gene silencing on cell cycle-related genes was determined using real-time PCR. The Ct values obtained for each gene were normalised against the Ct values of the housekeeping gene (GAPDH). The fold change relative to the control was measured individually for each gene. The image above depicts the fold change in the gene expression profile of CCND1, CDKN1A, and BCL2L1 in MDA-MB-231 for control (scramble), shRHOA, and shβ-catenin cells. Values are mean ± SE, n=5-6 independent samples, *p<0.05, ***p<0.0005.*

6.2.2.3 β-catenin silencing affects 3D growth of breast cancer cells

Since a simultaneous decrease in the transcript levels of CCND1 and CDKN1A was observed in shβ-catenin-MDA-MB-231 cells, a spheroid assay was also carried out to understand how the gene modification regulates the 3D growth of the breast cancer cells. The shRHOA and shβ-catenin cells were seeded for spheroid formation and the spheroid growth was monitored for 14 days and documented periodically. The growth of MCF7 cells was dramatically reduced when RHOA and β-catenin were downregulated (Figures 6.11 A and B). However, the growth of MDA-MB-231 cells in spheroids was not affected by the silencing of β-catenin and RHOA (Figures 6.11 A and C). This indicates that the involvement of these proteins in the three-dimensional expansion of breast cancer cells is contingent upon the specific circumstances. While there was a notable decline in the Ki67 % in MDA-MB-231 cells following the silencing of both RHOA and β-catenin, this decrease did not correspond to a reduction in 3D dimensional growth.

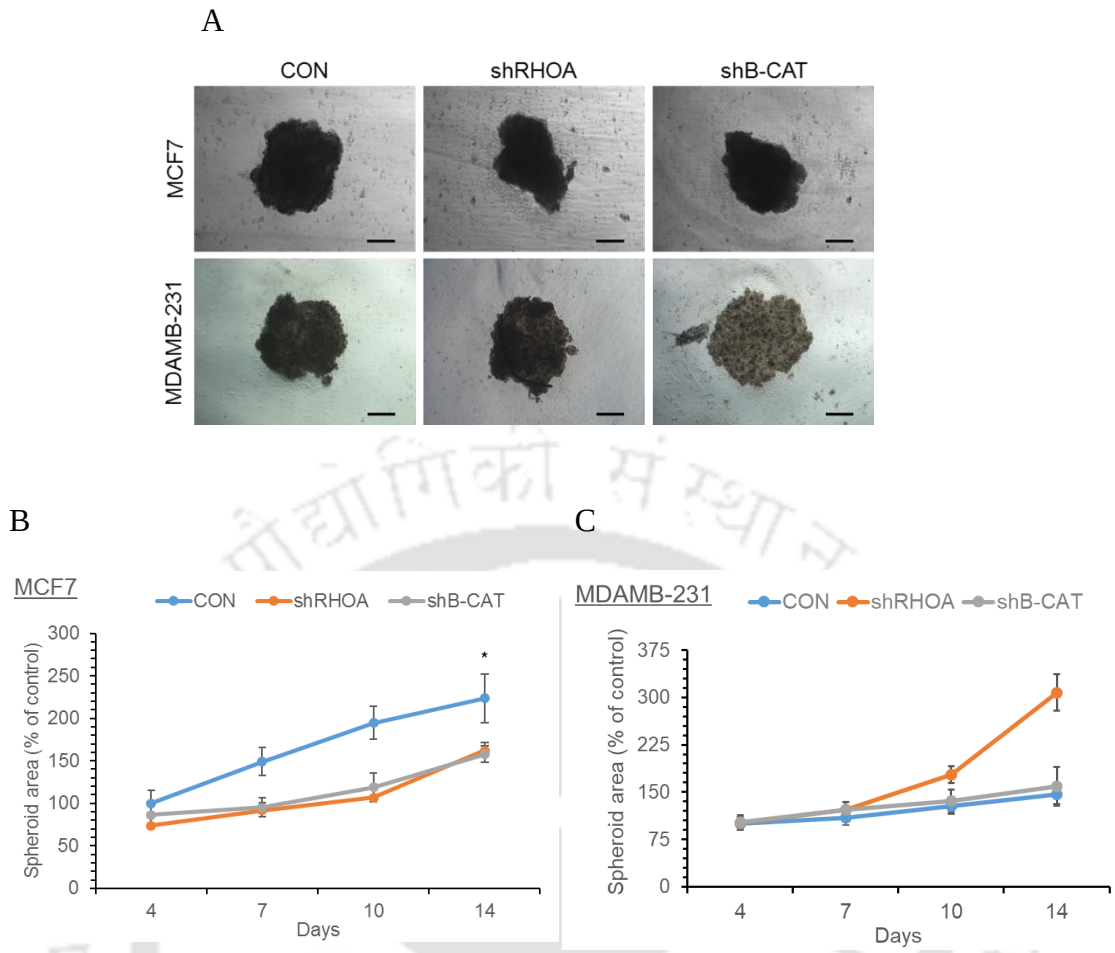

Figure 6.11: Effect of silencing on three-dimensional growth of cells. *The silenced breast cancer cells for control, RHOA and β-catenin were seeded on anchorage-independent surfaces to form spheroids. Images were taken on regular intervals of 3-4 days and the area was analysed using Fiji software.* ***A.*** *Represents spheroid images for control (transduced with scramble) and shRHOA and shβ-catenin MCF7 and MDA-MB-231 cells (scale = 200 µm) and* ***B.*** *Represents the spheroid area of MCF7 and* ***C.*** *represents the spheroid area of MDA-MB-231 for each condition, calculated as a percentage of the area of the controls. Values are mean ± SE, n=5 independent samples, *p<0.05.*

To ascertain whether treatment with Y27632 during RHOA or β-catenin silencing can impact the spheroid formation and 3D growth, shRHOA and shβ-catenin transduced MCF7 and MDA-MB-231 were allowed to form spheroid in the presence of Y27632. The growth of the spheroids was monitored and documented.

In MCF7, Y27632 treatment resulted in the formation of smaller spheroids in all the conditions, however, Y27632 mediated inhibition of spheroid growth was less pronounced in shRHOA and shβ-catenin conditions compared to the control. In the Y27632 treatment condition, compared to the control, shβ-catenin cells formed larger spheroids although Y27632 treatment in general reduced the spheroid size and growth significantly in MCF7. In MDA-MB-231, however, Y27632 treatment did not alter the spheroid size or growth during the observation period. Thus, ROCK inhibition in the presence of RHOA and β-

catenin downregulation differentially affects the 3D growth of MCF7 and MDA-MB-231 cells (Figures 6.12).

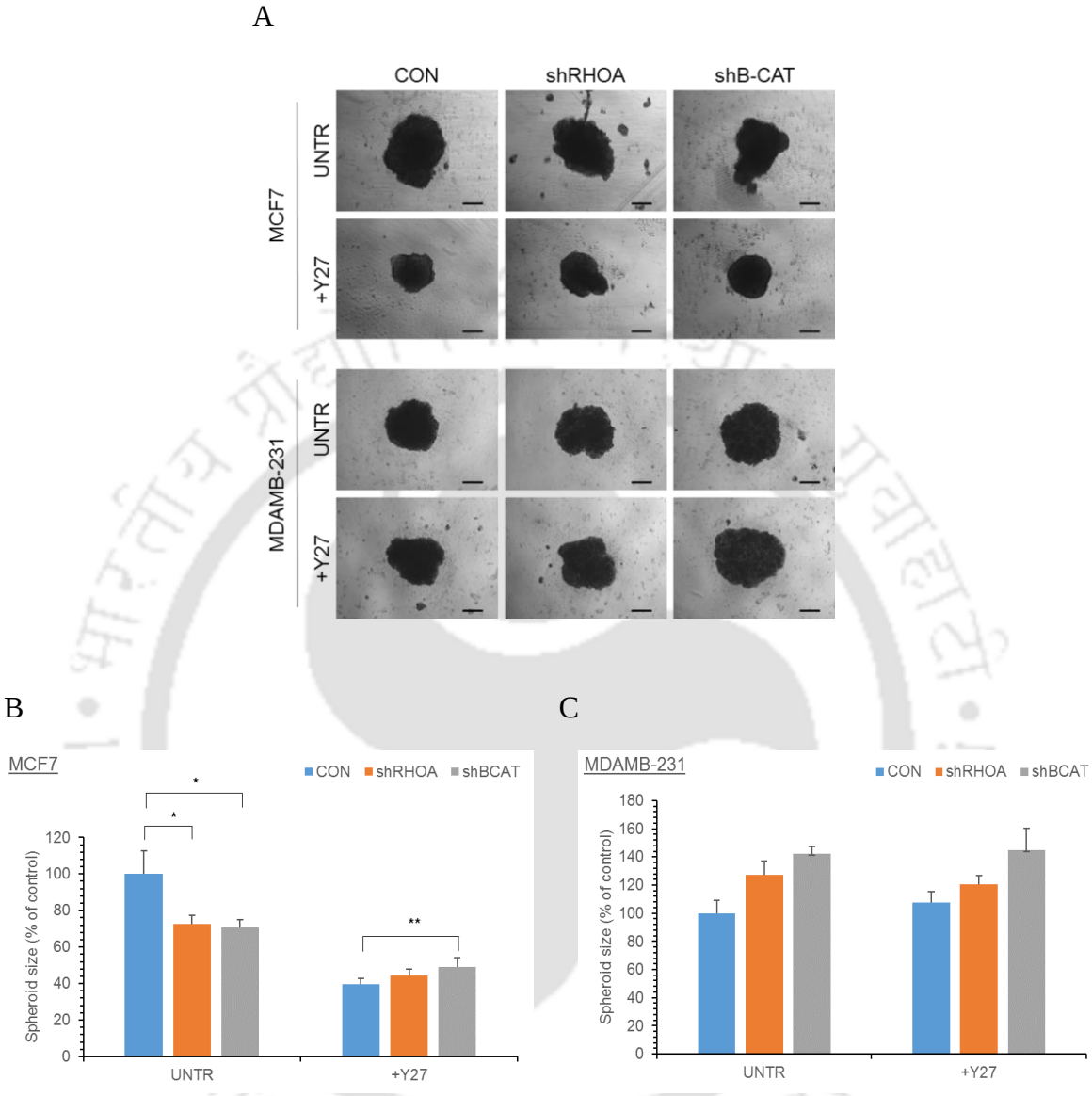

Figure 6.12: Combined effect of silencing and ROCK inhibitor on three-dimensional growth of cells. *The silenced breast cancer cells for control, RHOA and β-catenin were seeded along with Y27632 (10μM/ml) on the anchorage-independent surface to form spheroids. Images were taken on regular intervals of 3-4 days and the area was analysed using Fiji software.* ***A.*** *Represents spheroid images (scale = 200 μm) of MCF7 and MDA-MB-231 for control (transduced with scramble) and shRHOA and shβ-catenin cells with and without Y27632 and* ***B.*** *Represents the spheroid area of MCF7 and* ***C.*** *represents the spheroid area of MDA-MB-231 for each condition, calculated as a percentage of the area of their respective controls. Values are mean ± SE, n=5 independent samples, *p<0.05, **p<0.005.*

6.2.2.4 RHOA and β-catenin silencing affects self-renewal ability

As RHOA and β-catenin regulate the proliferation and cell cycle status of the breast cancer cells, their ability to impact the self-renewal of breast cancer cells was assessed by colony formation assay. RHOA and β-catenin downregulation significantly affected the self-

renewal ability of both MCF7 and MDA-MB-231 cells as seen by the decrease in their colony formation ability. However, shRHOA-MCF7 formed significantly larger colonies compared to the control and no changes in the colony size were observed in shRHOA-MDA-MB-231 cells (Figure 6.13 A, B and C).

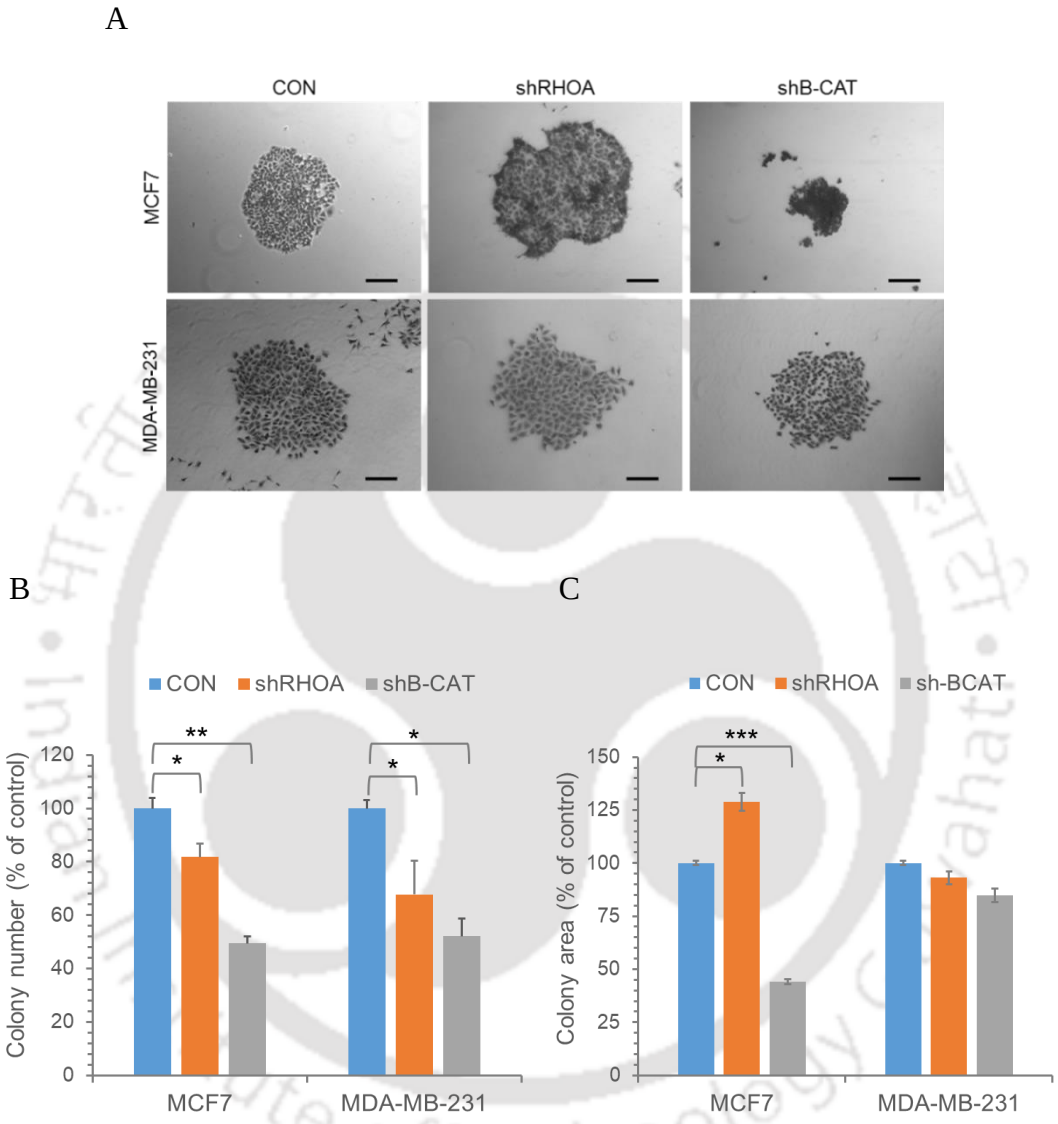

Figure 6.13: Effect of silencing on the clonogenic assay. *The silenced cells for RHOA, β-catenin, and scramble (control) were seeded and incubated to form colonies for 14 days on tissue culture plates. Crystal violet was used to stain the colony plates, and colonies were enumerated using a microscope. The colony with a cell count greater than or equal to 50 was deemed optimal. Images were captured using a microscope, and the area was computed using Fiji software.* ***A.*** *depicts the colony images and the black line in images represents the scale bar of 200µm.* ***B.*** *and* ***C.*** *represent the percentage of colony number and colony area for MCF7 and MDA-MB-231 cells silenced for RHOA, β-catenin, and scramble (control), respectively. Values are mean ± SE, n=5 independent samples, *p<0.05, **p<0.005, ***p<0.0005*

To understand the impact of RHOA and β-catenin silencing on the downstream signalling, immunoblotting analysis was performed.

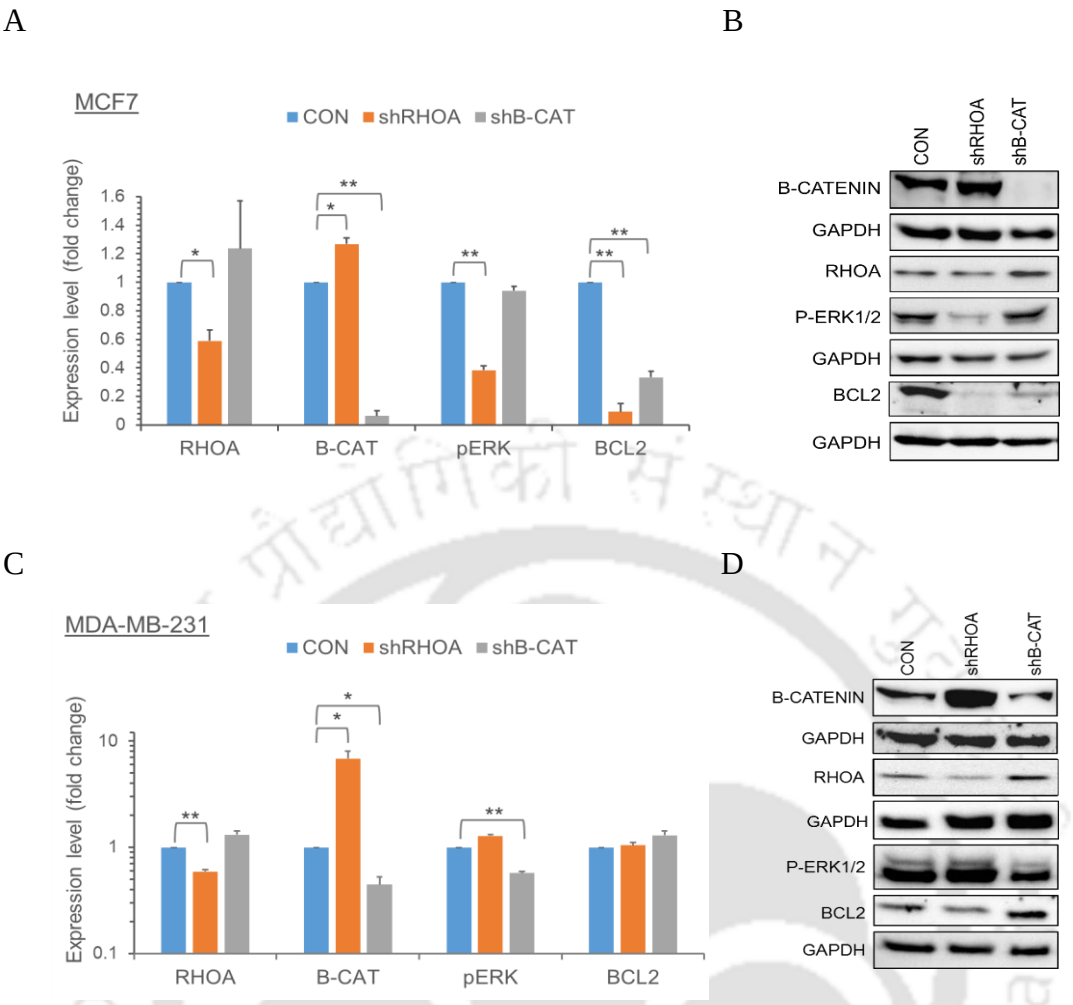

Figure 6.14: Effect of silencing on the downstream signalling. *Immunoblotting was done on silenced cells to test the effect of silencing on downstream targets. Before incubation with the targets antibody, the lysate from silenced cells in RIPA buffer was loaded on a polyacrylamide gel and protein bands were transferred to the nitrocellulose membrane. The blots were incubated with secondary HRP conjugated antibody to identify the primary antibody binding, and ECL chemiluminescent was added to visualise the protein band. Image Lab software was used to determine the band intensity, which was then normalised to the GAPDH protein. The fold change in expression was calculated relative to the control and is shown in* ***A.*** *for MCF7 and* ***C*** *for MDA-MB-231, while* ***B.*** *and* ***D.*** *represent immunoblot images of RHOA (~21 KDa), β-catenin (~92 KDa), pERK1/2 (~42-44 KDa), BCL2 (~26 KDa), and GAPDH (~37 KDa) for MCF7 and MDA-MB-231 cells silenced for RHOA, β-catenin, and scramble (control). Values are mean ± SE, n=5-6 independent samples, *p<0.05, **p<0.005.*

Silencing of RHOA resulted in a significant reduction in the expression levels of phosphoERK1/2 (pERK1/2) and BCL2 levels in MCF7 cells. Similarly, β-catenin silencing resulted in a substantial reduction in the expression levels of BCL2 (Figure 6.14 A and B), which correlates with the reduced growth and self-renewal observed during RHOA and β-catenin silencing. When β-catenin was silenced in MDA-MB-231 cells, it specifically decreased the levels of pERK1/2 but did not change the level of BCL2. However, silencing RHOA did not have any effect on the expression of either pERK1/2 or BCL2 (Figure 6.14 C and D). Remarkably, the inhibition of RHOA in both cell lines led to a noteworthy

elevation in the expression level of β-catenin. Conversely, the inhibition of β-catenin did not result in a significant increase in the level of RHOA, although there was an observed increase in expression. Therefore, it appears that RHOA and β-catenin play a compensating function when suppressed in breast cancer cells.

Several molecular mechanisms control the self-renewal and proliferation of cancer cells and cancer stem cells. In order to understand how the silencing of RHOA and β-catenin regulate the expression of cancer stem cell genes, gene expression analysis was performed. Downregulation of RHOA in MCF7 dramatically increased the expression of genes directly related to the self-renewal property of cells, including *OCT4S1, SOX2, NANOG* and *ALDH1A3*. The relatively high expression of self-renewal genes may explain the large colony size observed in MCF7-shRHOA. Interestingly, the silencing of β-catenin also increased the expression of *OCT4S1, SOX2,* and *NANOG*, while it decreased the expression of *ALDH1A3*. The downregulation of β-catenin might have induced the expression of self-renewal genes as a compensatory mechanism, however, functional assays showed that this increase was not sufficient to rescue the decrease in the colony number and the size observed with β-catenin silencing in MCF7 cells (Figure 6.15 A).

In the case of MDA-MB-231 cells, silencing of both RHOA and β-catenin markedly decreased several stemness genes such as *SOX2, ALDH1A3,* and *CD44* whereas β-catenin silencing also resulted in the downregulation of *OCT4A, ABCG2 and EZH2* (Figure 6.15 B). The downregulation of key stem-cell-related genes explains the decrease in the KI67 population observed during β-catenin silencing in MDA-MB-231 cells. However, the increased self-renewal ability observed during β-catenin silencing suggests that they might have activated signalling pathways to compensate for the loss of β-catenin that resulted in increased proliferative ability.

A

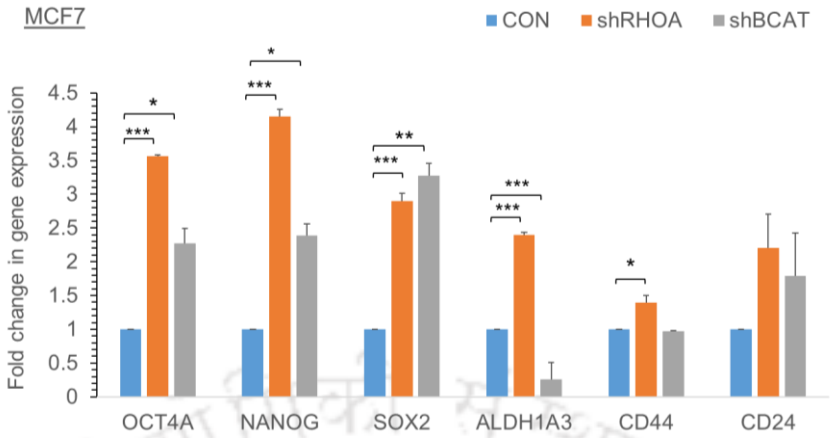

B

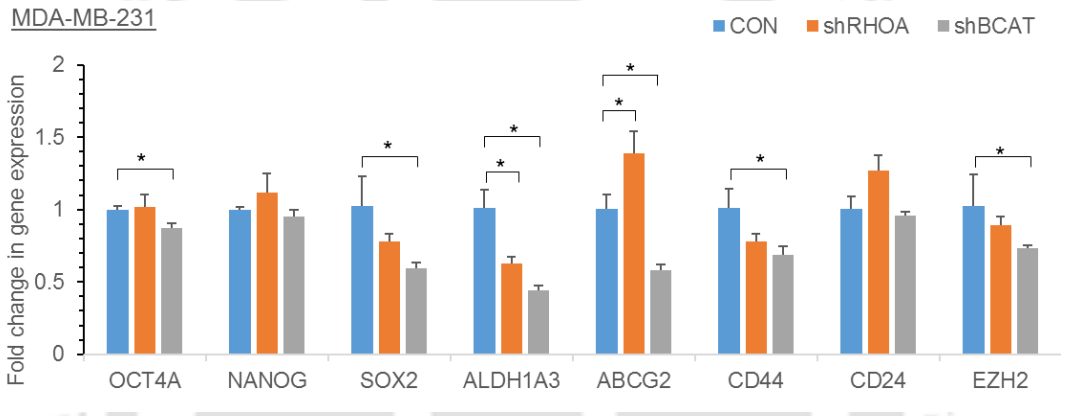

Figure 6.15: Effect of silencing on self-renewal and proliferation genes. *The effect of RHOA, β-catenin, and scramble (control) silencing on self-renewal and proliferation genes were determined using real-time PCR. The Ct values obtained for each gene were normalised against the Ct values of the housekeeping gene (GAPDH). The fold change relative to control was calculated with the ΔΔCt method.* ***A.*** *represents the bar graph for fold change in gene expression profiles of OCT4A, SOX2, NANOG, ALDH1A3, CD44, and CD24 in MCF7.* ***B.*** *represents the bar graph for fold change in gene expression profiles of OCT4A, NANOG, SOX2, ALDH1A3, ABCG2, CD44, CD24 and EZH2 in MDA-MB-231.Values are mean ± SE, n=3 independent samples, *p<0.05.*

6.2.3. RHOA and β-catenin in EMT and migration

EMT and metastasis are one of key properties of cancer cells which help them spread to secondary sites. To understand how RHOA or β-catenin control the metastatic ability of breast cancer cells, the migration potential of the cells was tested by wound healing assay and spheroid migration assay. Firstly, spheroids were formed with shRHOA and shβ-catenin –MCF7 cells. The spheroids were transferred to the collagen matrix to check their migration and invasion properties.

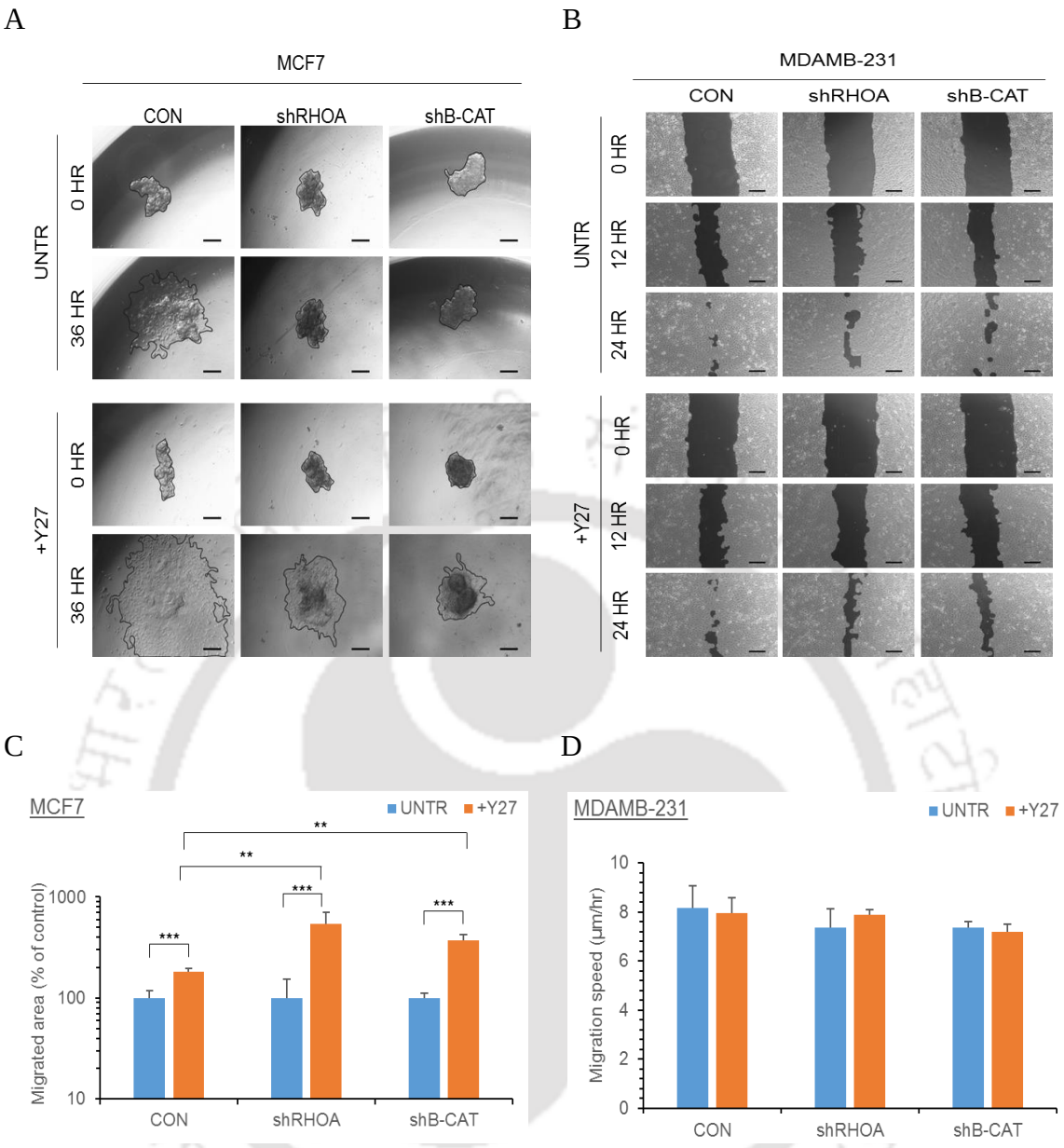

Figure 6.16: Impact of silencing and ROCK inhibitor on migration potential of cells. *The cells silenced for RHOA, β-catenin, and scramble (control) were analysed using invasion and wound healing assay. For invasion assay, cells were seeded on an anchorage-independent environment to form spheroids and then spheroids were transferred to a collagen-coated matrix. The cells were allowed to invade the collagen matrix in the presence of Y27632 and the area covered by migratory cells was measured by Fiji software. For the wound healing assay, silenced cancer cells were seeded and a scratch was made once the cells reached 90-95% confluence. Cells were allowed to migrate in the presence of Y27632 (10µM/ml) and the area covered by cells was calculated using T-scratch software.* ***A.*** *depict the spheroid migration of MCF7, and* ***B.*** *illustrate the wound healing assay of MDA-MB-231 in response to Y27632 (10µM/ml) treatment and the control group, respectively. In a similar vein, the migration area traversed by MCF7 is denoted in* ***C.*** *while the migration speed of MDA-MB-231 is denoted in* ***D.*** *under both the control (CON) and Y27632-treated conditions. The black line in images represents the scale bar (200µm). Values are mean ± SE, n=3 independent samples. **p<0.005, ***p<0.0005.*

Downregulation of RHOA and β-catenin in MCF7 reduced their migration potential, however, the addition of Y27632 significantly increased the migration ability of the cells

under control and silenced conditions (Figure 6.16 A). Interestingly, the fold increase in migration ability upon Y27632 treatment was significantly higher when RHOA and β-catenin were silenced compared to the control conditions (Figure 6.16 C). Y27632 treatment on RHOA silenced MCF7 induced the highest increase in the migration ability suggesting that ROCK inhibition increases migration ability as reported earlier. On the other hand, migration and the invasion ability of MDA-MB-231 cells were unaffected by RHOA or β-catenin silencing (Figure 6.16 B) and the addition of Y27632 did not alter the migration ability of the control or the silenced cells (Figure 6.16 D). The role of RHOA and β-catenin in controlling the migration of breast cancer cells seems to be context dependent; where the migration ability of drastically reduced by the downregulation of RHOA and β-catenin in MCF7 whereas no effect was observed in MDA-MB-231.

Although migration was not affected by RHOA and β-catenin silencing in MDA-MB-231, in order to understand its effect on the expression of the genes related to migration, gene expression analysis was performed. A significant downregulation in the mRNA levels of *ITGA6, CDH2, SNAI2, MMP14*, and *EpCAM* was detected in the β-catenin silenced MDA-MB-231 cells. Although the genes that control migration were affected, no functional changes in migration ability were detected. Possible causes include post-translational modifications or the activation of other signalling molecules. In contrast, silencing of RHOA has had no effect either on the gene expression or the migration potential (Figure 6.17).

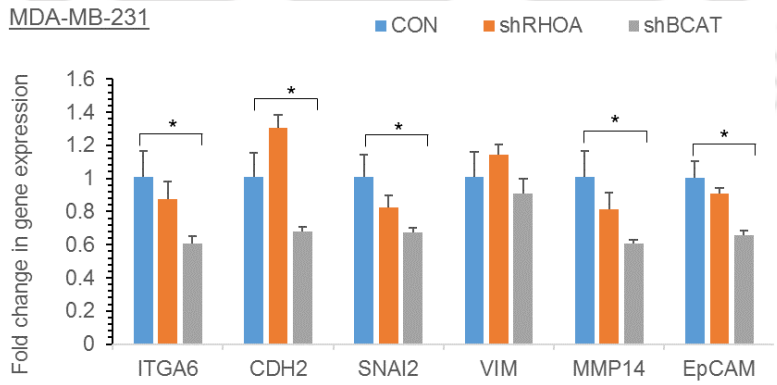

Figure 6.17: Effect of silencing on the migration-related gene. *MDA-MB-231 cells silenced for RHOA, β-catenin, and scramble (control) were lysed and RNA was isolated. After synthesizing cDNA using reverse transcription, qPCR was conducted to assess various gene-level expressions. The fold change in expression level was calculated with the ΔΔCt method. The bar graph represents the fold change in gene expression profiles of ITGA6, CDH2, SNAI2, VIM, MMP14 and EpCAM. Values are mean ± SE, n=3 independent samples, *p<0.05.*

6.2.4 RHOA silencing enhances the anoikis resistance

Cancer cells during metastasis acquire anoikis resistance and to understand the importance of RHOA and β-catenin in promoting anoikis resistance in the breast cancer cells, MDA-MB-231 and MCF7 cells were cultured in a non-adherent culture. The anoikis resistance ability was determined by colony-formation assay. In addition, the effect of the chemotherapeutic drug doxorubicin (Dox) on the anoikis resistance cells was also determined.

In case of MCF7, β-catenin silencing produced significantly less number of colonies (Figure 6.18 A), and the colonies were smaller in size when subjected to anoikis culture conditions, while no discernible difference was seen with RHOA silencing (Figure 6.18 B). Nonetheless, Dox treatment significantly reduced the colony formation ability in the MCF7 cell line regardless of their RHOA and β-catenin expression levels. Besides, no difference in the colony-forming ability was observed between the RHOA and β-catenin silenced cells during Dox treatment compared to the Control-Dox treated cells (Figure 6.18 C).

In the case of MDA-MB-231 cells, a significant increase in the number of colonies was observed when RHOA was silenced in untreated and Dox-treated conditions (Figure 6.18 D, E and F). Although Dox treatment reduced the overall colony-formation ability of MDA-MB-231 cells under anoikis conditions, RHOA silencing seems to provide a survival advantage to the cells resulting in the formation of more colonies compared to the control or shβ-catenin cells.

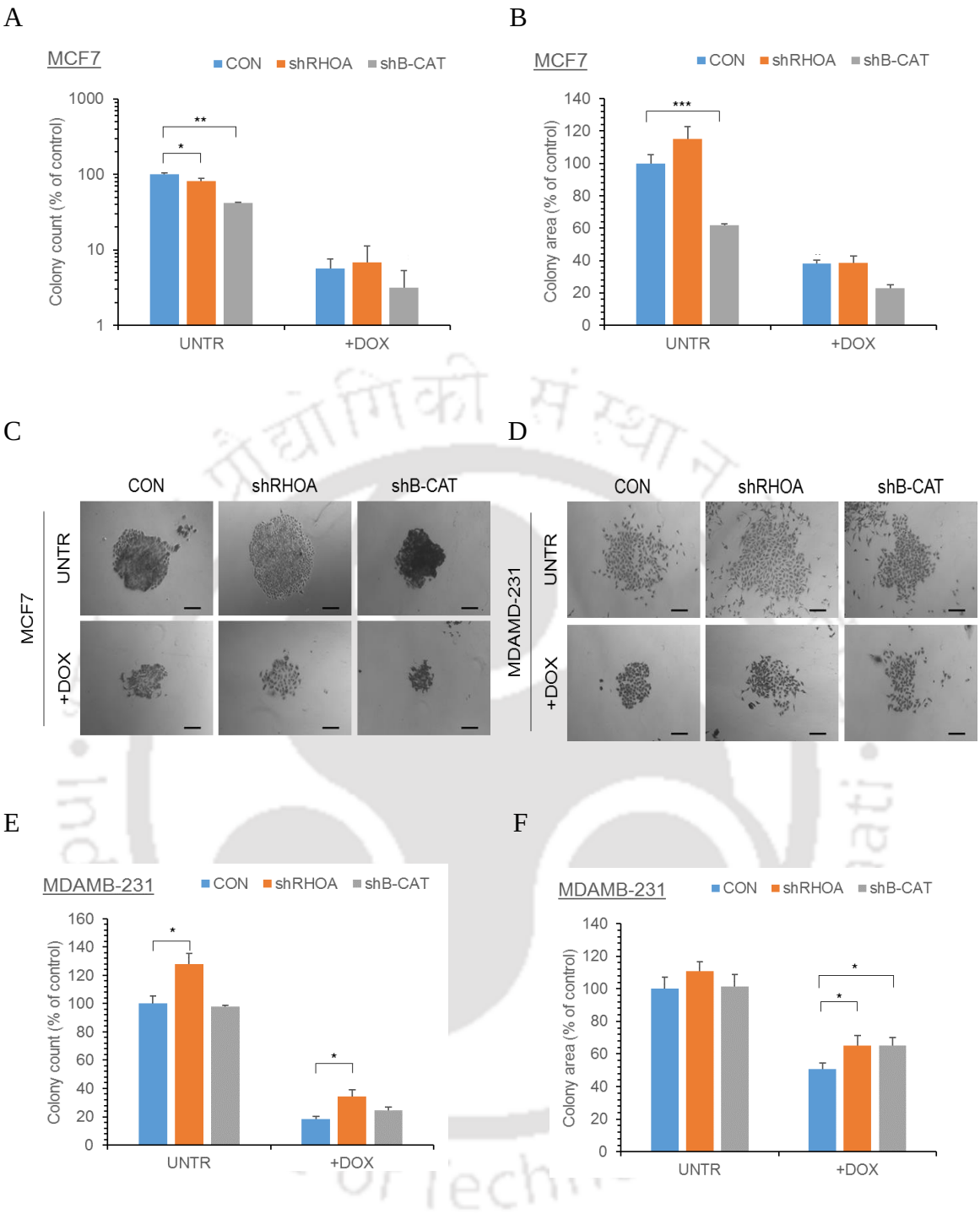

Figure 6.18: Effect of doxorubicin on anoikis resistance of silenced cells. *Silenced breast cancer cells for the scramble, RHOA and β-catenin were seeded on agar-coated wells along with doxorubicin (5μM/ml) for 48 hours and then transferred on tissue culture plates for colony formation in fresh media without doxorubicin. After successful incubation, the colonies were fixed with ice-cold 100% methanol and stained with crystal violet solution. Colonies were counted and the area was measured using Fiji software.* ***A.*** *and* ***B.*** *represent the graph indicating the colony number and area for MCF7,* ***C.*** *and* ***D.*** *represent the colony images of both silenced MCF7 and MDA-MB-231 (scale = 200 μm).* ***E.*** *and* ***F.*** *represent the graph indicating the colony number and area for MDA-MB-231 where cells were left untreated (CON) and treated with Dox. Values are mean ± SE, n=5-6 independent samples, *p<0.05, **p<0.005, ***p<0.0005*

In addition to surviving in the non-adherent state, the cancer cells are also subjected to shear stress during metastasis into distant organs. The shear stress in the cells was simulated by

culturing the cells in a shaker incubator. The effect of RHOA and β-catenin silencing on resisting the shear stress-induced cell death was determined by colony formation assay.

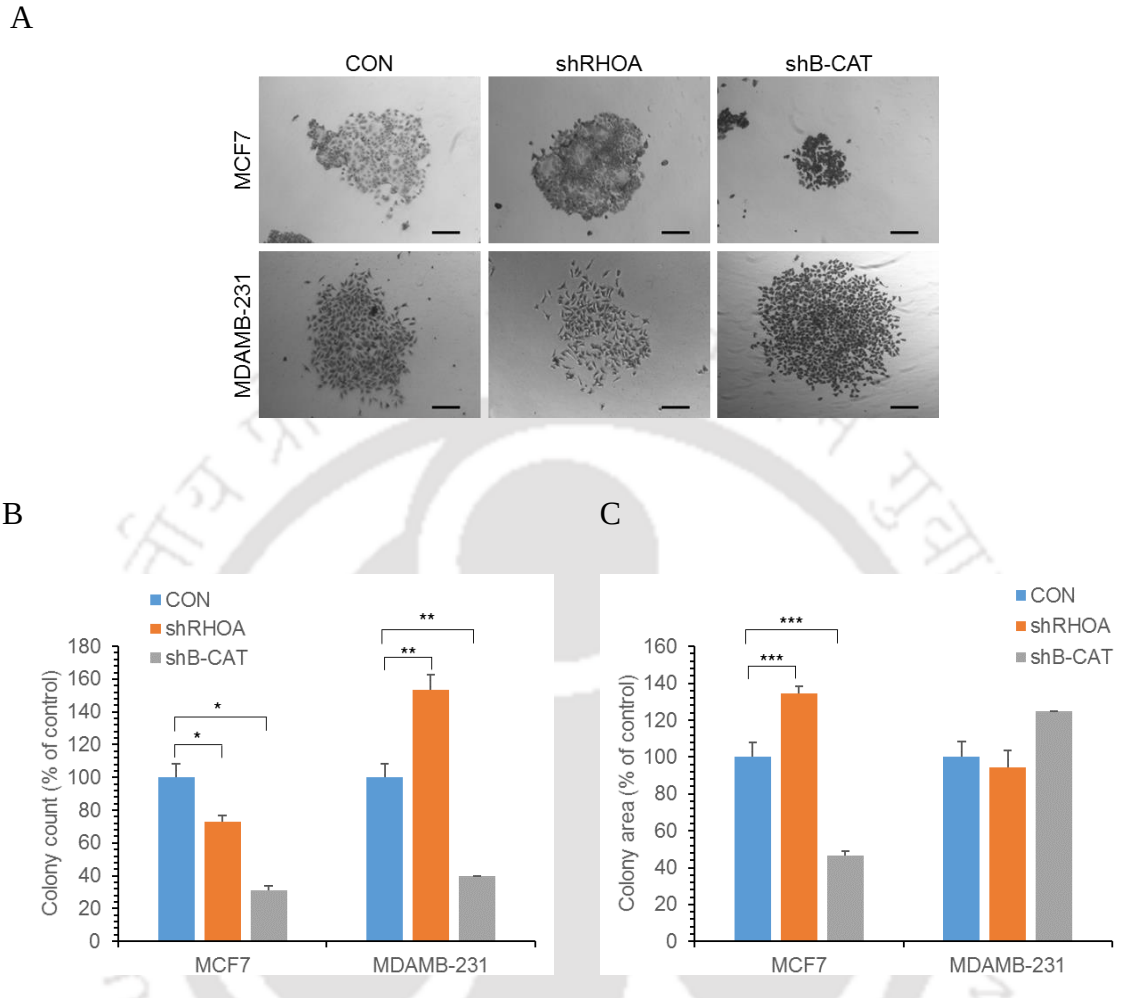

Figure 6.19: Effect of silencing on cellular tolerance to shear stress. *The shear stress resistance of silenced cancer cells was evaluated by subjecting them to stress by shaking them in an incubator for hours at 100 RPM and then assessing their growth potential using a colony assay. Following a successful incubation for 14 days, the colonies were fixed and stained using a crystal violet solution. Colonies were counted and photos were obtained with a microscope. The area covered by the colonies was determined using Fiji software.* ***A.*** *represents the colony images for both MCF7 and MDA-MB-231 (scale = 200 µm), while* ***B.*** *and* ***C.*** *represent the graph indicating the percentage of colony count and colony area of both control and silenced MCF7 and MDA-MB-231 cells with RHOA and β-catenin, respectively.* ***Values*** *are mean ± SE, n=5-6 independent samples, *p<0.05, **p<0.005, ***p<0.0005*

In MCF7, subjecting the cells to shear stress resulted in a drastic reduction in the colony-forming ability when RHOA and β-catenin were downregulated in the cells. During RHOA silencing, subjecting the cells to shear stress decreased the colony-forming ability; the cells formed larger colonies compared to control or β-catenin silenced cells. However, similar to that observed in the anoikis culture conditions, RHOA silencing promoted the survival and colony formation ability in MDA-MB-231 cells when subjected to shear stress. In contrast, β-catenin silencing drastically reduced the survival ability of MDA-MB-231 cells

under shear stress suggesting that β-catenin might play an important role in the survival of the cells during metastasis as displayed in Figure 6.19. The cells subjected to shear stress were also analysed for their gene expression through immunoblotting. Silencing RHOA in MCF7 resulted in the reduction of RHOA and BCL2 expression and an insignificant increase in pERK1/2 expression.

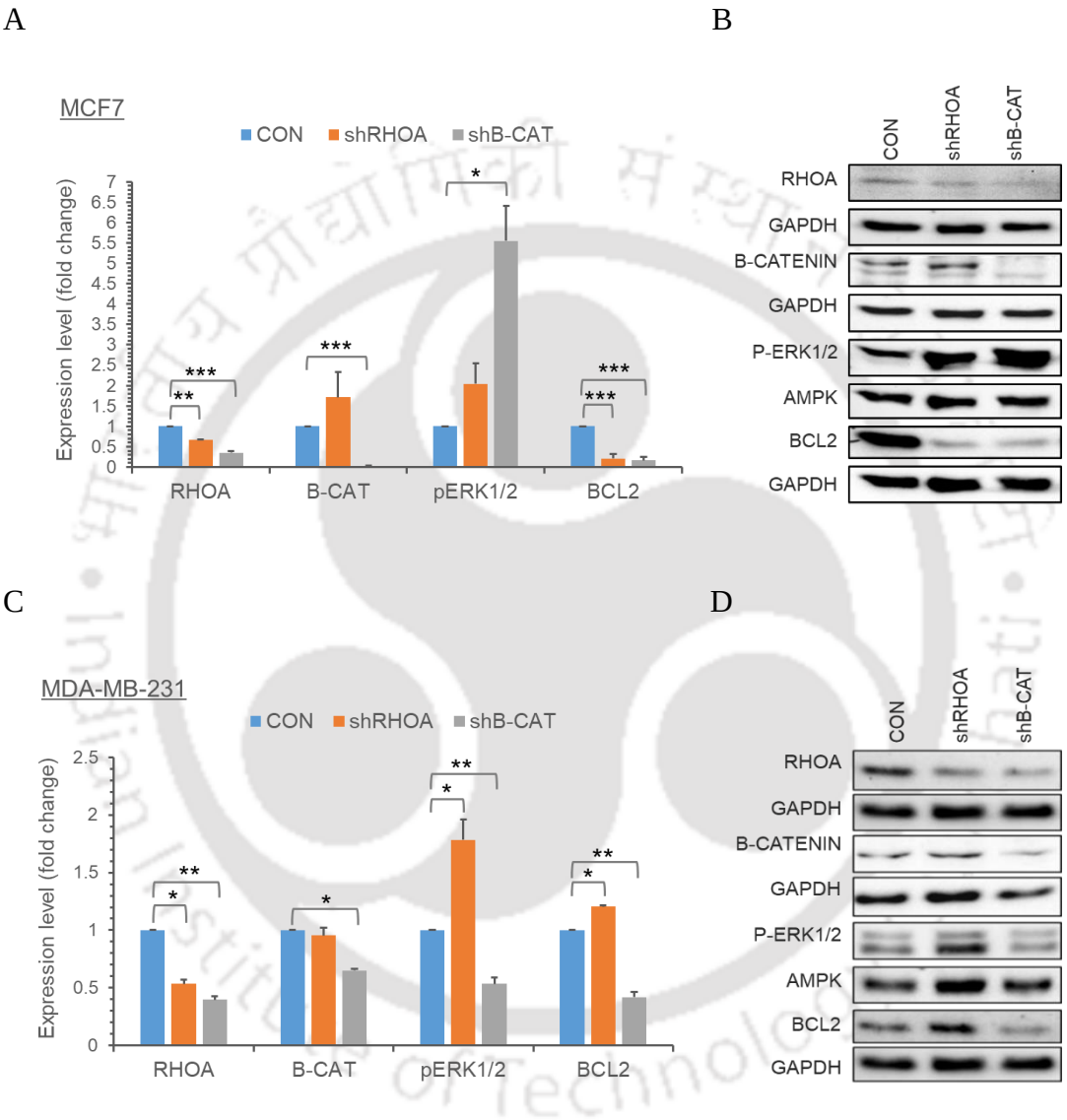

Figure 6.20: Alterations in gene expression of shear stress tolerant silenced cancer cells. *The alteration at the translational level for shear stress tolerant cells was analysed using immunoblotting. The collected lysate from cells was run using a polyacrylamide gel and transferred to a nitrocellulose membrane. The membrane was blocked with skim milk and incubated with primary antibodies such as RHOA (~21 KDa), β-catenin (~92 KDa), pERK1/2 (~42-44 KDa), BCL2 (~26 KDa), and GAPDH (~37 KDa). A secondary HRP-conjugated antibody was added prior to developing the blot using an ECL reagent. Image Lab software was used to determine the band intensity, which was then normalised to the GAPDH protein. The fold change in expression was calculated relative to the control and is shown in* ***A.*** *for MCF7 and* ***C.*** *for MDA-MB-231, while* ***B.*** *and* ***D.*** *represent immunoblot images for MCF7 and MDA-MB-231 cells silenced for RHOA, β-catenin, and scramble (control). Values are mean ± SE, n=4 independent samples, *p<0.05, **p<0.005, ***p<0.0005.*

In contrast, silencing β-catenin resulted in a significant decrease in RHOA, β-catenin, and BCL2 expression and an increase in pERK1/2 expression compared to the control (Figures 6.20 A and B).

Similarly, when MDA-MB-231 was analysed for the shear stress tolerance, silencing of RHOA in MDA-MB-231 decreased RHOA expression but induced the pERK1/2 and BCL2 expression. The increase in pERK1/2 and BCL2 explain the increase in the survival and colony-forming ability of the shRHOA-MDA-MB-231 cells subjected to shear stress. In contrast, β-catenin silencing led to a decrease in RHOA, β-catenin, pERK1/2, and BCL2 expression in MDA-MB-231 as shown in Figures 6.20 C and D. The presence of elevated pERK1/2 in RHOA-silenced cells suggests that the ERK pathway is active under stress and that this activation might have led to higher cell proliferation observed in these cells. Furthermore, cells grown under anchorage-dependent conditions were allowed to form spheroids and the changes in the gene expression were analysed.

RHOA and β-catenin silencing reduced the expression of pERK1/2 and β-catenin levels in MCF7 cells (Figure 6.21 A and B). Interestingly, in the case of MDA-MB-231, silencing of shRHOA increased pERK1/2 and β-catenin expression whereas β-catenin silencing led to the downregulation of β-catenin and abrogated the expression of pERK1/2 levels as shown in Figure 6.21 C and D. This increase in pERK1/2 in shRHOA-MDA-MB-231 cells suggests the survival advantage that these cells possess during anchorage-independent conditions.

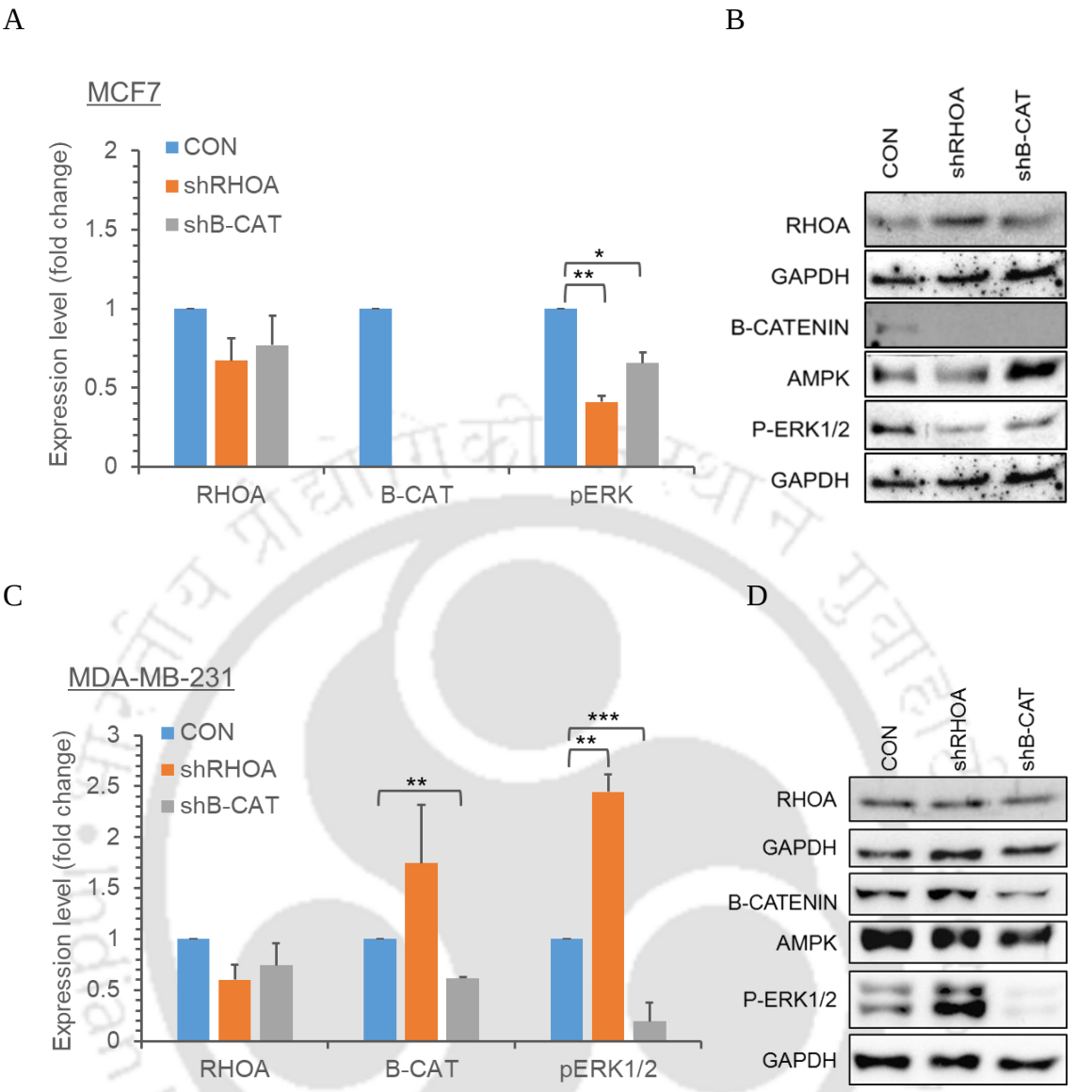

Figure 6.21: Gene expression study of anchorage-independent spheroids. *Immunoblotting was performed for the lysate collected from spheroids derived from the control and silenced MCF7 and MDA-MB-231 cells. Before incubation with the target antibody, the protein sample was loaded on a polyacrylamide gel and protein bands were transferred to the nitrocellulose membrane. The blots were incubated with secondary HRP conjugated antibody to identify the primary antibody binding, and ECL chemiluminescent was added to visualise the protein band. Image Lab software was used to determine the band intensity, which was then normalised to the GAPDH protein. The fold change in expression was calculated relative to the control and is shown in* ***A.*** *for MCF7 and* ***C.*** *for MDA-MB-231, while* ***B.*** *and* ***D.*** *represent immunoblot images of RHOA (~21 KDa), β-catenin (~92 KDa), pERK1/2 (~42-44 KDa), and GAPDH (~37 KDa) for MCF7 and MDA-MB-231 cells silenced for RHOA, β-catenin, and scramble (control). Values are mean ± SE, n=4 independent samples, *p<0.05, **p<0.005, ***p<0.0005.*

6.2.5 RHOA silencing augments chemoresistance in MDA-MB-231

RHOA and Wnt signalling were both found to be essential for shear stress tolerance. The change in pERK1/2 expression suggests that, under stress conditions, the ERK signalling pathway operates to adapt to the altered microenvironment. The intriguing result of shear stress tolerance prompted us to investigate the role of this pathway in chemoresistance.

The spheroid formation assay was carried out in the presence of Dox to determine the impact of silencing on the growth of the spheroids. Regardless of RHOA or β-catenin silencing, the addition of Dox to the cell line caused a substantial reduction in the spheroid size in MCF7 cells (Figure 6.22 A and B).

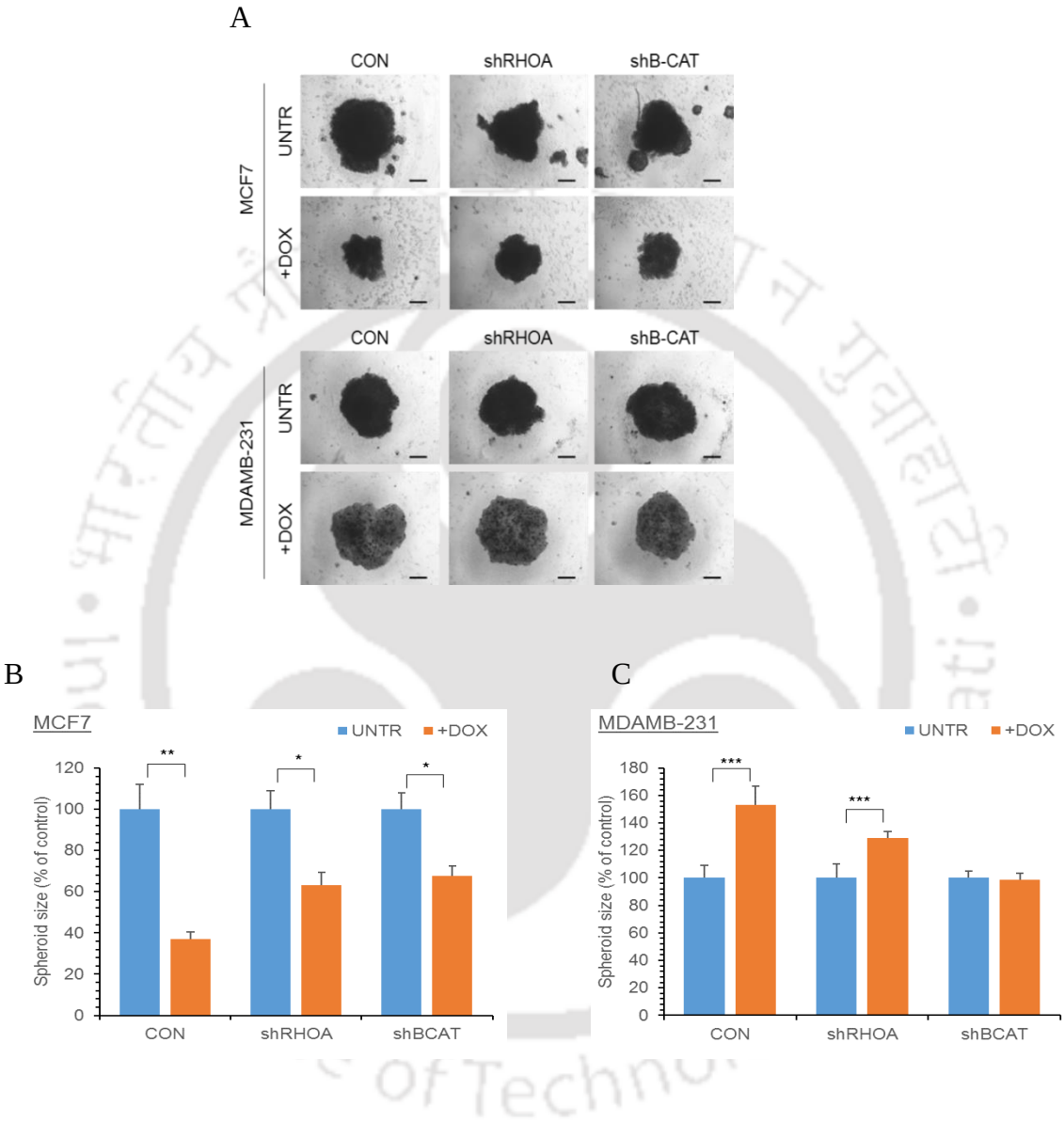

Figure 6.22: Effect of doxorubicin on the spheroid growth of silenced cells. *To test the effect of Dox (5μM/ml) on spheroids growth of silenced cells, scramble, RHOA and β-catenin silenced breast cancer cells were implanted in anchorage-independent conditions coupled with doxorubicin. Images were acquired at 3-4 day intervals and the area was evaluated with Fiji software.* ***A.*** *Represents spheroid images (scale = 200 μm) and* ***B.*** *Represents the spheroid area of MCF7 and* ***C.*** *represents the spheroid area of MDA-MB-231 for each condition control, shRHOA and shβ-catenin cells in presence and absence of Dox, calculated as the percentage of the area of their respective controls. Values are mean ± SE, n=5 independent samples, *p<0.05, **p<0.005, ***p<0.0005.*

It is interesting to note that the addition of Dox during spheroid formation in MDA-MB-231 increased the spheroid size of both control and RHOA-silenced cells in comparison to

their respective untreated conditions. On the other hand, β-catenin silencing did not have any effect on the spheroid size in either the untreated or Dox-treated condition as shown in Figure 6.22 A and C.

6.2.6 Silencing of RHOA and β-catenin reduces metastasis

The silenced MDA-MB-231 cell line was subjected to additional testing to determine its propensity for metastasis. Both control and silenced cells that had been pre-treated with doxorubicin in non-adherent anoikis conditions were seeded on bone marrow stromal cells, and their colony formation ability was determined. The ability to form colonies on the stromal cells was lower in shRHOA and shβ-catenin cells compared to the control cells. Also, treatment with Dox significantly reduced the colony formation ability in all the conditions (Figure 6.23). However, the addition of Dox to cells that have been silenced for shRHOA results in the induction of chemoresistance in comparison to control cells and cells silenced for shβ-catenin. Thus, in addition to modulating the anoikis resistance, RHOA and β-catenin regulate the ability of the cells to form colonies in the bone marrow microenvironment.

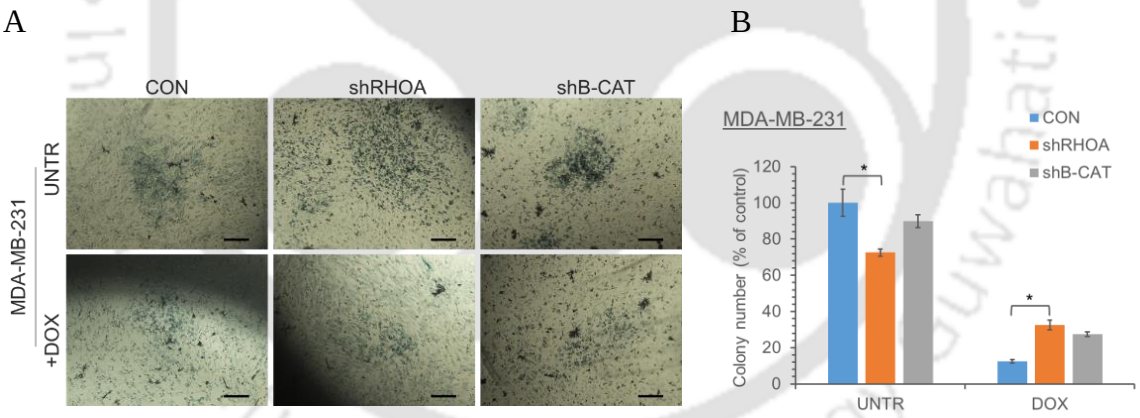

Figure 6.23: Effect of silencing on metastasis of anoikis-resistant cells. *To determine the metastatic potential of the scramble, RHOA, and β-catenin-silenced MDA-MB-231, the cells were first grown under anchorage-independent conditions with doxorubicin (5μM/ml). Silenced MDA-MB-231 cells were transferred to a monolayer of stromal cells that were already confluent and allowed to form colonies. The number of colonies formed by MDA-MB-231 on the stromal layer was enumerated using a microscope to determine its metastatic potential.* ***A.*** *Represents the colony images of MDA-MB-231 cells silenced with control (transduced with scramble) and RHOA and β-catenin formed on stromal cells (Scale bar = 200μm) and* ***B.*** *represents the graph of the colony number under each condition. Values are mean ± SE, n=12 independent samples, *p<0.05, **p<0.005, ***p<0.0005.*

6.3 Discussion

In numerous physiological and pathological processes, including embryonic development, wound healing, cancer metastasis, and inflammation, the Rho/Rock signalling pathway plays a crucial role in regulating cell migration. Rho, a small GTPase, initiates this pathway by activating Rho-associated protein kinase (ROCK). ROCK's phosphorylation and activation of MLC, which regulates the dynamics of the actin cytoskeleton and cell contractility, increases actomyosin contractility and cytoskeletal stress (Tan et al., 2011). The Rho/ROCK pathway is essential for the polarization, adhesion, and translocation of migrating cells due to its role in the formation and maintenance of stress fibres, focal adhesions, and cell-substrate traction forces. Rho/ROCK signalling has also been shown to regulate cell morphology, protrusion, adhesion turnover, and matrix metalloproteinase activity, which all contribute to cell migration (Anne J Ridley, 2015). The location of Rho-Rock signalling members determines the migratory front; for example, Cdc42 with mDIA forms filopodia and with Par complex regulates directional motility; Rho with ROCK regulates contraction in actin-myosin and adhesion to ECM (Lawson & Ridley, 2018; Anne J Ridley, 2015).

Wnt signalling is a highly conserved system that is essential for tissue homeostasis and embryonic development. Wnt signalling is another signalling pathway investigated in this research work. Wnt signalling dysregulation has been linked to several human illnesses, including cancer. Wnt signalling has been shown to support tumour growth, invasion, and metastasis in breast cancer when it is aberrantly activated. Studies have demonstrated that the activation of downstream target genes like Cyclin D1, c-Myc, and MMP-7 by Wnt/β-catenin signalling (Luu et al., 2004) increases breast cancer cell proliferation, survival, and invasion. Additionally, it has been demonstrated that Wnt signalling promotes cancer stem cell-like phenotype, increasing tumour-initiating potential and therapy resilience.

RHOA signalling was analysed by interrupting the downstream effector ROCK with the inhibitor Y27632. Several studies have utilized Y27632 to understand the role of RHOA in development and cell migration. In olfactory ensheathing cells, which were previously process-bearing and flattened in structure, neurite extension was induced by the Y27632 treatment (Li et al., 2018). Similarly, in another study (Lim & Joe, 2013), mesenchymal stromal cells treated with Y27632 acquired a neuronal cell-like structure by inhibiting the chondroitin sulfate proteoglycan, which inhibits the transformation of MSCs into a

neuronal morphology. The fact that we also observed protrusion in MCF7 and spike-like structures in MDA-MB-231 treated with Y27632 confirms the role of ROCK in actin remodelling. Y27632 induces development in individual cells rather than clusters in murine embryonic stem cells (CCE), and studies also found that inhibiting ROCK1/2 or silencing it with siRNA did not affect the marker essential for self-renewal (Chang et al., 2010). Our findings demonstrated that the Y27632 treatment improved the clonogenic potential of MCF7 in terms of colony size and density. However, we also discovered that Y27632 only promoted two-dimensional growth and had a detrimental impact on the formation of three-dimensional spheroids in MCF7.

Previous research indicated that inhibiting RHOA decreased human tongue cancer by halting the cell cycle (Yan et al., 2014) and the gastric cell line (MGC-803) by halting the proliferation of cells in the G0/G1 phase of the cell cycle (Duan et al., 2015). Another study discovered that eliminating β-catenin in H295R adenocarcinoma cells decreased cell proliferation, induced arrest in the G1 phase, and apoptosis (Gaujoux et al., 2013). In RHOA and β-catenin silenced MDA-MB-231 and RHOA silenced MCF7, we also noticed a cell cycle arrest in the G1 phase. It was discovered that inhibiting RHOA and RHOC with siRNAs can inhibit proliferation and invasion in MDA-MB-231 (Pillé et al., 2005); Our study, however, revealed that while RHOA silenced cells partially retained growth, it did not affect the invasion or migration of MDA-MB-231. When RHOA is silenced, PC3 cells develop long, thin protrusions triggered by Rac1, which promotes migration and invasion (Vega et al., 2011). In terms of morphology, this finding is consistent with our observations of projection in MDA-MB-231 and loose polygonal sheets of cells in MCF7; however, in terms of migration and invasion, we have found contradictory findings. In contrast to MDA-MB-231, whose migration was unaffected by RHOA silencing, MCF7 migration was suppressed entirely. One study found that E-cadherin expression was reduced when β-catenin was silenced, which inhibited lung cancer cells (Yu et al., 2017). The migration of MCF7 in our study was indeed inhibited, but after β-catenin silencing, we did not find any changes in E-cadherin expression.

GEF-1 is required for neutrophils to endure shear stress and drives its navigation or expansion via MLC and ROCK (Fine et al., 2020). MSC also require RHO-ROCK signalling to tolerate shear stress, indicating its essential role in shear stress tolerance (Gao et al., 2014). Recent research has shown that Wnt/β-catenin signalling plays a significant role in mechano activation (Warboys, 2018) and regulation (Strittmatter et al., 2022) in

determining the divergence of mesodermal heredity. Our findings with MCF7 are consistent with previous studies conducted on a variety of cancers in which silencing RHOA and β-catenin reduced the shear stress tolerance of cells, whereas, in contradiction, MDA-MB-231 exhibited a higher tolerance to shear stress when RHOA has silenced and a decrease in tolerance when Y27632 was added to the cells. Increased ERK expression is positively correlated with a variety of cancers, including prostate, colon, breast, and ovarian cancer (Levidou et al., 2012). Along the same lines, we have observed a decreased growth in MCF7 cells during adherent culture when RHOA silencing leads to a decrease in ERK1/2 level. On the other hand, increased expression of pERK1/2 during shear stress indicates that ERK is one of the stress-activated signalling pathways.

In colon cancer, Wnt signalling plays an important role and is associated with increased proliferation, whose regulation is increased by RHOA inactivation (Rodrigues et al., 2014b). In the current study, when RHOA was silenced, an increased expression of β-catenin was identified in both MCF7 and MDA-MB-231 cells. A similar effect was observed in lung cancer cells where inhibiting Rho GTPase activating protein 24 can stimulate Wnt/β-catenin signalling, which in turn can promote the dissemination of lung cancer (L. Wang et al., 2019). On the other hand, activating Rho GTPase activating protein 30 can suppress pancreatic cancer by deactivating Wnt/β-catenin signalling (Zhou et al., 2020). A relationship between Ras family members and BCL2 expression was observed (Kang & Pervaiz, 2013), where RAC1 levels correlate with BCL2 expression. In our studies, we observed that RHOA regulates BCL2 expression, where silencing RHOA in MCF7 reduced BCL2 expression, and the addition of Y27632 reduced its expression even further. However, when subjected to shear stress, RHOA and β-catenin silenced cells downregulated the BCL2 expression, although there was an increase in the pERK1/2 levels. The reduction in survival and the colony formation ability observed in MCF7 cells when subjected to shear stress during RHOA and β-catenin silencing also correlated with the reduced expression of the anti-apoptotic protein BCL2. Interestingly, in MDA-MB-231 cells, when RHOA was silenced, it induced the expression of pERK1/2 and BCL2, which explains the increased survival and self-renewal ability seen in these cells. In contrast, β-catenin silenced led to reduced colony formation ability and a significant decrease in the expression of pERK1/2 and BCL2.

Silencing of RHOA did not affect the migration of MDA-MB-231 cells. In contrast, highly aggressive rat A3 cells were found to use the Rho/ROCK/MLC pathway to invade the 3D

collagen matrix and the acellular dermis (Kosla et al., 2013), which supports our finding in MCF7 that RHOA silencing reduced the migration potential. Massive apoptosis of mammary tumour cells (Buechel et al., 2021) and head and neck cancer cells (Kleszcz et al., 2019) was caused by the elimination of β-catenin. The current study also observed that β-catenin silencing induced morphological changes in MCF7, reducing cell size and decreasing colony formation ability. Several studies supported the role of RHOA and β-catenin in controlling growth. When mice were injected with shRNAs of RHOA and RHOC, the tumour growth of HCT116 (colorectal cancer cell line) was inhibited (H. Wang et al., 2010). Similarly, in lung cancer (Yang et al., 2015) and ovarian cancer (Wang et al., 2015), RHOA silencing inhibited growth and proliferation. We also observed a reduction in the proliferation of MCF7 and MDA-MB-231 when RHOA was silenced. When RHOA was inhibited or silenced, human colon cancer cells lost their doxorubicin resistance (Doublier et al., 2008). Similarly, when β-catenin was suppressed via the NF-κB pathway, MG-63, an osteosarcoma cell, lost its chemoresistance to doxorubicin (Zhang et al., 2011). In addition, affecting the proximal target of Wnt signalling, such as LGR6 (leucine-rich, G protein-coupled receptor), can eliminate chemoresistance in ovarian cancer via β-catenin or canonical wnt signalling (Ruan et al., 2019). In the current study, RHOA or β-catenin silencing did not affect the chemosensitivity of MCF7 cells to doxorubicin, whereas RHOA silencing slightly decreased the chemosensitivity of MDA-MB-231 cells to doxorubicin. Thus, targeting β-catenin signalling in MCF7 can inhibit its proliferation (Saifo et al., 2010) but not in MDA-MB-231.

6.4 Conclusion

The finding in this chapter suggests that silencing RHOA and β-catenin can inhibit proliferation, migration, anoikis resistance, and chemoresistance in MCF7. However, the increased proliferation and migration of MCF7 in the presence of Y27632 and elevated pERK1/2 under shear stress remains debatable. Nonetheless, *in-vivo* studies are required to confirm the effect of RHOA and Wnt signalling in breast cancer. In contrast, the triple-negative cancer cell line MDA-MB-231 displayed a remarkable context-dependent effect (Figure 6.24). Surprisingly, suppressing RHOA enhanced tolerance to shear stress and resistance to anoikis and chemotherapeutic drug treatment. The finding also suggests that the activation of the ERK1/2 pathway can readily compensate for the absence of RHOA in MDA-MB-231 cells when subjected to shear stress.

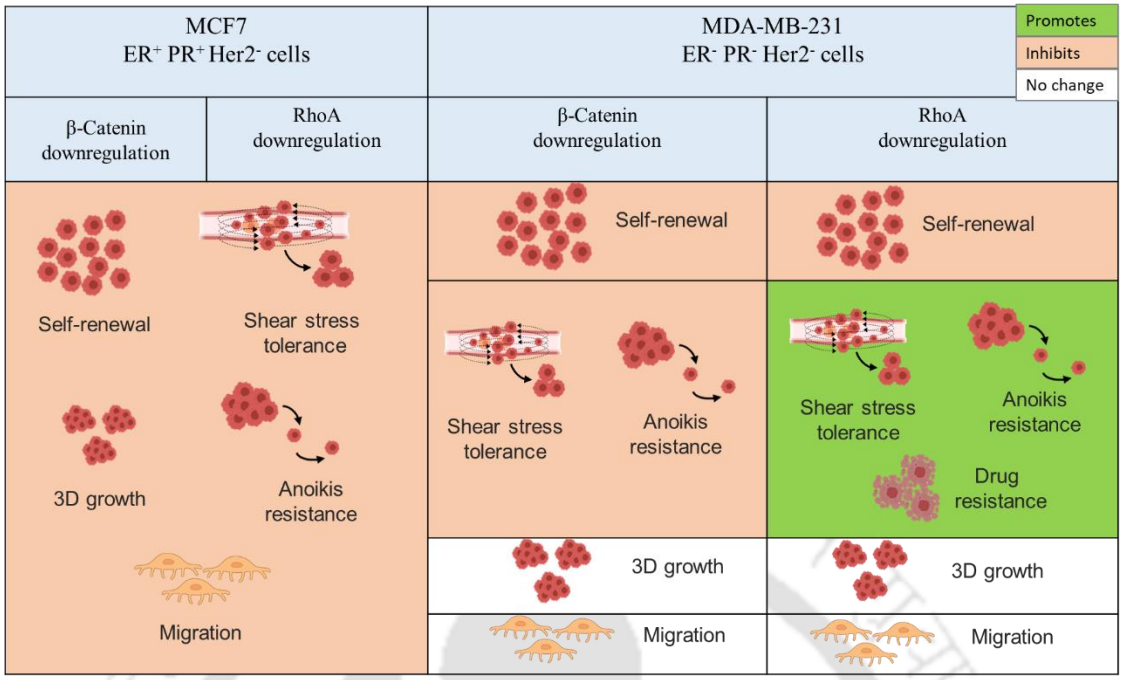

Figure 6.24: *Conclusive remark of canonical and non-canonical Wnt signalling in breast cancer cells.*

Even though a great deal of research has been conducted on RHOA and Wnt signalling in terms of various functions and cancer, there are still a great many things that have not been adequately studied to inhibit the progression of cancer. In order to uncover the complex and intricate behaviour of signalling, more research must be conducted.

Understanding the Crosstalk Between BMP4, RHOA and Wnt Signalling

7.1 Introduction

The regulation and coordination of different cellular processes rely on cross-talk between different signalling pathways. Several examples highlight the significance of cross-talk between signalling pathways: regulation of gene expression to carry out a physical function; integration of signals to improve response; feedback regulation to preserve homeostasis; and adaptation to novel microenvironments. Nevertheless, many diseases and disorders can develop when this complex or cross-talk signalling fails to operate in a healthy equilibrium. BMP and Wnt signalling cross-talk has been studied for its effects on a wide range of cellular and developmental processes, including embryogenesis, myoblast differentiation (Nakashima et al., 2005), dental stem cell regulation, and radial patterning of the mouse cochlea (Munnamalai & Fekete, 2016), but its dysregulation can cause a wide range of diseases and disorders. Wnt and BMP cross-talk at multiple stages, including reciprocal regulation of ligand production, and after nuclear localization in the nucleus, the downstream target of BMP, such as Smad, can cross-talk with the downstream target of Wnt, such as LEF/TCF (X. Guo & Wang, 2009). In the non-canonical Wnt signalling pathway, Wnt cross-talks with RHO-ROCK signalling using various mediators. Because of the intricate interplay between these pathways, developing an effective therapeutic strategy for cancer prevention has been challenging. Since no one reported the crosstalk between BMP, RHOA, and Wnt signalling, the silenced cells were subjected to functional and molecular investigations to identify this

7.2 Results

7.2.1 BMP4 and ROCK inhibitor in β-catenin and RHOA expression

Firstly, MDA-MB-231 and MCF7 cells were treated with BMP4, LDN, and Y27632 and their effect on the expression levels of β-catenin and RHOA were analysed by immunoblotting. Figure 7.1 A shows that after BMP4 treatment, β-catenin levels in MCF7 decreased slightly, although this effect could not be replicated. However, LDN or a combination of LDN and BMP4 did not affect β-catenin or RHOA expression. Treatment with BMP4 or LDN also did not affect β-catenin or RHOA expression levels in MDA-MB-231. The expression of β-catenin and RHOA did not change when exposed to Y27632 in both MCF7 and MDA-MB-231 cells (Figure 7.1 B).

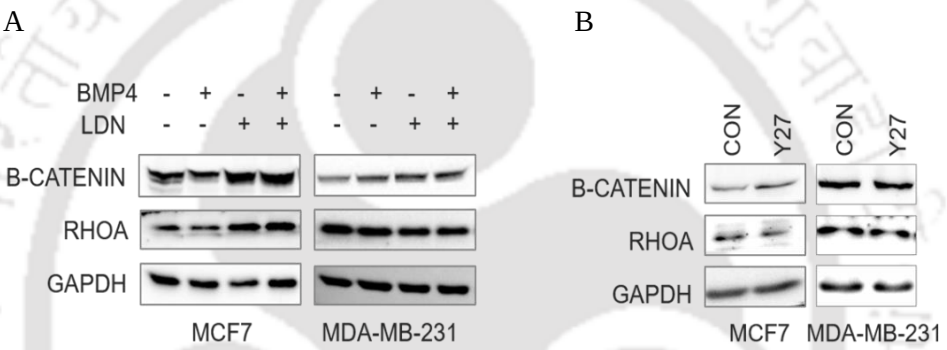

Figure 7.1: Effect of BMP4 and ROCK inhibitor on β-catenin and RHOA expression. *Immunoblotting was performed for the breast cancer cells treated with BMP4 (10ng/ml), LDN (1μM/ml) and Y27632 (10μM/ml) for 48 hours. Before incubating with β-catenin (~92 KDa), RHOA (~21 KDa) and GAPDH (~37 KDa) antibodies, the protein sample was loaded on a polyacrylamide gel and protein bands were transferred to the nitrocellulose membrane. The blots were then incubated with a secondary HRP-conjugated antibody to identify the primary antibody binding, and ECL chemiluminescent was added to visualise the protein band.* ***A.*** *depict the expression of β-catenin and RHOA in MCF7 and MDA-MB-231 cells, respectively, when treated with BMP4 and LDN and* ***B.*** *depict the expression of β-catenin and RHOA in MCF7 and MDA-MB-231 cells when treated with Y27632.*

7.2.2 BMP4 modulates clonogenic potential β-catenin and RHOA silenced cells

Although BMP4 or LDN treatment did not affect the expression levels of either RHOA or β-catenin, the self-renewal ability of the cells when treated with BMP4 or LDN during RHOA or β-catenin silencing was determined by colony formation assay. While BMP4 treatment decreased the colony formation ability in control and β-catenin silenced cells, RHOA silencing abrogated the inhibitory effect of BMP4 on the self-renewal ability of MCF7 cells. As reported earlier, LDN treatment increased the colony-forming ability of control cells; an increase in the colony-formation ability was also observed in LDN-treated RHOA-silenced cells but not in β-catenin silenced cells (Figures 7.2 A, B and C).

A

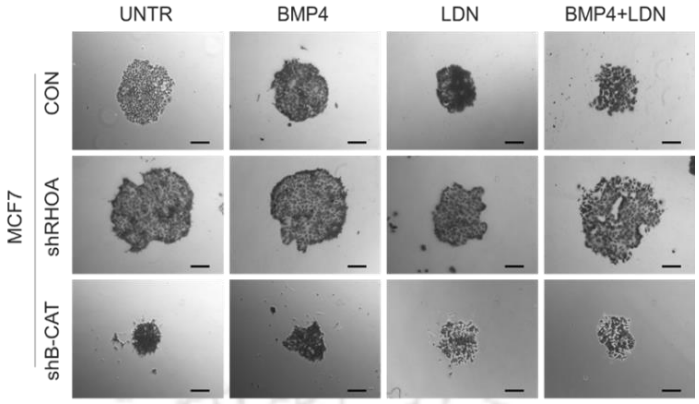

B

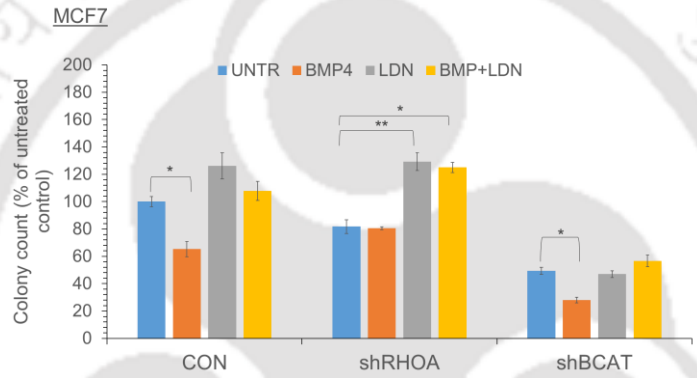

C

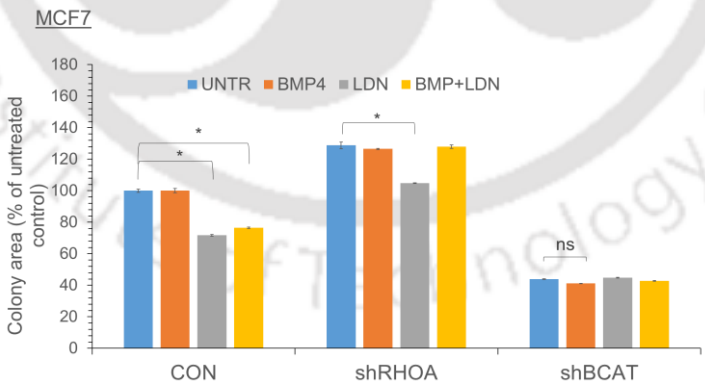

Figure 7.2: Effect of BMP4 on the clonogenic potential of silenced MCF7 cells. *The RHOA, β-catenin, and scramble (control) silenced cells were treated with BMP4 (10ng/ml) and LDN (1µM/ml), and their combination was incubated on tissue culture plates to form colonies for 14 days. The colony plates were stained with crystal violet, and colonies were counted using a microscope. The ideal colony has a cell count greater than or equal to 50. Images were taken with a microscope, and the area was calculated with Fiji software.* ***A.,*** *depict the colony images for silenced MCF7 cells, where cells left untreated (control) or treated with BMP4, LDN, BMP4+LDN and black line in images represents the scale bar of 200µm.* ***B.*** *and* ***C.*** *represent the percentage of colony number and colony area for MCF7. Values are mean ± SE, n=3-4 independent samples, *p<0.05, **p<0.005, not significant (ns), p>0.05*

A

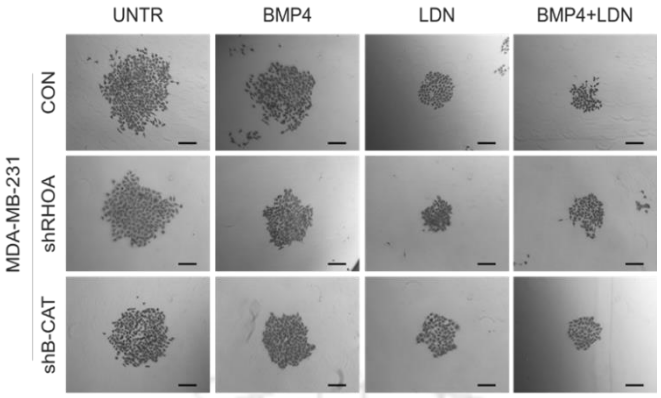

B

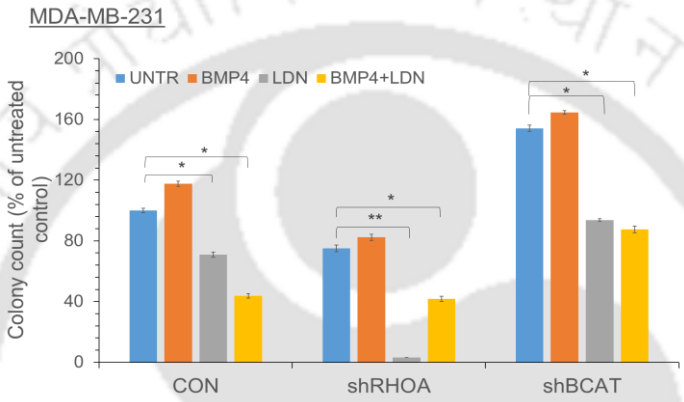

C

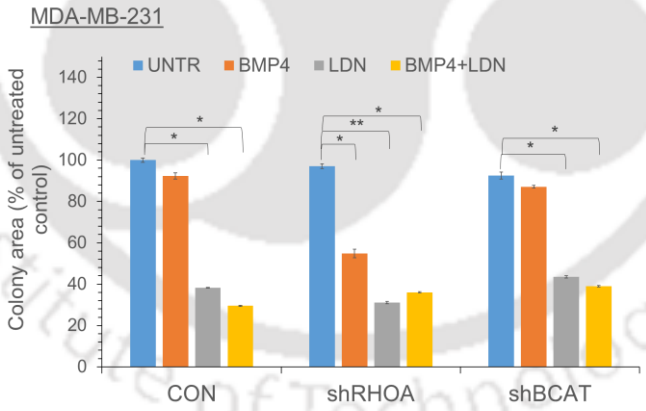

Figure 7.3: Effect of BMP4 on the clonogenic potential of silenced MDA-MB-231 cells. *The RHOA, β-catenin, and scramble (control) silenced cells were treated with BMP4 (10ng/ml) and LDN (1μM/ml), and their combination was incubated on tissue culture plates to form colonies for 14 days. The colony plates were stained with crystal violet, and colonies were counted using a microscope. The ideal colony has a cell count greater than or equal to 50. Images were taken with a microscope, and the area was calculated with Fiji software.* ***A.,*** *depict the colony images for silenced MDA-MB-231 cells, where cells left untreated (control) or treated with BMP4, LDN, BMP4+LDN and black line in images represents the scale bar of 200μm.* ***B.*** *and* ***C.*** *represent the percentage of colony number and colony area for MDA-MB-231. Values are mean ± SE, n=3-4 independent samples, *p<0.05, **p<0.005.*

In MDA-MB-231 cells, as expected, LDN treatment downregulated the colony-forming ability in all the conditions, such as control, shRHOA and shβ-catenin. However, RHOA silencing seems to have an additive effect where the colony-forming ability was drastically reduced upon LDN treatment. Interestingly, BMP4 treatment reduced the colony size when RHOA was silenced, whereas a reduction in colony size was observed during LDN treatment in control and β-catenin silenced cells. These results suggest a possible cross-talk between BMP signalling and the RHOA pathway (Figures 7.3 A, B and C).

To further analyse the cross-talk between the pathways, cells cultured under shear stress were treated with BMP4 or LDN, and their colony-formation ability was determined. Both the control and silenced cells underwent a considerable reduction in colony number after treatment with LDN and its co-treatment with BMP4. However, it was fascinating to note that BMP4 treatment affected only the cells in which β-catenin had been silenced, while control cells and cells in which RHOA had been silenced were unaffected by the treatment. Regarding colony area, both control and RHOA-silenced cells showed a reduction in colony area after being co-treated with BMP4 and LDN. On the other hand, the colony area was greatly reduced in control cells when LDN was added, and it was significantly reduced in shRHOA cells when BMP4 was added (Figure 7.4).

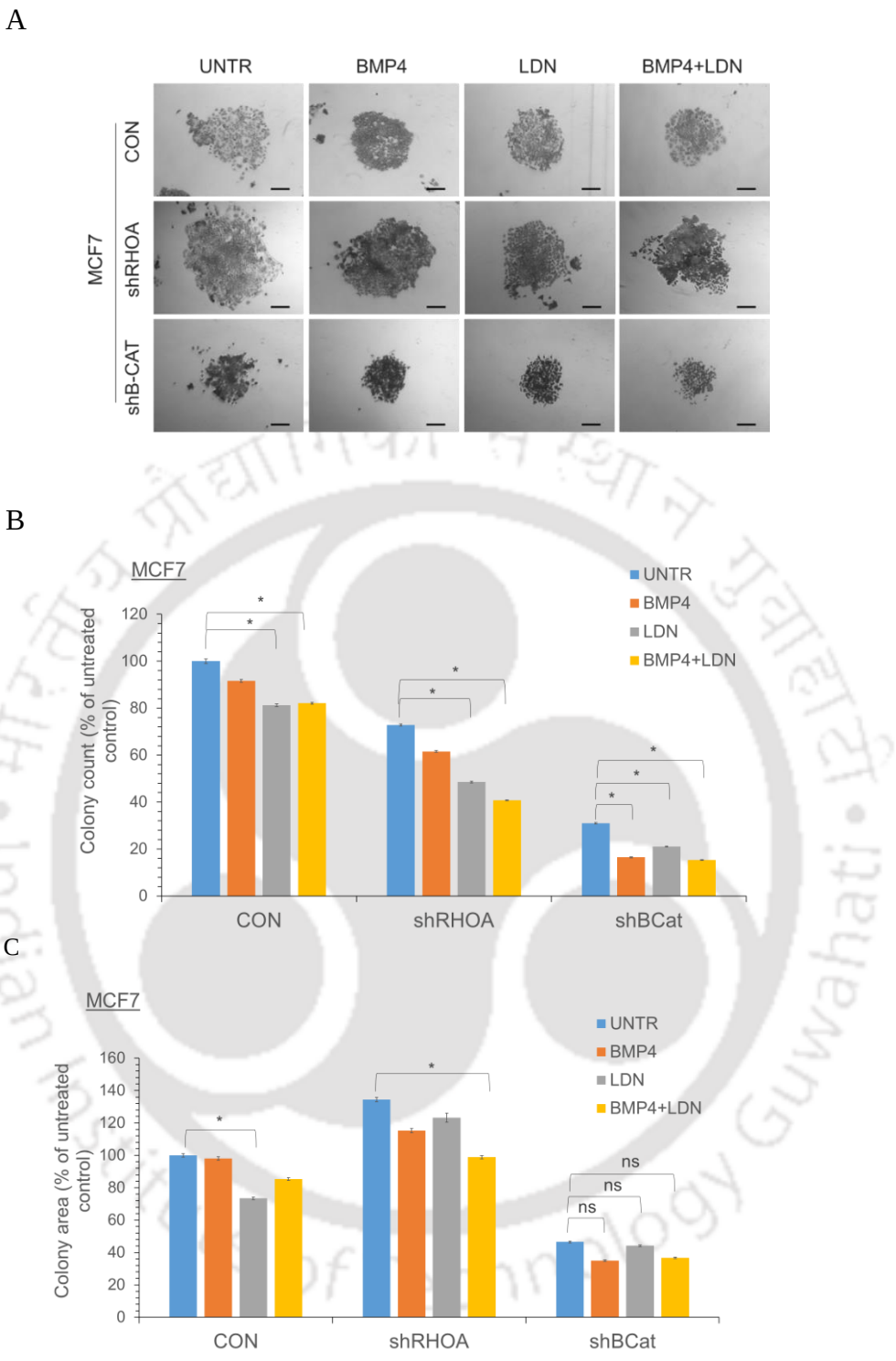

Figure 7.4: Effect of BMP4 on the clonogenic potential of shear-stressed silenced breast cancer cells. *To determine the effect of BMP on shear tolerance, silenced breast cancer cells subjected to shear stress in conjunction with BMP4 (10ng/ml) and LDN (1μM/ml) were plated to form colonies for 14 days. Following an effective incubation, colonies were fixed with methanol and stained with crystal violet solution. Images were taken with a microscope, and the area was calculated with Fiji software* ***A.*** *depicts the colony images for silenced MCF7 cells, where cells left untreated (control) or treated with BMP4, LDN, BMP4+LDN and black line in images represents the scale bar of 200μm.* ***B.*** *and* ***C.*** *represent the percentage of colony number and colony area for MCF7. Values are mean ± SE, n=3-4 independent samples, *p<0.05, **p<0.005, not significant (ns), p>0.05*

7.2.3 Silencing of β-catenin and RHOA modulates BMP, Wnt and Notch pathway genes

The above data suggests that a cross-talk may exist between the BMP4-Wnt and BMP4-RHOA pathways; however, how these pathways are interconnected remains unclear. So comprehensive gene expression analysis was conducted to determine the interactions.

The transcriptional factors associated with the BMP signalling pathway were examined to determine the nature of the interaction between pathways. When β-catenin was silenced in MCF7, the expression of *BMP4* was significantly upregulated, whereas the expression of *BMPR1A* and *BMPR2* was downregulated. In RHOA-suppressed cells, the expression of *BMPR1A* increased while that of *BMPR2* decreased (Figure 7.5 A). RHOA silencing in MDA-MB-231 reduced the expression of *BMPR1A* and *ID4*, whereas β-catenin silencing consistently decreased BMP signalling components such as *BMP4*, *BMPR1A*, *BMPR2*, and *ID4*. The expression of *BMP6* was notably upregulated in both silenced cells (Figure 7.5 B). This demonstrates that RHOA and Wnt signalling modulate BMP signalling in MCF7 and MDA-MB-231 in a context-dependent manner.

To further determine the effect of RHOA and β-catenin silencing on Wnt and Notch signalling, the expression of associated genes was also analysed. Suppressing β-catenin led to a significant reduction in Wnt signalling-related transcripts. *FZD2*, *LEF1*, and *S100A4* expression were found to be downregulated in shβ-cat-MDA-MB-231 cells. Similarly, β-catenin silencing substantially downregulated the Notch signalling pathway, as demonstrated by the decreased expression of *DLL1*, *NOTCH1*, *NOTCH2*, *NOTCH3*, and *HES2*. As shown in Figure 7.6, the RHOA silencing did not directly influence the Wnt and Notch signalling genes. Consequently, these results indicate that Wnt signalling can also modulate Notch signalling.

A

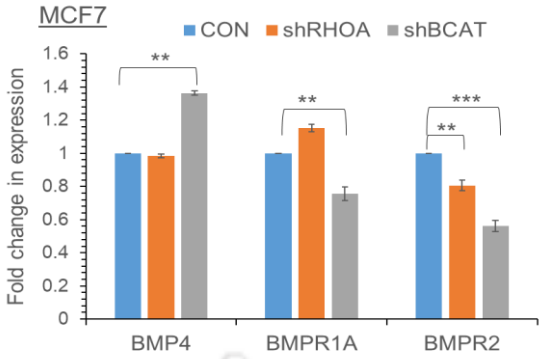

B

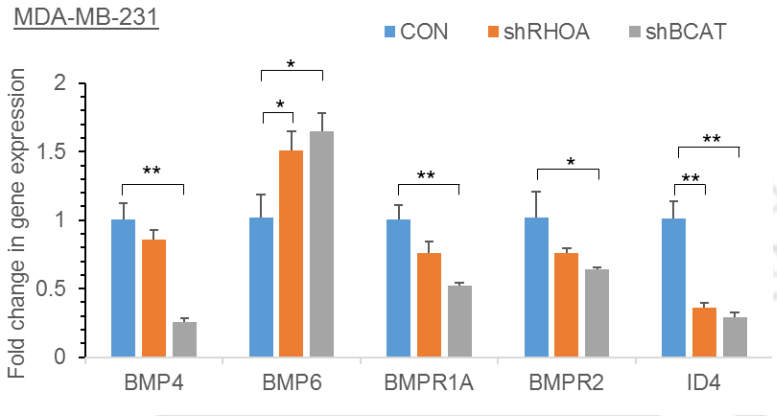

Figure 7.5: Effect of silencing on downstream targets of BMP signalling. *Silenced MCF7 and MDA-MB-231 for RHOA, β-catenin, and scramble (control)were lysed and RNA was isolated. After synthesizing cDNA using reverse transcription, qPCR was conducted to assess various gene-level expressions. The fold change in expression level was calculated with the ΔΔCt method. The bar graph depicts the fold change in gene expression profiles of BMP4, BMPR1A and BMPR2 in MCF7 as represented in* ***A.*** *and BMP4, BMP6, BMPR1A, BMPR2 and ID4 in MDA-MB-231 as represented in* ***B.*** *Values are mean ± SE, n=3 independent samples, *p<0.05, **p<0.005.*

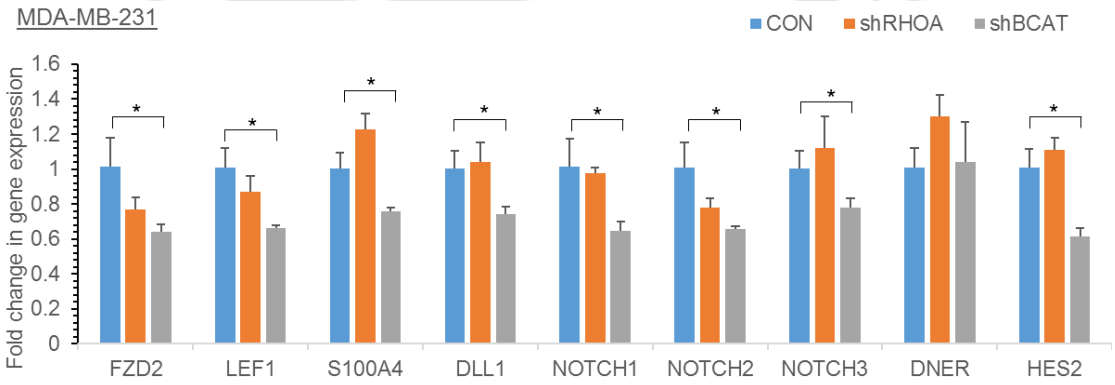

Figure 7.6: Effect of silencing on downstream targets of Wnt and Notch signalling*. MDA-MB-231 cells that have been silenced for RHOA, β-catenin, and scramble (control) were lysed and RNA was extracted. qPCR was used to examine various gene-level expressions after cDNA was synthesised using the reverse transcription. The fold change in expression level was calculated with the ΔΔCt method. The bar graph depicts the fold change in gene expression profiles of FZD2, LEF1, S100A4, DLL1, NOTCH1, NOTCH2, NOTCH3, DNER and HES2 in MDA-MB-231.Values are mean ± SE, n=3 independent samples, *p<0.05.*

7.3 Discussion

Cell proliferation, differentiation, and migration are just some cellular processes involving the BMP, RHOA, and Wnt networks. Activation of one route has been shown to affect the activity of others, a phenomenon known as "crosstalk". To establish the cross-talk between these three essential pathways, breast cancer cells (control cells, RHOA and β-catenin - silenced cells) were subjected to multiple analyses in the presence of BMP4, LDN, and Y27632.

The introduction of constitutively active RHOA, which reduces the expression of *SOX2* and *NANOG*, demonstrated that activated Rho decreased AKT phosphorylation and decreased human embryonic cell proliferation (Teramura et al., 2012). However, when RHOA and β-catenin were silenced in MCF7, our study found that the expression levels of *OCT4A*, *SOX2*, and *NANOG* elevated abruptly. Low proliferation in MCF7 was corroborated by reduced expression of *CCND1* and *ALDH1A3* during β-catenin silencing. (Masuko Katoh & Katoh, 2022) Katoh et al, reported directional control of Wnt/ β-catenin signalling to regulate *CCND1* expression, as well as context-dependent trajectories in the regulation of proliferation, immune survivability, plasticity, and migration (Fodde & Brabletz, 2007). The increased expression of *CDH2* after RHOA silencing suggests an increase in migration, but *in vitro*, we failed to see such an impact on the migration of MDA-MB-231. On the other hand, high expression of *CD24* at the mRNA level supported less growth of RHOA-silenced cells. The functional aspect of β-catenin silenced cells and mRNA levels of genes such as *CCND1*, *OCT4S1*, *SOX2*, and *ALDH1A3* showed opposite relationships. β-catenin silencing also downregulated the Notch signalling and Wnt signalling, which was confirmed by the downregulation of *NOTCH1*, *NOTCH2*, *HES2*, *DLL1* and *FZD2*, *LEF1* and *S100A4* expression respectively.

The increased β-catenin mRNA transcript level in MCF7 and the increased β-catenin protein level in MDA-MB-231 of RHOA-silenced cells indicate that RHOA can suppress β-catenin; however, this research did not identify whether it did so directly or through an intermediate molecule. In both cell types, RHOA silencing in the presence of BMP4 had the opposite effect on colony formation compared to the control, indicating that BMP4 regulates cellular function through RHOA signalling. One study found that the lack of Smad4, a downstream target of BMP signalling, enhanced the metastasis of colorectal

cancer cells via RHO-ROCK signalling, confirming the existence of cross-talk between BMP4 and RHOA (Voorneveld et al., 2014).

In contrast, BMP4 treatment of MCF7 cells decreased β-catenin expression, indicating that BMP4 can regulate Wnt/ β-catenin signalling. A similar pattern was reported by Zhang et al, (He et al., 2004), where BMP4 inhibited intestinal cell proliferation by inhibiting the Wnt/β-catenin pathway. Similarly, the development of arterial capillaries by bone morphogenetic protein requires a β-catenin-dependent transcription (Kashiwada et al., 2015). Multiple studies have demonstrated the parallel significance of BMP and Wnt signalling in osteoblast function and bone repair (Tang et al., 2010; Wu et al., 2012). However, this cannot be established from our investigation because the changes were not conclusively demonstrated.

Further reduction of *BMP4*, *BMPR1A*, *BMPR2*, and *ID4* expression in β-catenin silenced MDA-MB-231 indicates that Wnt signalling can influence BMP4 signalling in a variety of ways: by affecting the receptor before the signalling cascade begins, by inhibiting BMP4 binding to the receptor, and by downregulating the expression of *BMP4* and *ID4*. In contrast, RHOA silencing in MDA-MB-231 downregulated only *ID4*, indicating that it only influences the functional effect governed by ID4, not the entire BMP signalling pathway. Similarly, one of the findings in dental pulp repair demonstrates that both RHOA and Wnt/β-catenin can influence downstream targets of TGF-β signalling (Shao et al., 2011).

7.4 Conclusion

There exists a context-dependent cross-talk between Wnt and RHOA signalling (Figure 7.6). This study revealed, for example, that under shear stress conditions, Wnt regulates RHOA, but it remains uncertain whether this regulation is direct or mediated by transcription factors which get activated under stress conditions. In contrast, the inhibitory effect of RHOA in MCF7 and the regulatory effect in MDA-MB-231 discovered in this study further confirm the context-dependent cross-talk between RHOA and Wnt. Both Wnt and RHOA signalling can modulate BMP4 signalling in MDA-MB-231, but the cross-talk between Wnt and RHOA in the presence of BMP4 in MCF7 remains unclear. The regulatory or inhibitory effect of Wnt and RHOA is carried out exclusively at each stage of signalling; it can be receptor-oriented, affecting BMPR1A and BMPR2, or it can be downstream, affecting BMP4 and ID4. Thus, in MDA-MB-231, Wnt signalling controls

both BMP4 and RHO-ROCK signalling, whereas, in MCF7, Wnt regulates via RHO-ROCK signalling, but the context for BMP4 signalling is unclear. To thoroughly connect these three pathways and identify a common point at which the entire signalling cascade can be inhibited to control the progression of cancer, further research is required

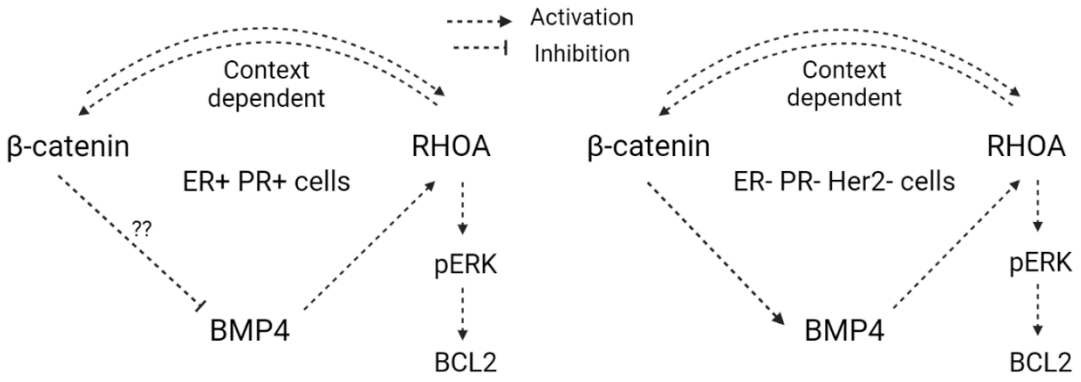

Figure 7.6: *Cross-talk between β-catenin, RHOA and BMP4 in breast cancer cell lines.*

Conclusion

Thus, the current study infers the context-dependent function of BMP4 signalling. Exogenous rhBMP4 protein increased the proliferation, migration, anoikis resistance, chemoresistance, and metastasis of triple-negative breast cancer cell lines. On the contrary, the inhibition of BMP4 signalling led to an increase in the ability of self-renewal and three-dimensional growth in breast cancer cell lines that are positive for ER/PR and Her2. Moreover, it additionally increased resistance to anoikis in Her2-positive breast cancer cells, and a temporary change in behaviour was observed in ER/PR breast cancer cells. Thus, it can be concluded that targeting BMP signalling may be an effective treatment for triple-negative breast cancer.

The non-canonical (RHO-ROCK signalling) and canonical (β-catenin) Wnt pathways were examined in the later section of the research. Alongside the silencing of RHOA and β-catenin, Y27632 was utilised to inhibit ROCK kinase. Migration was enhanced in both MCF7 and MDA-MB-231 cells when ROCK was inhibited. By silencing RHOA and β-catenin, proliferation, migration, anoikis resistance, and shear-stress tolerance were all diminished in MCF7 cells. In contrast, self-renewal was inhibited in MDA-MB-231 by suppressing RHOA and β-catenin, but 3D growth and migration remains unaffected. Anoikis resistance and shear stress tolerance were reduced when β-catenin was silenced, whereas suppressing RHOA increased these assays, suggesting that RHOA plays a compensatory role. The observed elevation in ERK levels in response to stress following the inhibition of RHOA and β-catenin in both MCF7 and MDA-MB-231 cell lines suggests that ERK signalling undertakes a compensatory role during stressful conditions. In relation to cross-talk, there appears to be a compensatory relationship between RHOA and β-catenin in a stage-specific manner in both cell lines. It has been observed that the Wnt/β-catenin signalling pathway modulates BMP4 pathway, whereas BMP4 regulates RHOA signalling via unknown transcription factors. Thus, there is a possibility that inhibiting Wnt signalling could serve as a potential treatment option for breast cancer.

A

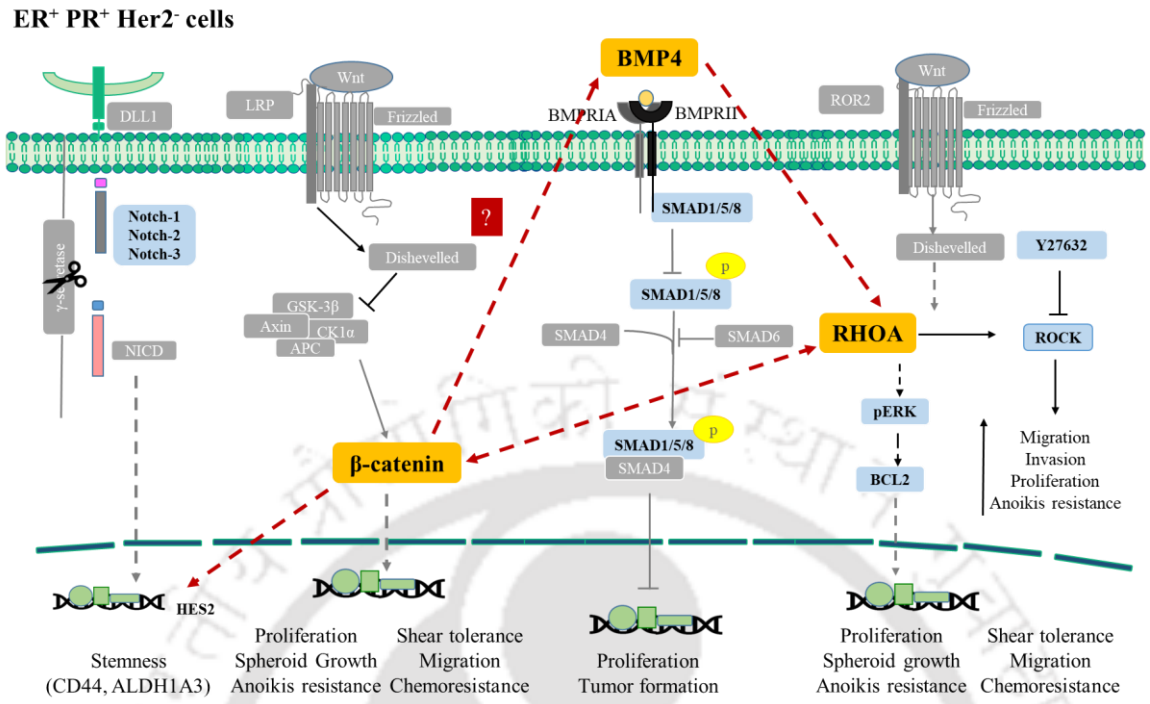

B

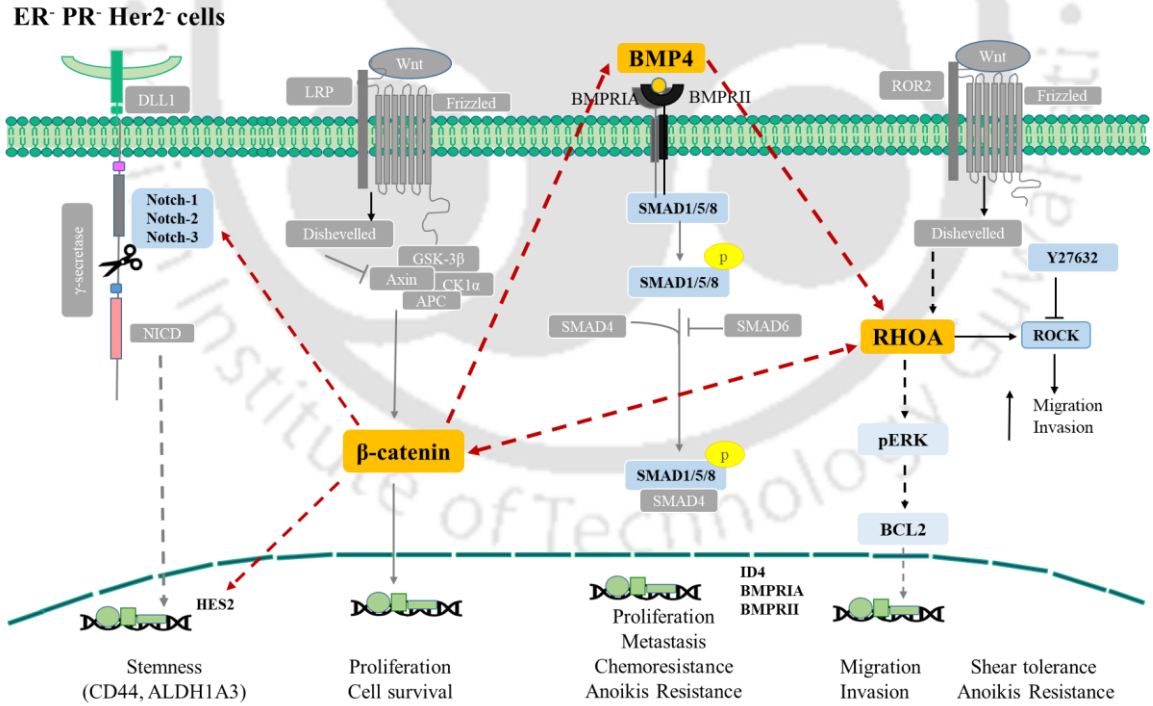

Figure 8.0: Cross-talk between signalling pathways. ***A.*** *represents the cross-talk between β-catenin, BMP4 and RHOA in ER+ PR+ cells (MCF7) and* ***B.*** *represents the cross-talk between Notch, BMP4, β-catenin, and RHOA signalling in ER- PR- Her2- cells (MDA-MB-231).*

Future Prospects

Possibilities for the future of this study include determining the contextual function of BMP signalling in breast cancer cells as a result of the presence or absence of the cell-surface BMP receptor or the differential expression of the ER, PR, and Her2 hormone receptors. In addition, in-vivo studies are required to investigate the impact of gene silencing on the progression of malignancy. To thoroughly comprehend the intricate dynamics between RHOA and β-catenin, more research is required. The upregulation of pERK1/2 under shear stress conditions has been extensively investigated in endothelial cells and smooth muscle cells. However, the implications of the increase in pERK1/2 levels in relation to cancer remain unknown.

References

Aguilar, Byron J, Zhao, Yaxue, Zhou, Huchen, Huo, Shouquan, Chen, Yan-Hua, & Lu, Qun (2019). Inhibition of Cdc42–intersectin interaction by small molecule ZCL367 impedes cancer cell cycle progression, proliferation, migration, and tumor growth. *Cancer biology & therapy, 20*(6), 740-749.

Ahandoust, Sina, Li, Kexin, Sun, Xun, Li, Bai-Yan, Yokota, Hiroki, & Na, Sungsoo (2023). Intracellular and extracellular moesins differentially regulate Src activity and β-catenin translocation to the nucleus in breast cancer cells. *Biochemical and biophysical research communications, 639*, 62-69.

Ai, Minrong, Holmen, Sheri L, Van Hul, Wim, Williams, Bart O, & Warman, Matthew L (2005). Reduced affinity to and inhibition by DKK1 form a common mechanism by which high bone mass-associated missense mutations in LRP5 affect canonical Wnt signaling. *Molecular and cellular biology, 25*(12), 4946-4955.

Akbarzadeh, Maryam, Mihanfar, Ainaz, Akbarzadeh, Shabnam, Yousefi, Bahman, & Majidinia, Maryam. (2021). Crosstalk between miRNA and PI3K/AKT/mTOR signaling pathway in cancer. *Life Sciences 285*, 119984.

Akoumianakis, Ioannis, Polkinghorne, Murray, & Antoniades, Charalambos (2022). Non-canonical WNT signalling in cardiovascular disease: mechanisms and therapeutic implications. *Nature Reviews Cardiology, 19*(12), 783-797.

Alarmo, Emma-Leena, Kuukasjärvi, Tuula, Karhu, Ritva, & Kallioniemi, Anne (2007). A comprehensive expression survey of bone morphogenetic proteins in breast cancer highlights the importance of BMP4 and BMP7. *Breast cancer research and treatment, 103*(2), 239-246.

Ali, Belal M, El Abhar, Hanan, Mohamed, Ghada, Sharaky, Marwa, Shouman, Samia A, & Kamel, Marwa. (2023). Enzalutamide and EPI-001 in T47D: Blocking Androgen receptor/Androgen receptor variant7 modulates NF-κB/c-Myc axis, cyclins A, E, & C, epithelial to mesenchymal transition markers, angiogenesis, and metastasis. *PeerJ*.

Amano, Mutsuki, Ito, Masaaki, Kimura, Kazushi, Fukata, Yuko, Chihara, Kazuyasu, Nakano, Takeshi,Kaibuchi, Kozo (1996). Phosphorylation and activation of myosin by Rho-associated kinase (Rho-kinase). *The Journal of biological chemistry, 271*(34), 20246-20249.

Ampuja, M, Alarmo, EL, Owens, P, Havunen, R, Gorska, AE, Moses, HL, & Kallioniemi, A (2016a). The impact of bone morphogenetic protein 4 (BMP4) on breast cancer metastasis in a mouse xenograft model. *Cancer letters, 375*(2), 238-244.

Anastas, Jamie N, & Moon, Randall T (2013). WNT signalling pathways as therapeutic targets in cancer. *Nature Reviews Cancer 13*(1), 11-26.

Ashikari, Roy, Park, Keun, Huvos, Andrew G, & Urban, Jerome A. (1970). Paget's disease of the breast. *Breast cancer research and treatment, 26*(3), 680-685.

Aspenström, Pontus (2022). The role of fast-cycling atypical RHO GTPases in Cancer. *Cancers, 14*(8), 1961.

Augeri, Dave J, Langenfeld, Elaine, Castle, Monica, Gilleran, John A, & Langenfeld, John (2016). Inhibition of BMP and of TGFβ receptors downregulates expression of XIAP and TAK1 leading to lung cancer cell death. *Molecular cancer, 15*, 1-16.

Bach, Duc-Hiep, Park, Hyen Joo, & Lee, Sang Kook. (2018). The Dual Role of Bone Morphogenetic Proteins in Cancer. *Molecular Therapy - Oncolytics, 8*, 1-13. doi:10.1016/j.omto.2017.10.002

Bach, Duc-Hiep, Park, Hyen Joo, & Lee, Sang Kook (2018). The dual role of bone morphogenetic proteins in cancer. *Molecular therapy oncolytics, 8*, 1-13.

Bagnell, Anna M, Sumner, Charlotte J, & McCray, Brett A (2022). TRPV4: A trigger of pathological RhoA activation in neurological disease. *BioEssay: news and reviews in molecular, cellular and developmental biology, 44*(6), 2100288.

Barbieri, Isaia, & Kouzarides, Tony (2020). Role of RNA modifications in cancer. *Nature Reviews Cancer 20*(6), 303-322.

Beck, Tim N, Korobeynikov, Vladislav A, Kudinov, Alexander E, Georgopoulos, Rachel, Solanki, Nehal R, Andrews-Hoke, Magda, Nicolas, Emmanuelle (2016). Anti-Müllerian hormone signaling regulates epithelial plasticity and chemoresistance in lung cancer. *Cell reports, 16*(3), 657-671.

Benson, John R (2003). The TNM staging system and breast cancer. *Oncology, 4*(1), 56-60.

Binello, Emanuela, & Germano, Isabelle M (2011). Targeting glioma stem cells: a novel framework for brain tumors. *Cancer science, 102*(11), 1958-1966.

Bishop, AL, & Ann, C (2000). Rho GTPases their effector proteins. *The Biochemical journal, 348*, 241-255.

Bist, Pradeep, Phua, Qian Hui, Shu, Shinla, Yi, Yuan, Anbalagan, Durkeshwari, Lee, Lay Hoon, Lim, Lina HK (2015). Annexin-A1 controls an ERK-RhoA–NFκB activation loop in breast cancer cells. *Biochemical and biophysical research communications, 461*(1), 47-53.

Bleckmann, Annalen, Conradi, Lena-Christin, Menck, Kerstin, Schmick, Nadine Annette, Schubert, Antonia, Rietkötter, Eva, Liersch, Torsten (2016). β-catenin-independent WNT signaling and Ki67 in contrast to the estrogen receptor status are prognostic and associated with poor prognosis in breast cancer liver metastases. *Clinical Experimental Metastasis 33*(4), 309-323.

Boix-Montesinos, Paz, Soriano-Teruel, Paula M, Armiñán, Ana, Orzáez, Mar, & Vicent, María J (2021). The past, present, and future of breast cancer models for nanomedicine development. *Advanced drug delivery reviews, 173*, 306-330.

Bolado-Carrancio, Alfonso, Rukhlenko, Oleksii S, Nikonova, Elena, Tsyganov, Mikhail A, Wheeler, Anne, Garcia-Munoz, Amaya, Kholodenko, Boris N. (2020). Periodic propagating waves coordinate RhoGTPase network dynamics at the leading and trailing edges during cell migration. *eLife, 9*, e58165.

Bourguignon, Lilly YW, Zhu, Hongbo, Shao, Lijun, & Chen, Yue Wei (2000). Ankyrin–Tiam1 interaction promotes Rac1 signaling and metastatic breast tumor cell invasion and migration. *The Journal of cell biology, 150*(1), 177-192.

Boustan, Arad, Jahangiri, Rosa, Ghalehno, Asefeh Dahmardeh, Khorsandi, Mahdieh, Mosaffa, Fatemeh, & Jamialahmadi, Khadijeh (2023). Expression analysis elucidates the roles of Nicastrin, Notch4, and Hes1 in prognosis and endocrine-therapy resistance in ER-positive breast cancer patients. *Research in pharmaceutical sciences, 18*(1), 78-88.

Boyce, BF, Yoneda, T, & Guise, TA. (1999). Factors regulating the growth of metastatic cancer in bone. *Endocrine-related cancer, 6*(3), 333-347.

Boyle, Sarah T, Kular, Jasreen, Nobis, Max, Ruszkiewicz, Andrew, Timpson, Paul, & Samuel, Michael S (2020). Acute compressive stress activates RHO/ROCK-mediated cellular processes. *Small GTPases, 11*(5), 354-370.

Brazil, Derek P, Church, Rachel H, Surae, Satnam, Godson, Catherine, & Martin, Finian (2015). BMP signalling: agony and antagony in the family. *Trends in cell biology, 25*(5), 249-264.

Brubaker, KD, Corey, E, Brown, LG, & Vessella, RL (2004). Bone morphogenetic protein signaling in prostate cancer cell lines. *Journal of cellular biochemistry, 91*(1), 151-160.

Buechel, David, Sugiyama, Nami, Rubinstein, Natalia, Saxena, Meera, Kalathur, Ravi KR, Lüönd, Fabiana, Cantù, Claudio (2021). Parsing β-catenin's cell adhesion and Wnt signaling functions in malignant mammary tumor progression. *Proceedings of the National Academy of Sciences 118*(34), e2020227118.

Burstein, Harold J, Polyak, Kornelia, Wong, Julia S, Lester, Susan C, & Kaelin, Carolyn M (2004). Ductal carcinoma in situ of the breast. *New England Journal of Medicine 350*(14), 1430-1441.

Buyuk, Busra, Jin, Sha, & Ye, Kaiming (2022). Epithelial-to-mesenchymal transition signaling pathways responsible for breast cancer metastasis. *Cellular and molecular bioengineering, 15*(1), 1-13.

Canel, Marta, Serrels, Alan, Frame, Margaret C, & Brunton, Valerie G (2013). E-cadherin–integrin crosstalk in cancer invasion and metastasis. *Journal of Cell Science 126*(2), 393-401.

Cao, Yuan, Slaney, Clare Y, Bidwell, Bradley N, Parker, Belinda S, Johnstone, Cameron N, Rautela, Jai, Anderson, Robin L (2014). BMP4 inhibits breast cancer metastasis by blocking myeloid-derived suppressor cell activity. *Cancer research*, *74*(18), 5091-5102.

Caswell-Jin, J. L., Plevritis, S. K., Tian, L., Cadham, C. J., Xu, C., Stout, N. K., Kurian, A. W. (2018). Change in Survival in Metastatic Breast Cancer with Treatment Advances: Meta-Analysis and Systematic Review. *JNCI Cancer Spectr*, *2*(4), pky062.

Cecchi, Fabiola, Rabe, Daniel C, & Bottaro, Donald P (2010). Targeting the HGF/Met signalling pathway in cancer. *European Journal of Cancer 46*(7), 1260-1270.

Chang, Tzu-Ching, Chen, Yen-Chung, Yang, Ming-Hua, Chen, Chien-Hung, Hsing, En-Wei, Ko, Bor-Sheng, Wu, Kenneth K (2010). Rho kinases regulate the renewal and neural differentiation of embryonic stem cells in a cell plating density–dependent manner. *PloS one*, *5*(2), e9187.

Charras, Guillaume T, Hu, Chi-Kuo, Coughlin, Margaret, & Mitchison, Timothy J (2006). Reassembly of contractile actin cortex in cell blebs. *The Journal of cell biology*, *175*(3), 477-490.

Chatakun, P, Núñez-Toldrà, R, Díaz López, EJ, Gil-Recio, C, Martínez-Sarrà, E, Hernández-Alfaro, Atari, M (2014). The effect of five proteins on stem cells used for osteoblast differentiation and proliferation: a current review of the literature. *Cellular Molecular Life Sciences 71*, 113-142.

Chen, Hui, He, Bin, & Ke, Feng (2022). Ceramide Synthase 6 Mediates Triple-Negative Breast Cancer Response to Chemotherapy Through RhoA-and EGFR-Mediated Signaling Pathways. *Journal of breast cancer*, *25*(6), 500-512.

Chen, Miaojuan, Pan, Yue, Liu, Hanbo, Ning, Fen, Lu, Qinsheng, Duan, Yaoyun, Zhang, Min. (2022). Ezrin accelerates breast cancer liver metastasis through promoting furin-like convertase-mediated cleavage of Notch1. *Cellular Oncology*, *46*(3), 571-587.

Chen, Weiling, Zhang, Yongqu, Li, Ronghui, Huang, Wenhe, Wei, Xiaolong, Zeng, De, Zhang, Lixin (2022). Notch3 transactivates glycogen synthase kinase-3-beta and inhibits epithelial-to-mesenchymal transition in breast cancer cells. *Cells*, *11*(18), 2872.

Chen, Xiaoliang, Yin, Lili, Xu, Hui, Rong, Jie, Feng, Miao, Jiang, Di, & Bai, Yunfeng (2023). Knockdown of RhoA Expression Reverts Enzalutamide Resistance via the p38 MAPK Pathway in Castration-resistant Prostate Cancer. *Recent patents on anti-cancer drug discovery*, *18*(1), 92-99.

Chen, Yan, Huang, Chong, Duan, Zhi-Bin, Chen, Yan-Xia, & Xu, Cheng-Yun (2023). LncRNA NEAT1 accelerates renal fibrosis progression via targeting miR-31 and modulating RhoA/ROCK signal pathway. *American Journal of Physiology; Cell Physiology*, *324*(2), C292-C306.

Chen, Zhuo, & Xu, XinHua (2016). Roles of nucleolin: Focus on cancer and anti-cancer therapy. *Saudi medical journal*, *37*(12), 1312-1318.

Chen, Zhuoyue, Zhang, Zhen, Feng, Juantao, Guo, Yayuan, Yu, Yuan, Cui, Jihong, Shang, Lijun (2018). Influence of mussel-derived bioactive BMP-2-decorated PLA on MSC behavior in vitro and verification with osteogenicity at ectopic sites in vivo. *ACS applied materials & interfaces*, *10*(14), 11961-11971.

Cheng, Shaoqiang, Huang, Yuanxi, Lou, Chun, He, Yanxia, Zhang, Yue, & Zhang, Qingyuan (2019). FSTL1 enhances chemoresistance and maintains stemness in breast cancer cells via integrin β3/Wnt signaling under miR-137 regulation. *Cancer biology & therapy*, *20*(3), 328-337.

Cheson, Bruce D (2004). What is new in lymphoma? *Cancer Journal for Clinicians*, *54*(5), 260-272.

Chhikara, Bhupender S, & Parang, Keykavous (2023). Global Cancer Statistics 2022: the trends projection analysis. *Chemical Biology Letters 10*(1), 451-451.

Chin, Koei, DeVries, Sandy, Fridlyand, Jane, Spellman, Paul T, Roydasgupta, Ritu, Kuo, Wen-Lin, Ryder, Tom (2006). Genomic and transcriptional aberrations linked to breast cancer pathophysiologies. *Cancer cell*, *10*(6), 529-541.

Chmielowiec, Jolanta, Szlachcic, Wojciech J, Yang, Diane, Scavuzzo, Marissa A, Wamble, Katrina, Sarrion-Perdigones, Alejandro, Borowiak, Malgorzata (2022). Human pancreatic

microenvironment promotes β-cell differentiation via non-canonical WNT5A/JNK and BMP signaling. *Nature communications, 13*(1), 1-18.

Christian, Jan (2021). A tale of two receptors: Bmp heterodimers recruit two type I receptors but use the kinase activity of only one. *Proceedings of the National Academy of Sciences of, 118*(19), e2104745118.

Chu, Jenny E, & Allan, Alison L (2012). The role of cancer stem cells in the organ tropism of breast cancer metastasis: a mechanistic balance between the "seed" and the "soil"? *International journal of breast cancer, 2012*.

Chung, Mei-I, Bujnis, Melissa, Barkauskas, Christina E, Kobayashi, Yoshihiko, & Hogan, Brigid LM (2018). Niche-mediated BMP/SMAD signaling regulates lung alveolar stem cell proliferation and differentiation. *Development, 145*(9), dev163014.

Colditz, Graham A (1998). Relationship between estrogen levels, use of hormone replacement therapy, and breast cancer. *Journal of the National Cancer Institute, 90*(11), 814-823.

Comşa, Şerban, Cimpean, Anca Maria, & Raica, Marius (2015). The story of MCF-7 breast cancer cell line: 40 years of experience in research. *Anticancer research, 35*(6), 3147-3154.

Costa, Eduardo, Ferreira-Gonçalves, Tânia, Chasqueira, Gonçalo, Cabrita, António S, Figueiredo, Isabel V, & Reis, Catarina Pinto. (2018). Experimental models as refined translational tools for breast cancer research. *Multidisciplinary Digital Publishing Institute, 88*(3), 32.

Coutte, Laetitia, Dreyer, Chantal, Sablin, Marie-Paule, Faivre, Sandrine, & Raymond, Eric (2012). PI3K-AKT-mTOR pathway and cancer. *Bulletin du cancer, 99*(2), 173-180.

Crosas-Molist, Eva, Samain, Remi, Kohlhammer, Leonie, Orgaz, Jose L, George, Samantha L, Maiques, Oscar, Sanz-Moreno, Victoria (2022). Rho GTPase signaling in cancer progression and dissemination. *Physiological reviews, 102*(1), 455-510.

Cserni, Gábor, Chmielik, Ewa, Cserni, Bálint, & Tot, Tibor (2018). The new TNM-based staging of breast cancer. *An International Journal of Pathology, 472*(5), 697-703.

Cyr-Depauw, Chanèle, Northey, Jason J, Tabariès, Sébastien, Annis, Matthew G, Dong, Zhifeng, Cory, Sean, Siegel, Peter M (2016). Chordin-like 1 suppresses bone morphogenetic protein 4-induced breast cancer cell migration and invasion. *Molecular Cellular Biology 36*(10), 1509-1525.

Darbre, PD (2001). Underarm cosmetics are a cause of breast cancer. *European Journal of Cancer Prevention 10*(5), 389-393.

De Boeck, Miriam, Cui, Chao, Mulder, Aat A, Jost, Carolina R, Ikeno, Souichi, & Ten Dijke, Peter (2016a). Smad6 determines BMP-regulated invasive behaviour of breast cancer cells in a zebrafish xenograft model. *Scientific reports, 6*(1), 24968.

De Boeck, Miriam, Cui, Chao, Mulder, Aat A, Jost, Carolina R, Ikeno, Souichi, & Ten Dijke, Peter (2016b). Smad6 determines BMP-regulated invasive behaviour of breast cancer cells in a zebrafish xenograft model. *Scientific reports, 6*(1), 1-10.

De Boer, Jan, Wang, Hong Jun, & Van Blitterswijk, Clemens (2004). Effects of Wnt signaling on proliferation and differentiation of human mesenchymal stem cells. *Tissue engineering, 10*(3-4), 393-401.

De Marchi, Tommaso, Foekens, John A., Umar, Arzu, & Martens, John W. M. (2016). Endocrine therapy resistance in estrogen receptor (ER)-positive breast cancer. *Drug Discovery Today, 21*(7), 1181-1188.

de Vinuesa, Amaya Garcia, Abdelilah-Seyfried, Salim, Knaus, Petra, Zwijsen, An, & Bailly, Sabine (2016). BMP signaling in vascular biology and dysfunction. *Cytokine & growth factor reviews, 27*, 65-79.

Deacon, Sean W, Beeser, Alexander, Fukui, Jami A, Rennefahrt, Ulrike EE, Myers, Cynthia, Chernoff, Jonathan, & Peterson, Jeffrey R (2008). An isoform-selective, small-molecule inhibitor targets the autoregulatory mechanism of p21-activated kinase. *Chemistry & biology, 15*(4), 322-331.

Dean-Colomb, Windy, & Esteva, Francisco J (2008). Her2-positive breast cancer: herceptin and beyond. *European Journal of Cancer, 44*(18), 2806-2812.

Deeb, Kristin K, Trump, Donald L, & Johnson, Candace S (2007). Vitamin D signalling pathways in cancer: potential for anticancer therapeutics. *Nature Reviews Cancer 7*(9), 684-700.

Del Pulgar, Teresa Gómez, Benitah, Salvador A, Valerón, Pilar F, Espina, Carolina, & Lacal, Juan Carlos (2005). Rho GTPase expression in tumourigenesis: evidence for a significant link. *BioEssays : news and reviews in molecular, cellular and developmental biology, 27*(6), 602-613.

Derks, Sarah, Postma, Cindy, Moerkerk, Peter, Van Den Bosch, Sandra M, Carvalho, Beatriz, Hermsen, Mario AJA, Bruïne, Adriaan P de (2006). Promoter methylation precedes chromosomal alterations in colorectal cancer development. *Analytical Cellular Pathology 28*(5-6), 247-257.

Devetzi, Marina, Kosmidou, Vivian, Vlassi, Margarita, Perysinakis, Iraklis, Aggeli, Chrysanthi, Choreftaki, Theodosia, Pintzas, Alexander (2016). Death receptor 5 (DR5) and a 5-gene apoptotic biomarker panel with significant differential diagnostic potential in colorectal cancer. *Scientific reports, 6*(1), 1-14.

Ding, Ziteng, Xu, Xudang, Li, Tiannv, Wang, Jia, Sun, Jin, & Tang, Lijun (2021). ZR-75-1 breast cancer models to study the utility of 18F-FES by PET imaging. *Translational cancer research, 10*(3), 1430.

Dorai, Haimanti, Vukicevic, Slobodan, & Sampath, T Kuber (2000). Bone morphogenetic protein-7 (osteogenic protein-1) inhibits smooth muscle cell proliferation and stimulates the expression of markers that are characteristic of SMC phenotype in vitro. *Journal of cellular physiology, 184*(1), 37-45.

Doublier, Sophie, Riganti, Chiara, Voena, Claudia, Costamagna, Costanzo, Aldieri, Elisabetta, Pescarmona, Gianpiero, Bosia, Amalia. (2008). RhoA silencing reverts the resistance to doxorubicin in human colon cancer cells. *Molecular Cancer Research 6*(10), 1607-1620.

Drabsch, Yvette, & Ten Dijke, Peter (2011). TGF-β signaling in breast cancer cell invasion and bone metastasis. *Journal of mammary gland biology and neoplasia, 16*(2), 97-108.

Duan, Ju-Tao, Wang, Xi-Mo, Zhang, Shu-Quan, & Zhao, Guan-Jie (2015). Effect of RhoA gene silencing on proliferation and migration of gastric MGC-803 cells. *International Journal of Clinical Experimental Medicine 8*(8), 14410-14415.

Duchartre, Y., Kim, Y. M., & Kahn, M. (2016). The Wnt signaling pathway in cancer. *Crit Rev Oncol Hematol, 99*, 141-149.

Dulong, C, Fang, YJ, Gest, C, Zhou, MH, Patte-Mensah, C, Mensah-Nyagan, AG, Cazin, L (2014). The small GTPase RhoA regulates the expression and function of the sodium channel Nav1. 5 in breast cancer cells. *International journal of oncology, 44*(2), 539-547.

Eckenstaler, Robert, Hauke, Michael, & Benndorf, Ralf A (2022). A current overview of RhoA, RhoB, and RhoC functions in vascular biology and pathology. *Biochemical pharmacology*, 115321.

Eckhardt, Bedrich L, Cao, Yuan, Redfern, Andrew D, Chi, Lap Hing, Burrows, Allan D, Roslan, Suraya, Ueno, Naoto T (2020a). Activation of Canonical BMP4-SMAD7 Signaling Suppresses Breast Cancer MetastasisBMP4: A Viable Antimetastasis Therapy in Breast Cancer. *Cancer Research, 80*(6), 1304-1315.

Eckhardt, Bedrich L, Cao, Yuan, Redfern, Andrew D, Chi, Lap Hing, Burrows, Allan D, Roslan, Suraya, Ueno, Naoto (2020b). Activation of canonical BMP4-SMAD7 signaling suppresses breast cancer metastasis. *Cancer research, 80*(6), 1304-1315.

Edwards, Abigail, & Brennan, Keith. (2021). Notch Signalling in Breast Development and Cancer. *Frontiers in cell and developmental biology, 9*, 692173. doi:10.3389/fcell.2021.692173

Eldridge, Lynne (2022). Cancer cells vs. normal cells: how are they different. *Verywell Health*

Eliyatkın, Nuket, Yalçın, Evrim, Zengel, Baha, Aktaş, Safiye, & Vardar, Enver (2015). Molecular classification of breast carcinoma: from traditional, old-fashioned way to a new age, and a new way. *The journal of breast health, 11*(2), 59-66.

Ettelt, Volker, Belitsky, Alice, Lehnert, Michael, Loidl-Stahlhofen, Angelika, Epple, Matthias, & Veith, Michael (2018). Enhanced selective cellular proliferation by multi-biofunctionalization of medical implant surfaces with heterodimeric BMP-2/6, fibronectin, and FGF-2. *Journal of Biomedical Materials Research, 106*(11), 2910-2922.

Evelyn, Chris R, Ferng, Timothy, Rojas, Rafael J, Larsen, Martha J, Sondek, John, & Neubig, Richard R (2009). High-throughput screening for small-molecule inhibitors of LARG-

stimulated RhoA nucleotide binding via a novel fluorescence polarization assay. *Journal of biomolecular screening, 14*(2), 161-172.

Fan, Chuannan, Wang, Qian, van der Zon, Gerard, Ren, Jiang, Agaser, Cedrick, Slieker, Roderick C, Ten Dijke, Peter (2022). OVOL1 inhibits breast cancer cell invasion by enhancing the degradation of TGF-β type I receptor. *Signal transduction and targeted therapy, 7*(1), 1-18.

Feng, Yixiao, Spezia, Mia, Huang, Shifeng, Yuan, Chengfu, Zeng, Zongyue, Zhang, Linghuan, Ren, Guosheng. (2018). Breast cancer development and progression: Risk factors, cancer stem cells, signaling pathways, genomics, and molecular pathogenesis. *Genes & Diseases, 5*(2), 77-106.

Filić, Vedrana, & Weber, Igor (2023). Rho GTPases in Model Systems. *Cells, 12*(5), 779.

Fillmore, Christine M, & Kuperwasser, Charlotte (2008). Human breast cancer cell lines contain stem-like cells that self-renew, give rise to phenotypically diverse progeny and survive chemotherapy. *Breast Cancer Research, 10*(2), 1-13.

Fine, Noah, Dimitriou, Ioannis D, & Rottapel, Robert. (2020). Go with the flow: GEF-H1 mediated shear stress mechanotransduction in neutrophils. *Small GTPases, 11*(1), 23-31.

Flanagan, Fidelma L, Dehdashti, Farrokh, & Siegel, Barry A. (1998). *PET in breast cancer.* Paper presented at the Seminars in Nuclear Medicine.

Fodde, Riccardo, & Brabletz, Thomas (2007). Wnt/β-catenin signaling in cancer stemness and malignant behavior. *Current Opinion in Cell Biology 19*(2), 150-158.

Foote Jr, Frank W, & Stewart, Fred W (1941). Lobular carcinoma in situ: a rare form of mammary cancer. *The American Journal of Pathology 17*(4), 491-496.493.

Friedl, Peter, Sahai, Erik, Weiss, Stephen, & Yamada, Kenneth M (2012). New dimensions in cell migration. *Molecular cell biology, 13*(11), 743-747.

Friedrichs, Melanie, Wirsdöerfer, Florian, Flohé, Stefanie B, Schneider, Sabine, Wuelling, Manuela, & Vortkamp, Andrea (2011). BMP signaling balances proliferation and differentiation of muscle satellite cell descendants. *BMC cell biology, 12*(1), 1-17.

Fu, Aikun, Yao, Bingqing, Dong, Tingting, & Cai, Shang (2022). Emerging roles of intratumor microbiota in cancer metastasis. *Trends in Cell Biology 33*(7), 583-593.

Fu, Minyang, Hu, Yuan, Lan, Tianxia, Guan, Kun-Liang, Luo, Ting, & Luo, Min (2022). The Hippo signalling pathway and its implications in human health and diseases. *Signal transduction and targeted therapy, 7*(1), 1-20.

Fukuda, Tomohiko, Fukuda, Risa, Tanabe, Ryo, Koinuma, Daizo, Koyama, Hiroo, Hashizume, Yoshinobu, Heldin, Carl-Henrik (2020). BMP signaling is a therapeutic target in ovarian cancer. *Cell Death Discovery, 6*(1), 139.

Gadalla, Salah-Eldin, Alexandraki, Anna, Lindström, Mikael S, Nistér, Monica, & Ericsson, Christer (2011). Uncoupling of the ERα regulated morphological phenotype from the cancer stem cell phenotype in human breast cancer cell lines. *Biochemical Biophysical Research Communications 405*(4), 581-587.

Gaggioli, Cedric, Hooper, Steven, Hidalgo-Carcedo, Cristina, Grosse, Robert, Marshall, John F, Harrington, Kevin, & Sahai, Erik (2007). Fibroblast-led collective invasion of carcinoma cells with differing roles for RhoGTPases in leading and following cells. *Nature cell biology, 9*(12), 1392-1400.

Gao, Xinghua, Zhang, Xu, Xu, Hui, Zhou, Bingpu, Wen, Weijia, & Qin, Jianhua (2014). Regulation of cell migration and osteogenic differentiation in mesenchymal stem cells under extremely low fluidic shear stress. *Biomicrofluidics, 8*(5), 052008.

Gao, Yuan, Dickerson, J Bradley, Guo, Fukun, Zheng, Jie, & Zheng, Yi (2004). Rational design and characterization of a Rac GTPase-specific small molecule inhibitor. *Proceedings of the National Academy of Sciences, 101*(20), 7618-7623.

García-Jiménez, Custodia, & Goding, Colin R (2019). Starvation and pseudo-starvation as drivers of cancer metastasis through translation reprogramming. *Cell metabolism, 29*(2), 254-267.

Garg, Priyanka, Mazur, Matthew M, Buck, Amy C, Wandtke, Meghan E, Liu, Jiayong, & Ebraheim, Nabil A (2017). Prospective review of mesenchymal stem cells differentiation into osteoblasts. *Orthopaedic surgery, 9*(1), 13-19.

Gaujoux, Sebastien, Hantel, Constanze, Launay, Pierre, Bonnet, Stéphane, Perlemoine, Karine, Lefevre, Lucile, Bertherat, Jerome (2013). Silencing mutated β-catenin inhibits cell proliferation and stimulates apoptosis in the adrenocortical cancer cell line H295R. *PloS one, 8*(2), e55743.

Georgouli, Mirella, Herraiz, Cecilia, Crosas-Molist, Eva, Fanshawe, Bruce, Maiques, Oscar, Perdrix, Anna, Cantelli, Gaia (2019). Regional activation of myosin II in cancer cells drives tumor progression via a secretory cross-talk with the immune microenvironment. *Cell, 176*(4), 757-774. e723.

Ghahhari, Nastaran Mohammadi, & Babashah, Sadegh (2015). Interplay between microRNAs and WNT/β-catenin signalling pathway regulates epithelial–mesenchymal transition in cancer. *European Journal of Cancer 51*(12), 1638-1649.

Ghasemi, Faezeh, Sarabi, Parisa Zia, Athari, Seyyed Shamsadin, & Esmaeilzadeh, Abdolreza (2019). Therapeutics strategies against cancer stem cell in breast cancer. *The International Journal of Biochemistry & Cell Biology, 109*, 76-81.

Ghosh, Noyel, Hossain, Uday, Mandal, Ankita, & Sil, Parames C (2019). The Wnt signaling pathway: a potential therapeutic target against cancer. *Annals of the New York Academy of Sciences, 1443*(1), 54-74.

Gipson, Gregory R, Goebel, Erich J, Hart, Kaitlin N, Kappes, Emily C, Kattamuri, Chandramohan, McCoy, Jason C, & Thompson, Thomas B (2020). Structural perspective of BMP ligands and signaling. *Bone, 140*, 115549.

Giuli, MV, Giuliani, E, Screpanti, I, Bellavia, D, & Checquolo, S (2019). Notch signaling activation as a hallmark for triple-negative breast cancer subtype. *Journal of oncology, 2019*, 8707053.

Giusti, Veronica, & Scotlandi, Katia (2021). CCN proteins in the musculoskeletal system: current understanding and challenges in physiology and pathology. *Journal of Cell Communication and Signaling 15*(4), 545-566.

Gligorijevic, Bojana, Wyckoff, Jeffrey, Yamaguchi, Hideki, Wang, Yarong, Roussos, Evanthia T, & Condeelis, John (2012). N-WASP-mediated invadopodium formation is involved in intravasation and lung metastasis of mammary tumors. *Journal of cell science, 125*(3), 724-734.

Gomez-Puerto, Maria Catalina, Iyengar, Prasanna Vasudevan, García de Vinuesa, Amaya, Ten Dijke, Peter, & Sanchez-Duffhues, Gonzalo (2019). Bone morphogenetic protein receptor signal transduction in human disease. *The Journal of pathology, 247*(1), 9-20.

Gong, Hua, Chen, Kang, Zhou, Lan, Jin, Yongchao, & Chen, Weihua (2023). Deleted in liver cancer 1 suppresses the growth of prostate cancer cells through inhibiting Rho-associated protein kinase pathway. *Asian journal of urology, 10*(1), 50-57.

Gong, Hua, Chen, Xingyi, Jin, Yongcao, Lu, Jiasun, Cai, Yuanjue, Wei, Ouyang, Wang, Yuemin (2019). Expression of ARHGAP10 correlates with prognosis of prostate cancer. *journal of clinical and experimental pathology, 12*(10), 3839.

Gordon, Kelly J, Kirkbride, Kellye C, How, Tam, & Blobe, Gerard C (2009). Bone morphogenetic proteins induce pancreatic cancer cell invasiveness through a Smad1-dependent mechanism that involves matrix metalloproteinase-2. *Carcinogenesis, 30*(2), 238-248.

Gul, Summer, Murad, Sheeba, Ehsan, Naureen, Bloodsworth, Peter, Sultan, Aneesa, & Faheem, M (2015). Transcriptional up-regulation of BMP-4 and BMPR-II genes in the peripheral blood of breast cancer patients: a pilot study. *Cancer Biomarkers, 15*(5), 551-557.

Gunasinghe, N. P., Wells, A., Thompson, E. W., & Hugo, H. J. (2012). Mesenchymal-epithelial transition (MET) as a mechanism for metastatic colonisation in breast cancer. *Cancer Metastasis Rev, 31*(3-4), 469-478. doi:10.1007/s10555-012-9377-5

Guo, Dan, Huang, Jiayi, & Gong, Jianping (2012). Bone morphogenetic protein 4 (BMP4) is required for migration and invasion of breast cancer. *Molecular Cellular Biochemistry 363*(1-2), 179-190.

Guo, Xing, & Wang, Xiao-Fan (2009). Signaling cross-talk between TGF-β/BMP and other pathways. *Cell Research 19*(1), 71-88.

Guyot, Boris, & Maguer-Satta, Veronique. (2019). A Potential New Mechanism for Bisphenol Molecules to Initiate Breast Cancer through Alteration of Bone Morphogenetic Protein

Signaling in Stem Cells and Their Microenvironment. In *Breast Cancer Biology*: IntechOpen.

Hanifa, Mohd, Singh, Mohini, Randhawa, Puneet, Jaggi, Amteshwar Singh, & Bali, Anjana (2023). A focus on Rho/ROCK signaling pathway: An emerging therapeutic target in depression. *European Journal of Pharmacology, 946*, 175648.

Haseeb, Muhammad, Pirzada, Rameez Hassan, Ain, Qurat Ul, & Choi, Sangdun (2019). Wnt signaling in the regulation of immune cell and cancer therapeutics. *Cells, 8*(11), 1380.

Hashemi, Seyed Hesam Bani, Karimi, Samieh, & Mahboobi, Hamidreza (2014). Lifestyle changes for prevention of breast cancer. *Electronic physician, 6*(3), 894-905.

He, Xi C, Zhang, Jiwang, Tong, Wei-Gang, Tawfik, Ossama, Ross, Jason, Scoville, David H, Wiedemann, Leanne M (2004). BMP signaling inhibits intestinal stem cell self-renewal through suppression of Wnt–β-catenin signaling. *Nature genetics, 36*(10), 1117-1121.

Heidenreich, Barbara, Rachakonda, P Sivaramakrishna, Hemminki, Kari, & Kumar, Rajiv (2014). TERT promoter mutations in cancer development. *Current Opinion in Genetics Development 24*, 30-37.

Hill, Billy Samuel, Sarnella, Annachiara, D'Avino, Giuliana, & Zannetti, Antonella. (2020). *Recruitment of stromal cells into tumour microenvironment promote the metastatic spread of breast cancer*. Paper presented at the Seminars in Cancer Biology.

Hodge, Richard G, & Ridley, Anne J (2016). Regulating Rho GTPases and their regulators. *Nature Reviews; Molecular Cell Biology, 17*(8), 496-510.

Hoe, Susan Ling Ling, Tan, Lu Ping, Abdul Aziz, Norazlin, Liew, Kitson, Teow, Sin-Yeang, Abdul Razak, Fazlyn Reeny, Mohd Kornain, Noor Kaslina. (2017). CD24, CD44 and EpCAM enrich for tumour-initiating cells in a newly established patient-derived xenograft of nasopharyngeal carcinoma. *Scientific reports, 7*(1), 1-13.

Hollestelle, Antoinette, Peeters, Justine K, Smid, Marcel, Timmermans, Mieke, Verhoog, Leon C, Westenend, Pieter J, Wiemer, Erik AC (2013). Loss of E-cadherin is not a necessity for epithelial to mesenchymal transition in human breast cancer. *Breast Cancer Research Treatment 138*(1), 47-57.

Holliday, Deborah L, & Speirs, Valerie (2011). Choosing the right cell line for breast cancer research. *Breast Cancer Research 13*(4), 1-7.

Horimoto, Yoshiya, Arakawa, Atsushi, Sasahara, Noriko, Tanabe, Masahiko, Sai, Sei, Himuro, Takanori, & Saito, Mitsue. (2016). Combination of cancer stem cell markers CD44 and CD24 is superior to ALDH1 as a prognostic indicator in breast cancer patients with distant metastases. *PloS one, 11*(10), e0165253.

Howe, Louise R, & Brown, Anthony MC (2004). Wnt signaling and breast cancer. *Cancer biology & therapy, 3*(1), 36-41.

Hu, Fen, Zhang, Yunfeng, Li, Mi, Zhao, Lina, Chen, Jing, Yang, Shuang, & Zhang, Xiujun. (2016). BMP-6 inhibits the metastasis of MDA-MB-231 breast cancer cells by regulating MMP-1 expression. *Oncology reports, 35*(3), 1823-1830.

Huang, Baolin, Yuan, Yuan, & Liu, Changsheng (2020). Biomaterial-guided immobilization and osteoactivity of bone morphogenetic protein-2. *Applied Materials Today, 19*, 100599.

Huang, Hui-Chuan, & Klein, Peter S (2004). Interactions between BMP and Wnt signaling pathways in mammalian cancers. *Cancer biology & therapy, 3*(7), 676-678.

Huang, Peide, Chen, Anan, He, Weiyi, Li, Zhen, Zhang, Guanglin, Liu, Zhong, Xiao, Gang (2017). BMP-2 induces EMT and breast cancer stemness through Rb and CD44. *Cell death discovery, 3*(1), 1-12.

Huang, Yongsheng, Liu, Sijia, Shan, Mengjie, Hagenaars, Sophie C, Mesker, Wilma E, Cohen, Danielle, Tollenaar, Rob AEM (2022). RNF12 is regulated by AKT phosphorylation and promotes TGF-β driven breast cancer metastasis. *Cell death & disease, 13*(1), 1-12.

Huelsken, Joerg, & Behrens, Juergen (2002). The Wnt signalling pathway. *Journal of cell science, 115*(21), 3977-3978.

Hulka, Barbara S, & Stark, Azadeh T. (1995). Breast cancer: cause and prevention. *The Lancet, 346*(8979), 883-887.

Humphries, Brock, Wang, Zhishan, Li, Yunfei, Jhan, Jing-Ru, Jiang, Yiguo, & Yang, Chengfeng. (2017). ARHGAP18 Downregulation by miR-200b Suppresses Metastasis of Triple-

Negative Breast Cancer by Enhancing Activation of RhoAARHGAP18 Downregulation Suppresses TNBC Metastasis. *Cancer research, 77*(15), 4051-4064.

Humphries, Brock, Wang, Zhishan, & Yang, Chengfeng (2020). Rho GTPases: big players in breast cancer initiation, metastasis and therapeutic responses. *Cells, 9*(10), 2167.

Hussain, Yaseen, Khan, Haroon, Alam, Waqas, Aschner, Michael, Alsharif, Khalaf F, & Saso, Luciano (2022). Flavonoids targeting the mTOR signaling cascades in cancer: A potential crosstalk in anti-breast cancer therapy. *Oxidative medicine and cellular longevity, 2022*, 4831833.

Hylton, Nola (2005). Magnetic resonance imaging of the breast: opportunities to improve breast cancer management. *Journal of Clinical Oncology 23*(8), 1678-1684.

Ibrahim, Sherif A, Yip, George W, Stock, Christian, Pan, Jun-Wei, Neubauer, Claudia, Poeter, Michaela, Schüle, Roland (2012). Targeting of syndecan-1 by microRNA miR-10b promotes breast cancer cell motility and invasiveness via a Rho-GTPase-and E-cadherin-dependent mechanism. *International Journal of Cancer, 131*(6), E884-E896.

Iqbal, Nida, & Iqbal, Naveed. (2014). Human Epidermal Growth Factor Receptor 2 (HER2) in Cancers: Overexpression and Therapeutic Implications. *Molecular Biology International, 2014*, 852748. doi:10.1155/2014/852748

Irshad, Shazia, Bansal, Mukesh, Guarnieri, Paolo, Davis, Hayley, Al Haj Zen, Ayman, Baran, Brygida, Bardella, Chiara (2017). Bone morphogenetic protein and Notch signalling crosstalk in poor-prognosis, mesenchymal-subtype colorectal cancer. *The Journal of pathology, 242*(2), 178-192.

Jaiyesimi, Ishmael A, Buzdar, Aman U, & Hortobagyi, Gabriel (1992). Inflammatory breast cancer: a review. *Journal of the American Society of Clinical Oncology, 10*(6), 1014-1024.

Jang, Gyu-Beom, Hong, In-Sun, Kim, Ran-Ju, Lee, Su-Youn, Park, Se-Jin, Lee, Eun-Sook, Lee, Kyoung-June (2015). Wnt/β-Catenin Small-Molecule Inhibitor CWP232228 Preferentially Inhibits the Growth of Breast Cancer Stem-like CellsTargeting Wnt Signaling in Breast Cancer Stem Cells. *Cancer research, 75*(8), 1691-1702.

Jesinger, Robert A (2014). Breast anatomy for the interventionalist. *Techniques in Vascular Interventional Radiology 17*(1), 3-9.

Jiang, Hao, Zu, Shijia, Lu, Yu, Sun, Zhongya, Adeerjiang, Akejiang, Guo, Qiao, Ding, Hong (2023). A RhoA structure with switch II flipped outward revealed the conformational dynamics of switch II region. *Journal of Structural Biology, 215*(5), 107942.

Juárez, Patricia, Fournier, Pierrick GJ, Mohammad, Khalid S, McKenna, Ryan C, Davis, Holly W, Peng, Xiang H, Guise, Theresa A (2017). Halofuginone inhibits TGF-β/BMP signaling and in combination with zoledronic acid enhances inhibition of breast cancer bone metastasis. *Oncotarget, 8*(49), 86447-86462.

Jung, Youn-Sang, & Park, Jae-Il (2020). Wnt signaling in cancer: therapeutic targeting of Wnt signaling beyond β-catenin and the destruction complex. *Experimental & molecular medicine, 52*(2), 183-191.

Kakiuchi, Miwako, Nishizawa, Takashi, Ueda, Hiroki, Gotoh, Kengo, Tanaka, Atsushi, Hayashi, Akimasa, Watanabe, Yoshiaki (2014). Recurrent gain-of-function mutations of RHOA in diffuse-type gastric carcinoma. *Nature genetics, 46*(6), 583-587.

Kallioniemi, Anne (2012). Bone morphogenetic protein 4—a fascinating regulator of cancer cell behavior. *Cancer genetics, 205*(6), 267-277.

Kalpana, Gardiyawasam, Figy, Christopher, Yeung, Miranda, & Yeung, Kam C (2019). Reduced RhoA expression enhances breast cancer metastasis with a concomitant increase in CCR5 and CXCR4 chemokines signaling. *Scientific reports, 9*(1), 1-12.

Kaneko, Masami, Saito, Yutaka, Saito, Hiromitsu, Matsumoto, Tadashi, Matsuda, Yuzuru, Vaught, Jeffry L, Neff, Nicola T (1997). Neurotrophic 3, 9-bis [(alkylthio) methyl]-and-bis (alkoxymethyl)-K-252a derivatives. *Journal of medicinal chemistry, 40*(12), 1863-1869.

Kang, Jia, & Pervaiz, Shazib (2013). Crosstalk between Bcl-2 family and Ras family small GTPases: potential cell fate regulation? *Frontiers in Oncology 2*, 206.

Kanzler, Benoît, Foreman, Ruth K, Labosky, Patricia A, & Mallo, Moisés (2000). BMP signaling is essential for development of skeletogenic and neurogenic cranial neural crest. *Development, 127*(5), 1095-1104.

Kashiwada, Takeru, Fukuhara, Shigetomo, Terai, Kenta, Tanaka, Toru, Wakayama, Yuki, Ando, Koji, Saito, Yoshinobu (2015). β-catenin-dependent transcription is central to Bmp-mediated formation of venous vessels. *Development 142*(3), 497-509.

Katagiri, Takenobu, Tsukamoto, Sho, & Kuratani, Mai (2021). Accumulated knowledge of activin receptor-like kinase 2 (ALK2)/activin A receptor, type 1 (ACVR1) as a target for human disorders. *Biomedicines, 9*(7), 736.

Katoh, Masaru. (2007). Networking of WNT, FGF, Notch, BMP, and Hedgehog signaling pathways during carcinogenesis. *Stem cell reviews, 3*(1), 30-38.

Katoh, Masuko, & Katoh, Masaru (2009). Transcriptional regulation of WNT2B based on the balance of Hedgehog, Notch, BMP and WNT signals. *International journal of oncology, 34*(5), 1411-1415.

Katoh, Masuko, & Katoh, Masaru (2022). WNT signaling and cancer stemness. *Essays in Biochemistry 66*(4), 319-331.

Katsuta, Eriko, Maawy, Ali A, Yan, Li, & Takabe, Kazuaki (2019). High expression of bone morphogenetic protein (BMP) 6 and BMP7 are associated with higher immune cell infiltration and better survival in estrogen receptor-positive breast cancer. *Oncology reports, 42*(4), 1413-1421.

Khammanivong, Ali, Mulligan, Miranda J, Brady, Nicholas J, Gopalakrishnan, Raj, & Dickerson, Erin B (2013). SMURF1 modulates BMP signaling and maintenance of HNSCC cancer stem cells. *Cancer Research, 73*(8_Supplement), 3759-3759.

Khosravi-Far, Roya, Solski, Patricia A, Clark, Geoffrey J, Kinch, Michael S, & Der, Channing J (1995). Activation of Rac1, RhoA, and mitogen-activated protein kinases is required for Ras transformation. *Molecular and cellular biology, 15*(11), 6443-6453.

Kim, Bo Ram, Oh, Sang Cheul, Lee, Dae-Hee, Kim, Jung Lim, Lee, Suk Young, Kang, Myoung Hee, Min, Byung Wook. (2015). BMP-2 induces motility and invasiveness by promoting colon cancer stemness through STAT3 activation. *Tumor Biology 36*, 9475-9486.

Kim, Seohyun, Kim, Seong A, Han, Jihoon, & Kim, In-San (2021). Rho-kinase as a target for cancer therapy and its immunotherapeutic potential. *International Journal of Molecular Sciences 22*(23), 12916.

Kim, Yong-Nyun, Koo, Kyung Hee, Sung, Jee Young, Yun, Un-Jung, & Kim, Hyeryeong (2012). Anoikis resistance: an essential prerequisite for tumor metastasis. *International journal of cell biology, 2012*, 306879.

Kimura, Kazushi, Ito, Masaaki, Amano, Mutsuki, Chihara, Kazuyasu, Fukata, Yuko, Nakafuku, Masato, Okawa, Katsuya (1996). Regulation of myosin phosphatase by Rho and Rho-associated kinase (Rho-kinase). *Science, 273*(5272), 245-248.

Klaus, Alexandra, & Birchmeier, Walter (2008). Wnt signalling and its impact on development and cancer. *Nature reviews; Cancer, 8*(5), 387-398.

Kleer, Celina G (2016). Dual roles of CCN proteins in breast cancer progression. *Journal of Cell Communication and Signaling 10*, 217-222.

Kleszcz, Robert, Szymańska, Anna, Krajka-Kuźniak, Violetta, Baer-Dubowska, Wanda, & Paluszczak, Jarosław. (2019). Inhibition of CBP/β-catenin and porcupine attenuates Wnt signaling and induces apoptosis in head and neck carcinoma cells. *Cellular Oncology 42*(4), 505-520.

Klumpe, Heidi E, Langley, Matthew A, Linton, James M, Su, Christina J, Antebi, Yaron E, & Elowitz, Michael B (2022). The context-dependent, combinatorial logic of BMP signaling. *Cell systems, 13*(5), 388-407. e310.

Koh, J., & Kim, M. J. (2019). Introduction of a New Staging System of Breast Cancer for Radiologists: An Emphasis on the Prognostic Stage. *20*(1), 69-82. doi:10.3348/kjr.2018.0231

Koh, Rhun Yian, Lim, Foong Ping, Ling, Leslie Siing Yie, Ng, Catherine Pei Ling, Liew, Siew Foong, Yew, Mei Yeng, Khuen Yen (2017). Anticancer mechanisms of Strobilanthes crispa Blume hexane extract on liver and breast cancer cell lines. *Oncology letters, 14*(4), 4957-4964.

Koh, Su Pin, Pham, Nhat Phi, & Piekny, Alisa (2022). Seeing is believing: tools to study the role of Rho GTPases during cytokinesis. *Small GTPases, 13*(1), 211-224.

Korzyńska, Anna, & Zychowicz, Marzena (2008). A method of estimation of the cell doubling time on basis of the cell culture monitoring data. *Biocybernetics and Biomedical Engineering, 28*(4), 75-82.

Kosla, Jan, Paňková, Daniela, Plachý, Jiří, Tolde, Ondřej, Bicanová, Kristýna, Dvořák, Michal, Brábek, Jan. (2013). Metastasis of aggressive amoeboid sarcoma cells is dependent on Rho/ROCK/MLC signaling. *Cell Communication Signaling 11*, 1-13.

Kumar, Atul, Bhattacharyya, Jina, & Jaganathan, Bithiah Grace (2017). Adhesion to stromal cells mediates imatinib resistance in chronic myeloid leukemia through ERK and BMP signaling pathways. *Scientific reports, 7*(1), 9535.

Lai, Lachlan Yuek Shun, Gracie, Nicholas Peter, Gowripalan, Anjali, Howell, Liam Michael, & Newsome, Timothy Peter (2022). SMAD proteins: Mediators of diverse outcomes during infection. *European journal of cell biology, 101*(2), 151204.

Lau, Marco Chi-Chung, Ng, Kai Yu, Wong, Tin Lok, Tong, Man, Lee, Terence K, Ming, Xiao-Yan, Qin, Yan-Ru (2017). FSTL1 Promotes Metastasis and Chemoresistance in Esophageal Squamous Cell Carcinoma through NFκB–BMP Signaling Cross-talkFSTL1-Mediated NFκB and BMP Pathway Deregulation in ESCC. *Cancer research, 77*(21), 5886-5899.

Lawson, Campbell D, & Ridley, Anne J (2018). Rho GTPase signaling complexes in cell migration and invasion. *Journal of Cell Biology 217*(2), 447-457.

Leask, Andrew (2016). CCN6: A modulator of breast cancer progression. *Journal of Cell Communication and Signaling 10*, 163-164.

Lee, Dae-Hee, Lee, Suk-young, & Oh, Sang Cheul (2017). Hedgehog signaling pathway as a potential target in the treatment of advanced gastric cancer. *Journal of the International Society for Oncodevelopmental Biology and Medicine, 39*(6), 1010428317692266.

Lee, Jae-Ho, Lee, Geun Taek, Woo, Seung Hyo, Ha, Yun-Sok, Kwon, Seok Joo, Kim, Wun-Jae, & Kim, Isaac Yi (2013). BMP-6 in renal cell carcinoma promotes tumor proliferation through IL-10–dependent M2 polarization of tumor-associated macrophages. *Cancer research, 73*(12), 3604-3614.

Leukemia. (1958). Grune & Stratton.

Leung, H, Yan, C, & Chan, B (2023). Osteochondral Tissue Engineering For Osteoarthritis Using Infrapatellar Fat-Pad Derived Mesenchymal Stem Cells. *Osteoarthritis and Cartilage, 31*, S225-S226.

Levidou, Georgia, Saetta, Angelica A, Gigelou, Fanie, Karlou, Maria, Papanastasiou, Polyanthi, Stamatelli, Angeliki, Patsouris, Efstratios (2012). ERK/pERK expression and B-raf mutations in colon adenocarcinomas: correlation with clinicopathological characteristics. *World Journal of Surgical Oncology 10*(1), 1-11.

Li, Haiying, Li, Juan, Cheng, Juan, Chen, Xuan, Zhou, Lanxia, & Li, Zhao (2019). AML-derived mesenchymal stem cells upregulate CTGF expression through the BMP pathway and induce K562-ADM fusiform transformation and chemoresistance. *Oncology reports, 42*(3), 1035-1046.

Li, Junliang, Ma, Jianxia, Zhang, Xuxia, Tai, Xiaohui, Liu, Le, & Zhang, Lingfang (2020). Long non-coding RNA (lncRNA) BMP/OP-responsive gene (BORG) promotes development of chemoresistance of colorectal cancer cells to carboplatin. *International Medical Journal of Experimental Clinical Research 26*, e919103.

Li, Nianshuang, Lu, Nonghua, & Xie, Chuan (2019). The Hippo and Wnt signalling pathways: crosstalk during neoplastic progression in gastrointestinal tissue. *The FEBS journal, 286*(19), 3745-3756.

Li, Qi, Kou, Xiaotong, Qin, Xiaoling, Li, Zhongsha, Li, Jingyu, & Chen, Chang (2022). BMP-4 impedes endothelial cell migration in neointimal hyperplasia via FoXO-3 specific modulation of reactive oxygen species. *Atherosclerosis, 351*, 9-17.

Li, Shulin, Hoefnagel, Sanne JM, Read, Matthew, Meijer, Sybren, van Berge Henegouwen, Mark I, Gisbertz, Suzanne S, Calpe, Silvia (2022). Selective targeting BMP2 and 4 in SMAD4 negative esophageal adenocarcinoma inhibits tumor growth and aggressiveness in preclinical models. *Cellular Oncology, 45*(4), 639-658.

Li, Wenzhe, Ma, Huailei, Zhang, Jin, Zhu, Ling, Wang, Chen, & Yang, Yanlian (2017). Unraveling the roles of CD44/CD24 and ALDH1 as cancer stem cell markers in tumorigenesis and metastasis. *Scientific reports, 7*(1), 1-15.

Li, Yan, Randriantsilefisoa, Rotsiniaina, Chen, Jie, Cuellar-Camacho, Jose Luis, Liang, Wanjun, & Li, Wenzhong (2020). Matrix stiffness regulates chemosensitivity, stemness characteristics, and autophagy in breast cancer cells. *ACS A Applied Biomaterials, 3*(7), 4474-4485.

Li, Yihao, Jin, Ke, van Pelt, Gabi W, van Dam, Hans, Yu, Xiao, Mesker, Wilma E, Zhang, Long (2016). c-Myb Enhances Breast Cancer Invasion and Metastasis through the Wnt/β-Catenin/Axin2 Pathwayc-Myb Potentiates Wnt Signaling in Breast Cancer. *Cancer research, 76*(11), 3364-3375.

Li, Yijian, Huo, Shujia, Fang, Yajie, Zou, Ting, Gu, Xianliang, Tao, Qin, & Xu, Haiwei (2018). ROCK inhibitor Y27632 induced morphological shift and enhanced neurite outgrowth-promoting property of olfactory ensheathing cells via YAP-dependent up-regulation of L1-CAM. *Frontiers in Cellular Neuroscience 12*, 489.

Li, Yujing, Zeng, Beilei, Li, Yunhai, Zhang, Chong, & Ren, Guosheng (2019). Downregulated expression of ARHGAP10 correlates with advanced stage and high Ki-67 index in breast cancer. *PeerJ, 7*, e7431.

Lian, Wen-Jing, Liu, Geng, Liu, Yuan-Jie, Zhao, Zhi-Wei, Yi, Tao, & Zhou, Hong-Ying (2013). Downregulation of BMP6 enhances cell proliferation and chemoresistance via activation of the ERK signaling pathway in breast cancer. *Oncology reports, 30*(1), 193-200.

Liao, YC, Ruan, JW, Lua, I, Li, MH, Chen, WL, Wang, JRY, Chen, JH (2012). Overexpressed hPTTG1 promotes breast cancer cell invasion and metastasis by regulating GEF-H1/RhoA signalling. *Oncogene, 31*(25), 3086-3097.

Licciulli, Silvia, Maksimoska, Jasna, Zhou, Chun, Troutman, Scott, Kota, Smitha, Liu, Qin, Field, Jeffrey (2013). FRAX597, a small molecule inhibitor of the p21-activated kinases, inhibits tumorigenesis of neurofibromatosis type 2 (NF2)-associated Schwannomas. *The Journal of biological chemistry, 288*(40), 29105-29114.

Lim, Hee-Suk, & Joe, Young. (2013). A ROCK inhibitor blocks the inhibitory effect of chondroitin sulfate proteoglycan on morphological changes of mesenchymal stromal/stem cells into neuron-like cells. *Biomolecules Therapeutics 21*(6), 447-453.

Lionarons, Daniël A, Hancock, David C, Rana, Sareena, East, Philip, Moore, Christopher, Murillo, Miguel M, Stamp, Gordon (2019). RAC1P29S induces a mesenchymal phenotypic switch via serum response factor to promote melanoma development and therapy resistance. *Cancer cell, 36*(1), 68-83. e69.

Liu, Mengmeng, Goldman, Graham, MacDougall, Mary, & Chen, Shuo (2022). BMP signaling pathway in dentin development and diseases. *Cells, 11*(14), 2216.

Liu, Peipei, Li, Wenhui, Hu, Yuanyuan, & Jiang, Youhong (2018). Absence of AIF1L contributes to cell migration and a poor prognosis of breast cancer. *OncoTargets and therapy, 11*, 5485-5498.

Liu, Qinghua, Huang, Xinjian, Li, Qingyuan, He, Lixin, Li, Siqi, Chen, Xiangfu, Lin, Chuyong (2020). Rhophilin-associated tail protein 1 promotes migration and metastasis in triple negative breast cancer via activation of RhoA. *FASEB journal : official publication of the Federation of American Societies for Experimental Biology, 34*(8), 9959-9971.

Liu, Qiqi, Sun, Hefen, Liu, Yang, Li, Xuan, Xu, Baojin, Li, Liangdong, & Jin, Wei (2022). HTR1A Inhibits the Progression of Triple-Negative Breast Cancer via TGF-β Canonical and Noncanonical Pathways. *Advanced science, 9*(12), e2105672.

Liu, Shuang, Ni, Chunsheng, Zhang, Danfang, Sun, Huizhi, Dong, Xueyi, Che, Na, Bai, Jingru (2019). S1PR1 regulates the switch of two angiogenic modes by VE-cadherin phosphorylation in breast cancer. *Cell death & disease, 10*(3), 1-15.

Liu, Xi, Zhang, Min, Ying, Songmin, Zhang, Chong, Lin, Runhua, Zheng, Jiaxuan, Du, Caiwen (2017). Genetic alterations in esophageal tissues from squamous dysplasia to carcinoma. *Gastroenterology, 153*(1), 166-177.

Liu, Ying-Ying, Liu, Hong-Yi, Yu, Tian-Jian, Lu, Qin, Zhang, Fang-Lin, Liu, Guang-Yu, Li, Da-Qiang (2022). O-GlcNAcylation of MORC2 at threonine 556 by OGT couples TGF-β signaling to breast cancer progression. *Cell death and differentiation, 29*(4), 861-873.

Lobbezoo, D. J., van Kampen, R. J., Voogd, A. C., Dercksen, M. W., van den Berkmortel, F., Smilde, T. J., Tjan-Heijnen, V. C. (2015). Prognosis of metastatic breast cancer: are there differences between patients with de novo and recurrent metastatic breast cancer? *Br J Cancer, 112*(9), 1445-1451. doi:10.1038/bjc.2015.127

Lowery, Jonathan W, & de Caestecker, Mark P (2010). BMP signaling in vascular development and disease. *Cytokine & growth factor reviews, 21*(4), 287-298.

Lu, Xin, & Kang, Yibin. (2007). Organotropism of breast cancer metastasis. *Journal of mammary gland biology and neoplasia, 12*(2), 153-162.

Luczak, Michał W, & Jagodziński, Paweł P (2006). The role of DNA methylation in cancer development. *Folia Histochemica et Cytobiologica 44*(3), 143-154.

Luo, N, Guo, J, Chen, L, Yang, W, Qu, X, & Cheng, Z (2016). ARHGAP10, downregulated in ovarian cancer, suppresses tumorigenicity of ovarian cancer cells. *Cell death & disease, 7*(3), e2157-e2157.

Luu, Hue H, Zhang, Ruiwen, Haydon, Rex C, Rayburn, Elizabeth, Kang, Quan, Si, Weike, Jiang, Wei (2004). Wnt/β-catenin signaling pathway as novel cancer drug targets. *Current Cancer Drug Targets 4*(8), 653-671.

Ma, Junli, Zeng, Shan, Zhang, Yan, Deng, Ganlu, Qu, Yanling, Guo, Cao, Li, Yiyi. (2017). BMP4 promotes oxaliplatin resistance by an induction of epithelial-mesenchymal transition via MEK1/ERK/ELK1 signaling in hepatocellular carcinoma. *Cancer letters, 411*, 117-129.

Ma, Yuxi, Xia, Zihan, Ye, Chunmei, Lu, Chong, Zhou, Sheng, Pan, Juan, Hu, Ting (2019). AGTR1 promotes lymph node metastasis in breast cancer by upregulating CXCR4/SDF-1α and inducing cell migration and invasion. *Aging, 11*(12), 3969-3992.

Makarem, Nour, Chandran, Urmila, Bandera, Elisa V, & Parekh, Niyati (2013). Dietary fat in breast cancer survival. *Annual Review of Nutrition 33*, 319-348.

Malhotra, Gautam K, Zhao, Xiangshan, Band, Hamid, & Band, Vimla (2010). Histological, molecular and functional subtypes of breast cancers. *Cancer biology & therapy, 10*(10), 955-960.

Malyuchik, SS, & Kiyamova, RG (2008). Medullary breast carcinoma. *Experimental oncology*.

Margadant, Coert, & Sonnenberg, Arnoud. (2010). Integrin–TGF-β crosstalk in fibrosis, cancer and wound healing. *EMBO reports, 11*(2), 97-105.

Marrazzo, Emilia, Frusone, Federico, Milana, Flavio, Sagona, Andrea, Gatzemeier, Wolfgang, Barbieri, Erika, Eboli, Marco Gaetano (2020). Mucinous breast cancer: a narrative review of the literature and a retrospective tertiary single-centre analysis. *Breast Care, 49*, 87-92.

Massey, Joseph, Liu, Yida, Alvarenga, Omar, Saez, Teresa, Schmerer, Matthew, & Warmflash, Aryeh (2019). Synergy with TGFβ ligands switches WNT pathway dynamics from transient to sustained during human pluripotent cell differentiation. *Proceedings of the National Academy of Sciences 116*(11), 4989-4998.

McLean, Karen, Gong, Yusong, Choi, Yunjung, Deng, Ning, Yang, Kun, Bai, Shoumei, Cho, Kathleen R (2011). Human ovarian carcinoma–associated mesenchymal stem cells regulate cancer stem cells and tumorigenesis via altered BMP production. *The Journal of clinical investigation, 121*(8), 3206-3219.

Mehrotra, Ravi, & Yadav, Kavita (2022). WJCO. *13*(3), 209-218.

Meng, Xian-Guo, & Yue, Shou-Wei (2015). Dexamethasone disrupts cytoskeleton organization and migration of T47D human breast cancer cells by modulating the AKT/mTOR/RhoA pathway. *Asian Pacific journal of cancer prevention : APJCP, 15*(23), 10245-10250.

Mercatali, Laura, La Manna, Federico, Miserocchi, Giacomo, Liverani, Chiara, De Vita, Alessandro, Spadazzi, Chiara, Ghetti, Martina. (2017). Tumor-stroma crosstalk in bone tissue: the osteoclastogenic potential of a breast cancer cell line in a co-culture system and the role of EGFR inhibition. *International Journal of Molecular Sciences, 18*(8), 1655.

Meyer, Matthew J, Fleming, Jodie M, Ali, Mustapha A, Pesesky, Mitchell W, Ginsburg, Erika, & Vonderhaar, Barbara K (2009). Dynamic regulation of CD24 and the invasive, CD44 pos CD24 neg phenotype in breast cancer cell lines. *Breast Cancer Research 397*(1), 27-33.

Meyer, Matthew J, Fleming, Jodie M, Ali, Mustapha A, Pesesky, Mitchell W, Ginsburg, Erika, & Vonderhaar, Barbara K (2010). Dynamic regulation of CD24 and the invasive, CD44posCD24neg phenotype in breast cancer cell lines. *Cancer Research 11*(6), R82.

Mihajlović, Jelena, Diehl, Laura AM, Hochhaus, Andreas, & Clement, Joachim H (2019). Inhibition of bone morphogenetic protein signaling reduces viability, growth and migratory potential of non-small cell lung carcinoma cells. *Journal of Cancer Research Clinical Oncology 145*(11), 2675-2687.

Minard, Meghan E, Kim, Lee-Su, Price, Janet E, & Gallick, Gary E. (2004). The role of the guanine nucleotide exchange factor Tiam1 in cellular migration, invasion, adhesion and tumor progression. *Breast cancer research and treatment, 84*(1), 21-32.

Mintun, Mark A, Welch, Michael J, Siegel, Barry A, Mathias, Carla J, Brodack, JW, McGuire, Andrea H, & Katzenellenbogen, John A (1988). Breast cancer: PET imaging of estrogen receptors. *Radiology, 169*(1), 45-48.

Miyauchi, Maho, Matsumura, Reina, & Kawahara, Hiroyuki (2023). BAG6 supports stress fiber formation by preventing the ubiquitin-mediated degradation of RhoA. *Molecular biology of the cell, 34*(4), mbc. E22-08-0355.

Mock, Kerstin, Preca, Bogdan-Tiberius, Brummer, Tilman, Brabletz, Simone, Stemmler, Marc P, & Brabletz, Thomas (2015). The EMT-activator ZEB1 induces bone metastasis associated genes including BMP-inhibitors. *Oncotarget, 6*(16), 14399.

Mohamed, Ammar, Amer, Eslam, Eldin, Noor, Hossam, Maysoon, Elmasry, Noha, & Adnan, Ganna Tamer. (2022). The impact of data processing and ensemble on breast cancer detection using deep learning. *Journal of Computing and Communication, 1*(1), 27-37.

Mokhtari, Reza Bayat, Qorri, Bessi, Sambi, Manpreet, Baluch, Narges, Kumar, Sushil, Das, Bikul, Cheng, Hai-Ling Margaret (2021). 3D Multicellular Stem-Like Human Breast Tumor Spheroids Enhance Tumorigenicity of Orthotopic Xenografts in Athymic Nude Rat Model. *Cancers*, *13*(11), 2784.

Moniuszko, Tadeusz, Wincewicz, Andrzej, Koda, Mariusz, Domysławska, Izabela, & Sulkowski, Stanisław (2016). Role of periostin in esophageal, gastric and colon cancer. *Oncology letters*, *12*(2), 783-787.

Moradian, Cobra, & Rahbarizadeh, Fatemeh (2019). Targeted Toxin gene therapy of breast cancer stem cells using CXCR1 promoter and bFGF 5′ UTR. *OncoTargets Therapy 12*, 8809-8820.

Morgillo, Floriana, Della Corte, Carminia Maria, Fasano, Morena, & Ciardiello, Fortunato. (2016). Mechanisms of resistance to EGFR-targeted drugs: lung cancer. *ESMO open, 1*(3), e000060.

Mullen, Peter J, Yu, Rosemary, Longo, Joseph, Archer, Michael C, & Penn, Linda Z (2016). The interplay between cell signalling and the mevalonate pathway in cancer. *Nature Reviews Cancer 16*(11), 718-731.

Müller, Paul M, Rademacher, Juliane, Bagshaw, Richard D, Wortmann, Celina, Barth, Carolin, van Unen, Jakobus, Heinrich, Louise E (2020). Systems analysis of RhoGEF and RhoGAP regulatory proteins reveals spatially organized RAC1 signalling from integrin adhesions. *Nature cell biology*, *22*(4), 498-511.

Munnamalai, Vidhya, & Fekete, Donna M (2016). Notch-Wnt-Bmp crosstalk regulates radial patterning in the mouse cochlea in a spatiotemporal manner. *Development*, *143*(21), 4003-4015.

Murray, Brion W, Guo, Chuangxing, Piraino, Joseph, Westwick, John K, Zhang, Cathy, Lamerdin, Jane, Zager, Michael (2010). Small-molecule p21-activated kinase inhibitor PF-3758309 is a potent inhibitor of oncogenic signaling and tumor growth. *Proceedings of the National Academy of Sciences of the United States of America*, *107*(20), 9446-9451.

Nagumo, Hiromitsu, Sasaki, Yasuharu, Ono, Yoshitaka, Okamoto, Hiroyuki, Seto, Minoru, & Takuwa, Yoh (2000). Rho kinase inhibitor HA-1077 prevents Rho-mediated myosin phosphatase inhibition in smooth muscle cells. *American journal of physiology-Cell physiology*, *278*(1), C57-C65.

Nakashima, Aiko, Katagiri, Takenobu, & Tamura, Masato (2005). Cross-talk between Wnt and bone morphogenetic protein 2 (BMP-2) signaling in differentiation pathway of C2C12 myoblasts. *Journal of Biological Chemistry 280*(45), 37660-37668.

Neckmann, Ulrike, Wolowczyk, Camilla, Hall, Martina, Almaas, Eivind, Ren, Jiang, Zhao, Sen, Ten Dijke, Peter (2019). GREM1 is associated with metastasis and predicts poor prognosis in ER-negative breast cancer patients. *Cell communication and signaling : CCS, 17*(1), 140.

Neinavaie, Fargam, Ibrahim-Hashim, Arig, Kramer, Andrew M, Brown, Joel S, & Richards, Christina L. (2021). The genomic processes of biological invasions: From invasive species to cancer metastases and back again. *Frontiers in Ecology and Evolution, 9*, 681100.

Network, Cancer Genome Atlas Research. (2014). Comprehensive molecular characterization of gastric adenocarcinoma. *Nature, 513*(7517), 202-209.

Nguyen, Daniel P, Li, Jinyi, Yadav, Shalini S, & Tewari, Ashutosh K (2014). Recent insights into NF-κ B signalling pathways and the link between inflammation and prostate cancer. *BJU international, 114*(2), 168-176.

Nickel, Joachim, & Mueller, Thomas D (2019). Specification of BMP signaling. *Cells, 8*(12), 1579.

Ning, Junya, Zhao, Yi, Ye, Yingnan, & Yu, Jinpu (2019). Opposing roles and potential antagonistic mechanism between TGF-β and BMP pathways: Implications for cancer progression. *EBioMedicine, 41*, 702-710.

Obradovic Wagner, Darja, Sieber, Christina, Bhushan, Raghu, Börgermann, Jan H, Graf, Daniel, & Knaus, Petra. (2010). BMPs: from bone to body morphogenetic proteins. In (Vol. 3, pp. 107). Science signaling: American Association for the Advancement of Science.

Otsuka, Fumio (2010). Multiple endocrine regulation by bone morphogenetic protein system. *Endocrine journal, 57*(1), 3-14.

Owens, Philip, Pickup, Michael W, Novitskiy, Sergey V, Giltnane, Jennifer M, Gorska, Agnes E, Hopkins, Corey R, Moses, Harold L (2015). Inhibition of BMP signaling suppresses metastasis in mammary cancer. *Oncogene, 34*(19), 2437-2449.

Owens, Philip, Polikowsky, Hannah, Pickup, Michael W, Gorska, Agnieszka E, Jovanovic, Bojana, Shaw, Aubie K,Moses, Harold L (2013). Bone morphogenetic proteins stimulate mammary fibroblasts to promote mammary carcinoma cell invasion. *PloS one, 8*(6), e67533.

Öztürk, Ece, Despot-Slade, Evelin, Pichler, Michael, & Zenobi-Wong, Marcy (2017). RhoA activation and nuclearization marks loss of chondrocyte phenotype in crosstalk with Wnt pathway. *Experimental cell research, 360*(2), 113-124.

Pal, Anupama, Huang, Wei, Li, Xin, Toy, Kathy A, Nikolovska-Coleska, Zaneta, & Kleer, Celina G (2012). CCN6 modulates BMP signaling via the Smad-independent TAK1/p38 pathway, acting to suppress metastasis of breast cancer. *Cancer research, 72*(18), 4818-4828.

Pan, Meng, Chew, Ti Weng, Wong, Darren Chen Pei, Xiao, Jingwei, Ong, Hui Ting, Chin, Jasmine Fei Li, & Low, Boon Chuan (2020). BNIP-2 retards breast cancer cell migration by coupling microtubule-mediated GEF-H1 and RhoA activation. *Science advances, 6*(31), eaaz1534.

Panda, Abikshyeet, Mishra, Pallavi, Mohanty, Aishwariya, Sundaragiri, Krishna Sireesha, Singh, Arpita, & Jha, Kunal (2022). Is Epithelial-Mesenchymal Transition a New Roadway in the Pathogenesis of Oral Submucous Fibrosis: A Comprehensive Review. *Cureus, 14*(9), e29636.

Paplomata, Elisavet, & O'Regan, Ruth (2014). The PI3K/AKT/mTOR pathway in breast cancer: targets, trials and biomarkers. *Therapeutic advances in medical oncology, 6*(4), 154-166.

Park, So-Yeon, Choi, Jang-Hyun, & Nam, Jeong-Seok. (2019). Targeting cancer stem cells in triple-negative breast cancer. *Cancers, 11*(7), 965.

Parrotta, Elvira Immacolata, Procopio, Anna, Scalise, Stefania, Esposito, Claudia, Nicoletta, Giovanni, Santamaria, Gianluca, Laugwitz, Karl-Ludwig (2021). Deciphering the role of wnt and rho signaling pathway in IPSC-derived ARVC cardiomyocytes by in silico mathematical modeling. *International journal of molecular sciences, 22*(4), 2004.

Parthasarathy, Veda, & Rathnam, Usharani (2012). Nipple discharge: an early warning sign of breast cancer. *International Journal of Preventive Medicine 3*(11), 810-814.

Pasquier, Jennifer, Abu-Kaoud, Nadine, Abdesselem, Houari, Madani, Aisha, Hoarau-Véchot, Jessica, Thawadi, Hamda Al, Rafii, Arash. (2015). SDF-1alpha concentration dependent modulation of RhoA and Rac1 modifies breast cancer and stromal cells interaction. *BMC cancer, 15*(1), 1-17.

Passaro, Antonio, Jänne, Pasi A, Mok, Tony, & Peters, Solange (2021). Overcoming therapy resistance in EGFR-mutant lung cancer. *Nature cancer, 2*(4), 377-391.

Patel, Ronil A, Forinash, Kara D, Pireddu, Roberta, Sun, Ying, Sun, Nan, Martin, Mathew P, Sebti, Saïd M (2012). RKI-1447 Is a Potent Inhibitor of the Rho-Associated ROCK Kinases with Anti-Invasive and Antitumor Activities in Breast CancerRKI-1447, a Potent ROCK Inhibitor with Antitumor Activity. *Cancer research, 72*(19), 5025-5034.

Patel, Shashank J, Sanjana, Neville E, Kishton, Rigel J, Eidizadeh, Arash, Vodnala, Suman K, Cam, Maggie, Yamamoto, Tori N (2017). Identification of essential genes for cancer immunotherapy. *Nature, 548*(7669), 537-542.

Patwardhan, Sejal, Mahadik, Pratiksha, Shetty, Omshree, & Sen, Shamik (2021). ECM stiffness-tuned exosomes drive breast cancer motility through thrombospondin-1. *Biomaterials, 279*, 121185.

Peng, Jin, Yoshioka, Yumiko, Mandai, Masaki, Matsumura, Noriomi, Baba, Tsukasa, Yamaguchi, Ken, Abiko, Kaoru (2016). The BMP signaling pathway leads to enhanced proliferation in serous ovarian cancer—A potential therapeutic target. *Molecular carcinogenesis, 55*(4), 335-345.

Pickup, Michael W, Hover, Laura D, Guo, Yan, Gorska, Agnieszka E, Chytil, Anna, Novitskiy, Sergey V, Owens, Philip (2015). Deletion of the BMP receptor BMPR1a impairs mammary tumor formation and metastasis. *Oncotarget, 6*(26), 22890-22904.

Pillé, J-Y, Denoyelle, C, Varet, J, Bertrand, J-R, Soria, J, Opolon, P, Malvy, C (2005). Anti-RhoA and anti-RhoC siRNAs inhibit the proliferation and invasiveness of MDA-MB-231 breast cancer cells in vitro and in vivo. *Molecular therapy, 11*(2), 267-274.

Politi, Katerina, Feirt, Nikki, & Kitajewski, Jan. (2004). *Notch in mammary gland development and breast cancer.* Paper presented at the Seminars in Cancer Biology.

Porchia, Leonardo M, Guerra, Marcy, Wang, Yu-Chieh, Zhang, Yunlong, Espinosa, Allan V, Shinohara, Motoo, Chen, Ching-Shih (2007). 2-amino-N-{4-[5-(2-phenanthrenyl)-3-(trifluoromethyl)-1H-pyrazol-1-yl]-phenyl} acetamide (OSU-03012), a celecoxib derivative, directly targets p21-activated kinase. *Molecular pharmacology, 72*(5), 1124-1131.

Privat, Maud, Cavard, Amélie, Zekri, Yanis, Ponelle-Chachuat, Flora, Molnar, Ioana, Sonnier, Nicolas, & Bignon, Yves-Jean (2020). A high expression ratio of RhoA/RhoB is associated with the migratory and invasive properties of basal-like Breast Tumors. *International journal of medical sciences, 17*(17), 2799-2808.

Pulciani, S, Santos, E, Long, LK, Sorrentino, V, & Barbacid, M (1985). ras gene Amplification and malignant transformation. *Molecular and cellular biology, 5*(10), 2836-2841.

Rahman, Md Shaifur, Akhtar, Naznin, Jamil, Hossen Mohammad, Banik, Rajat Suvra, & Asaduzzaman, Sikder M (2015). TGF-β/BMP signaling and other molecular events: regulation of osteoblastogenesis and bone formation. *Bone research, 3*(1), 1-20.

Rahman, Syed Azizur, Al–Marzouki, Amina, Otim, Michael, Khayat, Nour El Hoda Khalil, Yousef, Reham, & Rahman, Prama (2019). Awareness about breast cancer and breast self-examination among female students at the University of Sharjah: A cross-sectional study. *Asian Pacific journal of cancer prevention, 20*(6), 1901-1908.

Rathinam, Rajamani, Berrier, Allison, & Alahari, Suresh K (2011). Role of Rho GTPases and their regulators in cancer progression. *Frontiers in bioscience : a journal and virtual library, 16*(7), 2561-2571.

Reedijk, Michael, Odorcic, Silvia, Chang, Lynn, Zhang, Hui, Miller, Naomi, McCready, David R, Egan, Sean E (2005). High-level coexpression of JAG1 and NOTCH1 is observed in human breast cancer and is associated with poor overall survival. *Cancer research, 65*(18), 8530-8537.

Regard, Jean B, Zhong, Zhendong, Williams, Bart O, & Yang, Yingzi (2012). Wnt signaling in bone development and disease: making stronger bone with Wnts. *Cold Spring Harbor perspectives in biology*, *4*(12), a007997.

Ren, Weimin, Guan, Wencai, Zhang, Jinguo, Wang, Fanchen, & Xu, Guoxiong (2019). Pyridoxine 5′-phosphate oxidase is correlated with human breast invasive ductal carcinoma development. *Aging*, *11*(7), 2151-2176.

Riaz, Syeda Kiran, Ke, Yuepeng, Wang, Fen, Kayani, Mahmood Akhtar, & Malik, Muhammad Faraz Arshad (2019). Influence of SHH/GLI1 axis on EMT mediated migration and invasion of breast cancer cells. *Scientific reports*, *9*(1), 1-13.

Riddle, Ryan C, Diegel, Cassandra R, Leslie, Julie M, Van Koevering, Kyle K, Faugere, Marie-Claude, Clemens, Thomas L, & Williams, Bart O. (2013). Lrp5 and Lrp6 exert overlapping functions in osteoblasts during postnatal bone acquisition. *PloS one*, *8*(5), e63323.

Ridley, Anne J (2015). Rho GTPase signalling in cell migration. *Current opinion in cell biology*, *36*, 103-112.

Ridley, Anne J, & Hall, Alan (1992). The small GTP-binding protein rho regulates the assembly of focal adhesions and actin stress fibers in response to growth factors. *Cell*, *70*(3), 389-399.

Rodrigues, Paulo, Macaya, Irati, Bazzocco, Sarah, Mazzolini, Rocco, Andretta, Elena, Dopeso, Higinio, Nieto, Rocio (2014a). RHOA inactivation enhances Wnt signalling and promotes colorectal cancer. *Nature Communications*, *5*(1), 1-15.

Rodrigues, Paulo, Macaya, Irati, Bazzocco, Sarah, Mazzolini, Rocco, Andretta, Elena, Dopeso, Higinio, Nieto, Rocio (2014b). RHOA inactivation enhances Wnt signalling and promotes colorectal cancer. Nature communications, *5*(1), 5458.

Rodriguez-Martinez, Alejandra, Alarmo, Emma-Leena, Saarinen, Lilli, Ketolainen, Johanna, Nousiainen, Kari, Hautaniemi, Sampsa, & Kallioniemi, Anne (2011). Analysis of BMP4 and BMP7 signaling in breast cancer cells unveils time-dependent transcription patterns and highlights a common synexpression group of genes. *BMC medical genomics*, *4*(1), 80.

Roganovic, Dragana, Djilas, Dragana, Vujnovic, Sasa, Pavic, Dag, & Stojanov, Dragan (2015). Breast MRI, digital mammography and breast tomosynthesis: comparison of three methods for early detection of breast cancer. *Bosnian Journal of Basic Medical Sciences 15*(4), 64-68.

Rosenblatt, Adena E, Garcia, Maria Ines, Lyons, Leah, Xie, Yingqiu, Maiorino, Carol, Desire, Laurent, Burnstein, Kerry L (2011). Inhibition of the Rho GTPase, Rac1, decreases estrogen receptor levels and is a novel therapeutic strategy in breast cancer. *Endocrine-related cancer*, *18*(2), 207-219.

Ruan, Xiaohong, Liu, Aibin, Zhong, Meigong, Wei, Jihong, Zhang, Weijian, Rong, Yingrou, .Chen, Gaowen (2019). Silencing LGR6 attenuates stemness and chemoresistance via inhibiting Wnt/β-Catenin signaling in ovarian cancer. *Molecular Therapy-Oncolytics 14*, 94-106.

Ryspayeva, Dinara, Halytskiy, Volodymyr, Kobyliak, Nazarii, Dosenko, Iryna, Fedosov, Artem, Inomistova, Mariia,Sulaieva, Oksana (2022). Response to neoadjuvant chemotherapy in breast cancer: do microRNAs matter? *Oncology*, *13*(1), 1-10.

Saadeldin, Islam M, Tukur, Hammed A, Aljumaah, Riyadh S, & Sindi, Ramya A (2021). Rocking the boat: the decisive roles of Rho kinases during oocyte, blastocyst, and stem cell development. *Frontiers in Cell Developmental Biology 8*, 616762.

Saha Roy, Sudipa, & Vadlamudi, Ratna K (2012). Role of estrogen receptor signaling in breast cancer metastasis. *International journal of breast cancer*, *2012*.

Sahai, Erik, Olson, Michael F, & Marshall, CJ (2001). Cross-talk between Ras and Rho signalling pathways in transformation favours proliferation and increased motility. *The EMBO journal 20*(4), 755-766.

Saifo, Maher S, Rempinski, Donald R, Rustum, Youcef M, & Azrak, Rami G (2010). Targeting the oncogenic protein beta-catenin to enhance chemotherapy outcome against solid human cancers. *Molecular Cancer 9*, 1-11.

Sakamori, Ryotaro, Yu, Shiyan, Zhang, Xiao, Hoffman, Andrew, Sun, Jiaxin, Das, Soumyashree, Walker, Francesca (2014). CDC42 Inhibition Suppresses Progression of Incipient

Intestinal TumorsCdc42 Favors Growth of Intestinal Tumor Cells. *Cancer research, 74*(19), 5480-5492.

Sakamoto, Shinichi, & Kyprianou, Natasha (2010). Targeting anoikis resistance in prostate cancer metastasis. *Molecular Aspects of Medicine 31*(2), 205-214.

Sambanje, Martha Nyanungo, & Mafuvadze, Benford (2012). Breast cancer knowledge and awareness among university students in Angola. *Pan African Medical Journal 11*(1).

Sarwar, Makhdoom, Sykes, Peter H, Chitcholtan, Kenny, & Evans, John J (2020). Extracellular biophysical environment: Guilty of being a modulator of drug sensitivity in ovarian cancer cells. *Biochemical and biophysical research communications, 527*(1), 180-186.

Sauzeau, Vincent, Beignet, Julien, Vergoten, Gérard, & Bailly, Christian (2022). Overexpressed or hyperactivated Rac1 as a target to treat hepatocellular carcinoma. *Pharmacological research, 179*, 106220.

Saxena, Monika, Agnihotri, Nitin, & Sen, Jonaki (2020). Correction: Perturbation of canonical and non-canonical BMP signaling affects migration, polarity and dendritogenesis of mouse cortical neurons (doi: 10.1242/dev. 147157). *Development, 147*(2), dev188243.

Schinner, Sven (2009). Wnt-signalling and the metabolic syndrome. *Hormone and metabolic research, 41*(02), 159-163.

Schmidt, Sissel Ida, Blaabjerg, Morten, Freude, Kristine, & Meyer, Morten (2022). RhoA signaling in neurodegenerative diseases. *Cells, 11*(9), 1520.

Seo, Dongyeob, Jung, Su Myung, Park, Jin Seok, Lee, Jaewon, Ha, Jihoon, Kim, Minbeom, & Park, Seok Hee (2019). The deubiquitinating enzyme PSMD14 facilitates tumor growth and chemoresistance through stabilizing the ALK2 receptor in the initiation of BMP6 signaling pathway. *EBioMedicine, 49*, 55-71.

Sethi, Nilay, Dai, Xudong, Winter, Christopher, & Kang, Yibin. (2011). Tumor-Derived Jagged1 Promotes Osteolytic Bone Metastasis of Breast Cancer by Engaging Notch Signaling in Bone Cells. *Cancer cell, 19*, 192-205. doi:10.1016/j.ccr.2010.12.022

Shang, Xun, Marchioni, Fillipo, Evelyn, Chris R, Sipes, Nisha, Zhou, Xuan, Seibel, William, Zheng, Yi (2013). Small-molecule inhibitors targeting G-protein–coupled Rho guanine nucleotide exchange factors. *The journal of Proceedings of the National Academy of Sciences 110*(8), 3155-3160.

Shang, Xun, Marchioni, Fillipo, Sipes, Nisha, Evelyn, Chris R, Jerabek-Willemsen, Moran, Duhr, Stefan, Zheng, Yi (2012). Rational design of small molecule inhibitors targeting RhoA subfamily Rho GTPases. *Chemistry & biology, 19*(6), 699-710.

Shao, Mei-Ying, Cheng, Ran, Wang, Feng-Ming, Yang, Hui, Cheng, Li, & Hu, Tao (2011). β-Catenin and Rho GTPases as downstream targets of TGF-β1 during pulp repair. *Cell Biology International 35*(2), 105-109.

Sharma, Ganesh N, Dave, Rahul, Sanadya, Jyotsana, Sharma, Piush, & Sharma, KK3255438 (2010). Various types and management of breast cancer: an overview. *Journal of Advanced Pharmaceutical Technology 1*(2), 109-126.

Shaw, Holly Victoria, Koval, Alexey, & Katanaev, Vladimir (2019). Targeting the Wnt signalling pathway in cancer: prospects and perils. *Swiss medical weekly, 149*, w20129.

Shee, Kevin, Jiang, Amanda, Varn, Frederick S, Liu, Stephanie, Traphagen, Nicole A, Owens, Philip, Golub, Todd R (2019). Cytokine sensitivity screening highlights BMP4 pathway signaling as a therapeutic opportunity in ER+ breast cancer. *Federation of American Societies for Experimental Biology, 33*(2), 1644-1657.

Sheridan, Carol, Kishimoto, Hiromitsu, Fuchs, Robyn K, Mehrotra, Sanjana, Bhat-Nakshatri, Poornima, Turner, Charles H, Nakshatri, Harikrishna (2006). CD44+/CD24-breast cancer cells exhibit enhanced invasive properties: an early step necessary for metastasis. *Breast Cancer Research 8*(5), 1-13.

Shih, Hung-Yu, Chang, Chia-Wei, Chen, Yi-Chieh, & Cheng, Yi-Chuan (2023). Identification of the Time Period during Which BMP Signaling Regulates Proliferation of Neural Progenitor Cells in Zebrafish. *International journal of molecular sciences, 24*(2), 1733.

Sickles, Edward A (1984). Mammographic features of" early" breast cancer. *American Journal of Roentgenology 143*(3), 461-464.

Siegel, R. L., & Miller, K. D. (2021). Cancer Statistics, 2021. *CA Cancer J Clin, 71*(1), 7-33. doi:10.3322/caac.21654

Siegel, Rebecca L, Miller, Kimberly D, Wagle, Nikita Sandeep, & Jemal, Ahmedin. Cancer statistics, 2023. *Cancer Journal for Clinicians 73*(1), 17-48.

Sinn, H. P., & Kreipe, H. (2013). A Brief Overview of the WHO Classification of Breast Tumors, 4th Edition, Focusing on Issues and Updates from the 3rd Edition. *Breast Care, 8*(2), 149-154. doi:10.1159/000350774

Skovrlj, Branko, Koehler, Steven M, Anderson, Paul A, Qureshi, Sheeraz A, Hecht, Andrew C, Iatridis, James C, & Cho, Samuel K (2015). Association between BMP-2 and carcinogenicity. *Spine, 40*(23), 1862-1871.

Song, Robert X-D, & Santen, Richard J (2006). Membrane initiated estrogen signaling in breast cancer. *Biology of reproduction, 75*(1), 9-16.

Srivastava, Swayam Prakash, Koya, Daisuke, & Kanasaki, Keizo (2013). MicroRNAs in kidney fibrosis and diabetic nephropathy: roles on EMT and EndMT. *BioMed research international, 2013*, 125469.

Stepp, Marcus W, Salazar-González, Raúl A, Hong, Kyung U, Doll, Mark A, & Hein, David W (2019). N-acetyltransferase 1 knockout elevates acetyl coenzyme A levels and reduces anchorage-independent growth in human breast cancer cell lines. *Journal of oncology, 2019*, 3860426.

Stoletov, Konstantin, Montel, Valerie, Lester, Robin D, Gonias, Steven L, & Klemke, Richard (2007). High-resolution imaging of the dynamic tumor cell–vascular interface in transparent zebrafish. *Proceedings of the National Academy of Sciences of the United States of America, 104*(44), 17406-17411.

Strittmatter, Tobias, Haellman, Viktor, Argast, Paul, Buchman, Peter, Teixeira, Ana Palma, & Fussenegger, Martin (2022). Mechano-regulation of Wnt/β-Catenin signaling to control paraxial versus lateral mesoderm lineage bifurcation. *Biotechnology progress, 39*(2), e3312.

Sumbaly, Ronak, Vishnusri, N, & Jeyalatha, S. (2014). Diagnosis of breast cancer using decision tree data mining technique. *International Journal of Computer Applications, 83*(5).

Sun, Fengfeng, Sun, Peng, Yang, Xiaofeng, Hu, Liangliang, Gao, Jianguo, & Tian, Tao (2021). Inhibition of FSTL3 abates the proliferation and metastasis of renal cell carcinoma via the GSK-3β/β-catenin signaling pathway. *Aging, 13*(18), 22528-22543.

Sung, Hyuna, Ferlay, Jacques, Siegel, Rebecca L, Laversanne, Mathieu, Soerjomataram, Isabelle, Jemal, Ahmedin, & Bray, Freddie (2021). Global cancer statistics 2020: GLOBOCAN estimates of incidence and mortality worldwide for 36 cancers in 185 countries. *A cancer journal for clinicians, 71*(3), 209-249.

Sung, Nam Ji, Kim, Na Hui, Surh, Young-Joon, & Park, Sin-Aye (2020). Gremlin-1 promotes metastasis of breast cancer cells by activating STAT3-MMP13 signaling pathway. *International journal of molecular sciences, 21*(23), 9227.

Svensmark, Julius H, & Brakebusch, Cord (2019). Rho GTPases in cancer: friend or foe? *Oncogene, 38*(50), 7447-7456.

Taipale, Jussi, & Beachy, Philip A (2001). The Hedgehog and Wnt signalling pathways in cancer. *Nature, 411*(6835), 349-354.

Tan, Hai-Bo, Zhong, Yi-Sheng, Cheng, Yu, & Shen, Xi (2011). Rho/ROCK pathway and neural regeneration: a potential therapeutic target for central nervous system and optic nerve damage. *International Journal of Ophthalmology 4*(6), 652-657.

Tanaka, Arowu R, Noguchi, Kohji, Fukazawa, Hidesuke, Igarashi, Yasuhiro, Arai, Hiroyuki, & Uehara, Yoshimasa (2013). p38MAPK and Rho-dependent kinase are involved in anoikis induced by anicequol or 25-hydroxycholesterol in DLD-1 colon cancer cells. *Biochemical Biophysical Research Communications 430*(4), 1240-1245.

Tang, De-Zhi, Hou, Wei, Zhou, Quan, Zhang, Minjie, Holz, Jonathan, Sheu, Tzong-Jen, Harris, Stephen E (2010). Osthole stimulates osteoblast differentiation and bone formation by activation of β-catenin–BMP signaling. *Journal of Bone Mineral Research 25*(6), 1234-1245.

Tang, Yanyan, He, Yi, Zhang, Ping, Wang, Jinpeng, Fan, Chunmei, Yang, Liting, Nie, Shaolin (2018). LncRNAs regulate the cytoskeleton and related Rho/ROCK signaling in cancer metastasis. *Molecular cancer, 17*(1), 1-10.

Telloni, Stacy M. (2017). Tumor staging and grading: A primer. *Molecular Profiling: Methods 1606*, 1-17.

Teng, Ji-Ping, Yang, Zhi-Ying, Zhu, Yu-Ming, Ni, Da, Zhu, Zhi-Jun, & Li, Xiao-Qiang (2017). The roles of ARHGAP10 in the proliferation, migration and invasion of lung cancer cells. *Oncology letters, 14*(4), 4613-4618.

Teo, Cui Rong, Casey, Patrick J, & Rasheed, Suhail Ahmed Kabeer (2016). The GNA13-RhoA signaling axis suppresses expression of tumor protective Kallikreins. *Cellular signalling, 28*(10), 1479-1488.

Teramura, Takeshi, Takehara, Toshiyuki, Onodera, Yuta, Nakagawa, Koichi, Hamanishi, Chiaki, & Fukuda, Kanji (2012). Mechanical stimulation of cyclic tensile strain induces reduction of pluripotent related gene expressions via activation of Rho/ROCK and subsequent decreasing of AKT phosphorylation in human induced pluripotent stem cells. *Biochemical Biophysical Research Communications 417*(2), 836-841.

Tesauro, Cinzia, Simonsen, Anne Katrine, Andersen, Marie Bech, Petersen, Kamilla Wandsoe, Kristoffersen, Emil Laust, Algreen, Line, Stougaard, Magnus (2019). Topoisomerase I activity and sensitivity to camptothecin in breast cancer-derived cells: a comparative study. *BMC cancer, 19*(1), 1-15.

Thawani, Jayesh P, Wang, Anthony C, Than, Khoi D, Lin, Chia-Ying, La Marca, Frank, & Park, Paul (2010). Bone morphogenetic proteins and cancer: review of the literature. *Neurosurgery, 66*(2), 233-246.

Thiberville, Luc, Payne, Peter, Vielkinds, Jüergen, LeRiche, Jean, Horsman, Douglas, Nouvet, Georges, Lam, Stephen (1995). Evidence of cumulative gene losses with progression of premalignant epithelial lesions to carcinoma of the bronchus. *Cancer research, 55*(22), 5133-5139.

Thomas, David B (1984). Do hormones cause breast cancer? *Cancer, 53*(S3), 595-604.

Thomas, Sachin, & Jaganathan, Bithiah Grace (2022). Signaling network regulating osteogenesis in mesenchymal stem cells. *Journal of cell communication and signaling, 16*(1), 47-61.

Tian, Qi, Gao, Huan, Zhou, Yan, Zhu, Lizhe, Yang, Jiao, Wang, Bo, Yang, Jin (2022). RICH1 inhibits breast cancer stem cell traits through activating kinases cascade of Hippo signaling by competing with Merlin for binding to Amot-p80. *Cell death & disease, 13*(1), 1-13.

Tong, Jiaci, Li, Haoran, Hu, Ye, Zhao, Z, & Li, Man (2022). TMEM158 Regulates the Canonical and Non-Canonical Pathways of TGF-β to Mediate EMT in Triple-Negative Breast Cancer. *Journal of Cancer, 13*(8), 2694-2704.

Trichopoulos, Dimitrios, Li, Frederick P, & Hunter, David J (1996). What causes cancer? *Scientific American 275*(3), 80-87.

Trinh, XB, Tjalma, WAA, Vermeulen, PB, Van den Eynden, G, Van der Auwera, I, Van Laere, SJ, Van Dam, PA (2009). The VEGF pathway and the AKT/mTOR/p70S6K1 signalling pathway in human epithelial ovarian cancer. *British Journal of Cancer 100*(6), 971-978.

Trop, Isabelle, LeBlanc, Sophie M, David, Julie, Lalonde, Lucie, Tran-Thanh, Danh, Labelle, Maude, & El Khoury, Mona M (2014). Molecular classification of infiltrating breast cancer: toward personalized therapy. *Radiographics : a review publication of the Radiological Society of North America, Inc., 34*(5), 1178-1195.

Tse, Gary MK, Niu, Yun, & Shi, Hui-Juan (2010). Phyllodes tumor of the breast: an update. *Breast Cancer, 17*(1), 29-34.

Tu, Chao, Yang, Kexin, Wan, Lu, He, Jieyu, Qi, Lin, Wang, Wanchun, Li, Zhihong (2020). The crosstalk between lncRNAs and the Hippo signalling pathway in cancer progression. *Cell Proliferation 53*(9), e12887.

Turner, David A, Hayward, Penelope C, Baillie-Johnson, Peter, Rué, Pau, Broome, Rebecca, Faunes, Fernando, & Martinez Arias, Alfonso (2014). Wnt/β-catenin and FGF signalling direct the specification and maintenance of a neuromesodermal axial progenitor in ensembles of mouse embryonic stem cells. *Development, 141*(22), 4243-4253.

Ugrinova, Iva, Petrova, Maria, Chalabi-Dchar, Mounira, & Bouvet, Philippe (2018). Multifaceted nucleolin protein and its molecular partners in oncogenesis. *Advances in Protein Chemistry Structural Biology, 111*, 133-164.

Vega, Francisco M, Fruhwirth, Gilbert, Ng, Tony, & Ridley, Anne J (2011). RhoA and RhoC have distinct roles in migration and invasion by acting through different targets. *Journal of Cell Biology 193*(4), 655-665.

Vega, Francisco M, & Ridley, Anne J (2008). Rho GTPases in cancer cell biology. *FEBS letters, 582*(14), 2093-2101.

Venetis, Konstantinos, Piciotti, Roberto, Sajjadi, Elham, Invernizzi, Marco, Morganti, Stefania, Criscitiello, Carmen, & Fusco, Nicola. (2021). Breast cancer with bone metastasis: molecular insights and clinical management. *Cells*, *10*(6), 1377.

Venkatesh, Vandana, Nataraj, Raghu, Thangaraj, Gopenath S, Karthikeyan, Murugesan, Gnanasekaran, Ashok, Kaginelli, Shanmukhappa B, Basalingappa, Kanthesh M (2018). Targeting Notch signalling pathway of cancer stem cells. *Stem Cell Investigation 5*(5).

Vikram, Rajeev, Chou, Wen Cheng, Hung, Shih-Chieh, & Shen, Chen-Yang. (2020). Tumorigenic and metastatic role of CD44−/low/CD24−/low cells in luminal breast cancer. *Cancers, 12*(5), 1239.

Vincent, Thomas L, & Gatenby, Robert A (2008). An evolutionary model for initiation, promotion, and progression in carcinogenesis. *International Journal of Oncology 32*(4), 729-737.

Voorneveld, Philip W, Kodach, Liudmila L, Jacobs, Rutger J, Liv, Nalan, Zonnevylle, A Christiaan, Hoogenboom, Jacob P, De Rooij, Karien (2014). Loss of SMAD4 alters BMP signaling to promote colorectal cancer cell metastasis via activation of Rho and ROCK. *Gastroenterology, 147*(1), 196-208. e113.

Voorneveld, Philip W, Kodach, Liudmila L, Jacobs, Rutger J, Van Noesel, CJM, Peppelenbosch, MP, Korkmaz, KS, Van Pelt, GW (2015). The BMP pathway either enhances or inhibits the Wnt pathway depending on the SMAD4 and p53 status in CRC. *British journal of cancer, 112*(1), 122-130.

Vorburger, Stephan A, Xing, Yan, Hunt, Kelly K, Lakin, Gregory E, Benjamin, Robert S, Feig, Barry W, Trent III, Jonathan (2005). Angiosarcoma of the breast. *International Journal of the American Cancer Society 104*(12), 2682-2688.

Wang, Daisong, Liu, Chunye, Wang, Jingqiang, Jia, Yingying, Hu, Xin, Jiang, Hai, Zeng, Yi Arial (2018). Protein C receptor stimulates multiple signaling pathways in breast cancer cells. *The Journal of biological chemistry, 293*(4), 1413-1424.

Wang, Dongdong, Naydenov, Nayden G., Dozmorov, Mikhail G., Koblinski, Jennifer E., & Ivanov, Andrei I. (2020). Anillin regulates breast cancer cell migration, growth, and metastasis by non-canonical mechanisms involving control of cell stemness and differentiation. *Breast Cancer Research, 22*(1), 3. doi:10.1186/s13058-019-1241-x

Wang, Haibo, Zhao, Gang, Liu, Xiangping, Sui, Aihua, Yang, Kun, Yao, Ruyong, Shi, Qiang (2010). Silencing of RhoA and RhoC expression by RNA interference suppresses human colorectal carcinoma growth in vivo. *Journal of Experimental Clinical Cancer Research 29*(1), 1-7.

Wang, Jennifer Y, Wang, Erica B, & Swetter, Susan M (2023). What Is Melanoma? *Journal of the American Medical Association, 329*(11), 948-948.

Wang, Kai, Yuen, Siu Tsan, Xu, Jiangchun, Lee, Siu Po, Yan, Helen HN, Shi, Stephanie T, Law, Simon (2014). Whole-genome sequencing and comprehensive molecular profiling identify new driver mutations in gastric cancer. *Nature genetics, 46*(6), 573-582.

Wang, Lei, Shen, Saie, Wang, Mingsong, Ding, Fangbao, Xiao, Haibo, Li, Guoqing, & Hu, Fengqing (2019). Rho GTPase activating protein 24 (ARHGAP24) silencing promotes lung cancer cell migration and invasion by activating β-catenin signaling. *International Medical Journal of Experimental Clinical Research 25*, 21-31.

Wang, Lin, Park, Paul, La Marca, Frank, Than, Khoi D, & Lin, Chia-Ying (2015). BMP-2 inhibits tumor-initiating ability in human renal cancer stem cells and induces bone formation. *Journal of Cancer Research Clinical Oncology 141*, 1013-1024.

Wang, Lulu (2017). Early diagnosis of breast cancer. *Sensors, 17*(7), 1572.

Wang, Richard N, Green, Jordan, Wang, Zhongliang, Deng, Youlin, Qiao, Min, Peabody, Michael, Denduluri, Sahitya (2014). Bone Morphogenetic Protein (BMP) signaling in development and human diseases. *Genes & diseases,, 1*(1), 87-105.

Wang, Shan, Englund, Emelie, Kjellman, Pontus, Li, Zhen, Ahnlide, Johannes Kumra, Rodriguez-Cupello, Carmen, Lindgren, David (2021). CCM3 is a gatekeeper in focal adhesions regulating mechanotransduction and YAP/TAZ signalling. *Nature cell biology, 23*(7), 758-770.

Wang, Shuo, Li, Gui-Xi, Tan, Cong-Cong, He, Rui, Kang, Li-Juan, Lu, Jun-Tao, Zhai, Qiong-Li (2019). FOXF2 reprograms breast cancer cells into bone metastasis seeds. *Nature communications, 10*(1), 2707.

Wang, Shuo, Li, Gui-Xi, Tan, Cong-Cong, He, Rui, Kang, Li-Juan, Lu, Jun-Tao, Zhai, Qiong-Li. (2019). FOXF2 reprograms breast cancer cells into bone metastasis seeds. *Nature communications, 10*(1), 2707.

Wang, Wei, Rana, Priyanka S, Markovic, Vesna, & Sossey-Alaoui, Khalid. (2022). The WAVE3/β-Catenin oncogenic signaling regulates chemoresistance in triple negative breast cancer. *Breast cancer research : BCR, 25*(1), 31.

Wang, Xiaoxia, Jiang, Wenyan, Kang, Jiali, Liu, Qicai, & Nie, Miaoling (2015). Knockdown of RhoA expression alters ovarian cancer biological behavior in vitro and in nude mice. *Oncology Reports 34*(2), 891-899.

Wang, Yi-Qing, Wang, Nuo-Xin, Luo, Yi, Yu, Chang-Yin, & Xiao, Jian-Hui (2020). Ganoderal A effectively induces osteogenic differentiation of human amniotic mesenchymal stem cells via cross-talk between Wnt/β-catenin and BMP/SMAD signaling pathways. *Biomedicine Pharmacotherapy 123*, 109807.

Wang, Zhijie, Shen, Zhirong, Li, Zhenxiang, Duan, Jianchun, Fu, Shuai, Liu, Zhentao, Wang, Xiaodong (2015). Activation of the BMP-BMPR pathway conferred resistance to EGFR-TKIs in lung squamous cell carcinoma patients with EGFR mutations. *Proceedings of the National Academy of Sciences, 112*(32), 9990-9995.

Wang, Zhishan, & Yang, Chengfeng. (2019). *Metal carcinogen exposure induces cancer stem cell-like property through epigenetic reprograming: A novel mechanism of metal carcinogenesis.* Paper presented at the Seminars in Cancer Biology.

Warboys, Christina M (2018). Mechanoactivation of Wnt/β-catenin pathways in health and disease. *Emerging Topics in Life Sciences 2*(5), 701-712.

Wei, Changran, Wang, Ying, & Li, Xiangqi (2018). The role of Hippo signal pathway in breast cancer metastasis. *OncoTargets and therapy, 11*, 2185.

Wei, Congcong, Chen, Xingyong, Peng, Jinzhou, Yu, Shiqi, Chang, Penghui, Jin, Kaiming, & Geng, Zhaoyu (2023). BMP4/SMAD8 signaling pathway regulated granular cell proliferation to promote follicle development in Wanxi white goose. *Poultry science, 102*(1), 102282.

Weigelt, Britta, Lo, Alvin T, Park, Catherine C, Gray, Joe W, & Bissell, Mina J (2010). HER2 signaling pathway activation and response of breast cancer cells to HER2-targeting agents is dependent strongly on the 3D microenvironment. *Breast cancer research and treatment, 122*(1), 35-43.

Wellenstein, Max D, Coffelt, Seth B, Duits, Danique EM, van Miltenburg, Martine H, Slagter, Maarten, de Rink, Iris, Hau, Cheei-Sing (2019). Loss of p53 triggers WNT-dependent systemic inflammation to drive breast cancer metastasis. *Nature, 572*(7770), 538-542.

Welsh, JoEllen. (2013). Animal models for studying prevention and treatment of breast cancer. In *Animal Models for the Study of Human Disease* (pp. 997-1018): Elsevier.

Whiteside, TL (2008). The tumor microenvironment and its role in promoting tumor growth. *Oncogene, 27*(45), 5904-5912.

Whooley, Brian P, Gibbs, John F, Mooney, Margaret M, McGrath, Brian E, & Kraybill, William G (2000). Primary extremity sarcoma: what is the appropriate follow-up? *Annals of Surgical Oncology 7*(1), 9-14.

Wogan, Gerald N, Hecht, Stephen S, Felton, James S, Conney, Allan H, & Loeb, Lawrence A. (2004). *Environmental and chemical carcinogenesis.* Paper presented at the Seminars in Cancer Biology.

Wolf, Rebecca M, Draghi, Nicole, Liang, Xiquan, Dai, Chengkai, Uhrbom, Lene, Eklöf, Charlotta, Resh, Marilyn D (2003). p190RhoGAP can act to inhibit PDGF-induced gliomas in mice: a putative tumor suppressor encoded on human chromosome 19q13. 3. *Genes & development*, *17*(4), 476-487.

Wong, Darren Chen Pei, Pan, Catherine Qiurong, Er, Shi Yin, Thivakar, T, Rachel, Tan Zi Yi, Seah, Sock Hong, Chaudhuri, Parthiv Kant (2023). The Scaffold RhoGAP Protein ARHGAP8/BPGAP1 Synchronizes Rac and Rho Signaling to Facilitate Cell Migration. *Molecular biology of the cell*, *34*(3), mbc. E21-03-0099.

Worzfeld, Thomas, Swiercz, Jakub M, Looso, Mario, Straub, Beate K, Sivaraj, Kishor K, & Offermanns, Stefan (2012). ErbB-2 signals through Plexin-B1 to promote breast cancer metastasis. *The Journal of clinical investigation*, *122*(4), 1296-1305.

Wu, Jiuping, Li, Linlong, Fu, Chuan, Yang, Fan, Jiao, Zixue, Shi, Xincui, Zhang, Peibiao (2018). Micro-porous polyetheretherketone implants decorated with BMP-2 via phosphorylated gelatin coating for enhancing cell adhesion and osteogenic differentiation. *Colloids Surfaces B: Biointerfaces 169*, 233-241.

Wu, Longhuo, Huang, Xianhua, Li, Linfu, Huang, Hao, Xu, Ruian, & Luyten, Walter (2012). Insights on biology and pathology of HIF-1α/-2α, TGFα/BMP, Wnt/β-catenin, and NF-κB pathways in osteoarthritis. *Current pharmaceutical design*, *18*(22), 3293-3312.

Wu, Wenya, Li, Xiaomin, Qi, Meng, Hu, Xin, Cao, Fenghua, Wu, Xiaoping, & Fu, Junsheng (2022). Cordycepin inhibits growth and metastasis formation of MDA-MB-231 xenografts in nude mice by modulating the hedgehog pathway. *International journal of molecular sciences*, *23*(18), 10362.

Wu, Zhao-Qiu, Li, Xiao-Yan, Hu, Casey Yuexian, Ford, Michael, Kleer, Celina G, & Weiss, Stephen J (2012). Canonical Wnt signaling regulates Slug activity and links epithelial–mesenchymal transition with epigenetic Breast Cancer 1, Early Onset (BRCA1) repression. *Proceedings of the National Academy of Sciences of the United States of America*, *109*(41), 16654-16659.

Xiang, Yu-chen, Peng, Peng, Liu, Xue-wen, Jin, Xin, Shen, Jie, Zhang, Te, Yu, Qing-qing (2022). Paris saponin VII, a Hippo pathway activator, induces autophagy and exhibits therapeutic potential against human breast cancer cells. *Acta pharmacologica Sinica*, *43*(6), 1568-1580.

Xiao, Wen, Wang, Xuegang, Wang, Tao, & Xing, Jinchun (2020). Overexpression of BMP1 reflects poor prognosis in clear cell renal cell carcinoma. *Cancer gene therapy*, *27*(5), 330-340.

Xiao, Yang, Lin, Vivian Y, Ke, Shi, Lin, Gregory E, Lin, Fang-Tsyr, & Lin, Weei-Chin. (2014). 14-3-3τ promotes breast cancer invasion and metastasis by inhibiting RhoGDIα. *Molecular and cellular biology*, *34*(14), 2635-2649.

Xiao, Yi, Liu, Qin, Peng, Nanyin, Li, Yuzhang, Qiu, Danyang, Yang, Tianlun, Borlongan, Cesario V (2022). Lovastatin Inhibits RhoA to Suppress Canonical Wnt/β-Catenin Signaling and Alternative Wnt-YAP/TAZ Signaling in Colon Cancer. *Cell transplantation*, *31*, 09636897221075749.

Xie, Tingying, Zahid, Husam, Ali, Ahmed R, Joyce, Ryan, Yang, Ge, Winz, Cassandra, Hu, Longqin (2023). Inhibitors of Keap1-Nrf2 protein-protein interaction reduce estrogen responsive gene expression and oxidative stress in estrogen receptor-positive breast cancer. *Toxicology and applied pharmacology*, *460*, 116375.

Xue, Chen, Li, Ganglei, Lu, Juan, & Li, Lanjuan (2021). Crosstalk between circRNAs and the PI3K/AKT signaling pathway in cancer progression. *Signal Transduction Targeted Therapy 6*(1), 400.

Yadin, David, Knaus, Petra, & Mueller, Thomas D (2016). Structural insights into BMP receptors: Specificity, activation and inhibition. *Cytokine & growth factor reviews*, *27*, 13-34.

Yamaguchi, H., Wyckoff, J., & Condeelis, J. (2005). Cell migration in tumors. *Curr Opin Cell Biol*, *17*(5), 559-564. doi:10.1016/j.ceb.2005.08.002

Yan, Gang, Dai, Meiou, Zhang, Chenjing, Poulet, Sophie, Moamer, Alaa, Wang, Ni, Lebrun, Jean-Jacques. (2021). TGFβ/cyclin D1/Smad-mediated inhibition of BMP4 promotes breast cancer stem cell self-renewal activity. *Oncogenesis*, *10*(3), 21.

Yan, Guoxin, Zou, Ronghai, Chen, Zhenggang, Fan, Bing, Wang, Zhaoyan, Wang, Ying, Yang, Fang (2014). Silencing RhoA inhibits migration and invasion through Wnt/β-catenin pathway and growth through cell cycle regulation in human tongue cancer. *Acta Biochim Biophys Sin 46*(8), 682-690.

Yan, Ting, Zhang, Ailiang, Shi, Fangfang, Chang, Fei, Mei, Jie, Liu, Yongjian, & Zhu, Yichao (2018). Integrin αvβ3–associated DAAM1 is essential for collagen-induced invadopodia extension and cell haptotaxis in breast cancer cells. *The Journal of biological chemistry, 293*(26), 10172-10185.

Yang, Huijie, Xue, Min, Su, Peng, Zhou, Yan, Li, Xin, Li, Zhongbo, Zheng, Xiuxia (2022). RNF31 represses cell progression and immune evasion via YAP/PD-L1 suppression in triple negative breast Cancer. *Journal of experimental & clinical cancer research, 41*(1), 1-18.

Yang, J., Li, X., Li, Y., Southwood, M., Ye, L., Long, L., Morrell, N. W. (2013). Id proteins are critical downstream effectors of BMP signaling in human pulmonary arterial smooth muscle cells. *Am J Physiol Lung Cell Mol Physiol, 305*(4), L312-321. doi:10.1152/ajplung.00054.2013

Yang, Min, Fan, Zhiqin, Wang, Fei, Tian, Zhi-hua, Ma, Bo, Dong, Bin, Zhao, Wei (2018). BMP-2 enhances the migration and proliferation of hypoxia-induced VSMCs via actin cytoskeleton, CD44 and matrix metalloproteinase linkage. *Experimental cell research, 368*(2), 248-257.

Yang, Xueying, Zheng, Fushuang, Zhang, Suning, & Lu, Jibin. (2015). Loss of RhoA expression prevents proliferation and metastasis of SPCA1 lung cancer cells in vitro. *Biomedicine Pharmacotherapy 69*, 361-366.

Yap, Timothy A, Walton, Mike I, Grimshaw, Kyla M, Te Poele, Robert H, Eve, Paul D, Valenti, Melanie R, Heaton, Simon P (2012). AT13148 is a novel, oral multi-AGC kinase inhibitor with potent pharmacodynamic and antitumor activity. *Clinical Cancer Research, 18*(14), 3912-3923.

Yarden, Yosef (2001). Biology of HER2 and its importance in breast cancer. *Oncology, 61*(Suppl. 2), 1-13.

Yerushalmi, R, Hayes, MM, & Gelmon, KA (2009). Breast carcinoma—rare types: review of the literature. *Journal of the European Society for Medical Oncology, 20*(11), 1763-1770.

Ying, Xuexiang, Sun, Yunpo, & He, Pingqing (2015). Bone morphogenetic protein-7 inhibits EMT-associated genes in breast cancer. *Cellular Physiology Biochemistry 37*(4), 1271-1278.

Ying, Xuexiang, Sun, Yunpo, & He, Pingqing (2017). MicroRNA-137 inhibits BMP7 to enhance the epithelial-mesenchymal transition of breast cancer cells. *Oncotarget, 8*(11), 18348-18358.

Yousefnia, Saghar, Ghaedi, Kamran, Seyed Forootan, Farzad, & Nasr Esfahani, Mohammad Hossein (2019). Characterization of the stemness potency of mammospheres isolated from the breast cancer cell lines. *Tumor Biology 41*(8), 1010428319869101.

Yu, Wendan, Li, Liren, Zheng, Fufu, Yang, Wenjing, Zhao, Shilei, Tian, Chunfang, Zou, Lijuan (2017). β-catenin cooperates with CREB binding protein to promote the growth of tumor cells. *Cellular Physiology Biochemistry 44*(2), 467-478.

Yuan, Bo, Liu, Jinquan, Shi, Aiping, Cao, Jin, Yu, Yi, Zhu, Yezhang, Shi, Jiaxian (2023). HERC3 promotes YAP/TAZ stability and tumorigenesis independently of its ubiquitin ligase activity. *The EMBO journal, 42*(4), e111549.

Zahra, Maram H, Nawara, Hend M, Hassan, Ghmkin, Afify, Said M, Seno, Akimasa, & Seno, Masaharu. (2022). Cancer Stem Cells Contribute to Drug Resistance in Multiple Different Ways. In *Cancer Stem Cell Markers and Related Network Pathways* (Vol. 1393, pp. 125-139). Advances in Experimental Medicine and Biology: Springer.

Zeng, Yongqiu, Cao, Yang, Liu, Lan, Zhao, Jiao, Zhang, Ting, Xiao, Lifan, Disease. (2019). SEPT9_i1 regulates human breast cancer cell motility through cytoskeletal and RhoA/FAK signaling pathway regulation. *10*(10), 1-16.

Zhan, Tailan, Rindtorff, Niklas, & Boutros, Michael (2017). Wnt signaling in cancer. *Oncogene, 36*(11), 1461-1473.

Zhang, Chao, Wang, Hui-Jie, Bao, Qi-Chao, Wang, Lei, Guo, Tian-Kun, Chen, Wei-Lin, Yang, Ying-Rui (2016). NRF2 promotes breast cancer cell proliferation and metastasis by increasing RhoA/ROCK pathway signal transduction. *Oncotarget, 7*(45), 73593-73606.

Zhang, Fan, Chen, Anmin, Chen, Jianfeng, Yu, Tian, & Guo, Fengjing (2011). SiRNA-mediated silencing of beta-catenin suppresses invasion and chemosensitivity to doxorubicin in MG-63 osteosarcoma cells. *Asian Pacific journal of cancer prevention, 12*(1), 239-245.

Zhang, Fengyu, Liu, Ruilai, Liu, Cheng, Zhang, Haishi, & Lu, Yuan (2020). Nanos3, a cancer-germline gene, promotes cell proliferation, migration, chemoresistance, and invasion of human glioblastoma. *Cancer cell international, 20*(1), 1-14.

Zhang, Jingyao, Guo, Fengzhu, Li, Chunxiao, Wang, Yang, Wang, Jinsong, Sun, Fangzhou, Qian, Haili (2023). Loss of TTC17 promotes breast cancer metastasis through RAP1/CDC42 signaling and sensitizes it to rapamycin and paclitaxel. *Cell & bioscience, 13*(1), 1-19.

Zhang, RF, Liu, JW, Yu, SP, Sun, D, Wang, XH, Fu, JS, & Xie, Z (2019). LncRNA UCA1 affects osteoblast proliferation and differentiation by regulating BMP-2 expression. *European review for medical and pharmacological sciences, 23*(16), 6774-6782.

Zhang, Rui, Tu, Juchuanli, & Liu, Suling. (2022). Novel molecular regulators of breast cancer stem cell plasticity and heterogeneity. *Seminars in Cancer Biology, 82*, 11-25.

Zhang, Shuning, Dong, Yuqing, Zhao, Shuangyuan, Bi, Fei, Xuan, Ming, Zhu, Guiquan, Zhang, Zhuang (2023). CXCL1 promoted the migration and invasion abilities of oral cancer cells and might serve as a promising marker of prognosis in tongue cancer. *Journal of oral pathology & medicine*.

Zhang, Yiran, Cheng, Shihao, Zhong, Peiyu, Wang, Ziying, Liu, Rui, & Ding, Yu (2022). Structural insights into the binding of nanobody Rh57 to active RhoA-GTP. *Biochemical and biophysical research communications, 616*, 122-128.

Zhang, Yu, Xie, Zi-Yan, Guo, Xuan-Tong, Xiao, Xing-Hua, & Xiong, Li-Xia (2019). Notch and breast cancer metastasis: Current knowledge, new sights and targeted therapy. *Oncology letters, 18*(3), 2743-2755.

Zhao, Lin, Lei, Jianjun, Gu, Shanzhi, Zhang, Yujiao, Jing, Xin, Wang, Lu, Qi, Yifan (2022). A yes-associated protein 1-Notch1 receptor positive feedback loop promotes breast cancer lung metastasis by attenuating the bone morphogenetic protein 4-SMAD family member 1/5 signaling. *Carcinogenesis, 43*(12), 1162-1175.

Zhao, Lin, Lei, Jianjun, Gu, Shanzhi, Zhang, Yujiao, Jing, Xin, Wang, Lu, Shao, Shan. (2022). A yes-associated protein 1- Notch1 receptor positive feedback loop promotes breast cancer lung metastasis by attenuating the bone morphogenetic protein 4-SMAD family member 1/5 signaling. *Carcinogenesis*. doi:10.1093/carcin/bgac081

Zheng, Lewei, Yang, Qian, Li, Chengxin, Xu, Gaoran, Yuan, Qianqian, Hou, Jinxuan, & Wu, Gaosong (2023). Ubiquitin-Specific Peptidase 8 Modulates Cell Proliferation and Induces Cell Cycle Arrest and Apoptosis in Breast Cancer by Stabilizing Estrogen Receptor Alpha. *Journal of oncology, 2023*, 8483325.

Zhong, Zheng, Yu, Jia, Virshup, David M, & Madan, Babita (2020). Wnts and the hallmarks of cancer. *Cancer Metastasis Reviews 39*(3), 625-645.

Zhou, Jin, Zhao, Li-Qun, Xiong, Mo-Miao, Wang, Xiu-Qin, Yang, Guan-Rui, Qiu, Zong-Liang, Liu, Zhi-Hua (2003). Gene expression profiles at different stages of human esophageal squamous cell carcinoma. *World Journal of Gastroenterology 9*(1), 9-15.

Zhou, Xuan, & Zheng, Yi (2013). Cell type-specific signaling function of RhoA GTPase: lessons from mouse gene targeting. *The Journal of biological chemistry, 288*(51), 36179-36188.

Zhou, Yongping, Hua, Zhiyuan, Zhu, Ye, Wang, Liying, Chen, Fangming, Shan, Ting, Dai, Tu (2020). Upregulation of ARHGAP30 attenuates pancreatic cancer progression by inactivating the β-catenin pathway. *Cancer cell international, 20*, 1-12.

Zhou, Yulian, Wang, Yanshu, Tischfield, Max, Williams, John, Smallwood, Philip M, Rattner, Amir, Nathans, Jeremy (2014). Canonical WNT signaling components in vascular development and barrier formation. *The Journal of Clinical Investigation, 124*(9), 3825-3846.

Zuo, Hao, Yang, Dengbao, & Wan, Yihong (2021). Fam20C regulates bone resorption and breast cancer bone metastasis through osteopontin and BMP4. *The Journal of Cancer research 81*(20), 5242-5254.

Zuo, Yan, Ulu, Arzu, Chang, Jeffrey T, & Frost, Jeffrey A (2018). Contributions of the RhoA guanine nucleotide exchange factor Net1 to polyoma middle T antigen-mediated mammary gland tumorigenesis and metastasis. *Breast cancer research : BCR*, *20*(1), 1-16.

Publications

- **Renu Sharma**, Amit Sharma, Sam P Mathew**,** Bithiah Grace Jaganathan*. RHOA and β-catenin in breast cancer progression. (Under preparation)
- **Renu Sharma**, Gayatri Gogoi, Snigdha Saikia, Amit Sharma, Deep Jyoti Kalita, Anupam Sarma, Anil Mukund Limaye, Manish Kumar Gaur, Jina Bhattacharyya, Bithiah Grace Jaganathan*. BMP4 enhances anoikis resistance and chemoresistance of breast cancer cells through canonical BMP signalling. J Cell Commun Signal. 2022;16;191-205. https://doi.org/10.1007 /s12079-021-00649
- **Renu Sharma,** Amit Sharma, Atul Kumar*, Bithiah Grace Jaganathan*. Phospho-protein Analysis in Adherent Cells Using Flow Cytometry. Bio-protocol. 2019;9(20);e3395. https://doi.org/10.21769/BioProtoc.3395
- Chinnapaka Somaiah[#], Atul Kumar[#], **Renu Sharma[#],** Amit Sharma, Trishna Anand, Jina Bhattacharyya, Damodar Das, Sewali Deka Talukdar, Bithiah Grace Jaganathan*. Mesenchymal stem cells show functional defects and decreased anti-cancer effects after exposure to chemotherapeutic drugs. J Biomed Sci. 2018;25;5. https://doi.org/10.1186/s12929-018-0407
- Sreeja Dattachoudhury, **Renu Sharma**, Atul Kumar, Bithiah Grace Jaganathan*. Sorafenib Inhibits Proliferation, Migration and Invasion of Breast Cancer Cells. Oncology. 2020;98(7);478-486. https://doi.org/10.1159/000505521
- Atul Kumar, **Renu Sharma**, Sreeja Dattachoudhury, Amit Sharma, Trishna Anand, Jina Bhattacharyya, Kasturi Bhattacharjee, Bithiah Grace Jaganathan*. OCT4A transcript level correlates with the proliferation potential of human mesenchymal stem cells. Gene reports. 2019;16;100459. https://doi.org/10.1016/j.genrep.2019.100459
- Darilang Mawrie, Kasturi Bhattacharjee, Amit Sharma, **Renu Sharma**, Jina Bhattacharyya, Harsha Bhattacharjee, Nilutparna Deori, Atul Kumar, Bithiah Grace Jaganathan*. Human orbital adipose tissue-derived mesenchymal stem cells possess neuroectodermal differentiation and repair ability. Cell Tissue Res. 2019;378;5312542. https://doi.org/10.1007/s00441-019-03072-0

# Equal contribution

Conferences and Workshops

- Participated in the "2 nd Indian Cancer Congress" held at Clark's Convention Centre, Bengaluru. (9 th -12 th November 2017).
- Participated in a workshop on "ZE5 & Droplet Digital PCR-QX200" organised by Bio-Rad laboratories and IIT-Guwahati, India. (30 th October-3 rd November 2017).
- Participated in a workshop on "ImageJ" at Research Conclave 2018 organised by Student's Academic Board, IIT-Guwahati, India. (8 th -11 th March 2018).
- Research Conclave-IIT Guwahati (March 2019) "Role of Rho-GTPase and BMP in breast cancer metastasis"
- Research Conclave-IIT Guwahati (Jan 2021) "Role of RHOA signalling in breast cancer metastasis"
- Online Workshop on "Flow Cytometry Techniques and Applications" NECBH, IIT Guwahati (21 st -22 nd December 2020).
- Poster Presented on "Role of RHOA Signalling in Breast Cancer Metastasis" during North-East Research Conclave, IIT Guwahati. (20 th -22 nd May, 2022

Acknowledgement

First and foremost, I want to express my sincere gratitude and respect for ***Prof. Bithiah Grace Jaganathan***, who supervised my PhD. I owe her a debt of gratitude for all of the scientific advice, perceptive comments and recommendations, ongoing support, and tolerance during my PhD. I want to thank her for providing the necessary resources and for setting up a great lab environment where different research ideas could be discussed and exchanged. She has inspired me to work independently and has consistently encouraged me to provide my best effort. I have been motivated to work hard by her enthusiasm for science and ability to multitask accurately and consistently. She has given me academic and emotional support, which has enabled me to complete this thesis. I consider myself fortunate to have a supervisor who genuinely cares about my work and answers my inquiries and concerns promptly. I recall feeling disoriented and perplexed. You were the one who recognised my potential and assisted me in seeing it, or at the very least in getting a glimpse of it. Thank you so much, Ma'am, for everything.

I would like to express my profound gratitude to the doctoral committee members, ***Prof. Pranab Goswami***, ***Prof. Biman Behari Mandal***, and ***Prof. Sachin Kumar***, for their insightful criticism and motivating recommendations, which helped me finish my thesis.

I am grateful to ***Prof. V. Venkata Dasu***, ***Prof. Kannan Pakshirajan***, ***Prof. Latha Rangan***, and ***Prof. Rakhi Chaturvedi***, previous and present Heads of the Department of Biosciences and Bioengineering, for their assistance in supplying all the departmental facilities during their tenure. I also acknowledge the Department of Biosciences and Bioengineering at IIT Guwahati for providing the facilities necessary for my research. I also like to thank the BSBE office team for their technical assistance. I wish to express my gratitude to the Ministry of Human Resources Development (MHRD), India for providing financial support during my PhD.

I am indebted to all former and current members of the Stem Cell and Cancer Biology Group; of which I have been a member for more than seven years. Before anything else, I would like to credit my seniors ***Dr Atul Kumar***, ***Dr Darilang Mawrie***, and ***Dr Chinnapaka Somaiah*** for establishing the standard protocol and fostering an environment conducive to research. Next, I would like to thank my seniors ***Trishna*** and ***Sreeja***, who were incredibly helpful during the beginning of my PhD career, both professionally and emotionally. Next, I would like to acknowledge ***Amit*** for providing me with transduced cells during a crucial phase of my thesis research. My peers ***Nikhil***, ***Rumela***, ***Soumik***, ***Sam***, ***Kritika***, and ***Shikha*** have been constant sources of encouragement and assistance. All of the dissertation students, beginning with ***Vishnu***, ***Pratyush***, ***Sanjukta***, ***Sachin***, ***Aswanth***,

Surya, ***Pakshal*** and ***Raghu*** with whom I have shared my research experience and learned a great deal.

During the ups and downs of my PhD journey, my companions and family away from home ***Bhagyashree***, ***Rachayeeta***, ***Christy***, ***Krishna***, ***Manash***, ***Nayan***, ***Sandeep*** and ***Varun*** were always by my side. I consider myself especially privileged to have received love and support from ***Alisha***, ***Divya*** and ***Nishant*** who were only a phone call away. We shared some priceless moments and created countless memories that I will cherish for a lifetime. Thanks a lot for everything.

Last, but certainly not least, I would like to express my sincere appreciation to my family for their unwavering support. Without them, I consider myself to be insignificant. I believe that nothing can ever go awry for me because I am always protected by your blessing. Your understanding and confidence in me are my greatest assets; I could not have reached this point without you.

I am eternally grateful to the Almighty for everything I have, including a beautiful existence surrounded by wonderful people.

Renu Sharma